

U.S. Geological Survey  
Toxic Substances Hydrology Program

Proceedings of the Technical Meeting,  
Charleston, South Carolina,  
March 8—12, 1999

Rec'd  
12/12/00  
CKim/  
Gleg)



Water-Resources Investigations Report 99-4018C  
Volume 3 of 3 - Subsurface Contamination From Point Sources

Section B - Ground Water Contamination by Crude Oil



**U.S. Geological Survey  
Toxic Substances Hydrology Program—  
Proceedings of the Technical Meeting,  
Charleston, South Carolina,  
March 8-12, 1999**

***David W. Morganwalp and Herbert T. Buxton, Editors***

---

U.S. GEOLOGICAL SURVEY

Water-Resources Investigations Report 99-4018C

Volume 3 of 3 - Subsurface Contamination From Point Sources

Section B - Ground Water Contamination by Crude Oil

West Trenton, New Jersey

1999



**U.S. DEPARTMENT OF THE INTERIOR**

BRUCE BABBITT, *Secretary*

**U.S. GEOLOGICAL SURVEY**

Charles G. Groat, *Director*

The use of brand, trade, or firm names, or the names of individuals in this report is for identification purposes only and does not imply endorsement by the U.S. Geological Survey or impute responsibility for any present or potential effects on water or other natural resources.

---

For additional information  
write to:

Coordinator  
Toxic Substances Hydrology Program  
U.S. Geological Survey  
412 National Center  
Reston, Virginia 22092

Copies of this report can be  
purchased from:

U.S. Geological Survey  
Branch of Information Services  
Box 25286  
Denver, CO 80225-0286



## CONTENTS

	Page
INTRODUCTION .....	1
ACKNOWLEDGMENTS .....	2
<b>VOLUME 3 - SUBSURFACE CONTAMINATION FROM POINT SOURCES</b>	
SECTION B—Ground Water Contamination by Crude Oil.....	121*
Long-term geochemical evolution of a crude-oil plume at Bemidji, Minnesota by I.M. Cozzarelli, M.J. Baedecker, R.P. Eganhouse, M.E. Tuccillo, B.A. Bekins, G.R. Aiken, and J.B. Jaeschke.....	123
Chemical and physical controls on microbial populations in the Bemidji Toxics Site crude-oil plume by B.A. Bekins, I.M. Cozzarelli, E.M. Godsy, Ean Warren, M.E. Tuccillo, H.I. Essaid, and V.V. Paganelli.....	133
Long-term monitoring of unsaturated-zone properties to estimate recharge at the Bemidji crude-oil spill site by G.N. Delin and W.N. Herkelrath.....	143
Coupled biogeochemical modeling of ground-water contamination at the Bemidji, Minnesota, crude oil spill site by G.P. Curtis, I.M. Cozzarelli, M.J. Baedecker, and B.A. Bekins .....	153
Determining BTEX biodegradation rates using in-situ microcosms at the Bemidji site, Minnesota: Trials and tribulations by E.M. Godsy, Ean Warren, I.M. Cozzarelli, B.A. Bekins, and R.P. Eganhouse .....	159
Mineralogy and mineral weathering: Fundamental components of subsurface microbial ecology by P.C. Bennett, J.R. Rogers, F.K. Hiebert, and W.J. Choi .....	169
Aromatic and polyaromatic hydrocarbon degradation under Fe(III)-reducing conditions by R.T. Anderson, J.N. Rooney-Varga, C.V. Gaw, and D.R. Lovley .....	177
Electrical geophysics at the Bemidji Research Site by R.J. Bisdorf.....	187
Impacts of remediation at the Bemidji oil-spill site by W.N. Herkelrath .....	195
Ground penetrating radar research at the Bemidji, Minnesota, crude-oil spill site by J.E. Lucius .....	201
Investigating the potential for colloid- and organic matter-facilitated transport of polycyclic aromatic hydrocarbons in crude oil-contaminated ground water by J.N. Ryan, G.R. Aiken, D.A. Backhus, K.G. Villholth, and C.M. Hawley .....	211
Inhibition of acetoclastic methanogenesis by crude oil from Bemidji, Minnesota by Ean Warren, B.A. Bekins, and E.M. Godsy .....	223
Polar metabolites of crude oil by K.A. Thorn and G.R. Aiken.....	231
Patterns of microbial colonization on silicates by J.R. Rogers, P.C. Bennett, and F.K. Hiebert .....	237
COMPLETE CONTENTS OF ORIGINAL MANUSCRIPT .....	243

\*Page numbers are those of the original manuscript.



## INTRODUCTION

This report contains papers presented at the seventh Technical Meeting of the U.S. Geological Survey (USGS), Toxic Substances Hydrology (Toxics) Program. The meeting was held March 8-12, 1999, in Charleston, South Carolina. Toxics Program Technical Meetings are held periodically to provide a forum for presentation and discussion of results of recent research activities.

The objectives of these meetings are to:

- Present recent research results to essential stakeholders,
- Encourage synthesis and integrated interpretations among scientists with different expertise who are working on a contamination issue, and
- Promote exchange of ideas among scientists working on different projects and issues within the Toxics Program.

The Proceedings is published in three volumes. Volume 1 contains papers that report on results of research on contamination from hard-rock mining. Results include research on contamination from hard rock mining in arid southwest alluvial basins, research on hard rock mining in mountainous terrain, and progress from the USGS Abandoned Mine Lands Initiative. This Initiative is designed to develop a watershed-based approach to characterize and remediate contamination from abandoned mine lands and transfer technologies to Federal land management agencies and stakeholders.

Volume 2 contains papers on contamination of hydrologic systems and related ecosystems. The papers discuss research on the response of estuarine ecosystems to contamination from human activities. They include research on San Francisco Bay; mercury contamination of aquatic ecosystems; and investigation of the occurrence, distribution, and fate of agricultural chemicals in the Mississippi River Basin. This volume also contains results on development and reconnaissance testing of new methods to detect emerging contaminants in environmental samples.

Volume 3 contains papers on subsurface contamination from point sources. The papers discuss research on: hydrocarbons and fuel oxygenates at gasoline release sites; ground-water contamination by crude oil; complex contaminant mixtures from treated wastewater discharges; waste disposal and subsurface transport of contaminants in arid environments; ground water and surface water affected by municipal landfill leachate; natural attenuation of chlorinated solvents; and characterizing flow and transport in fractured rock aquifers.

In all, the more than 175 papers contained in this proceedings reflect the contributions of more than 350 scientists who are co-authors. These scientists are from across the USGS, as well as from universities, other Federal and State agencies, and industry.

More information on the Toxic Substances Hydrology Program, including a searchable bibliography of publications and selected on-line publications, is available on the World Wide Web at: <http://toxics.usgs.gov/toxics/>

## ACKNOWLEDGMENTS

The editors acknowledge with great appreciation the assistance provided by Kim Crutchfield, Judy Salvo, Nana Snow, Judy Griffin, Patti Greene, and Ray Douglas. Their efforts in the planning, organization, and arrangements made for this seventh Technical Meeting of the Toxics Program made it both successful and enjoyable. Sincere thanks to Bill Ellis for assisting authors with preparation of papers for publication and for preparation and layout of this manuscript. Chet Zenone, Larry Slack, Anthony Buono, and John Flager assisted through review and improvement of the papers in this proceedings. Thanks are extended to the South Carolina District for their warm hospitality. Thanks also to the many scientists whose contributions and accomplishments are reflected in this proceedings; their continued efforts ensure continued success for the USGS Toxic Substances Hydrology Program.

## Ground Water Contamination By Crude Oil

Ground water contamination by crude oil, and other petroleum-based liquids, is a widespread problem. An average of 83 crude-oil spills occurred per year during 1994-96 in the United States, each spilling an average of about 50,000 barrels of crude oil (U.S. Office of Pipeline Safety, electronic commun., 1997). An understanding of the fate of organic contaminants (such as oil and gasoline) in the subsurface is needed to design innovative and cost-effective remedial solutions at contaminated sites.

A long-term, interdisciplinary research project by the U.S. Geological Survey (USGS) Toxic Substances Hydrology Program began in 1983 at a crude-oil spill site near Bemidji, Minnesota. The project involves research by scientists from the USGS and several academic institutions. Research at the site is directed toward understanding physical, chemical, and biological processes controlling the migration and fate of hydrocarbon contaminants in the subsurface. The goal is to provide information and methods to help evaluate the potential for, and long-term performance of, natural and enhanced bioremediation of hydrocarbons.

The crude-oil spill site near Bemidji is one of the better characterized sites of its kind in the world. Results of research conducted on processes affecting the migration and fate of crude oil at the site have provided fundamental knowledge that has been used to remediate similar sites worldwide. The Bemidji research project was first to document that the extent of crude-oil contamination can be limited by natural attenuation. Scientists studying natural attenuation at other contaminated sites have used many of the methods and approaches developed at the site.

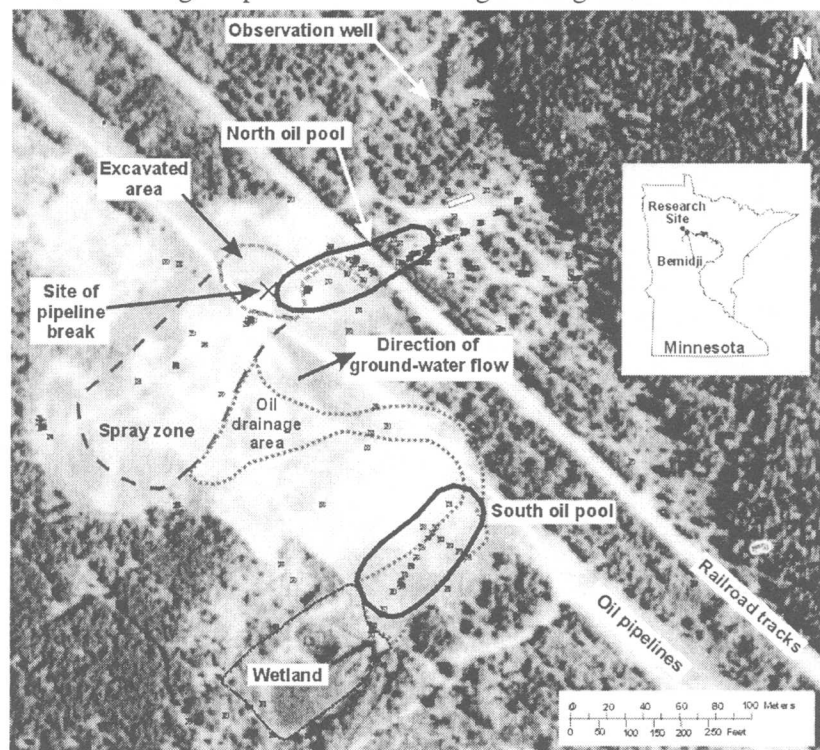


Figure 1. Features of the Bemidji, Minnesota crude-oil spill research site superimposed on a 1991 aerial photograph.

### DESCRIPTION AND HISTORY OF THE BEMIDJI SITE

On August 20, 1979, approximately 16 kilometers northwest of Bemidji, Minnesota, the land surface and shallow subsurface were contaminated when a crude-oil pipeline burst. About 1,700,000 L (liters) (about 10,700 barrels) of crude oil spilled onto a glacial outwash deposit. Crude oil also sprayed to the southwest covering an approximately 7,500-m<sup>2</sup> (square meters) area of land (spray zone, figure 1). After cleanup efforts were completed, about 400,000 L (about 2,500 barrels) of crude oil remained in the ground. Some crude oil percolated through the unsaturated zone to the water table near the rupture site (North oil pool). Some of the sprayed oil flowed over the surface toward a small wetland forming a second area of significant oil infiltration (South oil pool).

Ground water affected by the oil spill discharges to a small lake 400-m east of the pipeline. The land surface is a glacial outwash plain underlain by stratified glacial outwash deposits. At a depth of about 25 m, a regionally persistent and uniform layer of low permeability sediment restricts vertical ground-water movement. The water table ranges from near land surface to about 11 m below the land surface. About 370 wells and test holes had been installed at the Bemidji research site as of 1998.

## ONGOING AND FUTURE RESEARCH

The fate of hydrocarbons depends on the processes of transport, multiphase flow, volatilization, dissolution, geochemical reactions, biodegradation, and sorption (figure 2). An interdisciplinary investigation of these processes is critical for successful evaluation of the potential for migration of hydrocarbons in the subsurface. The investigation at the Bemidji site has involved the collection and analysis of crude oil, water, soil, vapor, and sediment samples. The oil phase that occurs as floating product on the water table and as residuum on sediment grains provides a continuing source of hydrocarbons to the ground water and vapor plumes. Studies have also been conducted to document the concentrations of gases in the unsaturated zone.

Numerical models are useful for integrating information collected in the field and have been used at the site for studying the importance of the simultaneously occurring processes. Multiphase flow modeling was used to study the oil movement after the spill. Transport and biodegradation modeling was used to simulate the evolution of the plume, to evaluate factors limiting biodegradation, and to develop a mass balance for contaminants at the site and thus evaluate the amount and rate of removal of hydrocarbons by biodegradation.

Although initial remediation of the research site was completed more than 15 years ago, a State regulatory agency has required the pipeline company to remove more of the remaining oil. While this renewed remediation may result in termination of ongoing research documenting natural attenuation, it has also provided an opportunity to work with industry in documenting the effects of the renewed remediation. One goal of ongoing research is to add to the published literature a thorough documentation of the remediation of this site; very few remediation efforts at crude-oil contamination sites are documented in the literature.

For additional information contact:

Geoffrey N. Delin, USGS, Mounds View,  
Minnesota, (email: delin@usgs.gov), or

William N. Herkelrath, USGS, Menlo Park,  
California, (email: wnherkel@usgs.gov)

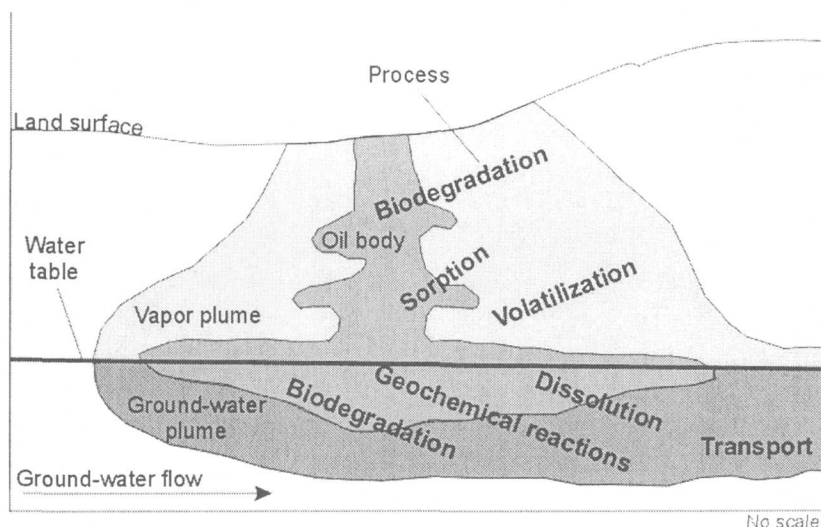


**Figure 2.** Processes critical to understanding the fate and transport of hydrocarbons in the subsurface at the Bemidji site.

# Long-Term Geochemical Evolution of a Crude-Oil Plume at Bemidji, Minnesota

By Isabelle M. Cozzarelli, Mary Jo Baedecker, Robert P. Eganhouse, Mary Ellen Tuccillo, Barbara A. Bekins, George R. Aiken, and Jeanne B. Jaeschke

## ABSTRACT

The long-term study of the development of the contaminant plume at the Bemidji site has provided an excellent opportunity to determine how natural attenuation of hydrocarbons is affected by evolving redox conditions in the aquifer. During the 16 years that data have been collected the shape and extent of the contaminant plume have changed as redox reactions, most notably iron reduction, have progressed over time. The downgradient extent of the  $\text{Fe}^{2+}$  and BTEX plume did not change between 1992 and 1995, indicating that, at the plume scale, the supply of these compounds from the upgradient contaminated water is balanced by the attenuation processes. However, depletion of the unstable Fe (III) oxides near the subsurface crude-oil source has caused the maximum dissolved iron concentration zone within the plume to spread at a rate of approximately 3 m/year. The zone of maximum benzene, toluene, ethylbenzene, and xylene (BTEX) concentrations has also spread within the anoxic plume. Analysis of sediment and water, collected at closely spaced vertical intervals, from cores in the contaminant plume provide further insight into the evolution of redox zones at a smaller scale. Contaminants that appeared not to be moving downgradient from the oil based on observation well data, such as ortho-xylene, are migrating in thin layers as the aquifer evolves to methanogenic conditions.

## INTRODUCTION

Concern over the contamination of ground-water resources combined with the realization that engineered clean up of contaminated sites is limited by technological and monetary constraints has led to an interest in remediation by natural attenuation (National Research Council, 1994). The processes that control the attenuation of organic compounds in contaminated aquifers are complex. The prevalence of hydrocarbon-contaminated sites and the high degree of toxicity and aqueous mobility of hydrocarbons has resulted in numerous investigations into the fate of hydrocarbons in the subsurface. It is well known that aromatic hydrocarbons can be degraded under both aerobic and anaerobic conditions, but the rates of degradation can vary significantly under different electron accepting conditions (e.g. Krumholz and others, 1996). It has been demonstrated that closely spaced sampling is required to identify microbiological processes in contaminated aquifers (e.g., Smith and others, 1991). Characterization of the small-

scale spatial variability of biogeochemical processes provides insight into how naturally occurring microbes degrade hydrocarbons in contaminated aquifers and may improve estimates of hydrocarbon degradation rates.

A number of electron acceptors in subsurface environments can be utilized by bacteria to mediate the oxidation of hydrocarbons. In the absence of oxygen, the oxidized forms of inorganic species are used by microorganisms as electron acceptors. In most sand and gravel aquifers, Fe (III) oxides are abundant, yet the spatial distribution of sedimentary iron may be heterogeneous at scales ranging from the entire formation, which may be tens of meters thick, to individual depositional layers that may be only a few centimeters (cm) thick (e.g. Knapp, 1997). The heterogeneity of iron oxides demonstrates the non-uniform availability of solid-phase electron acceptors in sedimentary aquifers. As degradation reactions progress in a contaminated aquifer, the distribution of solid iron phases can change over time and space, altering the

biogeochemical processes that affect the fate and transport of hydrocarbons.

Previous results (Baedecker and others, 1993; 1996) indicated that between 1984 and 1992, a ground-water contamination plume developed near the oil body and evolved from aerobic to manganese reducing to iron reducing and finally methanogenic conditions. The long-term study of the development of the contaminant plume at the Bemidji site has provided an excellent opportunity to look at how natural attenuation of hydrocarbons is affected by the evolving redox conditions in the aquifer. This paper describes the continued evolution of the contaminant plume over time and examines changes in aquifer geochemistry and the potential for hydrocarbon transport that occur at a small spatial scale. Detailed sampling of ground water and aquifer solids, on a centimeter scale, has allowed a more precise determination of the important oxidation-reduction reactions involved in the degradation of hydrocarbons at this site than would have been possible with ground-water sampling at a larger spatial scale.

## SITE DESCRIPTION

The field site is near Bemidji, Minnesota, in the Bagley outwash plain in north central Minnesota. Location maps are given in Bekins and others (1999). In 1979, a high-pressure oil pipeline burst, spraying oil over the land surface. Crude oil percolated through the unsaturated zone to the water table, creating two main subsurface oil bodies. One oil body, termed the "north pool", where a layer of oil approximately 1 meter (m) thick remains floating on the water table, has been an area of extensive research since 1984. The contaminated surficial aquifer is approximately 20 m thick, with the water table located 6-10 m below land surface. The aquifer sediment is glacially deposited, moderately calcareous, silty sand with local lenses of silty material and lenses of coarser sand and pebbles. The mineralogy of the sediments is roughly 50% quartz, 30% feldspar, 5-6% calcite and dolomite, and about 5% heavy minerals (Bennett and others, 1993).

## STUDY METHODS

### Field Procedures

Ground-water samples were collected from water-table wells and deeper wells along a transect in the direction of ground-water flow (fig. 1). Ground-water samples for analysis of unstable constituents (e.g. dissolved oxygen (DO)) were collected with a submersible pump, and ground-water samples for analysis of organic compounds were collected with a Teflon bailer by the methods of Baedecker and others (1993) and Eganhouse and others (1993). Cores were collected by drilling with a hollow-stem auger to the top of the desired coring interval, followed by driving of the core barrel beneath the augers to the desired depth.

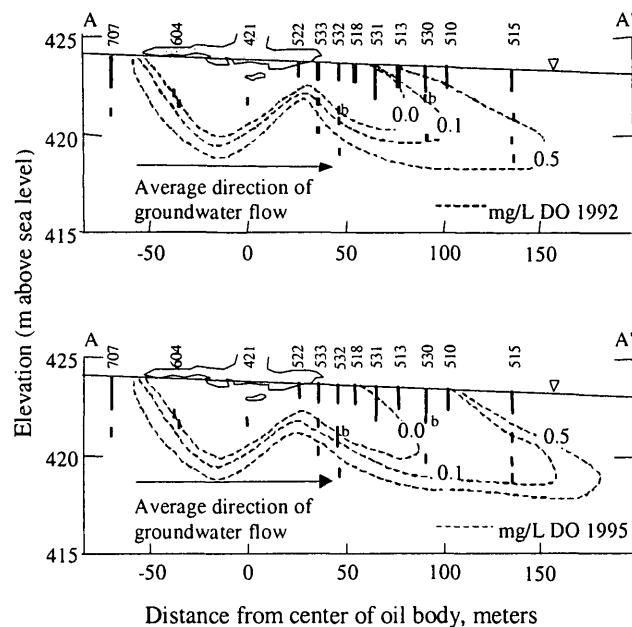


**Figure 1.** Dissolved oxygen (DO) contours in ground water downgradient from the crude oil source in 1992 and 1995. The location of the water table and observation wells are shown.

The coring method uses a piston that creates suction on saturated sediment within the core barrel as the barrel is driven into the sediment (Murphy and Herkelrath, 1996). The bottom of the core is frozen *in situ* to prevent loss of fluids out the core bottom. The 47-millimeter (mm) diameter cores were collected in clear



polycarbonate liners. The cores were removed from the core barrel and immediately sealed with plugs at the top and bottom after retrieval. The top plug was connected to N<sub>2</sub> gas, which was at a pressure of less than 30 kPa during sampling of the core.

Water from the cores was immediately collected at 15-cm intervals beginning at the top of the core. The core was drained at each interval by drilling a 4-mm-diameter hole in the polycarbonate liner and then inserting a luer-tip syringe snugly into the hole. Approximately 10 to 15 milliliters (mL) of pore water were collected at each interval. Glass syringes were used for the hydrocarbon sample; polycarbonate syringes were used for all other samples.

Concentrations of DO were measured in the field using a modified Winkler titration (Baedecker and Cozzarelli, 1992) and field-test kits available from CHEMetrics (Calverton, Virginia). Samples for monoaromatic hydrocarbon and methane (CH<sub>4</sub>) analyses were collected from wells and cores without filtration. Water samples collected for measurement of CH<sub>4</sub> concentrations were collected in glass syringes and transferred from the syringe into 25-mL serum bottles containing enough mercuric chloride (HgCl<sub>2</sub>) to produce a Hg concentration of 0.2 millimolar (mM). Ground water for determination of volatile hydrocarbons was transferred from the syringe into 1.8-mL glass vials containing HgCl<sub>2</sub>. Samples collected for cations, including total iron, and ferrous iron (Fe<sup>2+</sup>) were filtered through 0.2-micrometer (μm) filters. Samples collected for Fe<sup>2+</sup> analysis were fixed with reagents in the field and cation samples were preserved with nitric acid. Samples for volatile dissolved organic carbon (VDOC) were filtered through 0.4 μm Nuclepore filters and preserved with mercuric chloride (HgCl<sub>2</sub>). Samples for determination of δ<sup>13</sup>C of inorganic carbon were filtered through 0.4 μm Nuclepore filters and the carbon was precipitated as strontium carbonate in the field.

The drained cores were sectioned and subsamples of the sediments were transferred to airtight containers under a CO<sub>2</sub>-N<sub>2</sub> atmosphere. Sediment samples were stored frozen until they could be extracted for iron content (see sediment extraction procedure below).

## Analytical Procedures

### Water Chemistry

Concentrations of Fe<sup>2+</sup> were determined colorimetrically by a modified bipyridine method as described in Baedecker and Cozzarelli (1992). Cation samples were analyzed with an ARL Spectraspan V Direct Current Plasma spectrometer. Carbon isotopes were analyzed using an isotope-ratio mass spectrometer (Baedecker and others, 1993). Dissolved CH<sub>4</sub> concentrations were measured by headspace analysis and gas chromatography (Baedecker and Cozzarelli, 1992). Concentrations of volatile monoaromatic hydrocarbons were measured by purge-and-trap capillary gas chromatography using a DB-5 bonded-phase fused-silica capillary column, as described by Eganhouse and others (1999).

### Sediment Extractions

Sediment extractions were performed as described in Tuccillo and others (1999). To perform the extractions, 0.6 grams (g) to 1.5 g of sediment were placed in 30-mL serum bottles. Anoxic sediment samples were transferred to the bottles while the headspace of the sediment storage vial was flushed with N<sub>2</sub>. After adding samples to bottles, 30 mL of 0.5 molar (M) HCl was added, and the bottles were crimped, capped, covered with foil, and placed on a shaker table for 3 days. After removal from the shaker table, the liquid was then filtered through a 0.2 μm filter and analyzed for Fe(II) and Fe(total) using Ferrozine (Gibbs, 1979). The concentrations of Fe(III) were determined by difference.

## RESULTS AND DISCUSSION

### 2-D Plume-Scale Changes in Aquifer Chemistry

The distribution of DO in ground water along a transect downgradient from the oil body indicates that the anoxic plume extended

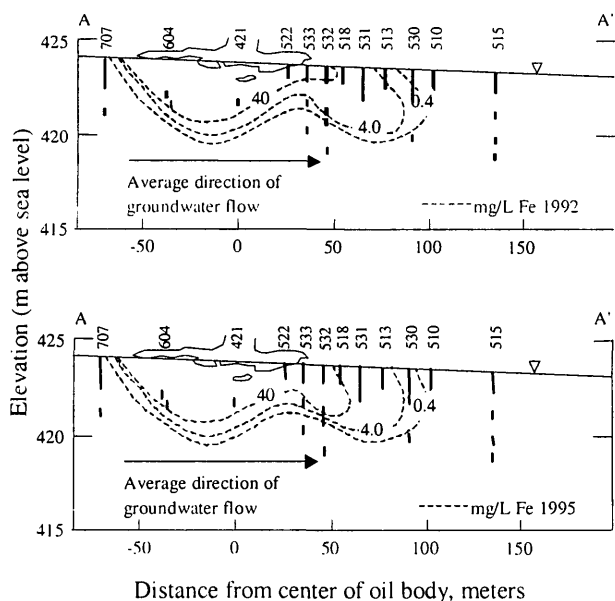


**Figure 2.** Dissolved iron (Fe) contours in ground water downgradient from the crude oil source in 1992, and 1995. The locations of the water table and observation wells are shown.

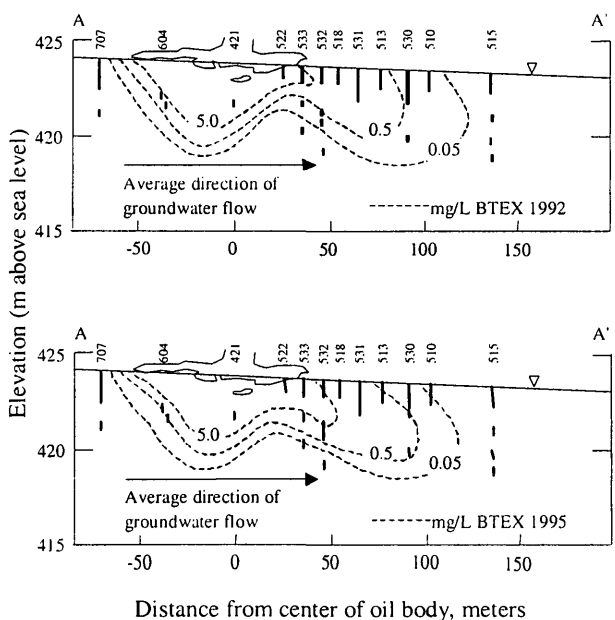


**Figure 3.** BTEX contours in ground water downgradient from the crude oil source in 1992, and 1995. The locations of the water table and observation wells are shown.

approximately 80 m downgradient from the crude oil in 1992 (fig. 1). The zone containing anoxic ground water and high  $\text{Fe}^{2+}$  and BTEX concentrations continues to spread (fig. 1-3), consistent with previous results for earlier years (Baedecker and others, 1993, 1996, Baedecker and Cozzarelli, 1994). Changes in chemistry

observed at the plume scale are defined in this paper as those changes that can be determined on the basis of data from the observation well network. Although the shape of the anoxic plume has remained the same, the zero D.O. contour line (D.O. below detection) is now several meters further downgradient (fig. 1). Within the anoxic plume, the zone with high dissolved-iron concentrations increased in vertical extent over time and the maximum benzene, toluene, ethylbenzene, and xylene (BTEX) concentrations have also spread in this zone. The rate of movement of the high dissolved  $\text{Fe}^{2+}$  plume (defined by the 40 milligrams (mg)/L contour, fig. 2) was approximately 3 m/year. The downgradient extent of the  $\text{Fe}^{2+}$  and BTEX (fig. 3) plumes, however, has not noticeably changed, indicating that the supply of these compounds from the upgradient contaminated water is balanced by the processes that impede the movement of these compounds. It has been well established that microorganisms degrade BTEX compounds in this aquifer (Baedecker and others, 1993, Cozzarelli and others, 1994, Lovley and others, 1989). The rate of degradation has been such that, in 11 years of study, the plume-scale movement of BTEX compounds has been much slower than would have been predicted by conservative transport. The downgradient edge of the BTEX plume moved about 8 meters per year from 1987 to 1992 (Baedecker and Cozzarelli, 1994) and appears to have moved even more slowly from 1992 to 1995 (fig. 3).

The balance between microbial iron reduction and precipitation and/or oxidation of  $\text{Fe}^{2+}$  controls the movement of the dissolved iron plume (fig. 2). Depth profiles of the Fe (III) concentrations (determined from the 0.5M HCl extraction) from several cores (fig. 4) show that Fe (III) is depleted, relative to background, in the anoxic zone and underneath the oil due to microbial reduction of iron coupled to degradation of the hydrocarbons (fig. 5). The dashed line in each panel represents the mean concentration of Fe (III) for that core. At the edge of the anoxic zone reduced iron that has been transported downgradient is oxidized. In this oxic/anoxic transition zone sediment Fe (III) accumulates and concentrations reach high levels (significantly greater than background) as the

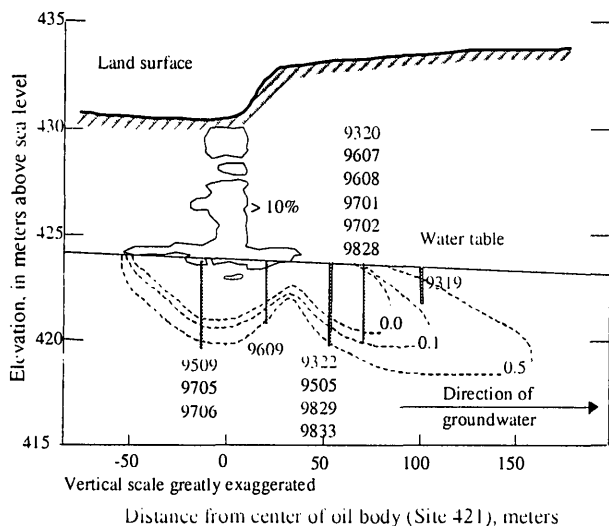


**Figure 4.** Location of cores collected underneath and downgradient from the crude oil source from 1993 through 1998. The locations of the DO contours in 1992 and the oil saturation values greater than 10 percent are shown.

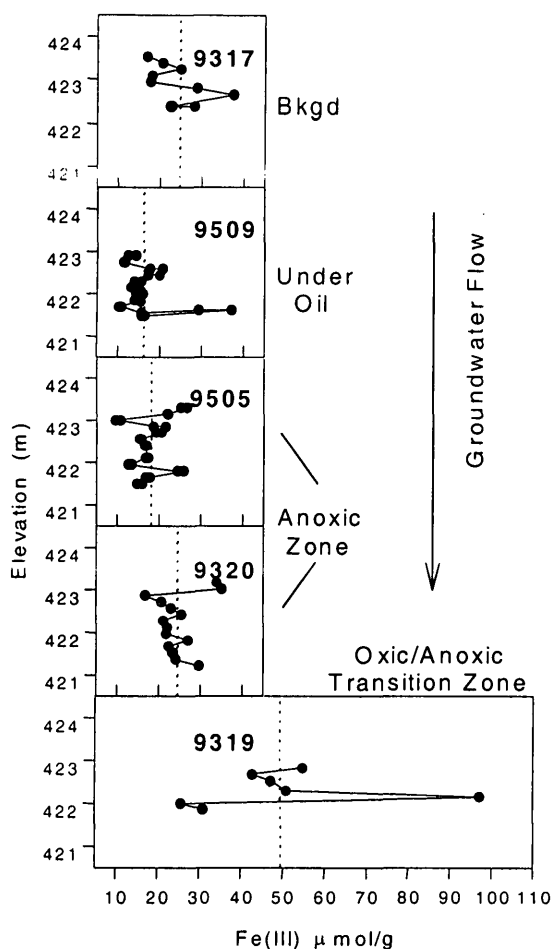


**Figure 5.** The concentration of Fe(III) in cores (located in fig. 4) collected downgradient from the oil body. The dashed lines represent the mean concentration of Fe (III) for that core.

aqueous  $Fe^{2+}$  oxidizes and precipitates. Plots of the Fe (II) concentrations (fig. 6) from the same cores show Fe (II) is very low in background sediments and highest underneath the oil where  $Fe^{2+}$  in the water precipitates as iron carbonates or in iron-rich clays (Tuccillo and others, 1999).

### Temporal Changes in Vertical Profiles

Analyses of water chemistry from cores collected from the center of the anoxic plume (fig. 7), and from the edge of the anoxic plume (fig. 8), indicate that significant changes are occurring at particular locations within the plume that are more difficult to see when chemistry is examined at the larger plume scale. The concentrations of  $Fe^{2+}$ ,  $CH_4$ , and BTEX indicate that the plume is increasing in vertical thickness over time. In the center of the anoxic plume,

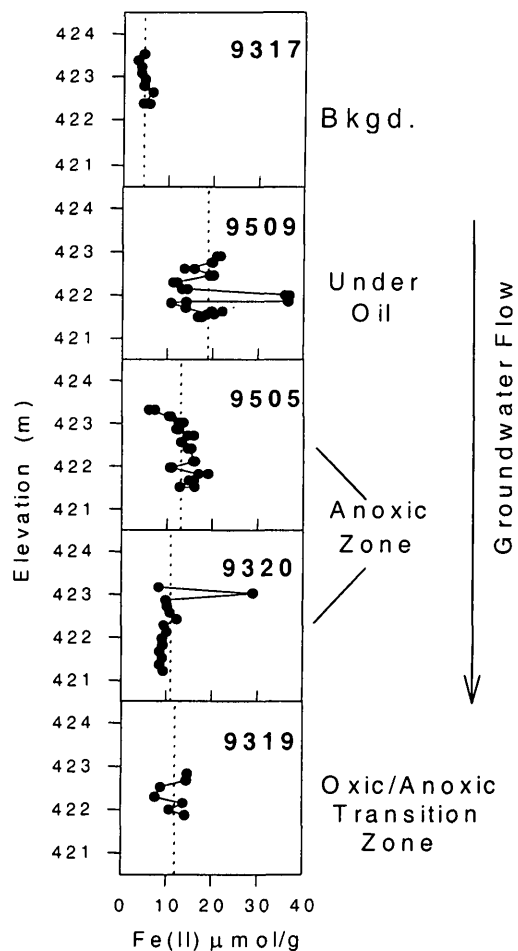


**Figure 6.** The concentration of Fe(II) in cores (located in fig. 4) collected downgradient from the oil body. The dashed lines represent the mean concentration of Fe (II) for that core.

although the maximum concentrations of methane and iron are approximately the same, the depths over which these high concentrations are observed have increased (fig. 7). A similar pattern was seen in the core profiles collected at the edge of the anoxic zone (fig. 8). The continued spreading of the dissolved methane and iron plumes indicate that iron reduction and methanogenesis continue to be important processes in the aquifer close to the oil body.

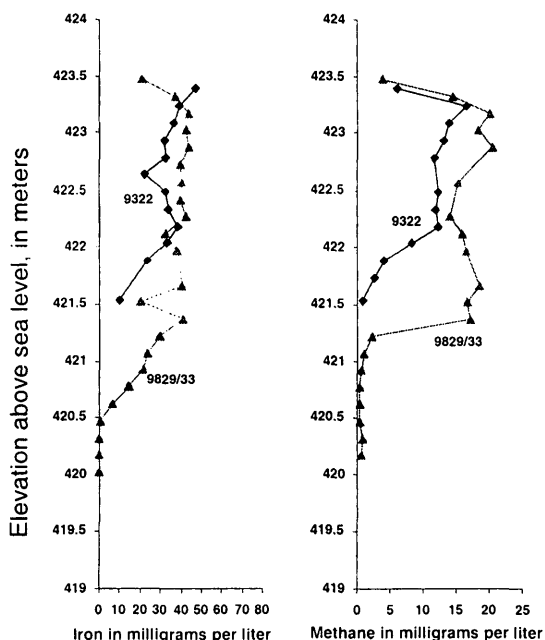


**Figure 7.** Concentrations of dissolved iron and methane in ground water in the center of the anoxic plume in 1993 and 1998. Core locations are shown on figure 4.

Prolonged iron reduction in the plume has caused measurable temporal changes in the sediment iron chemistry near the edge of the anoxic plume (fig. 8). Sediment extractions indicate that Fe (III) is being depleted from the sediment, while Fe (II) is being deposited. Scanning electron microscopy showed that some of the reduced iron is being stored in the plume sediments as Fe (II)-bearing minerals (e.g. ferroan calcite, Baedeker and others, 1993, Tuccillo and others, 1999). Additional pyrophosphate extractions by Tuccillo and others (1999) indicated that a portion of the Fe(II) may be present as organically bound iron. Reoxidation and precipitation of iron is taking place near the water table, as the anoxic plume

mixes with oxygenated recharge water, resulting in consistently higher concentrations of Fe (III) near the top of the core profiles (fig. 8).

The availability of reducible Fe (III) in the sediments is important for the continued biodegradation in the contaminant plume. Sediment Fe (III) is clearly being removed from the anoxic plume sediments (fig. 8), yet there is no evidence that Fe (III) has been depleted to the point of limiting iron reduction. There is evidence of methanogenesis near the oil body despite the presence of Fe (III) concentrations of 15-20  $\mu$ moles per gram under the oil. Bekins and others (1999) found that areas of high contaminant flux near the oil body contained the greatest numbers of culturable methanogens. Methanogenesis occurs concurrent with iron reduction in thin layers of sediment (on the order of 25 cm) beneath the oil body, indicating that the redox zones evolve on a small spatial scale. Further downgradient, within the anoxic plume, this evolution is likely slower since a greater amount of readily reducible Fe (III) is still available for iron reduction.

## Potential for Transport of Hydrocarbons

The evolution of the redox zones in the contaminant plume can have a significant effect on the fate and transport of hydrocarbons in ground water. Analysis of the hydrocarbon concentrations over time in two wells located within the plume (532b and 530b, locations on fig. 1) indicate that the concentrations of hydrocarbons vary in space and over time (fig. 9). The transport of different hydrocarbons is dependent to a large extent on the differences in degradability of these compounds (Eganhouse and others, 1993). Although the hydrocarbons appear to be attenuated at the plume scale, specific hydrocarbons appear to persist in local zones. At the location closer to the oil, 532b (fig. 9), hydrocarbon concentrations have gradually increased over time. Concentrations of all the hydrocarbons are higher after 10 years than they were in 1986 (by a factor ranging from 1.4 for ethylbenzene to 11.6 for benzene), indicating that

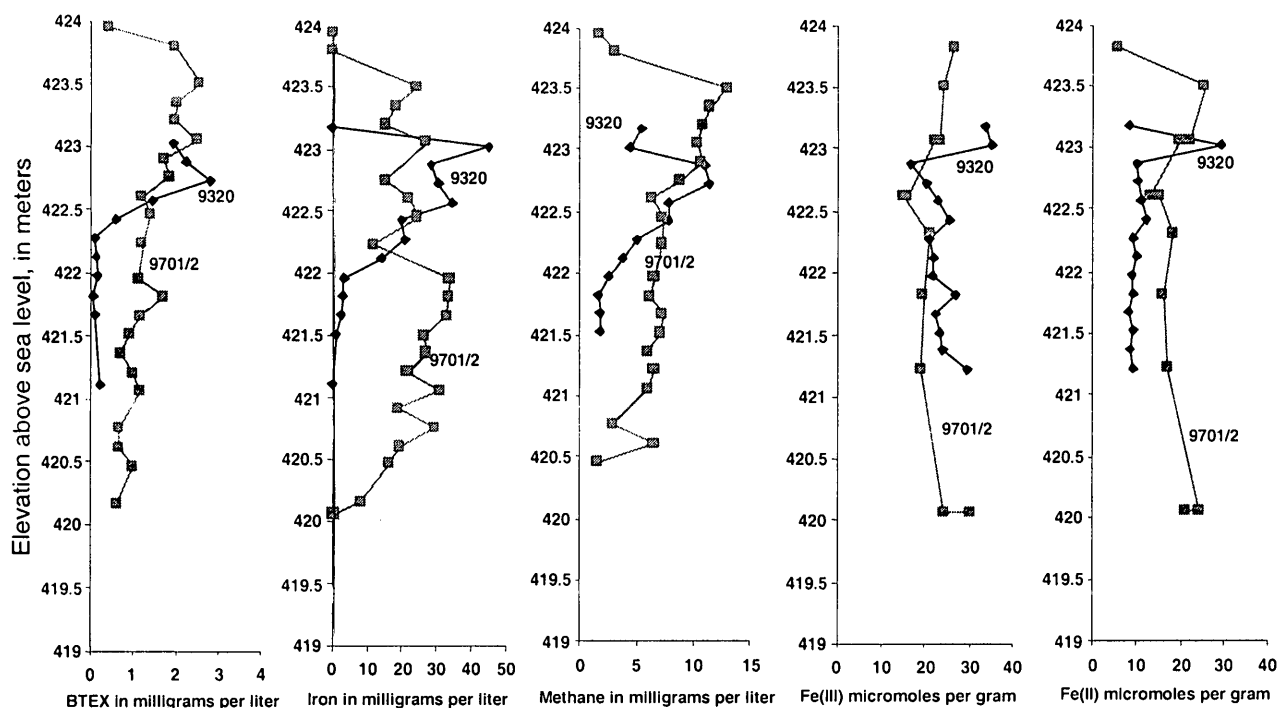


**Figure 8.** Concentrations of dissolved BTEX, iron and methane in ground water and Fe(III) and Fe(II) in aquifer solids at the edge of the anoxic plume in 1993 and 1997. Core locations are shown on figure 4.

the crude oil continues to provide a source for these compounds at a rate slightly above the rate at which they are attenuated. Less persistent compounds show greater temporal fluctuations in removal rates than more stable species. For example, the concentrations of *ortho*-xylene show the highest degree of variability. Benzene and ethylbenzene have consistently been shown to be stable in the anoxic plume, while toluene and *ortho*-xylene are consistently unstable (Eganhouse and others, 1996).

In ground water farther downgradient (well 530b), concentrations of most hydrocarbons are still increasing 16 years after the crude-oil spill (fig. 9). The more stable compounds increase in concentration earlier than the least stable compounds. The different hydrocarbons show markedly different transport rates in this part of the aquifer. The more stable compounds, such as ethylbenzene, appear to be approaching concentration levels similar to those found in the upgradient well. The concentrations of the least stable compound, *ortho*-xylene, are below detection 16 years after the original spill. Attenuation processes, most likely microbial

degradation, remove this contaminant from the ground water within a short distance from the source. It has been well documented that microorganisms in anaerobic aquifers can degrade *ortho*-xylene.

Examination of the data from the closely-spaced sampling of water from the cores indicates that there is potential for *ortho*-xylene transport despite the relatively stable patterns observed in the data from the ground-water wells. The cores (locations on fig. 4) at the edge of the anoxic plume, approximately 70 m from the center of the oil body (fig. 10), were collected just upgradient from well 530b. Analyses of the hydrocarbon concentrations in this profile (fig. 10) show that *ortho*-xylene moved into this part of the aquifer between 1993 and 1997. The very thin *ortho*-xylene plume corresponds to the zone of maximum concentrations of methane and iron (fig. 8). This thin zone has been identified as a methanogenic zone by Bekins and others (1999) on the basis of geochemical evidence combined with the evolution of microbial populations of different physiological types. The long-term potential for *ortho*-xylene transport, and perhaps

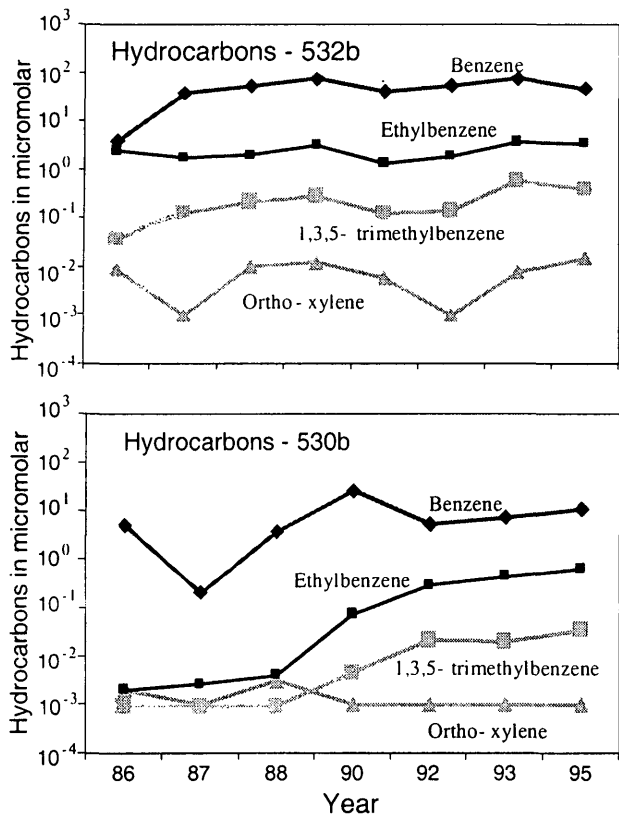


**Figure 9.** Concentrations of benzene, ethylbenzene, 1,3,5 trimethylbenzene and *ortho*-xylene in ground water from two wells between 1986 and 1996. Wells located on figure 1.

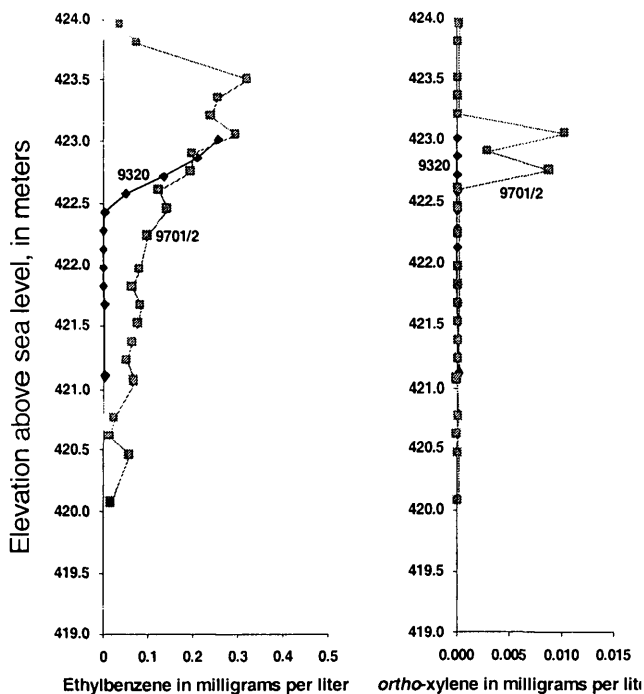


**Figure 10.** Concentrations of ethylbenzene and *ortho*-xylene in ground water at the edge of the anoxic plume in 1993 and 1997. Core locations are shown in figure 4.

transport of other hydrocarbons that show similar potential for degradation, is tied to the evolution of the redox zones in the plume. It is apparent that this evolution occurs at a small scale (on the order of tens of centimeters) in the contaminated aquifer.

## CONCLUSIONS

This study shows the importance of long-term monitoring and examination of processes at a small spatial scale when assessing the natural attenuation of hydrocarbons in a contaminated aquifer. Examination of the patterns in the hydrocarbon well data for the crude-oil contaminated aquifer at Bemidji, Minnesota show that there were periods of several years, for example 1988 through 1992, during which hydrocarbon concentrations in the heart of the contaminant plume showed decreases for many compounds. If these were the only data available, one might have concluded that hydrocarbons near the source were being depleted and the long-term potential for hydrocarbon transport would have been underestimated. Temporal data collected at closely spaced vertical intervals, however, indicate that hydrocarbon concentrations (e.g. ethylbenzene) have spread out, consistent with a vertical thickening of the plume. It is apparent that the availability of an electron acceptor such as Fe (III) oxides in this system has a significant impact on the transport of hydrocarbons downgradient and away from the crude-oil source. Examination of changes in the distribution of this electron acceptor at the plume scale and at the core scale provides insight into the progression of biogeochemical zones. This type of information is needed in order to predict the long-term impact of hydrocarbon spills on aquifer chemistry and to assess the potential for hydrocarbon transport through the aquifer.

## REFERENCES

- Baedecker, M.J., and Cozzarelli, I.M., 1992, The determination and fate of unstable constituents in contaminated groundwater in Lesage, S., and Jackson, R.E., eds, Groundwater Quality and Analysis at

- Hazardous Waste Sites, Marcel Dekker, p. 425-461.
- Baedecker, M.J., and Cozzarelli, I.M., 1994, Biogeochemical processes and migration of aqueous constituents in ground water contaminated with crude oil. in Dutton, A.R., ed, Toxic Substances and the Hydrologic Sciences, American Institute of Hydrology, p. 69-79.
- Baedecker, M.J., Cozzarelli, I.M., Eganhouse, R.P., Siegel, D.I., and Bennett, P.C., 1993, Crude oil in a shallow sand and gravel aquifer-III. Biogeochemical reactions and mass balance modeling in anoxic groundwater: *Applied Geochemistry*, v. 8, p. 569-586.
- Baedecker, M.J., Cozzarelli, I.M., Bennett, P.C., Eganhouse, R.P., and Hult, M.F., 1996, Evolution of the contaminant plume in an aquifer contaminated with crude oil, Bemidji, Minnesota, in Morganwalp, D.W., and Aronson, D.A., eds, U.S. Geological Survey Toxic Substances Hydrology Program—Proceedings of the technical meeting, Colorado Springs, Colorado, September 20-24, 1993: U.S. Geological Survey Water-Resources Investigations Report 94-4015, p. 613-620.
- Bekins, B.A., Cozzarelli, I.M., Godsy, E.M., Warren, Ean, Tuccillo, M.E., Essaid, H.I., and Paganelli, V.V., 1999, Chemical and physical controls on microbial populations in the Bemidji Toxics Site crude-oil plume, Morganwalp, D.W., and Buxton, H.T., eds, U.S. Geological Survey Toxic Substances Hydrology Program—Proceedings of the Technical Meeting, Charleston, South Carolina, March 8-12, 1999-- Volume 3 -- Subsurface Contamination from Point Sources: U.S. Geological Survey Water-Resources Investigations Report 99-4018C.
- Bennett, P.C., Siegel, D.E., Baedecker, M.J., and Hult, M.F., 1993, Crude oil in a shallow sand and gravel aquifer - I. Hydrogeology and inorganic geochemistry: *Applied Geochemistry*, v. 8, p. 529-549.
- Cozzarelli, I.M., Baedecker, M.J., Eganhouse, R.P., and Goerlitz, D.F., 1994, The geochemical evolution of low-molecular-weight organic acids derived from the degradation of petroleum contaminants in groundwater: *Geochimica et Cosmochimica Acta*, v. 58, p. 863-877.
- Eganhouse, R.P., Baedecker, M.J., Cozzarelli, I.M., Aiken, G.R., Thorn, K.A., and Dorsey, T.F., 1993, crude oil in a shallow sand and gravel aquifer - II. Organic geochemistry: *Applied Geochemistry*, v. 8, p. 551-567.
- Eganhouse, R.P., Dorsey, T.F., Phinney, C.S., and Westcott, A.M., 1996, Processes affecting the fate of monoaromatic hydrocarbons in an aquifer contaminated by crude oil: *Environmental Science and Technology*, v. 30, p. 3304-3312.
- Eganhouse, R.P., Matthews, L.L., Cozzarelli, I.M., and Scholl, M.A., 1999, Evidence for natural attenuation of volatile organic compounds in the leachate plume of the Norman, Oklahoma landfill, Morganwalp, D.W., and Buxton, H.T., eds, U.S. Geological Survey Toxic Substances Hydrology Program—Proceedings of the Technical Meeting, Charleston, South Carolina, March 8-12, 1999-- Volume 3 -- Subsurface Contamination from Point Sources: U.S. Geological Survey Water-Resources Investigations Report 99-4018C.
- Gibbs, M.M., 1979, A simple method for the rapid determination of iron in natural waters: *Water Resources Research*, v. 13, p. 295-297.
- Knapp, E. P, 1997, The influence of redox conditions on sorption to aquifer sediments: Transport of reactive solutes in groundwater. Ph.D. thesis, University of Virginia, Charlottesville, Virginia, USA.
- Krumholz, L.R., Caldwell, M.E., and Suflita, J.M., 1996, Biodegradation of "BTEX" hydrocarbons under anaerobic conditions, Crawford, R.L., and Crawford, D.L., eds, *Bioremediation: Principles and Applications*, Cambridge University Press, p. 61-99.
- Murphy, F. and Herkelrath, W.N., 1996, A sample-freezing drive shoe for a wire line piston core sampler: *Ground Water Monitoring and Remediation*, v. 16, p. 86-90.
- NRC, 1994, *Alternatives for Ground Water Cleanup*: Washington, D. C., National Academy Press, p. 315.
- Lovley, D.R., Baedecker, M.J., Lonergan, D.J., Cozzarelli, I.M., Phillips, E.J.P., and Siegel,

D.I., 1989, Oxidation of aromatic compounds coupled to microbial iron reduction: *Nature*, v. 339, p. 297-299.

Smith, R. L., Harvey, R. W., and LeBlanc, D. R., 1991, Importance of closely spaced vertical sampling in delineating chemical and microbiological gradients in groundwater studies: *Journal of Contaminant Hydrology*, v. 7, p. 285-300.

Tuccillo, M.E., Cozzarelli, I.M., and Herman, J.S., 1999, *Applied Geochemistry*, v. 14, no. 5, p. 71-83.

## **AUTHOR INFORMATION**

Isabelle M. Cozzarelli (icozzare@usgs.gov),  
Mary Jo Baedecker, Robert P. Eganhouse, Jeanne  
B. Jaeschke U.S. Geological Survey, Reston,  
Virginia

Mary Ellen Tuccillo, Department of  
Environmental Sciences, University of Virginia,  
Charlottesville, Virginia

Barbara A. Bekins, U.S. Geological Survey,  
Menlo Park, California

George R. Aiken, U.S. Geological Survey,  
Boulder, Colorado



# Chemical and Physical Controls on Microbial Populations in the Bemidji Toxics Site Crude-Oil Plume

By Barbara A. Bekins, Isabelle M. Cozzarelli, E. Michael Godsy, Ean Warren, Mary Ellen Tuccillo, Hedef I. Essaid, and Victor V. Paganelli

## ABSTRACT

Processes controlling the establishment of aquifer microbial populations that degrade organic ground-water contaminants are poorly understood. We provide insight into this problem with a combined data set that includes microbial populations, grain size, pore-water chemistry, and sediment iron content. Data from three vertical profiles through the anaerobic portion of the Bemidji crude-oil plume show similar patterns in the microbial populations. Within each profile, numbers of iron-reducers vary from lows of  $10^2$ - $10^4$ /g sediment to highs of  $10^5$ - $10^6$ /g. Areas that are evolving from iron-reducing conditions to methanogenic conditions are indicated by lower numbers of iron-reducers and the presence of culturable methanogens ( $10^1$ - $10^2$ /g). These conditions are found in areas of high contaminant flux either in the vicinity of the non-aqueous oil or where higher concentrations in the contaminant plume are associated with local increases in aquifer permeability. In all locations where methanogens are found, lower numbers of culturable iron reducers are also present. Moreover, in these areas, significant extractable Fe(III) ( $>10 \mu\text{mol/g}$ ) is still present, suggesting that the remaining iron on the sediments may be less available for microbial reduction. The methanogenic zones are vertically narrow, ranging from 0.25-1 m thick, but they are laterally continuous extending from the source area to at least 60 m downgradient.

## INTRODUCTION

Although it is well known that aquifer microbes degrade dissolved hydrocarbons under both aerobic and anaerobic conditions (see Wiedemeier and others, 1995, for a review), the ecology of the microbial populations performing the degradation reactions is poorly understood. As electron acceptors are depleted, a succession of physiologic types occurs. The spatial distribution of the physiologic types is generally inferred from aqueous concentrations of redox indicators such as dissolved oxygen, Fe(II), and dissolved methane. Although, these chemical species indicate that a particular reaction is occurring, measured concentration distributions do not accurately demarcate the regions of the aquifer where the specific microbial processes are active. This is because the concentrations are affected not only by microbial activity but also by advective transport, dispersion, and

inorganic reactions. For example, methane can be transported downgradient from zones where methanogenesis occurs, complicating the use of methane concentrations for determining the exact location and extent of the methanogenic zone. Moreover, because the anaerobic cores of plumes can be extremely narrow in vertical extent (e.g., Smith and others, 1991; Cherry, 1996), pore-water samples from wells with long screens may be sampling ground water from two or more redox zones.

The goal of this work was to examine the processes that control microbial redox zones in a ground-water plume at a crude-oil spill. Characterizing distribution of microbial physiologic types together with pore-water chemistry, sediment iron content, and sediment permeability provides insight into the patterns of ecological succession at the plume scale. Using the most probable number (MPN) method, the microbial population distributions

were estimated for six physiologic types: aerobes, iron-reducers, heterotrophic fermenters, methanogens, sulfate-reducers and denitrifiers. We concentrated on the anaerobic portion of the plume because anaerobic processes probably account for the majority of the hydrocarbon degradation at this site (Essaid and others, 1995). Moreover, anaerobic processes are estimated to be important at 90% of sites contaminated by non-aqueous phase petroleum hydrocarbons (T. Wiedemeier, Parsons Engineering Science, Inc., oral. comm., 1998).

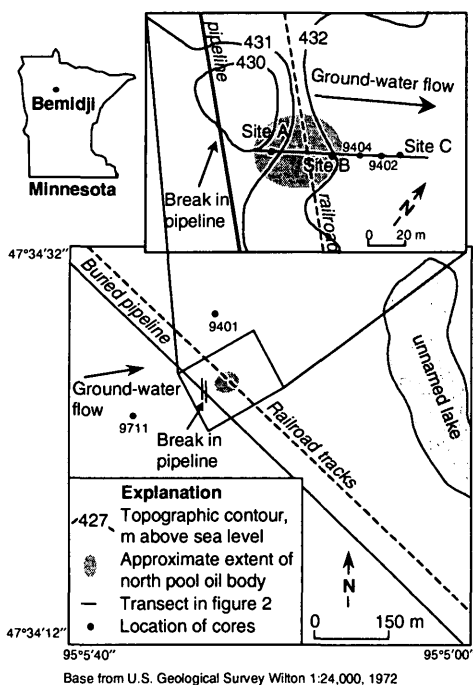


**Figure 1.** Site of 1979 crude oil spill near Bemidji, Minnesota, with locations of cores.

## SITE DESCRIPTION

The study aquifer, located near Bemidji, Minnesota, is a surficial formation of pitted and dissected glacial outwash sediments (fig. 1). It was contaminated with crude oil when a pipeline ruptured in August, 1979. After clean-up operations by the pipeline company, residual spilled oil infiltrated into the aquifer forming bodies of oil floating on the water table (Hult, 1984). The largest oil body (the "north pool") is

estimated to contain 147,000 liters of oil (Herkelrath, 1999).

A set of papers (Baedecker and others, 1993; Bennett and others, 1993; Eganhouse and others, 1993) described the geochemistry of the contaminant plume emanating from the north pool. Starting in 1984, concentrations of both reduced iron and methane began to increase in the anoxic zone immediately downgradient from the oil body. From 1986 to 1989, profiles of dissolved organic compounds indicated the plume reached a quasi steady-state in which dissolution from the non-aqueous oil was approximately balanced by biotransformation by iron-reduction (Lovley and others, 1989) and methanogenesis (Baedecker and others, 1993). Recent results on the continued chemical evolution of the plume are presented by Cozzarelli and others (1999).

## METHODS

Using the existing geochemical data, locations for three vertical profiles were chosen to characterize the microbial population in the anaerobic portion of the plume (A, B, and C in figure 1). In September of 1996, two cores with a horizontal separation of 1 m were collected from Site B with a freezing drive shoe (Murphy and Herkelrath, 1996). Each core was 2.3 m long, which was sufficient to span the entire vertical extent of the anaerobic plume at this location. One core was analyzed for the microbial population on the sediments, along with extractable iron [Fe(III) and Fe(II)], and grainsize. The second core was used for pore-water chemical analyses. Because the drill rig depth measurements were imprecise, data from the two cores were aligned vertically using the grainsize distributions.

In August of 1997, five additional cores were collected. Three cores were needed to span a vertical interval from the oil body to the base of the contaminant plume at Site A, and two cores were sufficient to obtain a vertical profile of the plume at Site C. In these cores, the pore water was drained for chemical analyses and the sediments were analyzed for microbial numbers, grain-size distributions and extractable iron. Five additional cores were collected in 1994-

**Table 1.** Log<sub>10</sub> of microbial numbers from seven locations marked in figure 2 plus two uncontaminated background locations (fig. 1). Abbreviations: Dist – Distance from center of oil body, meters; Elev – Elevation above mean sea level, meters; Fe-red – Iron-reducers; Aer – Aerobes; Ferm – Heterotrophic fermenters; Meth – Methanogens; and Bkgd – Background.

Sample	Dist	Elev	Fe-red	Aer	Ferm	Meth
9510-22s	19.8	421.5	<0.3	2.43	2.32	<0.3
9402-1s	55.3	423.0	4.00	4.00	<0.3	<0.3
9402-2s	55.3	422.1	4.46	3.32	1.53	2.32
9402-3s	55.3	421.3	4.03	3.03	1.70	<0.3
9404-1s	40.4	423.3	3.23	2.23	0.30	<0.3
9404-2s	40.4	422.5	4.38	2.90	2.15	0.90
9404-3s	40.4	421.7	2.70	1.85	<0.3	1.23
9711	Bkgd		1.15	2.85	<0.3	<0.3
9401	Bkgd		<0.3	1.76	1.98	<0.3

1997 and from these, nine samples were analyzed for sediment microbial numbers (figs. 1 and 2 and table 1).

For pore-water chemical analyses, water was drained from the core at 15 centimeter (cm) intervals. The pH was measured in the field and the water samples were preserved for laboratory analyses of hydrocarbons, dissolved organic carbon, methane, and major cations, according to the methods described by Cozzarelli and others (1999). Sediment samples were collected at 20-70 cm intervals and analyzed for populations of aerobes, iron-reducers, heterotrophic fermenters, methanogens, sulfate-reducers, and denitrifiers, using the MPN method. The methods of sediment sampling and MPN determination are described by Essaid and others (1995). The sediment grain-size analyses were performed using the method described by Hess and others (1992). The extractable iron method, described by Tuccillo and others (1999), was expected to extract the bioavailable Fe(III) as well as poorly crystalline Fe(II) from the sediments.

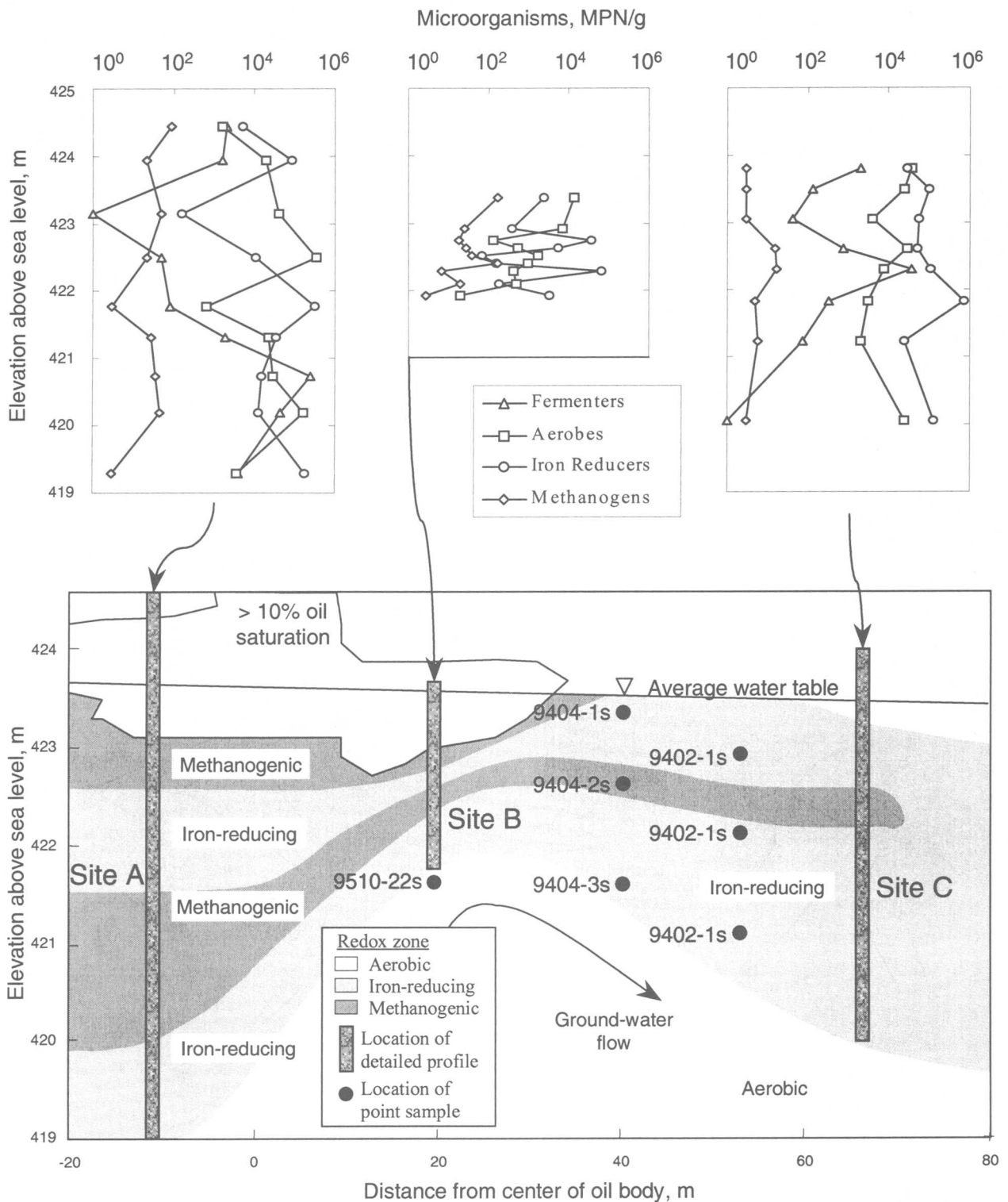
## RESULTS

Figure 2 shows the vertical profile MPN data for the four major physiologic types found in the aquifer: aerobes, iron-reducers, fermenters, and methanogens. Data for sulfate

reducers and denitrifiers are not presented here because these organisms were present in low numbers in the plume. This observation is consistent with the low concentrations of sulfate and nitrate in the uncontaminated ground water (Baedecker and others, 1993; Bennett and others, 1993). The populations of aerobes and iron-reducers vary by two to three orders of magnitude over short vertical distances of 10-20 cm. The peak populations of the methanogens are only 10<sup>2</sup>/gram (g) of sediment but these contrast sharply with nondetectable background numbers. These results are similar to those of Godsy and others (1992) who reported a 100-fold increase in methanogens in a plume of dissolved creosote compounds compared to an uncontaminated background location. Like the aerobes and iron-reducers, the methanogenic populations vary vertically on a scale of 10-20 cm.

In all three profiles it appears that peaks in iron-reducer numbers alternate with those of methanogens. A Pearson correlation analysis of the combined data set from the three profiles shows that there is an inverse correlation between iron-reducers and methanogens of -0.62 (p<0.0007; 24 samples). In the Site A profile, located below the oil, iron-reducers are dominant at three levels: 424.0 meters (m), 421.8 m, and 419.0 m above sea level. At these same levels, there are lower numbers of fermenters, methanogens, and aerobes. Conversely, locations with lower numbers of iron-reducers, found at levels 424.5 m and 420.0-421.5 m, correspond to higher numbers of fermenters, methanogens, and aerobes. The increase in culturable aerobes at the same horizons where methanogens are present suggests that these are facultative organisms that can survive either aerobically or anaerobically.

The profile from Site B, located in the upwelling area, shows small-scale oscillations between methanogenic and iron-reducing conditions. Two levels in the aquifer (422.7 m and 422.3 m) have peak iron-reducing numbers together with relatively low numbers of aerobes and methanogens. At two other levels, peak values of aerobes and methanogens are found together with lower numbers of iron-reducers.



**Figure 2.** Vertical MPN profiles and interpreted cross section showing the distribution of microbial physiologic types in the anaerobic portion of the Bemidji plume. The vertical profiles correspond to Site A, B, and C locations in figure 1. The interpreted cross-section is based on the vertical profile data combined with data for point samples from seven locations marked on the section.

One level is located within the oil body at 423.4 m and the other is at 422.6-422.3 m in the core of the plume. A third level exhibiting this pattern is possibly also present at 422.1 m. Thus, this profile has methanogenic zones alternating with iron-reducing zones on a scale of only 25 cm.

The profile from Site C, located downgradient from the oil body, shows signs of being less evolved toward methanogenic conditions. Peak aerobic numbers are found at the top and base of the profile where aerobic conditions exist at the edge of the plume. A third peak in aerobes also exists between 422-423 m above sea level, where methanogens and fermenters increase, and iron-reducers decline. The maximum number of methanogens found is almost 10 times lower than at the sites below the oil. Moreover, the number of culturable iron-reducers still present in the evolving methanogenic zone exceeds  $10^4/g$  compared to values as low as  $10^2/g$  in methanogenic zones closer to the oil. These data suggest that this location may be in the early stages of switching from iron-reducing to methanogenic conditions.

Although the MPN method is not reliable for determining absolute numbers, the consistent pattern in relative numbers among the three profiles is significant. We have taken the vertical profile data together with microbial data from seven broadly-spaced sediment samples (fig. 2 and table 1) and interpolated them to provide a qualitative picture of the redox zones in the aquifer (fig. 2). A location was classified as methanogenic if more than  $10/g$  total methanogens were present on the sediments and the iron-reducer numbers were relatively low compared to other locations in the same vertical profile. Where iron-reducer populations achieved maximum values and numbers of attached methanogens declined, the location was classified as iron-reducing. Finally, if only aerobes and fermenters were found, the location was classified as aerobic.

Within the contaminant plume, the contours of the population distribution appear to generally conform to the ground-water flow lines. Our results indicate that the anaerobic core of the plume attains a minimum vertical thickness of about one meter at the

downgradient edge of the non-aqueous oil body. Essaid and others (1995) hypothesized that restricted recharge through a low permeability horizon causes the observed upwelling of oxygenated water in this location. Upwelling of the flow at Site B causes vertical focussing of the contaminated ground water, creating an especially narrow methanogenic zone centered at 422.5 m that spans a distance of only 25 cm. This contrasts with the thicker profiles upgradient at Site A and downgradient at Site C. Methanogenic zones have evolved in two places: one within the area where separate-phase oil is present, and a second below the oil in the laterally migrating plume of contaminated ground water. In the laterally migrating plume there is a classic pattern of a methanogenic core progressing with depth to iron-reducing and then aerobic conditions.

## Controls on the Microbial Population Distribution

For each site, figure 3 shows the microbial data for iron-reducers and methanogens together with plots of the extractable Fe(II) and Fe(III) concentrations from the sediments; pore-water concentrations of ethylbenzene and *m*- and *p*-xylene; permeabilities estimated from sediment grain-size distributions (Krumbein and Monk, 1942), and pore-water Fe(II) concentrations.

### Extractable Iron on Sediments

In general, extractable concentrations of sediment Fe(III) are lower, and Fe(II) are higher in the area of the aquifer affected by the plume than background values. Sediment Fe(III) values at the base of the core at Sites B and C are consistent with background concentrations indicating that the profiles span the entire anoxic portion of the plume. The overall picture is consistent with the results of Tuccillo and others (1999) who found that microbial iron-reduction of the petroleum hydrocarbons has resulted in depletion of solid phase Fe(III) and precipitation of authigenic Fe(II) minerals on the sediments in the anoxic zone.

Within the areas where culturable methanogens are found, extractable Fe(III) and

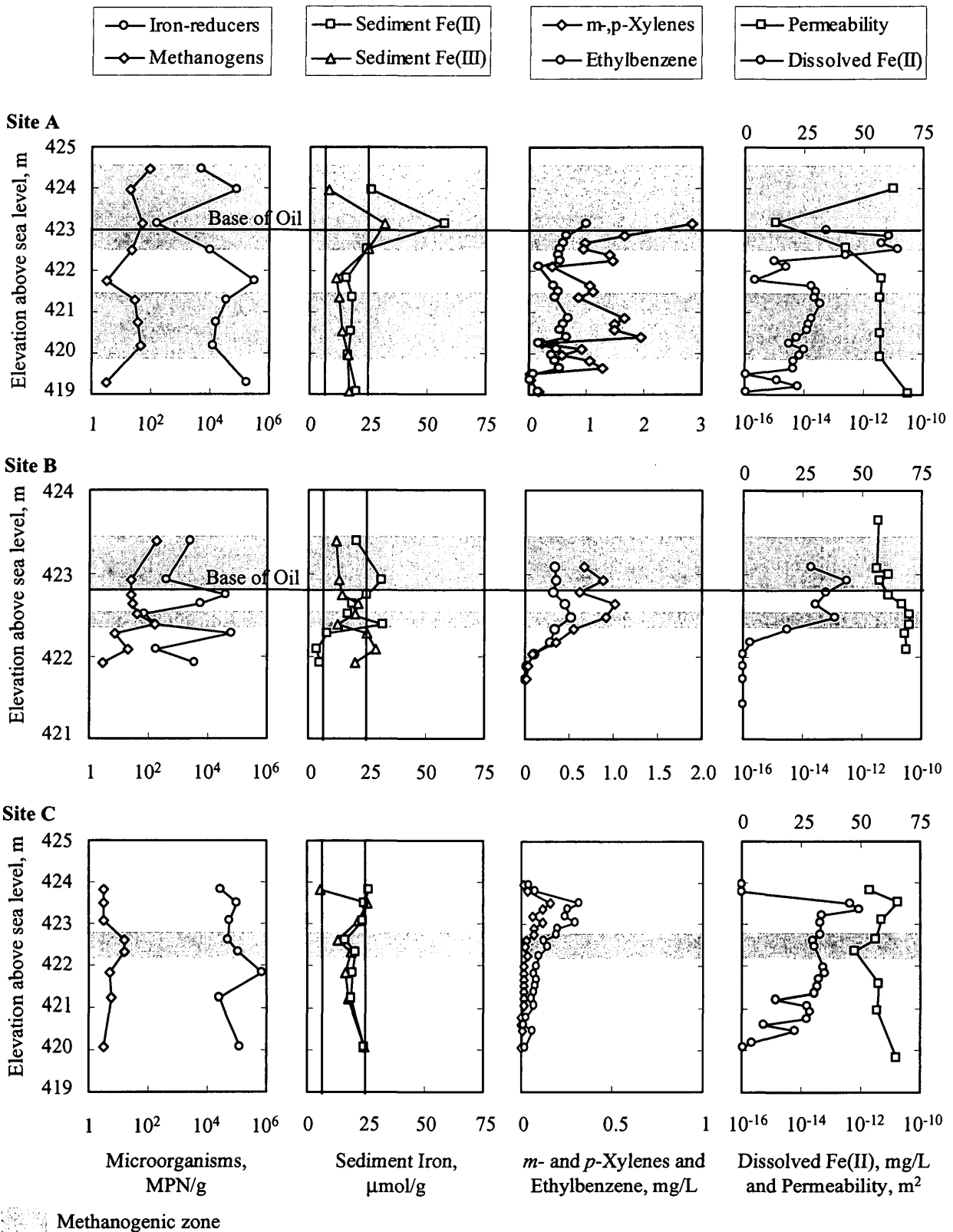


**Figure 3.** Vertical profiles for Sites A, B, and C of microbial data for iron-reducers and methanogens together with plots of the Fe(II) and Fe(III) concentrations from the sediments; pore-water concentrations of ethylbenzene and *m*- and *p*-xylene; and permeabilities estimated from sediment grain-size distributions and pore-water Fe(II) concentrations. Uncontaminated background concentrations of sediment Fe(II) and Fe(III) are shown in the sediment iron plots, averaging 6 and 25 μmol/g, respectively.

culturable iron-reducing organisms are still present. The lowest value of extractable Fe(III) found in all of the cores is 11 micromole/g ( $\mu\text{mol/g}$ ) which is almost 50% of the average background concentration. Apparently, only about half of the Fe(III) available on the aquifer sediments is used before methanogenesis begins. Postma (1993) showed that simultaneous methanogenesis and iron-reduction is thermodynamically feasible if microorganisms are forced to use less soluble Fe phases than the poorly crystalline material that typically comprises hydroxypolymer coatings on mineral grains.

A detailed examination of the iron and microbial data shows that solid-phase Fe(III) depletion alone cannot explain the succession of iron-reducers by methanogens. For example, in the center of the dissolved plume at Site B (422.5 m) very low numbers of Fe-reducers are found with high values of extractable Fe(III). Also, high numbers of iron-reducers exist where Fe(III) values are low below the base of the oil body at Sites A (421.8 m) and B (422.7 m). Other factors are important that are not apparent from consideration of the extractable Fe(III) concentrations alone.

In several cases, peak values in Fe(II) are associated with low numbers of iron-reducers, and peaks in active methanogens (fig. 3: Site A, 423.2 m; Site B, 422.4 m and 422.9 m). This suggests that coating of the Fe(III) phases by Fe(II) precipitates is inhibiting iron-reduction and providing an advantage to the methanogens in these locations.

### Organic concentrations

To illustrate the influence of the organic contaminants on the microbial populations the concentrations of ethylbenzene and *m*- and *p*-xylene for the three sites are shown in figure 3. Ethylbenzene was selected because it has similar biodegradability to benzene but is present at concentrations similar to *m*- and *p*-xylene. The behavior of *m*- and *p*-xylene is intermediate compared to toluene, which is highly degradable, and benzene, which is less degradable (Eganhouse and others, 1993). Between Sites B and C the average

concentration of ethylbenzene drops slightly from about 0.4 to 0.3 milligrams per liter (mg/L). In contrast, the concentration of *m*- and *p*-xylene drops from 1-2 mg/L at Sites A and B to  $\sim 0.1$  mg/L at Site C.

At Sites A and B, the methanogenic zones are associated with higher concentrations of ethylbenzene, *m*- and *p*-xylene, and dissolved iron (fig. 3). The correspondence between methanogenic zones and higher concentrations of contaminants suggests that these areas have been subjected to greater cumulative hydrocarbon fluxes over time. A comparison of the permeability profiles and the aqueous concentration data for Sites A and B indicates that there are two types of high organic concentration areas in the aquifer below the oil body. One is a relatively low permeability zone in the vicinity of the separate-phase oil where the flux rate is probably controlled by dissolution and diffusion. The second is a high permeability zone below the oil where the hydrocarbon flux is probably controlled by horizontal advection of water contaminated by separate-phase oil located upgradient.

The dissolved iron concentration profiles at Sites A and B closely correspond to the shapes of the hydrocarbon concentration profiles in this contaminant plume. Because total dissolved concentration can be quickly determined in the field with a portable spectrophotometer, it was useful as a field indicator to formulate our 1997 microbial sampling scheme. The peaks in the dissolved iron plume gave a good indication of where the methanogenic zones were located.

At Site C, near the edge of the anoxic zone (Cozzarelli and others, 1999), the picture is more complex. In the top two meters below the water table, the profiles of hydrocarbon concentrations correspond closely to the permeability profile. However, the peak in methanogens is found about a meter below the maximum hydrocarbon concentrations and the sediment Fe(III) is only slightly depleted. It is also not clear from the MPN data alone where transitions between iron-reducing and aerobic conditions are located. The MPN data show that iron-reducers and aerobes coexist at both the top and base of the profile. However, at both levels

dissolved Fe(II) is below detection and the cores were visually more orange colored compared to the center of the profile. These observations suggest that DO is at least intermittently present on the fringes of the profile. It seems possible that temporal changes in the ground water flow may create conditions that alternate between aerobic and iron-reducing on the fringes of the plume. Intermittent replenishing of the Fe(III) supply near the water table by oxidation of dissolved Fe(II) during water table fluctuations might also explain the off-center position of the methanogenic zone at this location.

## DISCUSSION AND CONCLUSIONS

The data set provides a consistent picture of methanogenic zones at various levels of development at the Bemidji site. The dominant physiologic type of the microbial population changes from iron-reducing to methanogenic over vertical scales as small as 25 cm. Near the oil body, methanogenic zones have evolved in two high-flux areas. One zone is found within the non-aqueous oil where high fluxes are due to local dissolution and diffusion of contaminants from the oil. A second zone exists along high permeability horizons in a laterally migrating contaminant plume. This zone appears to be continuous for more than 60 m downgradient.

Calculations based on the dissolution rate and total mass of the non-aqueous oil at the Bemidji site, indicate that the oil body may provide a continuous contaminant source for hundreds of years (Bekins and others, 1999). During this period, the methanogenic zones will continue to develop as sediment Fe(III) is depleted along the high permeability horizons. Although some recycling of Fe is expected, it is clear from the data (fig. 3) that some of the dissolved Fe(II) precipitates as Fe(II) solids in the anoxic zone.

The development of laterally continuous methanogenic zones along high permeability horizons has implications for risk analysis at sites where petroleum hydrocarbon contaminants are degrading by iron-reduction and methanogenesis. Because the hydrocarbon flux is greatest along high permeability horizons, worst-case migration scenarios should

be based on two assumptions: first, continued iron reduction over the long term requires plume growth into previously uncontaminated aquifer sediments with fresh or recycled Fe(III); second, any projections of steady-state behavior should be based on methanogenic degradation capabilities and on estimated flow rates in the highest permeability horizons.

High permeability zones where methanogenic conditions develop may be very thin vertically, making them difficult to locate. At Site B, the methanogenic niche spans an interval of only 25 cm. This aspect of the plume also complicates interpretations of terminal electron processes. Cozzarelli (1993) noted that geochemical indicators became mixed when redox zones were very thin at a gasoline-contaminated site. At the Bemidji site, the strategy of collecting pore waters over 15 cm intervals and analyzing dissolved iron in the field was useful in locating the methanogenic zones.

Several aspects of the data warrant further investigation. Although Fe(III) is generally depleted in the methanogenic zones, significant extractable iron and culturable iron-reducers are still present, suggesting ongoing low levels of iron-reduction. At Sites A and B, high numbers of iron-reducers are present just below the oil at locations where the sediment Fe(III) is highly depleted. In contrast, very low numbers of iron-reducers are found at the center of the plume at Site B in spite of moderate levels of sediment Fe(III). Preferential use of favorable Fe(III) phases, along with natural variability of the Fe(III) phases on the sediments, may play a role in these observations. Another possibility is that proximity to the oil provides access to more favorable substrates such as toluene or to organic ligands. Cozzarelli and others (1994) demonstrated that organic ligands are present in higher concentrations near the oil body and Lovley and others (1994) demonstrated that organic ligands facilitate chelation of solid Fe(III) phases.

## REFERENCES

- Baedecker, M.J., Cozzarelli, I.M., Eganhouse, R.P., Siegel, D.I., and Bennett, P.C., 1993,



- Crude oil in a shallow sand and gravel aquifer-III. Biogeochemical reactions and mass balance modeling in anoxic groundwater: *Applied Geochemistry*, v. 8, p. 569-586.
- Bekins, B.A., Baehr, A.L., Cozzarelli, I.M., Essaid, H.I., Haack, S.K., Harvey, R.W., Shapiro, A.M., Smith, J.A., and Smith, R.L., 1999, Capabilities and challenges of natural attenuation in the subsurface: Lessons from the U. S. Geological Survey Toxics Substances Hydrology Program, in U.S. Geological Survey Toxic Substances Hydrology Program--Proceedings of the Technical Meeting, Charleston, South Carolina, March 8-12, 1999-- Volume 3 -- Subsurface Contamination from Point Sources: U.S. Geological Survey Water-Resources Investigations Report 99-4018C.
- Bennett, P.C., Siegel, D.E., Baedecker, M.J., and Hult, M.F., 1993, Crude oil in a shallow sand and gravel aquifer-I. Hydrogeology and inorganic geochemistry: *Applied Geochemistry*, v. 8, p. 529-549.
- Cherry, J.A., 1996, Conceptual models for chlorinated solvent plumes and their relevance to intrinsic remediation, in Proceedings of the Symposium on Natural Attenuation of Chlorinated Organics in Ground Water: Dallas, Texas, US EPA, p. 29-31.
- Cozzarelli, I.M., Baedecker, M.J., Eganhouse, R.P., and Goerlitz, D.F., 1994, The geochemical evolution of low-molecular-weight organic acids derived from the degradation of petroleum contaminants in groundwater: *Geochimica et Cosmochimica Acta*, v. 58, p. 863-877.
- Cozzarelli, I.M., Baedecker, M.J., Eganhouse, R.P., Tuccillo, M.E., Aiken, G.R., Bekins, B.A., and Jaeschke, J.B., 1999, Long-term geochemical evolution of the Bemidji Toxics site crude-oil plume, in U.S. Geological Survey Toxic Substances Hydrology Program--Proceedings of the Technical Meeting, Charleston, South Carolina, March 8-12, 1999-- Volume 3 -- Subsurface Contamination from Point Sources: U.S. Geological Survey Water-Resources Investigations Report 99-4018C.
- Cozzarelli, I.M., 1993, The biogeochemical fate of organic acids in a shallow aquifer contaminated with gasoline: Charlottesville, University of Virginia, 240 p.
- Eganhouse, R.P., Baedecker, M.J., Cozzarelli, I.M., Aiken, G.R., Thorn, K.A., and Dorsey, T.F., 1993, Crude oil in a shallow sand and gravel aquifer-II. Organic geochemistry: *Applied Geochemistry*, v. 8, p. 551-567.
- Essaid, H.I., Bekins, B.A., Godsy, E.M., Warren, Ean, Baedecker, M.J., and Cozzarelli, I.M., 1995, Simulation of aerobic and anaerobic biodegradation processes at a crude oil spill site: *Water Resources Research*, v. 31, no. 12, p. 3309-3327.
- Godsy, E.M., Goerlitz, D.F., and Grbic-Galic, D., 1992, Methanogenic biodegradation of creosote contaminants in natural and simulated ground water ecosystems: *Ground Water*, v. 30, no. 2, p. 232-242.
- Herkelrath, W.N., 1999, Impacts of remediation at the Bemidji oil spill site, in U.S. Geological Survey Toxic Substances Hydrology Program--Proceedings of the Technical Meeting, Charleston, South Carolina, March 8-12, 1999-- Volume 3 -- Subsurface Contamination from Point Sources: U.S. Geological Survey Water-Resources Investigations Report 99-4018C.
- Hess, K.M., Herkelrath, W.N., and Essaid, H.I., 1992, Determination of subsurface fluid contents at a crude-oil spill site: *Journal of Contaminant Hydrology*, v. 10, p. 75-96.
- Hult, M.F., 1984, Groundwater contamination by crude oil at the Bemidji, Minnesota, research site-An introduction, in Groundwater Contamination by Crude Oil at the Bemidji, Minnesota, Research Site: U.S. Geological Survey Water-Resources Investigations Report 84-4188, p. 1-15.
- Krumbein, W.C. and Monk, G.D., 1942, Permeability as a function of the size parameters of unconsolidated sand: *Transactions of the American Institute of Mining and Metallurgical Engineering*, v. 151, p. 153-163.
- Lovley, D.R., Baedecker, M.J., Lonergan, D.J., Cozzarelli, I.M., Phillips, E.J.P., and Siegel, D.I., 1989, Oxidation of aromatic

- compounds coupled to microbial iron reduction: *Nature*, v. 339, p. 297-299.
- Lovley, D.R., Woodward, J.C., and Chapelle, F.H., 1994, Stimulated anoxic biodegradation of aromatic hydrocarbons using Fe(III) ligands: *Nature*, v. 370, no. 14, p. 128-131.
- Murphy, Fred and Herkelrath, W.N., 1996, A sample-freezing drive shoe for a wire line piston core sampler: *Ground Water Monitoring and Remediation*, v. 16, p. 86-90.
- Postma, D., 1993, The reactivity of iron oxides in sediments: A kinetic approach: *Geochimica et Cosmochimica Acta*, v. 57, p. 5027-5034.
- Smith, R.L., Harvey, R.W., and LeBlanc, D.R., 1991, Importance of closely spaced vertical sampling in delineating chemical and microbiological gradients in groundwater studies: *Journal of Contaminant Hydrology*, v. 7, p. 285-300.
- Tuccillo, M.E., Cozzarelli, I.M., and Herman, J.S., 1999, Iron reduction in the sediments of a hydrocarbon-contaminated aquifer: *Applied Geochemistry*, v. 4, no. 5, p. 71-83.
- Wiedemeier, Todd, Wilson, J.T., Kampbell, D.H., Miller, R.N., and Hansen, J.E., 1995, Technical protocol for implementing intrinsic remediation with long-term monitoring for natural attenuation of fuel contamination dissolved in groundwater, Volume I: Air Force Center for Environmental Excellence, Technology Transfer Division, Brooks Air Force Base.

## AUTHOR INFORMATION

Barbara A. Bekins, Hedef I. Essaid, E. Michael Godsy, Victor V. Paganelli, Ean Warren, U.S. Geological Survey, Menlo Park, California

Isabelle M. Cozzarelli, U.S. Geological Survey, Reston, Virginia

Mary Ellen Tuccillo, University of Virginia, Charlottesville, Virginia

# Long-Term Monitoring of Unsaturated-Zone Properties to Estimate Recharge at the Bemidji Crude-Oil Spill Site

By Geoffrey N. Delin and William N. Herkelrath

## ABSTRACT

Ground-water recharge is an important factor affecting the Bemidji, Minnesota crude-oil spill site. About 400,000 liters of crude oil remained in the ground after remediation was completed following the 1979 pipeline break. An automated data logging system was used to measure unsaturated zone properties relevant to estimating recharge and to evaluate their effects on dissolution of the oil. Laboratory and field testing of several soil-moisture probes indicated that the CS615 probe was better suited to estimating recharge in the glacial outwash at the Bemidji crude-oil spill site than the CS605 probes. Both probes are manufactured by Campbell Scientific Inc. The CS615 probe provided dependable and accurate data over long time periods, using a limited power supply, under the extreme weather conditions typical of northern Minnesota. Based on results of the testing, arrays of the CS615 probes, zero-maintenance tensiometers, and thermocouples were installed in the unsaturated zone at the north oil pool in the fall of 1998. Computer simulations indicated that the rate of dissolution from the oil body is linearly related to the recharge rate. Additional multiphase flow model analyses are being conducted to quantify this increased dissolution. Additional model analyses are also being conducted to evaluate how dissolution is affected by recharge that varies in relation to the presence of crude oil in the unsaturated and saturated zones, discontinuous lenses of lacustrine silt and clay, and topography. The VS2DT code is also being used to estimate recharge rates and to evaluate the movement of water through the oil.

## INTRODUCTION

Ground-water recharge is an important factor affecting the Bemidji, Minnesota crude-oil spill site. Although most recharge occurs as a result of spring snowmelt, its spatial and temporal variability at the site is complex and poorly understood. Recharge varies spatially in relation to the presence of crude oil in the unsaturated and saturated zones, discontinuous lenses of lacustrine silt and clay, and topography. Little is known of how ground-water recharge (in relation to these factors) affects the dissolution, transport, and degradation of oil at the site. Preliminary model analyses have indicated that ground-water recharge is a critical factor affecting the transport and dissolution rates of oil at the site.

This paper presents preliminary results of an investigation to better understand the effects of recharge on the dissolution and movement of oil through the unsaturated and saturated zones at the

Bemidji, Minnesota crude-oil spill site. Included are selected results of measurements being used to monitor water movement through the unsaturated zone and to quantify ground-water recharge. Recharge estimates based on unsaturated-zone measurements are compared to estimates based on hydrograph analysis.

## Site Description

On August 20, 1979, approximately 16 kilometers northwest of Bemidji, Minnesota, the land surface and shallow subsurface were contaminated when a crude-oil pipeline burst, spilling about 1,700,000 L (liters) (about 10,700 barrels) of crude oil onto a glacial outwash deposit. Crude oil also sprayed to the southwest covering an approximately 7,500 m<sup>2</sup> (square meter) area of land. After cleanup efforts were completed about 400,000 L (about 2,500 barrels)

of crude oil remained at the site. Some crude oil percolated through the unsaturated zone to the water table near the rupture site (north oil pool, fig. 1). Some of the sprayed oil flowed over the land surface toward a small wetland forming a second area of oil infiltration (south oil pool).

Ground water affected by the oil spill discharges to a small lake 400-m east of the pipeline. The land surface is a glacial outwash plain underlain by stratified glacial outwash deposits. Sediments at the test site consist of poorly sorted glacial outwash sand of fine to very coarse grain size, with some fine gravel and cobbles. One- to 10-mm (millimeter) thick iron-cemented laminations occur between depths of 0.3 and 1.0 m. At a depth of about 25 m, a regionally persistent and uniform layer of low permeability sediment (till) restricts vertical ground-water movement. Crude oil (about 0.4-0.5- m thick) floats on the water table, which is about 2.7 m below land surface at the south

oil pool. The water table is about 6 m below the land surface at the north oil pool.

## Methods

An automated data logging system was installed near Well 981 (south oil pool) in late 1996 primarily to compare the performance of several different soil-moisture probes manufactured by Campbell Scientific Inc.<sup>1</sup> Three different soil-moisture probes were compared to determine which was the most appropriate for evaluating recharge at the north oil pool, which is the primary area of research interest. Other data collected at the site included soil temperature (at 1/2-meter depth intervals), ground-water level, and precipitation. The soil moisture and other data were collected 6 times per day from late 1996 to present. Solar-charged batteries initially powered the CR10X data logger and time-domain reflectometry (TDR) system. The batteries were

replaced in the fall of 1997 with 110-volt AC power.

Three types of Campbell Scientific soil-moisture probes were compared at the Well 981 site (fig. 2). The CS615 probes were 30-cm (centimeter) long and had 2 prongs. The CS615 is a self-contained "reflectometer" that does not require a TDR cable tester to determine water content. This probe was compared to two CS605 three-prong TDR probes (30-cm long and 50-cm long) that require a cable tester. An array of 4

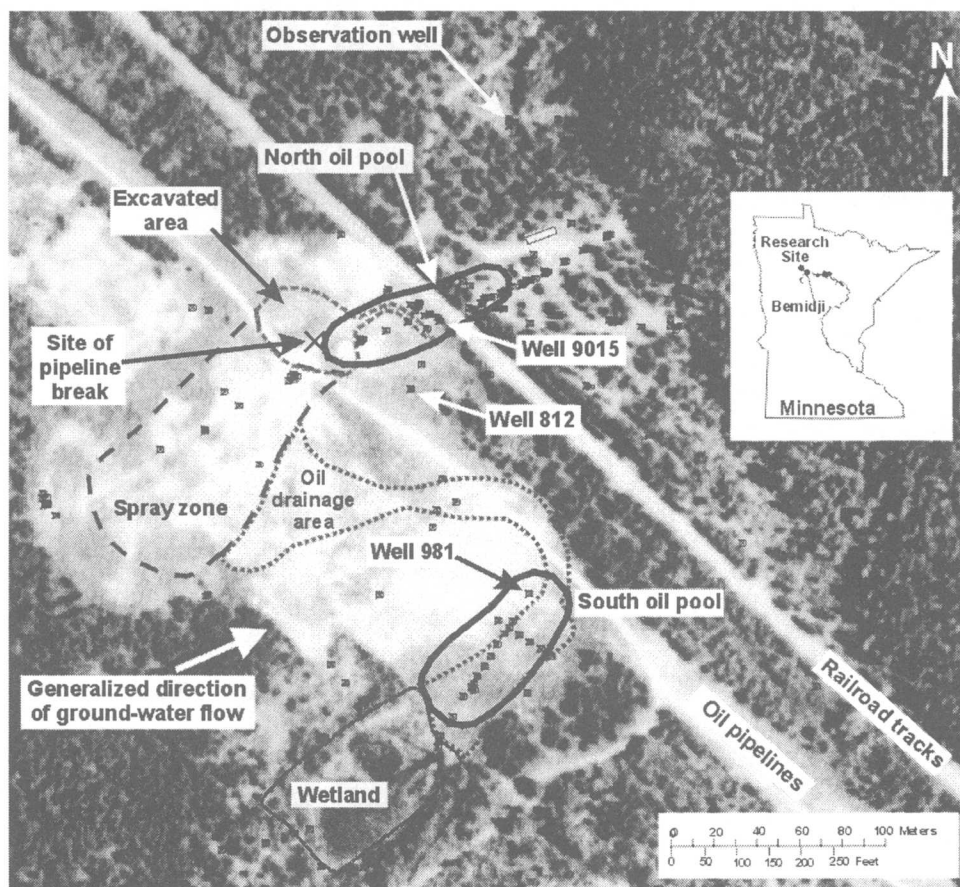


**Figure 1.** Features of the Bemidji crude-oil spill research site superimposed on a 1991 aerial photograph.

<sup>1</sup> The use of brand names herein is for identification purposes only and does not constitute endorsement by the U.S. Government.

probes of each type was installed horizontally at ½-meter depth intervals in the wall of a 2-meter-deep pit. A fourth array of vertically oriented

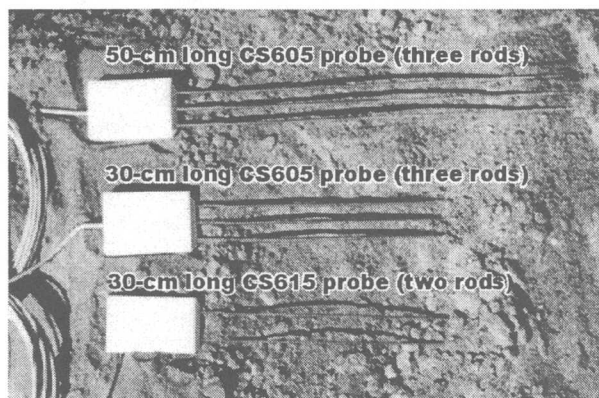


**Figure 2.** Campbell Scientific soil moisture probes used at the Bemidji crude-oil spill site.

CS605 30-cm long probes was also installed at ½-m depth intervals in small-diameter boreholes to evaluate how probe orientation affected soil-moisture measurements.

Using the methods described in Herkelrath and others (1991), the three types of soil-moisture probes were calibrated in the laboratory using repacked columns of sandy sediments obtained from the field site. The columns were saturated from the bottom through a tube. Relative permittivity of the sediments was determined for the saturated sample using each soil-moisture probe. The column mass was determined by weighing. Water was removed incrementally through the bottom of the column by suction with permittivity and mass being measured for each increment. Total water content corresponding to each measurement was calculated from the difference between the measured column mass and the oven-dry mass. Volumetric water contents were determined by the ratio of total water content to soil volume.

Ground-water recharge estimated using the soil-moisture data near Well 981 was based on a rudimentary water balance. The primary assumption is that water in the soil above a certain depth (boundary) in the unsaturated zone moves upward in response to evapotranspiration and water below that boundary drains to the water table. Seasonal movement of the evapotranspiration/drainage boundary is typically measured directly using

soil-water tensiometers. Several tensiometers were installed at the site, but the instruments failed, and the measured data could not be reliably used. Therefore, the depth of the boundary was assumed to be 50 cm during the summer months based on previous research (unpublished data). These recharge estimates were compared to estimates based on the method of hydrograph analysis (Rasmussen and Andreason, 1959). The hydrograph analysis method is based on relating changes in water-table elevation measured in a well with changes in the amount of water stored in the aquifer. The change in storage is attributed to ground-water recharge. Recharge is equivalent to the water table rise over a given time period multiplied by the aquifer specific yield of 0.3.

## RESULTS AND DISCUSSION

Results of laboratory tests indicated that the moisture content calculated using the factory-supplied calibration for the CS615 probe was accurate to within about +/- 0.02 cc/cc (cubic centimeters per cubic centimeter) of the actual value over the whole moisture content range (fig. 3). This error was deemed acceptable and the field data were not adjusted. The moisture content values calculated using the factory-supplied calibration for the CS605 probes were generally higher than the actual moisture content. Therefore, the field data were shifted downward

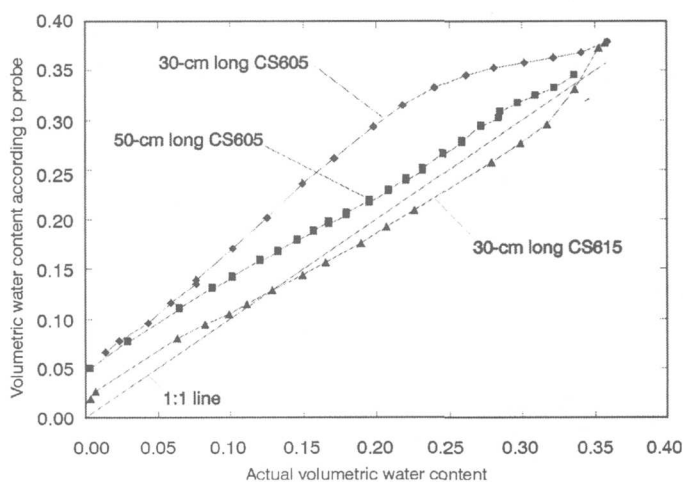


**Figure 3.** Calibration results for the Campbell Scientific soil moisture probes used at the Bemidji crude-oil spill site.

0.07 and 0.02 cc/cc, respectively, for the 30-cm-long and 50-cm-long CS605 probes.

### Temperature Measurements

Analysis of the temporal variation in soil temperature was both qualitatively and quantitatively useful in estimating the timing, depth, and duration of recharge events. The typical profile of soil temperature with depth is observed in figure 4 where the normal summer pattern of decreasing temperature with depth becomes inverted during October, followed by increasing temperatures with depth during the winter months. The thermocouples detected wetting front movement following precipitation events that exceeded about 2 cm, most noticeably the event during early July 1997 (fig. 4). Soil temperatures generally decreased following each of these precipitation events, with slightly smaller decreases at greater depths. The shifting low temperature with depth following the July precipitation (recharge) event is evidence of movement of the recharge water through the

unsaturated zone. This shift in temperature with depth and time is not noticeable for precipitation events that did not result in ground-water recharge, such as the one on August 19th. In addition to the late summer and fall time period represented in figure 4, the temperature data also proved very useful in determining the timing of recharge from spring snowmelt.

### Comparison Of Soil-Moisture Probes

Each type of soil-moisture probe simultaneously detected wetting front movement at the 150-cm depth following precipitation events (fig. 5). The greatest difference in measured soil moisture between the probes occurred during precipitation events when the magnitude of the soil-moisture changes for the vertically oriented CS605s were much greater than that for the other probes. This phenomenon was observed at both the 100- and 150-cm depths. The vertical probe orientation caused the wetting fronts to be detected for a much longer period of time than for the horizontally oriented probes.

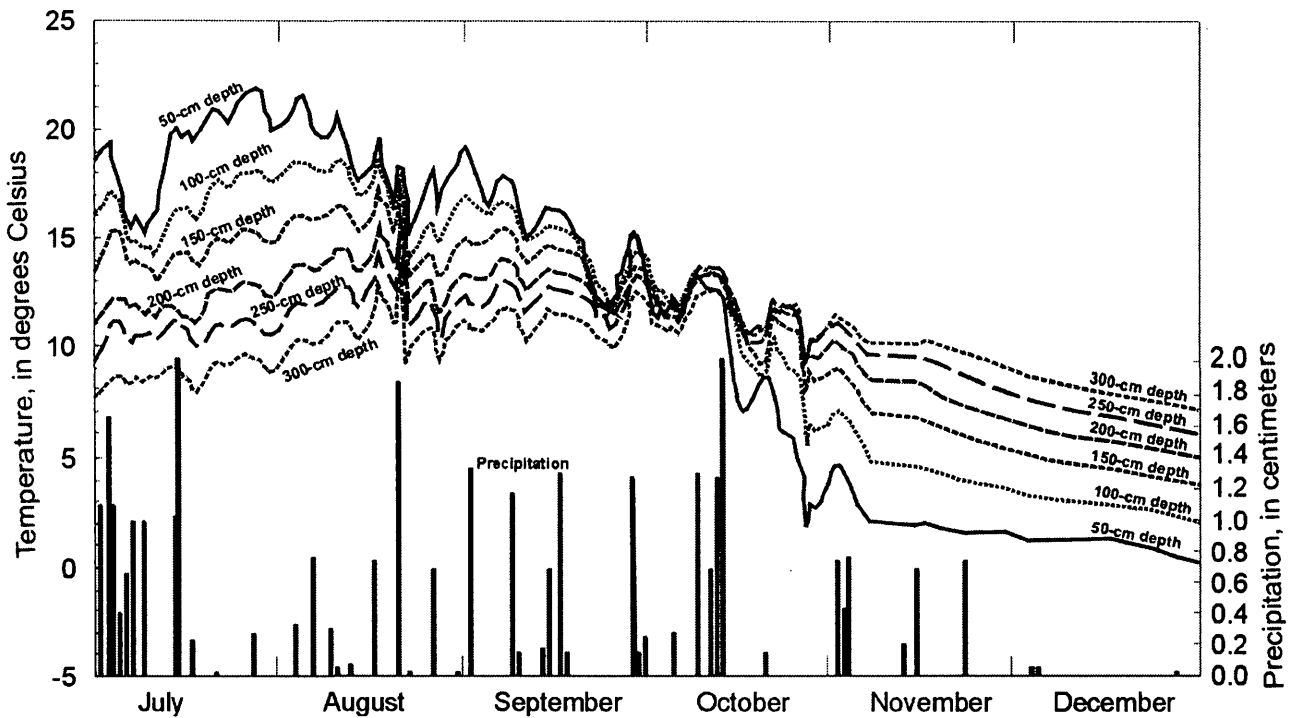


Figure 4. Soil temperature and precipitation near Well 981, July – December 1997.

The resultant apparent soil moisture during these recharge periods was necessarily greater. The slightly greater soil moisture measured by the CS615s than the horizontally oriented CS605s likely is due to localized differences in soils. Soil moisture measured with the 50-cm long CS605s did not fluctuate as much as for the 30-cm long CS605s. This may be an indication that a longer probe provides a more stable response to changes in soil moisture.

Soil-moisture values measured with the CS615s were much more stable and “clean” (less data fluctuation and data loss) than those measured with the CS605s, which were comparatively “noisy” (figs. 5 and 6). Data loss for the CS615s was less than 1 percent, with virtually all losses being unrelated to the probe itself. In contrast, data loss for the CS605s was notable with each of the CS605 probes having lost at least 5 percent of the data during each year of operation. During the first 6 months of 1997, for example, data loss for the CS605s was as follows: 12 percent for the 30-cm long (horizontally oriented) probes; 15 percent for the 30-cm long

(vertically oriented) probes; and 22 percent for the 50-cm long (horizontally oriented) probes. During the same time period in 1998 these data losses were about two times greater, indicating a progressive increase of data loss in time.

Data collected with all three of the CS605s at the 300-cm depth were very sparse, with data losses of greater than 80 percent per probe. A comparison of figures 5 and 6, which have the same vertical scales, provides a good indication of the “noise” in the CS605 probes at this depth. Each of the probes at this depth was located below the water table and thus the soil moisture should not have changed significantly over time. Some of the data loss for the CS605s likely resulted from variations in power supply voltage and line noise that caused out-of-range (positive and negative) values. Loss of data with the CS605s critically affects recharge estimates resulting in inaccurate or missing recharge estimates.

During the time when the monitoring system was initially powered by solar-charged batteries, data loss for the CS605s increased

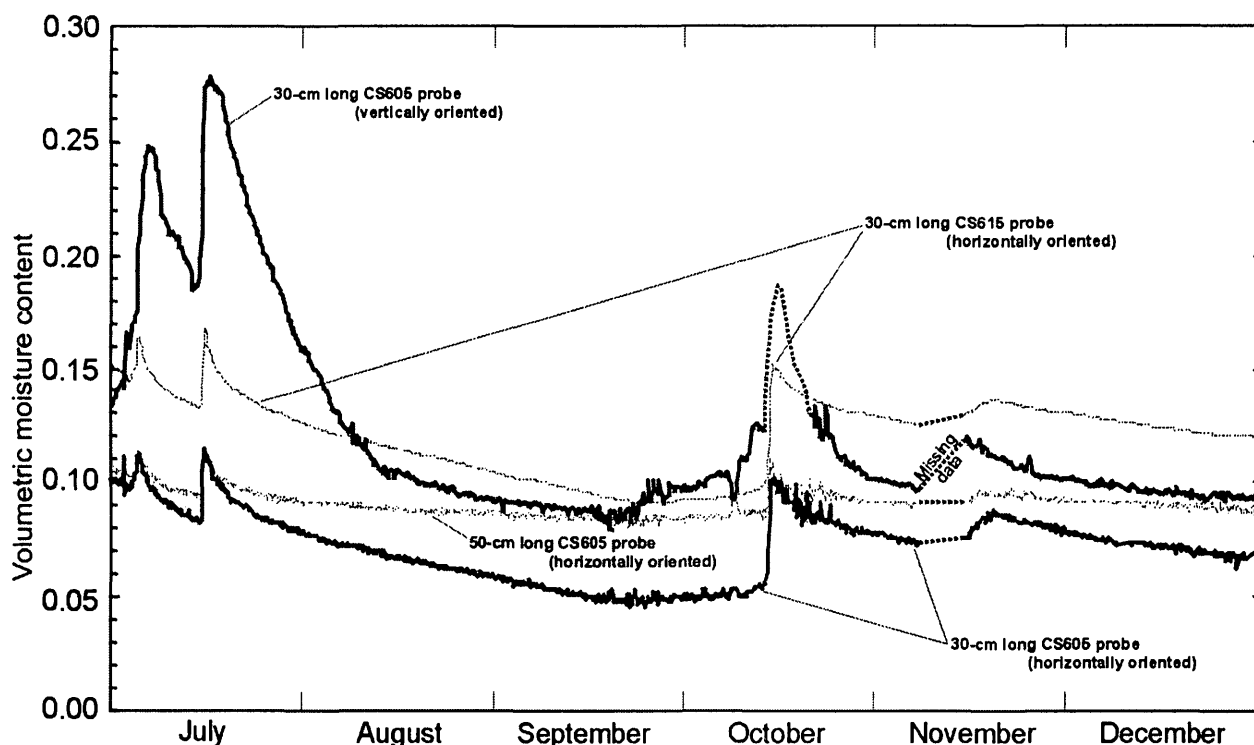


**Figure 5.** Soil moisture at the 150-cm depth near Well 981 measured with the different probes, July – December 1997.

during the winter months when air temperatures were below  $-10^{\circ}\text{C}$ . This increased data loss was likely due to insufficient solar radiation during the winter to charge the batteries to power the cable tester. Conversely, the CS615 probes had sufficient power to make their measurements during the winter months.

The two-pronged CS615 probe was easier to install than the three-pronged CS605 probe, largely because of increased friction and the enhanced likelihood of hitting gravel with the third prong. However, greater care was required during installation of the CS615s to ensure that the internal circuitry was not damaged. The 50-cm long CS605s were most difficult to install because of their greater length, which increased friction and the likelihood of hitting gravel.

### Recharge Estimates

Ground-water recharge was estimated using the soil moisture data and by the hydrograph analysis method for all events where precipitation exceeded about 2.0 cm. For the three precipitation events that occurred during the last six months of

1997 (fig. 7), for example, recharge based on data from the horizontally oriented 30-cm long CS615 and CS605 probes were similar. Small-scale soil heterogeneity rather than differences in the way soil moisture is measured by each probe likely cause the slightly different recharge estimates for these probes.

Recharge based on the vertically oriented 30-cm long CS605 probes during the early July event was about 70 percent greater than for the other probes (fig. 7). This greater recharge for the vertically oriented probe was typical during the study. The vertical probe orientation caused the wetting fronts to be detected for a much longer period of time than for the horizontally oriented probes, which generally resulted in a higher estimated recharge rate. This was not always the case, however, as evidenced by the less than average recharge estimate for the vertically oriented probes during the mid October 1997 event (fig. 7). These inconsistent results are further evidence that the vertical probe orientation is not appropriate for recharge estimation at this site.

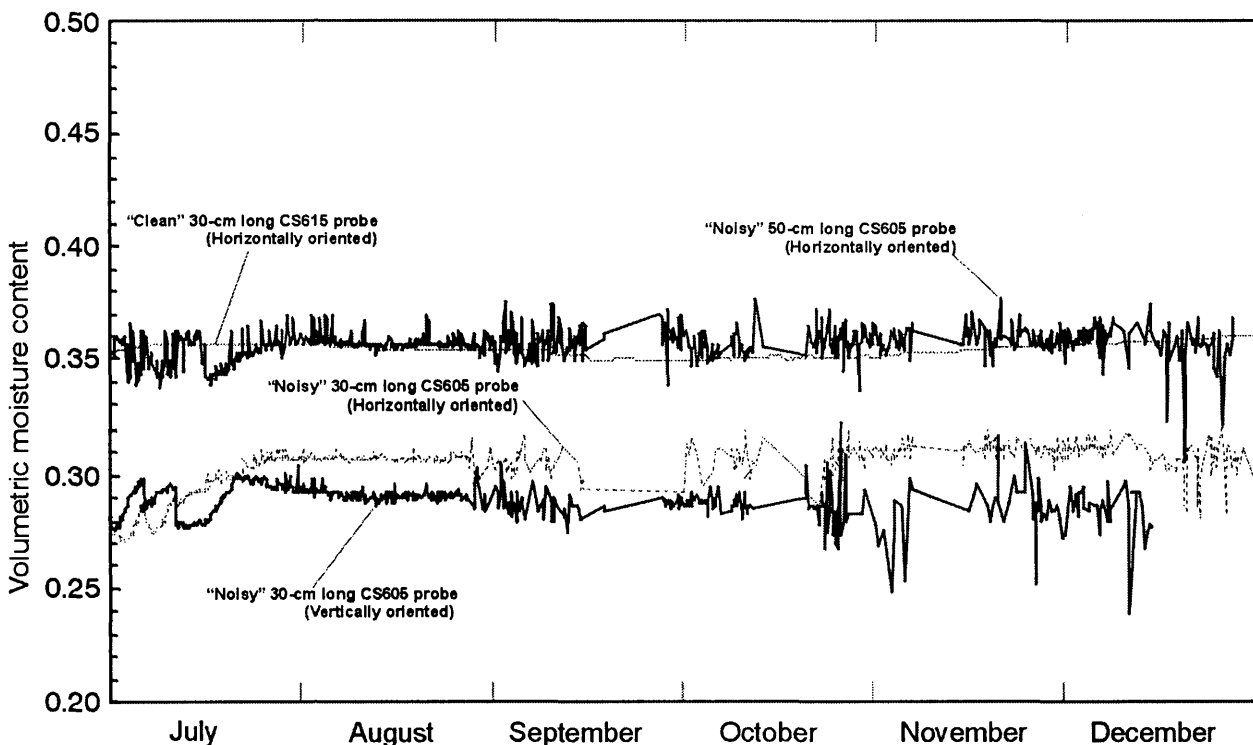


**Figure 6.** Soil moisture at the 300-cm depth near Well 981 measured with the different probes, July – December 1997.



The method of hydrograph analysis was applied to the three recharge events that occurred during the second half of 1997. Because the two July precipitation events occurred only about two weeks apart (fig. 5) the effects of both events were superimposed in the ground-water hydrograph response (figs. 7 and 8). Thus, only one recharge estimate is presented for the two July events. The well used for hydrograph analysis at the 981 site was installed in August 1997. Thus, data from a nearby datalogger at Well 812 were used for estimating recharge during the July recharge event (fig. 8). Use of water-level data from the two different wells shown in figure 8 may have introduced some error when comparing the recharge estimates for this time period.

Recharge estimates based on hydrograph analysis were generally 20-40 percent less than estimates based on the soil-moisture probes for events in 1997 and 1998. For example, total recharge based on hydrograph analysis for the three 1997 events shown in figure 7 was 11 cm

or about 30 percent less than estimates based on the horizontally oriented probes. The several limiting assumptions behind both of the recharge estimation methods are the most likely causes for the differing estimates. Application of other methods such as tritium/helium (Solomon and others, 1993) is being employed at the site to obtain a more accurate recharge estimate.

### Model Analyses

Computer simulations indicate that the rate of dissolution from an oil body is linearly related to the recharge rate. Water permeabilities estimated from a multiphase flow model (Essaid and others, 1995) were used in MODFLOW (McDonald and Harbaugh, 1988; Harbaugh and McDonald, 1996) and MODPATH (Pollock, 1994) simulations to evaluate steady state water movement through the oil body. When there is no recharge, most of the ground water flows around the oil body and does not come in contact with the oil. However, recharge water flows

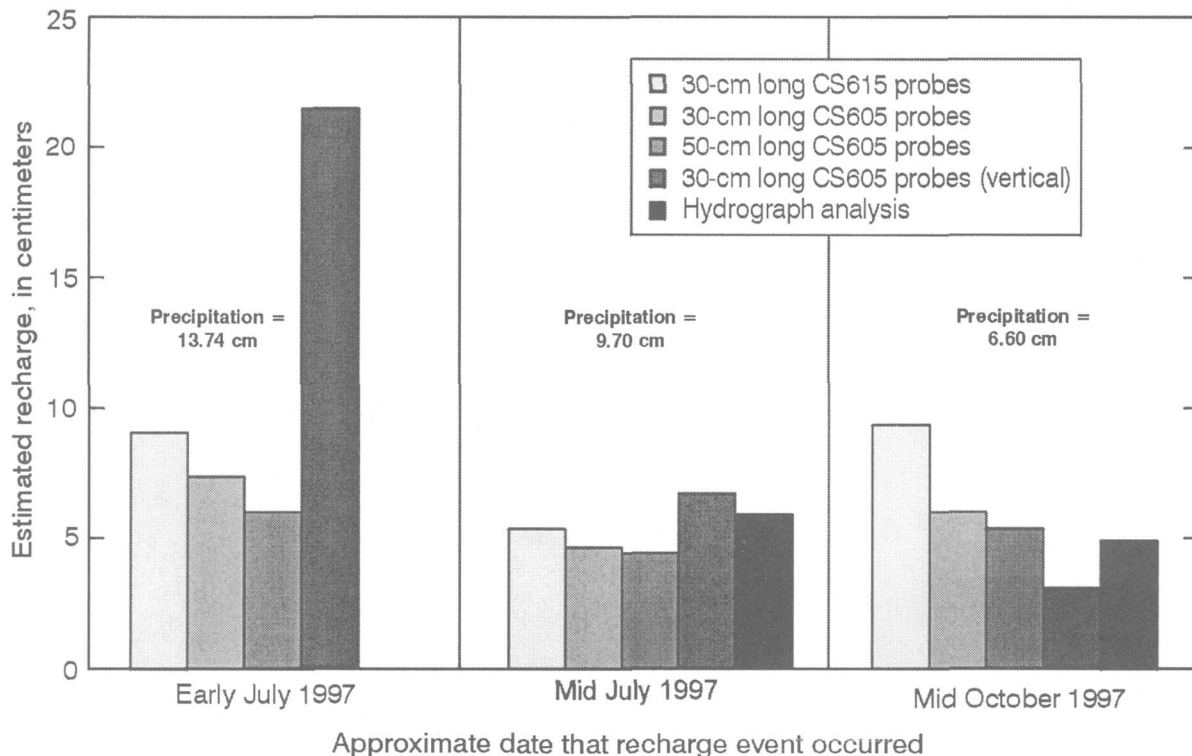


**Figure 7.** Recharge estimates based on the different probes near Well 981 compared to estimates based on hydrograph analysis, July – December 1997.

downward through the oil body and increases the contact between ground water and the oil, increasing the rate of dissolution.

## SUMMARY AND CONCLUSIONS

Ground-water recharge is an important factor affecting the Bemidji, Minnesota crude-oil spill site where about 400,000 liters of crude oil remained in the ground after remediation was completed following the 1979 pipeline break. An automated data logging system was used to measure unsaturated zone properties relevant to estimating recharge and evaluating their effects of the dissolution of oil. The performance of several different soil-moisture probes manufactured by Campbell Scientific Inc. was evaluated. Analysis of the temporal variation in soil temperature was both qualitatively and quantitatively useful in estimating the timing, depth, and duration of recharge events.

Laboratory and field testing of the soil-moisture probes indicated that the Campbell Scientific CS615 probe was better suited to estimating recharge at the Bemidji crude-oil spill site than the CS605 probes, given the local soil and climatic conditions. Field testing indicated that the CS615 probes are better suited to the needs at the Bemidji site for the following reasons: (1) the CS615 probes provided a dependable and accurate means for long-term monitoring of soil moisture in the glacial outwash being studied; (2) the CS615 probe is somewhat easier to install in sandy soils than the standard CS605 probe; (3) data from the CS615 probes had less "noise" than data from the standard CS605 probes; and (4) the CS615 probe provided dependable and accurate data using limited power under the extreme weather conditions typical of northern Minnesota. The greater soil moisture measured by some of the vertically-oriented CS605 probes is somewhat surprising. Further

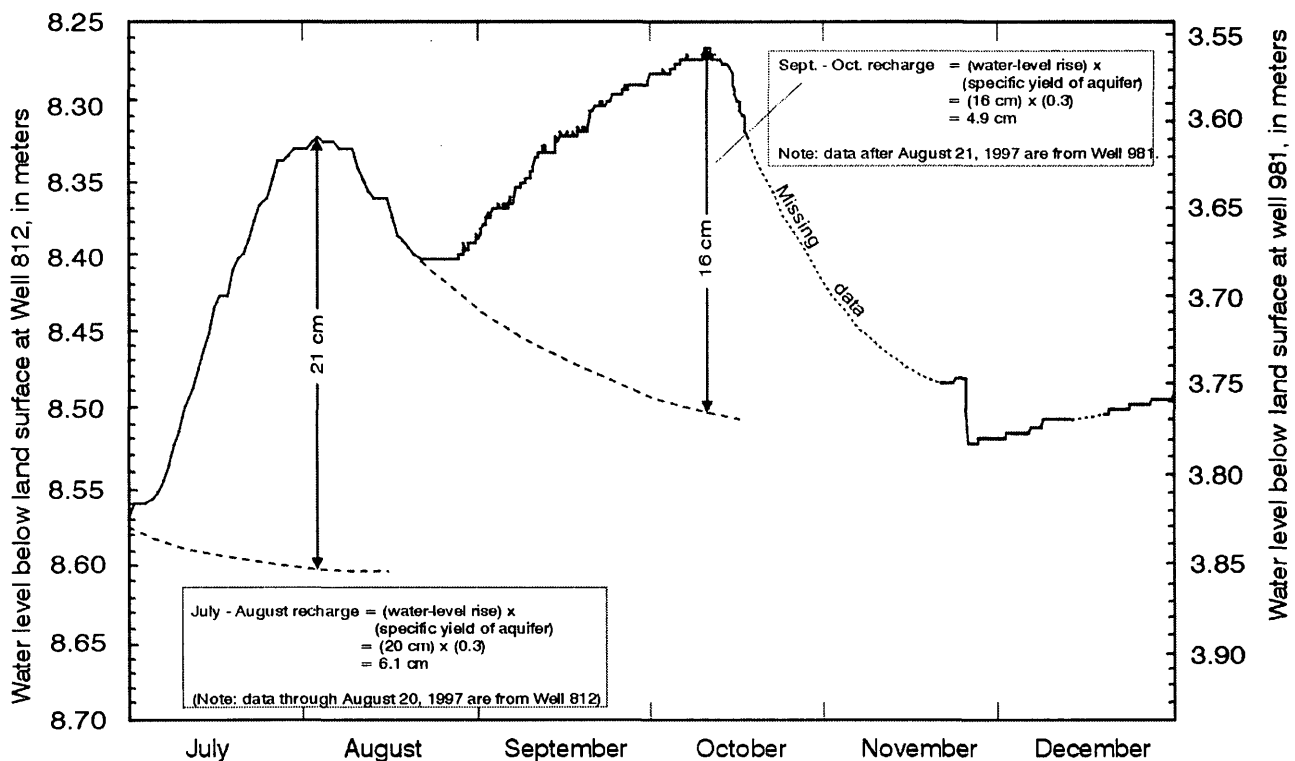


**Figure 8.** Water-level hydrograph and recharge calculations, July – December 1997.

laboratory or field research into this phenomenon may be warranted, the results of which would have transfer value to unsaturated-zone research using similar instrumentation.

Based on results of the preliminary testing, an array of CS615 soil-moisture probes, thermocouples, and zero-maintenance tensiometers were installed in the unsaturated zone near Well 9015 (north oil pool) in the fall of 1998. Seven CS615 probes and thermocouples were installed between the depths of 0.5 and 6.0 m. Four zero-maintenance tensiometers were installed between the depths of 1.0 and 2.5 m. The soil moisture and pressure data will be used to estimate ground-water recharge based on the zero flux plane method and to evaluate the effects of the dissolution of oil.

Computer simulations indicated that the rate of dissolution from the oil body is linearly related to the recharge rate. Additional multiphase flow model analyses are being conducted to quantify this increased dissolution. Additional multiphase flow model analyses are also being conducted to evaluate how dissolution is affected by recharge that varies in relation to the presence of crude oil in the unsaturated and saturated zones, discontinuous lenses of lacustrine silt and clay, and topography. The VS2DT code (Lappala and others, 1987; Healy, 1990) is also being used to estimate recharge rates and to evaluate the movement of water through the oil.

## CITED REFERENCES

- Essaid, H.I., Herkelrath, W.N., and Dillard, L.A., 1995, The influence of spatial variability of hydraulic properties on the flow of water near a subsurface oil body: EOS, Transactions, American Geophysical Union, v. 76, no. 46, p. F266.
- Harbaugh, A.W., and McDonald, M.G., 1996, User's documentation for MODFLOW-96, an update to the U.S. Geological Survey modular finite-difference ground-water flow model: U.S. Geological Survey Open-File Report 96-485, 56 p.
- Healy, R.W., 1990, Simulation of solute transport in variably saturated porous media with supplemental information on modifications to the U.S. Geological Survey's Computer Program VS2D: U.S. Geological Survey

- Water-Resources Investigations Report 90-4025, 125 p.
- Herkelrath, W.N., Hamburg, S.P., and Murphy, Fred, 1991, Automatic, real-time monitoring of soil moisture in a remote field area with time-domain reflectometry: Water Resources Research, v. 27, no. 5, p. 857-864.
- Lappala, E.G., Healy, R.W., and Weeks, E.P., 1987, Documentation of computer program VS2D to solve the equations of fluid flow in variably saturated porous media: U.S. Geological Survey Water-Resources Investigations Report 83-4099, 184 p.
- McDonald, M.G., and Harbaugh, A.W., 1988, A modular three-dimensional finite-difference ground-water flow model: U.S. Geological Survey Techniques of Water-Resources Investigations, book 6, chap. A1, 586 p.
- Pollock, D.W., 1994, User's Guide for MODPATH/MODPATH-PLOT, Version 3—A particle tracking post-processing package for MODFLOW, the U.S. Geological Survey finite-difference ground-water flow model: U.S. Geological Survey Open-File Report 94-464, 6 ch.
- Rasmussen, W.C., and Andreason, G.G., 1959, Hydrologic budget of the Beaver Dam Creek Basin Maryland. U.S. Geological Survey Water-Supply Paper 1472, 106 p.
- Solomon, D.K., Schiff, S.L., Poreda, R.J., and Clarke, W.B., 1993, A validation of the  $^3\text{H}/^3\text{He}$  method for determining groundwater recharge: Water Resources Research, v. 29, no. 9, p. 2951-2962.

## AUTHOR INFORMATION

- Geoffrey N. Delin, U.S. Geological Survey, Mounds View, Minnesota (delin@usgs.gov)
- William N. Herkelrath, U.S. Geological Survey, Menlo Park, California (wnherkel@usgs.gov)



# Coupled Biogeochemical Modeling of Ground-Water Contamination at the Bemidji, Minnesota, Crude Oil Spill Site

By Gary P. Curtis, Isabelle M. Cozzarelli, Mary Jo Baedecker, and Barbara A Bekins

## ABSTRACT

Fully-coupled multicomponent reactive solute transport simulations were performed for the groundwater contamination at the Bemidji, MN crude oil spill site. The simulations included the oxidation of the dissolved crude oil constituents by microorganisms using four different terminal electron acceptors:  $O_2$ ,  $MnO_2$ ,  $Fe(OH)_3$  and  $CO_2$ . The simulations also accounted for the dissolution of reactive phases resulting from the limited amount of each reactant, the formation of new phases containing  $Mn^{2+}$  and  $Fe^{2+}$ , and the outgassing of  $CO_2$  and  $CH_4$ . The simulations assumed that  $O_2$  was used preferentially and that all other terminal electron acceptors were used in parallel. Simulation results are presented that reproduce many of the features illustrated by the field data including the disappearance of the  $O_2$ , the appearance of  $Mn^{2+}$ ,  $Fe^{2+}$ , and  $CH_4$ , the pH values, the diminished concentrations of solid phases  $Fe^{+3}$  beneath the oil body as well as the increase in  $Fe^{+3}$ -containing solid phase concentrations in the dow

## INTRODUCTION

The dissolution and biodegradation of crude oil in an unconfined aquifer near Bemidji, MN has caused a diverse range of geochemical changes. Baedecker and others (1993) identified five geochemical zones that have developed as a result of these biodegradation reactions. These zones are depicted in figure 1 as zones I-V. Briefly, these zones have been described as: (I) the background water which is a Ca-Mg- $HCO_3$  water with a pH 7.6 to 7.8, that is saturated with oxygen, (II) a mixed zone characterized by low  $O_2$  and elevated dissolved organic carbon (DOC), (III) an anaerobic zone with high concentrations of DOC,  $Fe^{2+}$ ,  $Mn^{2+}$  and  $CH_4$ , and a pH of 6.8, (IV) a transition zone between highly reducing conditions and oxidized conditions, and (V) an impacted zone, that shows elevated concentrations of Ca and Mg.

There have been at least three previous reports on modeling the geochemical changes in the Bemidji aquifer but none have conducted fully coupled modeling. Bennett and others (1993)

matched the water composition in the anoxic core of the plume by conducting reaction path calculations that mixed water from a silty layer near zone II with water from the boundary between zones II and III followed by oxidation of DOC by goethite. Baedecker and others, (1993) reported on a reaction-path model along a flow path from the zone III toward zone IV. The simulations required outgassing of  $CO_2$  and  $CH_4$  even though the flow path was 2 meters below the water table surface. Although these mixing and reaction path calculations can account for some geochemical changes, they do not account for any limitations imposed on the hypothesized mixing by the flow system.

Essaid and others (1995) conducted two dimensional reactive transport simulations that accounted for the biodegradation of crude oil, the consumption of  $O_2$ , solid phase Mn(IV) and solid phase Fe(III) and the production of dissolved  $Mn^{2+}$ ,  $Fe^{2+}$ , and  $CH_4$ . These rate-controlled simulations showed that many of the features of the plume could be reproduced including the disappearance of  $O_2$ , the appearance of  $Mn^{2+}$ ,  $Fe^{2+}$ ,  $CH_4$  and the disappearance of DOC, and volatile DOC, the two forms of dissolved crude oil

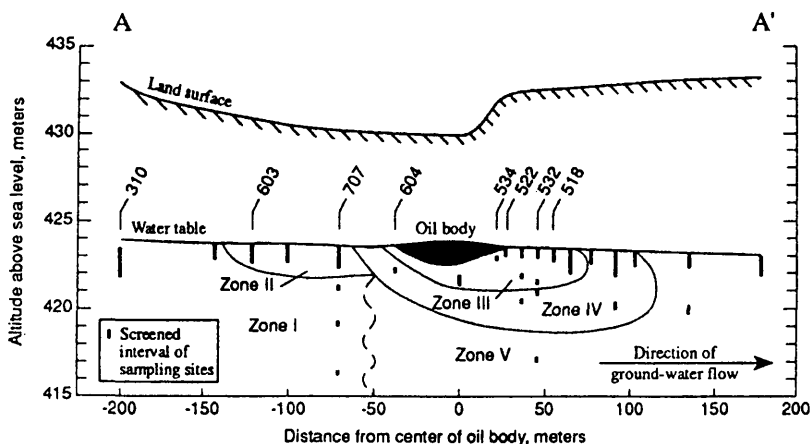


**Figure 1.** A cross section of the Bemidji aquifer (after Baedecker and others, 1993).

considered. These simulations did not include inorganic reactions including the carbonate system or the redox reactions involving  $O_2$  and the reduced forms of Mn and Fe. In addition, precipitation of new phases containing reduced Fe and Mn was accounted for using a single constant for each metal and the formation of new phases containing oxidized Fe and Mn in the transition zone was ignored. Accurately accounting for these reactions may be important because they involve the electron acceptors for the biodegradation reactions which cause the geochemical changes in the aquifer.

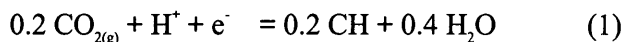
The objectives of this work were to demonstrate the use of RATEQ (Curtis, in preparation), a fully coupled model for simulating biogeochemical transport, and to reproduce the field observations for multiple inorganic and organic species.

## CONCEPTUAL MODEL

### Geochemical Reactions

Modeling reactions involving the degradation of dissolved crude oil is difficult, in part, because crude oil is a complex mixture of many individual compounds. In view of this complexity, the dissolved crude oil is represented here as a generic hydrocarbon and denoted as CH (Baedecker and others, 1993; Bennett and others, 1993). This approach establishes the nominal redox-state of the crude oil and allows one to

express the degradation reactions as stoichiometrically balanced reactions. Formulating these reactions is critical for both mathematically coupling the oxidation of the electron donors (CH) to the different terminal electron acceptors, and for formulating the fully-coupled, multicomponent mass balance model. The half-reaction for the formation of CH is



The logarithm of the equilibrium constant (log K) for this reaction was found to be 2.1 using the approach of MacFarlane and Sims (1993).

In the aquifer at Bemidji, the dominant electron acceptors available for the oxidation of CH are  $O_2$ , solid phase Mn(IV), solid phase Fe(III), and  $CO_2$ . Neither  $NO_3^-$  nor  $SO_4^{2-}$  are significant electron acceptors in this system because the concentration is too small (Baedecker and others, 1993; Bennett and others, 1993). The half-reactions for the electron acceptors are coupled with that for the electron donor (eqn 1) to give the final, stoichiometrically balanced reaction for the oxidation of the hydrocarbon (table 1). Each reaction in table 1 is written for the oxidation of 0.2 moles of CH. Thus, the log K values illustrate the thermodynamic basis for the sequential use of electron acceptors that is often observed for microbial processes.

In addition to the reactions involving the biodegradation of the dissolved crude oil, many other geochemical reactions occur in the aquifer.

**Table 1:** Reactions for the oxidation of CH by various electron acceptors.

Reactions	logK
$.2 \text{ CH} + .25 \text{ O}_2(\text{g}) + .1 \text{ H}_2\text{O} = .2 \text{ HCO}_3^- + .2 \text{ H}^+$	18.6
$.2 \text{ CH} + .5 \text{ MnO}_{2(\text{s})} + .8 \text{ H}^+ = .2 \text{ HCO}_3^- + .5 \text{ Mn}^{2+} + .4 \text{ H}_2\text{O}$	18.6
$.2 \text{ CH} + \text{Fe}(\text{OH})_{3(\text{s})} + 1.8 \text{ H}^+ = 2 \text{ HCO}_3^- + \text{Fe}^{2+} + 2.4 \text{ H}_2\text{O}$	13.9
$.2\text{CH} + .225 \text{ H}_2\text{O} = .075 \text{ HCO}_3^- + .125 \text{ CH}_4 + .075 \text{ H}^+$	.9

The bulk mineralogy of the Bemidji aquifer consists primarily of quartz, feldspars, calcite and dolomite, (Bennett and others, 1993). For the simulations presented here, calcite and dolomite were included in the simulations, as were the aqueous carbonate and hydroxide species. In addition, a number of other redox reactions, sometimes called secondary reactions (Hunter and others, 1998), such as the oxidation of  $\text{Fe}^{+2}$  by  $\text{MnO}_2$  or  $\text{O}_2$  have been included.

One-dimensional reactive transport simulations were conducted along a 400m flow tube that extends from A to A' on figure 1. The initial conditions and the influent boundary condition were taken to match the average groundwater chemistry at well 310. The reactive phases and their relative amounts, expressed in units of moles of solid per liter of groundwater were; calcite (2M), dolomite (.25M),  $\text{MnO}_2$  (0.001M) and  $\text{Fe}(\text{OH})_3$  (0.12M). Given that the  $\text{O}_2$  concentration in the aquifer was  $2.5 \times 10^{-4}\text{M}$ ,  $\text{Fe}(\text{OH})_3$  clearly has the potential to be one of the most important electron acceptors in the aquifer. Note that if all of  $\text{Fe}(\text{OH})_3$  was reduced by CH, there would be a consumption of approximately 0.2 mole of  $\text{H}^+$  per liter of aquifer (table 1). Extractions of cores taken from the site showed that after approximately 14 years half of the initial of  $\text{Fe}(\text{OH})_3$  present beneath the oil body had been removed ( Tuccillo and others, 1998) suggesting that there was a large consumption of  $\text{H}^+$ . Because of this large consumption of  $\text{H}^+$ , which tends to increase the pH, matching the observed decrease in the field pH was difficult.

## REACTIVE TRANSPORT SIMULATIONS

The crude oil was assumed to dissolve into the groundwater according to a first order dissolution process:

$$\frac{\partial C}{\partial t} = k_{diss} (C_s - C) \quad (2)$$

where

- $C$  is the concentration of CH
- $C_s$  is the concentration of the CH in equilibrium with the crude oil, and
- $k_{diss}$  is the first order dissolution constant.

The dissolution rate used in the simulations varied with distance along the flow path. The first order dissolution rate constant was zero except in Zone II ( 25 to 100 m upgradient from the center of the oil body) where the value was  $5 \times 10^{-4} \text{ d}^{-1}$  and in Zone III ( 25 upgradient to 25m down gradient from the center of the oil body) where the value was  $5 \times 10^{-2} \text{ d}^{-1}$ . Outside of the zones where oil was assumed to be dissolving into the groundwater, the system was assumed to be in contact with atmospheric concentrations of  $\text{O}_2$ . This was included downgradient of the oil body as an approximation to the annual water table fluctuations of approximately 0.5 m.

## Degradation Rates

The reactive transport simulations presented here assumed that the microbial populations were constant in space and time. This assumption simplified the parameter estimation because it was difficult to obtain

growth and decay parameters that gave acceptable simulation results. This difficulty may have been because of the autocatalytic nature of the reaction stoichiometry; if the biomass is allowed to vary, then the rate of the biodegradation reaction depends on the biomass produced by the reaction. A second difficulty encountered with simulating microbial growth was that the populations tended to grow unbounded which contrasts with moderate populations observed in the field (Essaid and others 1995). The actual growth may be limited by nutrients such as phosphorous (Rodgers and others, 1999), or nitrogen (Essaid and others, 1995), although in the latter study it was found that it was still necessary to artificially limit growth. The assumption of a constant biomass is consistent with the approach used to simulate biodegradation with very low amounts of biomass produced per mole of carbon oxidized for methanogens at a creosote spill at Pensacola, FL (Bekins and others, 1993).

Although the biomass was assumed to be constant in time, a dual Monod kinetics formulation was used to simulate the reaction between the electron donor and the electron acceptor. For example, the oxidation of CH by Fe(OH)<sub>3</sub>, has a rate law of the following form:

$$r = v_{max} \left( \frac{C_{CH}}{C_{CH} + K_{CH}} \right) \left( \frac{C_{Fe}}{C_{Fe} + K_{Fe}} \right) \left( \frac{I_{O_2}}{C_{O_2} + I_{O_2}} \right)$$

where

- $v_{max}$  the maximum rate of substrate utilization,
- $C_{CH}$  is the concentration of CH,
- $K_{CH}$  is the half-velocity coefficient for the oxidation of CH by Fe(OH)<sub>3</sub>,
- $C_{Fe}$  is the concentration of Fe(OH)<sub>3</sub>,
- $K_{Fe}$  is the half-velocity coefficient for the reduction of Fe(OH)<sub>3</sub> by CH,
- $I_{O_2}$  is the inhibition constant for the effect of O<sub>2</sub> on the Fe reduction rate, and
- $C_{O_2}$  is the concentration of O<sub>2</sub>.

Rate expressions of this form are used for each of the reactions listed in table 1.

## Results and Discussion

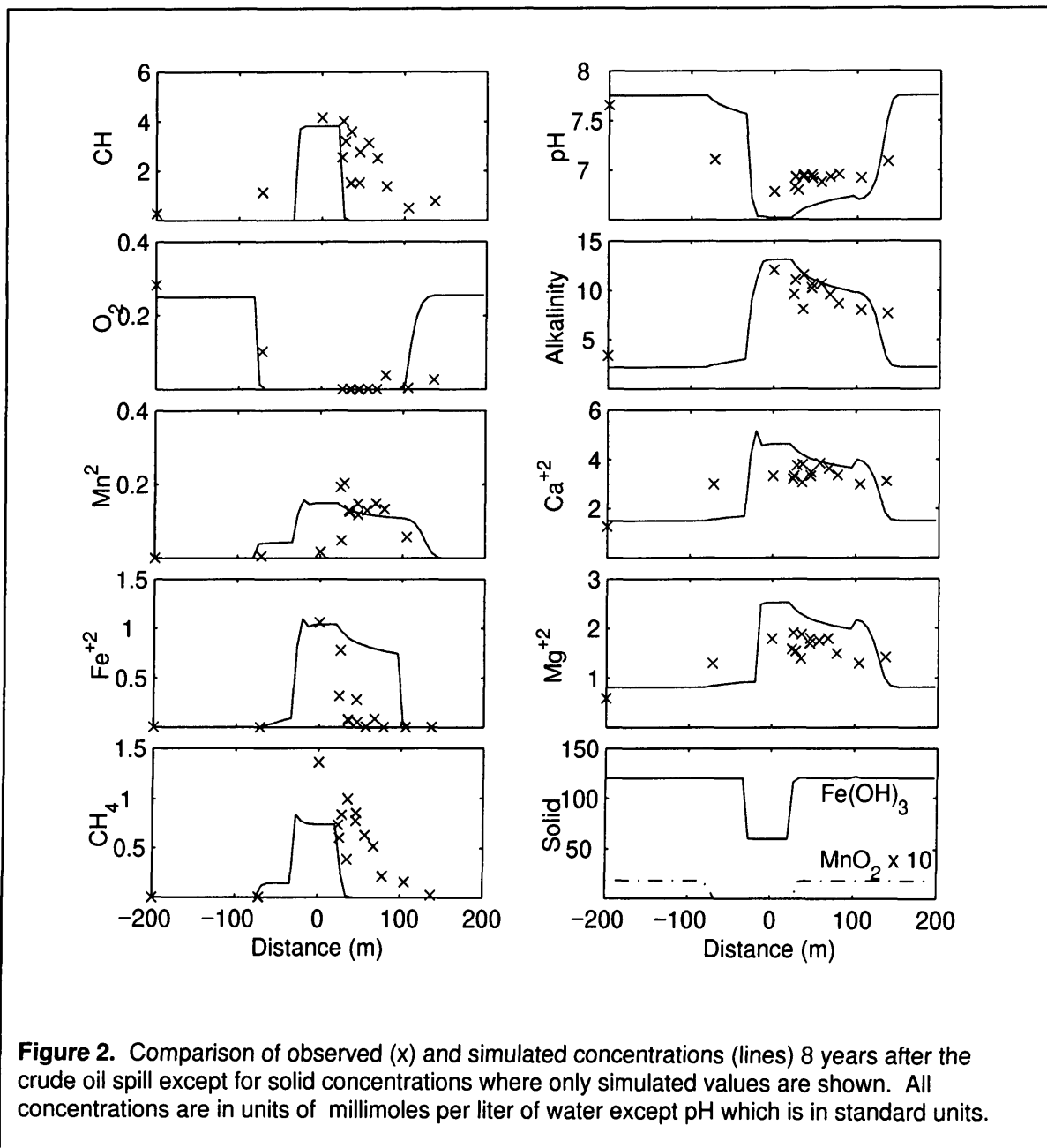
The simulation results are presented in figure 2 and are compared with data obtained in 1987 (Baedecker and others, 1993, Cozzarelli and others, 1999). The Monod parameters used in these simulations were obtained by setting the half velocity coefficient to the initial concentration of the electron acceptor, or the saturated concentration in the case of CH, and adjusting the value of  $v_{max}$  to obtain an acceptable visual fit to the data. The values used in the final simulations are summarized in Table 2. Note that only anaerobic processes were inhibited by using an inhibition constant of  $10^{-7}$  M O<sub>2</sub>. Fe(OH)<sub>3</sub> reduction was not inhibited by MnO<sub>2</sub> because Fe<sup>2+</sup> produced can be oxidized back to Fe<sup>3+</sup> by an equilibrium controlled redox reaction with MnO<sub>2</sub>. Methanogenesis was not inhibited by the presence of Fe(OH)<sub>3</sub> for reasons discussed below.

The simulations in figure 2 reproduce the observed trends illustrated by the data. These trends include the appearance of CH<sub>4</sub>, Fe<sup>2+</sup>, Mn<sup>2+</sup> and CH<sub>4</sub>, and the disappearance of O<sub>2</sub>. For CH<sub>4</sub>, only about 10% of the quantity produced by methanogenesis is illustrated in figure 2. The balance of the methane was removed in the model as a gas. A gas phase containing both CH<sub>4(g)</sub> and CO<sub>2(g)</sub> in equilibrium with aqueous solution was assumed to form when the sum of the partial pressures of CH<sub>4(g)</sub> and CO<sub>2(g)</sub> exceeded 1 atmosphere. The simulations also reproduce the observed decrease in the field pH, as well as increases in Ca<sup>2+</sup>, Mg<sup>2+</sup>, and alkalinity. The simulated solid phase Fe(OH)<sub>3</sub> is not completely depleted which agrees with observations from sediments samples taken from cores obtained at the site (Tuccillo and others, 1999). For CH, the simulations show little migration downgradient

**Table 2:** Reaction constants used for RATEQ simulation. Values not used in simulations are denoted by a '-'

Acceptor	$v_{max}$ (d <sup>-1</sup> )	$K_{CH}$ (M)	$K_{Acr.}$ (M)	$I_{O_2}$ (M)
O <sub>2</sub>	1x10 <sup>1</sup>	1x10 <sup>-3</sup>	1x10 <sup>-4</sup>	-
MnO <sub>2</sub>	5x10 <sup>-3</sup>	1x10 <sup>-3</sup>	1x10 <sup>-4</sup>	10 <sup>-8</sup>
Fe(OH) <sub>3</sub>	4x10 <sup>-5</sup>	1x10 <sup>-3</sup>	6x10 <sup>-2</sup>	10 <sup>-8</sup>
CO <sub>2</sub>	2x10 <sup>-4</sup>	1x10 <sup>-3</sup>	-	10 <sup>-8</sup>





from the source area probably because the crude oil has been approximated in these initial simulations by a single compound which is assumed to be completely biodegradable. It is known that even slight structural differences of individual compounds has a large impact on the extent of degradation (Eagenhouse and others, 1993). Similarly, the  $O_2$  concentration increased to saturated values 100 meters downgradient from the source to reflect reoxygenation of the groundwater, possibly from fluctuations of the water table.

The simulations illustrated in figure 2 were obtained by assuming that iron reduction and

methanogenesis occurred simultaneously. This approach contradicts the often assumed process of sequential use of electron acceptors by microorganisms, but is supported by the observed co-occurrence of iron reducing and methanogenic bacteria (Bekins and others, 1999). This was the only set of reaction constants that was found that matched the observed decrease in pH and gave relatively close agreement for dissolved  $Fe^{2+}$  and solid phase  $Fe^{+3}$ . The protons consumed in the oxidation of  $Fe(OH)_3$ , are balanced by protons produced simultaneously by methanogenesis.

## CONCLUSIONS

Coupled reactive transport simulations were performed to reproduce the observed geochemical trends in ground water at the Bemidji crude oil spill site. The simulations accounted for oxidation of CH<sub>4</sub>, a dissolved crude oil constituent, by four electron acceptors: O<sub>2</sub>, MnO<sub>2</sub>, Fe(OH)<sub>3</sub> and CO<sub>2</sub>. The simulations reproduced the general observed trends in CH<sub>4</sub>, Fe<sup>+2</sup>, Mn<sup>+2</sup>, CH<sub>4</sub>, Ca<sup>+2</sup>, Mg<sup>+2</sup>, alkalinity, and pH. In this model, it was necessary to allow Fe(OH)<sub>3</sub> reduction to occur simultaneously with methanogenesis to match the pH observed in the field. This approach contradicts the concept of sequential use of electron acceptors by micro-organisms, but it is supported by the coexisting iron-reducing and methanogenic microbial populations at the site (Bekins and others, 1999).

## REFERENCES

- Baedecker, M.J., Cozzarelli, I.M., Eganhouse, R.P., Siegel, D.I., and Bennett, P.C., 1993, Crude oil in a shallow sand and gravel aquifer, III—Biogeochemical reactions and mass balance modeling in anoxic groundwater: *Applied Geochemistry*, v8, p529-549.
- Bekins, B.A. Cozzarelli, I.M., Godsy, E.M. Warren, E., Tuccillo, M.E., Essaid, H.I., and Paganelli, V.V., 1999, Chemical and Physical Controls on Microbial Populations in the Bemidji Toxics Site Cured-Oil Plume, in U.S. Geological Survey Toxic Substances Hydrology Program—Proceeding of the Technical Meeting, Charleston, South Carolina, March 8-12, 1999—Volume 3—Subsurface Contamination from Point Sources: U.S. Geological Survey Water Resources Investgations Report 99-4018C.
- Bekins, B.A., Godsy, E.M. and Goerlitz, D.F., 1993, Modeling Steady-State Methanogenic Degradation of Phenols in Groundwater: *Journal of Contaminant Hydrology*, v. 14, no. 3-4, p. 279-294.
- Bennett, P.C., Siegel, D.I., Baedecker, M.J. and Hult, M.F., 1993, Crude oil in a shallow sand and gravel aquifer, I – Hydrogeology and inorganic geochemistry; *Applied Geochemistry*, v8, p529-549.
- Cozzarelli, I.M., Baedecker, M.J., Eganhouse, R.P., Tuccillo, M.E., Aiken, G.R., Bekins, G.A., Jaeschke, J.B., 1999, Long-term geochemical evolution of the Bemidji Toxics site cured-oil plum, in U.S. Geological Survey Toxic Substances Hydrology Program—Proceeding of the Technical Meeting, Charleston, South Carolina, March 8-12, 1999—Volume 3—Subsurface Contamination from Point Sources: U.S. Geological Survey Water Resources Investgations Report 99-4018C.
- Eganhouse, R.P., Baedecker, M.J., Cozzarelli, I.M., Aiken, G.R., Thorn, K.A., and Dorsey, T.F., 1993, Crude oil in a shallow sand and gravel aquifer-II. Organic geochemistry: *Applied Geochemistry*, v. 8, p. 551-557.
- Essaid, H.I., Bekins, B.A., Godsy, E.M., Warren, E., Baedecker, M.J. and Cozzarelli, I.M., Simulation of aerobic and anaerobic biodegradation processes at a crude oil spill site, *Water Resources. Research.*, 31, p3309-3327.
- Hunter, K.S., Wang, Y, Van Cappellen, P., 1998, Kinetic modeling of microbially-driven redox chemistry of subsurface environments: coupling transport, microbial metabolism and geochemistry, *Journal of Hydrology*, v 209, p 53-80.
- McFarlane, M.J. and Sims, R.C., 1991, Thermodynamic framework for evaluating PAH degradation in the subsurface, *Ground Water*, 29, p 885-896.
- Rodgers, J.R., P.C. Bennett, and W.J. Choi, 1998, Feldspars as a source of nutrients for microorganisms, *American Mineralogist*, v. 83, 1532-1540.
- Tuccillo, M.E., Cozzarelli, I.M., and Herman, J.S., 1999, Iron reduction in the sediments of a hydrocarbon-contaminated aquifer: *Applied Geochemistry*, v. 4, no. 5, p. 71-83.

## AUTHOR INFORMATION

Gary P. Curtis and Barbara A. Bekins, U.S. Geological Survey, Menlo Park, California

Isabelle M. Cozzarelli and Mary Jo Baedecker, U.S. Geological Survey, Reston, Virginia

# Determining BTEX Biodegradation Rates Using In Situ Microcosms at the Bemidji site, Minnesota: Trials and Tribulations

By E. Michael Godsy, Ean Warren, Isabelle M. Cozzarelli, Barbara A. Bekins, and Robert P. Eganhouse

## ABSTRACT

In situ microcosms (ISMs) were installed in an aquifer contaminated by crude oil to study the in situ biodegradation of monoaromatic hydrocarbons. One was placed in an area where iron reduction predominates (ISM-Fe) and the other in an area where methanogenesis predominates (ISM-CH<sub>4</sub>). Numerous problems were encountered during installation and operation of the ISM-CH<sub>4</sub> microcosm and therefore monitoring of it has been temporarily discontinued. Biodegradation rates determined from field concentrations suggested that degradation for the ISM-Fe should proceed in the following order: (1) toluene and *o*-xylene – ~12 days; (2) *m*-, *p*-xylene – ~400 days; (3) benzene – 700 days; (4) ethylbenzene – ~1600 days. Samples taken from the ISM-Fe at days 36 and 68 indicated that toluene biodegradation was occurring. Iron, manganese, CO<sub>2</sub>, alkalinity, and low molecular weight volatile fatty acids increased while toluene concentration decreased by approximately 20 percent. All other organic and inorganic compounds remained at initial levels including the tracer with the exception of sodium, chloride, and sulfate. These species increased sharply starting at approximately day 8 and have remained elevated since then for an unknown reason.

## INTRODUCTION

On August 20, 1979, approximately  $1.7 \times 10^6$  liters (L) of crude oil was released in northern Minnesota due to a high-pressure pipeline rupture. At the completion of cleanup,  $4.0 \times 10^5$  L of the oil remained. The majority of the oil pooled near the rupture site in the north pool while a smaller amount flowed overland to the southeast to a local depression and pooled to the south (fig. 1). At both sites, the remaining oil percolated through the unsaturated zone and pooled on the water table (Hult, 1984).

The fate, transport, and multiphase flow of the hydrocarbons present in the oil depend not only on geochemical processes, but also on volatilization, dissolution, biodegradation, transport, and sorption. All of these processes have been studied in detail by an interdisciplinary team from the U.S. Geological Survey and a number of universities.

The natural attenuation of water-soluble crude-oil organic due to biodegradation in the subsurface plume at Bemidji, Minn. is now well documented (Baedecker and others, 1993; Eganhouse and others, 1993, Essaid and others, 1995). In this paper we focus on the fate of a subset of the monoaromatic hydrocarbons: benzene, toluene, ethylbenzene, and *ortho*-, *meta*-, and *para*-xylene (BTEX). The major factor in the natural attenuation of the BTEX compounds is the ubiquitous degradative activity of the resident microbial populations. In order to formulate numerical models that simulate the transport and biodegradation processes, the biodegradation potentials and rates must be determined under naturally-occurring redox conditions.

The availability of electron acceptors is believed to determine the biodegradation potentials and rates of BTEX compounds. Availability and thermodynamic principles predict the sequence of electron acceptors used for biodegradation (Stumm and Morgan, 1981). The theoretical sequence is

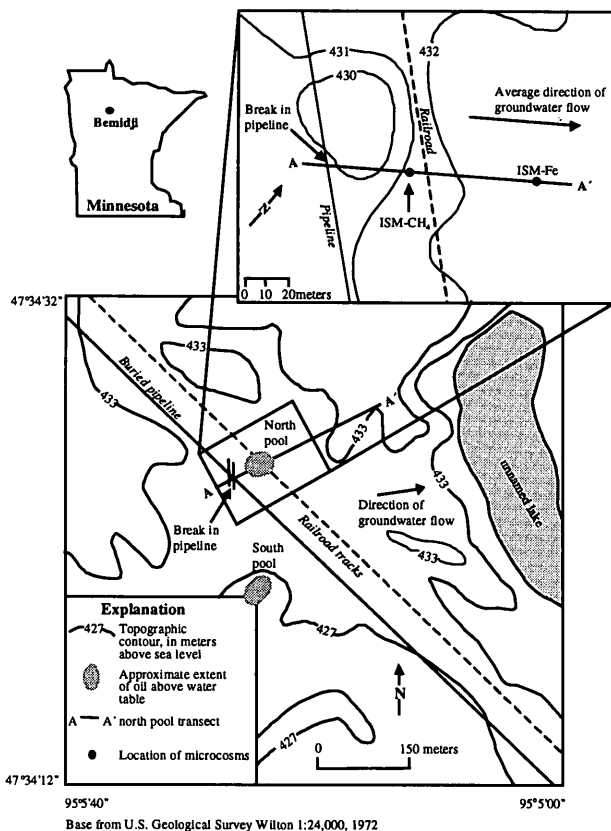


**Figure 1.** The study site at Bemidji, Minnesota, showing A-A' transect, oil bodies, and oil pipeline.

aerobic biodegradation, followed by denitrification, manganese and iron reduction, sulfate reduction, and methanogenesis. This sequence has been shown to cause zonation in a contaminant plume with different electron accepting biodegradation processes dominating in different redox zones. At Bemidji, over fifteen years of observations have demonstrated that three redox zones predominate in the contaminant plume: (1) aerobic, (2) iron reducing, and (3) methanogenic (Baedecker and others, 1993; Bekins and others, 1999).

In situ biodegradation rates of the volatile organic carbon fraction at the site have been determined by fitting field concentrations using a two-dimensional reactive solute transport model with Monod biodegradation kinetics (Essaid and others, 1995). Monod kinetic constants for the individual BTEX compounds, determined by fitting field concentrations to a steady-state one-dimensional advective equation that incorporates Monod kinetics (Parlange and others, 1984), were used to predict time required for biodegradation of

the individual BTEX compounds. We report here the results of an ongoing BTEX biodegradation experiment conducted with in situ microcosms (ISMs).

## IN SITU MICROCOSM TECHNIQUE

The in situ microcosm (ISM) technique to determine biodegradation potentials and rates was developed at the University of Waterloo (Gillham and others, 1990a; Gillham and others, 1990b). The ISM consists of a stainless steel cylinder that encloses a volume of the aquifer that, once loaded with ground water spiked with specific hydrocarbon compounds, can be monitored over time for degradation. Unlike a field injection-tracer test where there is of the contaminant plume encountering areas of different redox potentials, differing microbial populations, and heterogeneity in the aquifer, this technique isolates a portion of the aquifer assuring the same conditions throughout the experiment.

## Location of ISM

Both ISMs were placed along the A-A' transect (figs. 1 and 2). The microcosm identified as ISM-CH<sub>4</sub> (borehole 9828) was placed in an area of the contaminant plume where biodegradation processes were predominately methanogenic. The

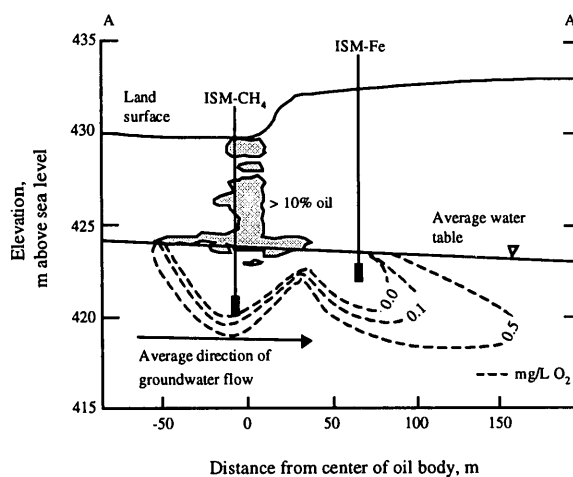


**Figure 2.** Cross section along transect A-A' showing locations of the oil body, microcosms and concentrations of dissolved oxygen within the saturated zone, Bemidji, Minnesota.

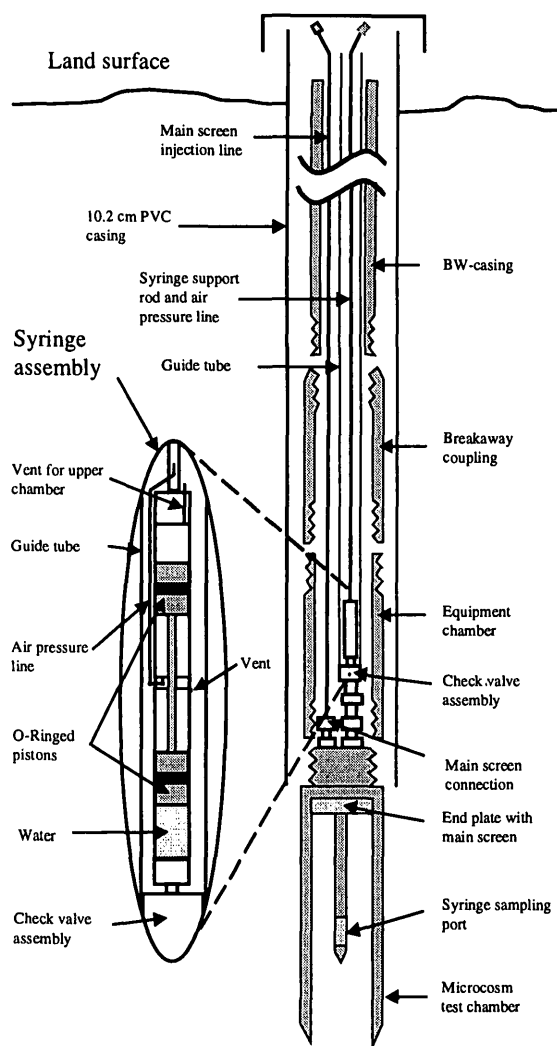


**Figure 3.** Cross section of the in-situ microcosm with an exploded view of the sampling syringe. Drawing not to scale.

top of the microcosm test chamber was set at an elevation of 421.1 meters (m) above sea level. ISM-Fe (borehole 9825) was placed in an area where biodegradation was predominantly by iron-reduction and set at an elevation of 432.3 m above sea level (Bekins and others, 1999).

### Description of ISM

The ISM consists of an 8.3 centimeter (cm) inside diameter (id) x 88 cm stainless steel cylindrical test chamber open at the bottom and bounded at the inside-top by a set of coarse and fine stainless steel mesh screens (fig. 3). The main screens are used to remove and reinject spiked ground water into the test chamber. The design

allows even flow through the screens assuring plug flow into the test chamber during reinjection. The test chamber isolates a total aquifer volume of 4.76 L or 1.43 L of ground water (assuming a porosity of 0.3). A depth adjustable, stainless steel sampling port, with a fine mesh screen, extends 26 cm into the test chamber. Water samples are collected from the central port with a syringe assembly (see expanded section of figure 3).

The stainless steel syringe is 70 cm x 1.5 cm outside diameter (od) and was developed by Fred Murphy (U.S. Geological Survey, Menlo Park, Calif.). It is divided into two chambers – a lower 30 cm x 1.2 cm id water sampling chamber and an upper compressed air chamber. The bottom of the syringe is fitted with a nipple (not shown in figure 3) that fits into and releases the spring-loaded ball in the check valve assembly for sample collection from the central spike port. Connected to the top of the syringe are 2 m lengths of 0.6 cm (od) stainless steel tubing that act as both the syringe support rod and the compressed air line.

An equipment chamber, threaded onto the top of the test chamber, protects the tubing connector and the syringe check valve assembly. A breakaway coupling with reverse threads adapts the equipment chamber to the lengths of BW-casing. A 6.4 millimeter (mm) Teflon tube for spiking and a polypropylene syringe guide tube (2.5 cm) connect to the ISM and pass through the large diameter metal (BW) casing to the surface.

### Installation of ISM

The ISM and the attached BW casing were installed through the center of 15.2 cm hollow stem augers equipped with a wire-line, surface-connected knockout-plug in the cutting bit to prevent the cuttings from being carried up the interior of the augers. After drilling to the desired depth, the ISM was lowered through the augers until it rested on the knockout plug. The augers were pulled up slightly to allow the displacement of the knockout plug by the ISM. After the knockout plug was opened, the ISM was advanced into the undisturbed aquifer sediment using an electric vibrating hammer until the top of the test chamber was just below the bottom of the augers. A 10.2 cm PVC casing was then installed to the bottom of the augers and the augers removed leaving the ISM with sampling tubes and both the

BW and PVC casings in place. The space between the PVC casing and the aquifer sediment was filled with the drill cuttings.

### Loading of ISM

Ground water was pumped from a nearby well that was screened at the target depth of the ISM (532 B for the ISM-CH<sub>4</sub> and 531 B for the ISM-Fe) until temperature and pH stabilized (approximately 5 casing volumes). At this time, 10 L of ground water was pumped into a 20 L Tedlar gas-sampling bag that was immersed in an ice filled picnic cooler. This was equivalent to approximately 7 ISM test chamber volumes. Prior to filling, the sampling bag was flushed five times with O<sub>2</sub>-free Argon. The hydrocarbon and conservative tracer spike compounds were added carefully to the ground water in the sampling bag to exclude O<sub>2</sub>. The hydrocarbon solution was thoroughly mixed and introduced by gravity into the ISM through the main screen injection line.

### Sampling of ISM

Prior to sampling, the pistons were pushed to the bottom of each chamber by a set rod inserted in the upper chamber vent. The stainless steel syringe was then attached to the support tubing and adjusted to withdraw 10 milliliters (mL) of water.

This was accomplished by placing a set rod in the upper chamber vent to stop the piston from travelling the complete 30 cm distance. Ten mL was determined to be the dead volume of the sampling port and check valve assembly. The syringe was lowered down the guide tube until reaching the check valve assembly. The syringe was then raised approximately 30 cm and jammed down into the check valve assembly. Approximately 400 kilopascals (kPa) of pressure was applied to the syringe from a portable air compressor. This compressed air displaced the pistons to the top of each chamber of the syringe. The lower chamber was simultaneously filled with a water sample from the microcosm. The dead volume was discarded. The set rod was removed and the syringe was again lowered to the ISM and a full 30 mL water sample was taken. The syringe was detached from the ISM by a gentle pull, elevated to land surface, and aliquots of the sample were transferred to the appropriate bottle by manually depressing the upper piston with a metal rod passed through the upper vent.

## MATERIALS AND METHODS

### BTEX Solution

The spiked ground-water solution could not

**Table 1.** Concentrations of compounds used in the BTEX solution for the ISM-Fe compared to the observed maximum field concentration in well 531 B at the Bemidji site, Minnesota.

Compound	Concentration (µg/L)	
	Maximum field	Spike solution
Benzene-D6	2100	2000
Toluene	10	1000
Ethylbenzene	323	650
<i>m</i> -xylene	78	250
<i>p</i> -xylene	78	250
<i>o</i> -xylene	20	150
isopropylbenzene	36	200
1-methyl-3-ethylbenzene	29	150
1-methyl-2-isopropylbenzene	6	100
1-methyl-4-isopropylbenzene	10	100
1,3-dimethyl-2-ethylbenzene	26	100
1,3-dimethyl-4-ethylbenzene	17	100
1,2,3,5-tetramethylbenzene	34	150
1,2,3,4-tetramethylbenzene	58	150

**Table 2.** Sampling scheme and methods for the ISM-Fe.

Parameter	Container	Bottle volume (mL)	Sample volume (mL)	Preservation (all chilled)	Analysis method
pH	Vial	5	2	None	Electrode
Alkalinity	Vial	5	2	0.2 $\mu\text{m}$ nylon filter	Titration
Dissolved gases	Serum bottle, evacuated	10	2	HgCl <sub>2</sub>	Headspace GC
Organic intermediates	Vial	5	10	Zero headspace	Acid ether extract, GC/MS
BTEX compounds	Glass vial	5	5	HgCl <sub>2</sub> , zero headspace	Purge & trap GC/MS
Fatty acids	Vial	5	2.5	HgCl <sub>2</sub>	IC
Cations	Plastic bottle	10	4	0.2 $\mu\text{m}$ nylon filter, 0.5% nitric acid	ICP/MS
Anions	Vial	5	2.5	0.2 $\mu\text{m}$ nylon filter	IC

be loaded into the ISM-CH<sub>4</sub> for unknown reasons; therefore, the composition of the solution is given only for the ISM-Fe (table 1). A hydrocarbon mixture was prepared in the laboratory by mixing the desired volumes of the neat compounds in an ampoule. A concentrated hydrocarbon solution was prepared in the field by injecting 59.5 microliters of this mixture into 200 mL of the ground water and mixing in a sonication bath for 60 min. Then, all of the concentrated solution was injected into approximately 10 L of ground water from well 531B. A conservative tracer, KBr was then added to a final concentration of 30 milligrams/liter (mg/L) as Br.

### Sampling Protocol

Samples from ISM-Fe were analyzed for pH, alkalinity, intermediate organic acids, anions including low molecular weight volatile fatty acids (VFAs), cations, hydrocarbons, and dissolved CH<sub>4</sub> and CO<sub>2</sub> as outlined in table 2. Biodegradation rates determined from field concentrations suggested that the BTEX compounds for the iron reducing ISM should degrade in the following order: (1) toluene and *o*-xylene – ~12 days; (2) *m*-, *p*-xylene – ~400 days; (3) benzene – ~700 days; (4) ethylbenzene – ~1600 days. The sampling scheme was designed to obtain as many samples as possibly for each compound within the limits of the total volume present in the ISM.

### Analytical Techniques

Alkalinity was determined in the laboratory with an automatic titrator and pH was determined in the field with an electrode. The cations were determined using an ICPMS. Dissolved gasses were determined according to the method described Godsy and others (1992). The hydrocarbons were analyzed by purge and trap capillary gas chromatography with ion trap detection as described by Eganhouse and others (1999).

The anions and low-molecular weight fatty acids (formate, acetate, propionate, and butyrate; VFA) were determined using a Dionex Ion Chromatography System equipped with an advanced gradient pump with a conductivity detector, an anion self-regenerating suppressor with an autosuppression external water mode, and a 4 mm Dionex AS15 analytical column. The system was equipped with a guard column, a column heater set at 30°C, and an anion trap column.

Intermediate organic acids were determined by a single 2:1 acid extraction into diethylether. The extract was injected in a Finnigan GCQ GC/MS equipped with a 30 m x 0.25 mm (0.25 micrometer film) DB-WAXETR fused silica column (J&W Scientific, Folsom, Calif.). The oven temperature was programmed from 35 to 245°C at 8°C/min and held at the final temperature for 5 min. The injection port temperature was 265°C and helium carrier gas velocity was 40 cm/sec.

**Table 3.** Selected parameters and cations from the iron reducing ISM at the Bemidji site, Minnesota. All concentrations are in mg/L except for pH. Alk = laboratory alkalinity.

Time	pH	Alk	CO <sub>2</sub>	CH <sub>4</sub>	Fe	Mn	Na	K
Prespike	<i>6.95</i>	<i>503.7</i>	<i>233.7</i>	<i>4.90</i>	<i>1.30</i>	<i>3.07</i>	<i>4.91</i>	<i>2.56</i>
0	6.78	485.7	397.5	7.96	33.60	0.66	3.01	15.10
1	<i>6.90</i>	<i>497.0</i>	<i>357.1</i>	<i>5.58</i>	<i>15.90</i>	<i>0.70</i>	<i>3.83</i>	<i>16.13</i>
2	6.75	491.7	263.2	6.38	13.10	0.99	4.31	15.50
5	6.74	497.0	235.6	6.64	11.40	1.02	4.46	15.60
8	6.78	500.6	383.2	6.03	10.70	1.08	15.30	17.90
13	6.80	491.2	342.9	6.09	8.64	1.08	20.40	19.00
18	7.21	413.2	404.7	4.78	NS	NS	NS	NS
36	6.89	515.8	351.4	3.54	13.80	1.39	29.50	22.70
69	6.66	576.2	479.3	6.07	28.60	1.69	15.10	17.30

italics = average of 3 analyses

ND = not detected

NS = no sample

## RESULTS

### Anions and Cations

The pH, alkalinity, and concentrations of anions and cations for ISM-Fe are given in tables 3 and 4. Evidence that biodegradation was occurring by day 36 is given by the increase from day 13 in the terminal electron accepting cations Fe and Mn, and the increase from day 18 in alkalinity. The concentration of CH<sub>4</sub> remained constant over the

experiment, but the VFAs, acetate, and formate, increased by day 36, and propionate increased at day 69.

The concentrations of the conservative tracers, K and Br, show some variability but did not decrease significantly over the experiment. It is of interest to point out that the concentrations of Na, Cl, and SO<sub>4</sub> increased dramatically after day 5. It is unknown why the concentration of these species would increase while the conservative tracers do not increase.

**Table 4.** Selected anions and low-molecular weight volatile fatty acids from the iron reducing ISM at the Bemidji site, Minnesota. All concentrations are in mg/L. Ace = acetate, For = formate, and Pro = propionate.

Time	SO <sub>4</sub>	Cl	Br	Ace	For	Pro
Prespike	<i>4.58</i>	<i>3.13</i>	ND	<i>0.31</i>	<i>0.60</i>	ND
0	0.68	0.95	28.95	0.27	0.44	ND
1	<i>0.70</i>	<i>1.87</i>	<i>29.04</i>	<i>0.23</i>	<i>0.47</i>	ND
2	0.74	2.27	29.31	0.25	0.44	ND
5	0.71	2.31	28.82	0.26	0.44	ND
8	8.55	19.05	34.13	ND	ND	ND
13	11.97	30.65	37.56	ND	1.87	ND
18	17.52	NS	28.75	3.06	1.51	ND
36	19.51	43.47	32.20	ND	ND	ND
69	11.44	16.73	33.32	2.51	ND	0.74

italics = average of 3 analyses

ND = not detected

NS = no sample



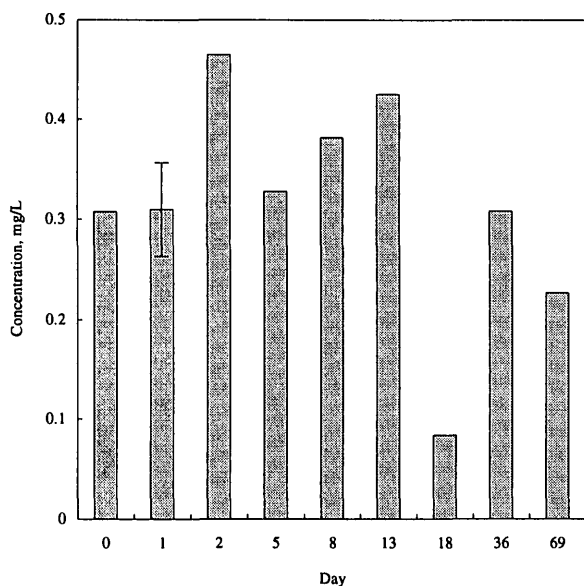


**Figure 4.** Concentrations of toluene in the ISM at the Bemidji site, Minnesota. Prespike concentrations were at method detection limit (MDL). Bar on day 1 represents the range of 3 replicates.

## Organic Compounds

Over the course of the experiment only toluene showed any perceptible signs of biodegradation. Between days 13 and 69, there appeared to be a significant decrease in the amount of this compound (fig. 4) relative to the Br tracer. We have not established a sampling error at this time, and the next sampling is not scheduled until approximately day 170, at which time toluene degradation potential should be understood.

Benzoic acid, the major monoaromatic intermediate in the methanogenic biodegradation of monoaromatic compounds (Godsy and others, 1996) and presumably under iron reducing conditions, was detected on day 36, suggesting that biodegradation of monoaromatic hydrocarbons may be occurring in this time frame.

## DISCUSSION AND CONCLUSIONS

The biodegradation of monoaromatic and polynuclear aromatic compounds under methanogenic conditions has been studied in detail in the last several years (Godsy and others, 1992; Godsy and others, 1996) and recently has been the subject of investigations under iron reducing

conditions (Lovley and others, 1989). One of the questions surrounding the microbial ecology of the contaminant plume at the Bemidji site is the role of the individual members and the terminal member of the microbial consortia in different redox zones of the plume. Previous studies have shown that anaerobic iron reducing microorganisms can degrade some of the BTEX compounds in pure culture (Lovley and others, 1989; Lovley and Lonergan, 1990) while a consortia is required for these hydrocarbons under methanogenic conditions.

Investigations by Bekins and others (1999) into the nature of the microbial consortia at the Bemidji site have shown that iron-reducing microorganisms capable of utilizing acetate and  $H_2$  as substrates are prevalent throughout the contaminant plume. They are present in both methanogenic and iron reducing redox zones, but are at lower numbers in the methanogenic zones. This finding, coupled with the appearance of VFAs and benzoate in the ISM-Fe suggests that the iron reducing microorganisms are acting as a terminal member of the consortium by utilizing the acetate and  $H_2$  produced and not degrading the BTEX compounds directly. If the iron reducing microorganisms were degrading the BTEX directly, VFAs and benzoic acid would not appear as intermediates. Proof of this observation will require further study in the ISMs and in laboratory investigations.

Microorganisms in the zone of the plume where the iron-reducing ISM was placed have not previously encountered toluene or *o*-xylene in significant concentrations. In the past, these compounds have been degraded before reaching this distance down gradient in the aquifer (Eganhouse and others, 1993; Cozzarelli and others, 1994, Cozzarelli and others, 1999). The time elapsed for toluene biodegradation to begin, may be the time required for the microbial consortia to adapt to this compound. In addition, disturbance of aquifer material during installation may effect the degradation rate. It is not clear at this time whether a single microorganism is responsible for the ring cleavage of a single compound or its analogs or if a microorganism can open the ring structure of several classes of compounds. The preliminary results of the ISM suggest that the individual microorganism or consortia of microorganisms might be specific for a

limited number of compounds as was observed for creosote derived compounds (E.M. Godsy, unpub. data, 1993)

The reasons for the failure of the methanogenic ISM to accept the spike solution will remain a mystery until the ISM is recovered in the spring.

## REFERENCES

- Baedecker, M.J., Cozzarelli, I.M., Eganhouse, R.P., Siegel, D.I., and Bennett, P.C., 1993, Crude oil in a shallow sand and gravel aquifer-III. Biogeochemical reactions and mass balance modeling in anoxic groundwater: *Applied Geochemistry*, v. 8, p. 569-586.
- Bekins, B.A., Cozzarelli, I.M., Godsy, E.M., Warren, Ean, Tuccillo, M.E., Essaid, H.I., and Paganelli, V.V., 1999, Chemical and physical controls on microbial populations in the Bemidji Toxics Site crude-oil plume, Morganwalp, D.W., and Buxton, H.T., eds., U.S. Geological Survey Toxic Substances Hydrology Program—Proceedings of the Technical Meeting, Charleston, South Carolina, March 8-12, 1999-- Volume 3 -- Subsurface Contamination from Point Sources: U.S. Geological Survey Water-Resources Investigations Report 99-4018C, this volume.
- Cozzarelli, I.M., Baedecker, M.J., Eganhouse, R.P., and Goerlitz, D.F., 1994, The geochemical evolution of low-molecular-weight organic acids derived from the degradation of petroleum contaminants in groundwater: *Geochimica et Cosmochimica Acta*, v. 58, no. 2, p. 863-877.
- Cozzarelli, I.M., Baedecker, M.J., Eganhouse, R.P., Tuccillo, M.E., Aiken, G.R., Bekins, B.A., and Jaeschke, J.B., 1999, Long-term geochemical evolution of the Bemidji Toxics site crude-oil plume, Morganwalp, D.W., and Buxton, H.T., eds., U.S. Geological Survey Toxic Substances Hydrology Program—Proceedings of the Technical Meeting, Charleston, South Carolina, March 8-12, 1999-- Volume 3 -- Subsurface Contamination from Point Sources: U.S. Geological Survey Water-Resources Investigations Report 99-4018C, this volume.
- Eganhouse, R.P., Baedecker, M.J., Cozzarelli, I.M., Aiken, G.R., Thorn, K.A., and Dorsey, T.F., 1993, crude oil in a shallow sand and gravel aquifer - II. Organic geochemistry: *Applied Geochemistry*, v. 8, p. 551-567.
- Eganhouse, R.P., Matthews, L.L., Cozzarelli, I.M., and Scholl, M.A., 1999, Evidence for natural attenuation of volatile organic compounds in the leachate plume of the Norman, Oklahoma landfill, Morganwalp, D.W., and Buxton, H.T., eds., U.S. Geological Survey Toxic Substances Hydrology Program—Proceedings of the Technical Meeting, Charleston, South Carolina, March 8-12, 1999-- Volume 3 -- Subsurface Contamination from Point Sources: U.S. Geological Survey Water-Resources Investigations Report 99-4018C, this volume.
- Essaid, H.I., Bekins, B.A., Godsy, E.M., Warren, Ean, Baedecker, M.J., and Cozzarelli, I.M., 1995, Simulation of aerobic and anaerobic biodegradation processes at a crude oil spill site: *Water Resources Research*, v. 31, no. 12, p. 3309-3327.
- Gillham, R.W., Robin, M.L., and Ptacek, C.J., 1990a, A device for in situ determination of geochemical transport parameters 1. Retardation: *Ground Water*, v. 28, no. 6, p. 666-672.
- Gillham, R.W., Starr, R.C., and Miller, D.J., 1990b, A device for in situ determination of geochemical transport parameters 2. Biochemical reactions: *Ground Water*, v. 28, no. 6, p. 858-862.
- Godsy, E.M., Goerlitz, D.F., and Grbić-Galić, Dunja, 1992, Methanogenic biodegradation of creosote-derived contaminants in natural and simulated ground water ecosystems: *Ground Water*, v. 30 no. 2, p. 232-242.
- Godsy, E.M., Goerlitz, D.F., and Grbić-Galić, Dunja, 1996, Pathways of methanogenic biodegradation of creosote-derived aromatic compounds, Morganwalp, D.W., and Aronson, D.A., eds., U.S. Geological Survey Toxic Substances Hydrology Program—Proceedings of the Technical Meeting, Colorado Springs, Colorado, September 20-24, 1993-- Volume 2: U.S. Geological Survey Water-Resources Investigations Report 94-4015, p. 835-841.

- Hult, M.F., 1984, Groundwater contamination by crude oil at the Bemidji, Minnesota, Research Site - An Introduction, in Groundwater Contamination by Crude Oil at the Bemidji, Minnesota, Research Site: U.S. Geological Survey Water-Resources Investigations Report 84-4188, p. 1-15.
- Lovley, D.R., Baedecker, M.J., Lonergan, D.J., Cozzarelli, I.M., Phillips, E.J.P., and Siegel, D.I., 1989, Oxidation of aromatic contaminants coupled to microbial iron reduction: *Nature*, v. 339, p. 297-300.
- Lovley, D.R. and Lonergan, D.J., 1990, Anaerobic oxidation of toluene, phenol, and p-cresol by the dissimilatory iron-reducing organism, GS-15: *Applied and Environmental Microbiology*, v. 56, no. 6, p. 1858-1864.
- Parlange, J.Y., Starr, J.L., Barry, D.A., and Braddock, R.D., 1984, Some approximate solutions of the transport equation with irreversible reactions: *Soil Science*, v. 137, no. 6, p. 434-442.
- Stumm, Werner and Morgan, J.J., 1981, *Aquatic Chemistry*: New York, N.Y., J. Wiley and Sons, 780 p.

#### **AUTHOR INFORMATION**

E. Michael Godsy, Ean Warren, and Barbara A. Bekins, U.S. Geological Survey, Menlo Park, California (emgodsy@usgs.gov)

Isabelle M. Cozzarelli and Robert P. Eganhouse, U.S. Geological Survey, Reston, Virginia



# Mineralogy and Mineral Weathering: Fundamental Components of Subsurface Microbial Ecology

By Philip C. Bennett, Jennifer Roberts Rogers, Franz K. Hiebert, and Wan Joo Choi.

## ABSTRACT

This is an investigation of the interplay between mineral chemistry, microbial ecology, and mineral weathering in the oil-contaminated Bemidji aquifer using field and laboratory observations and experiments over a period of 8 years. We observed microbe-mineral interactions at two scales of interaction: a *macroscale* interaction where the metabolism of both attached and planktonic organisms perturb the bulk groundwater chemistry and therefore, the mineral-water equilibria; and a *microscale* interaction where attached organisms perturb mineral-water equilibria only in the near vicinity of the organism or biofilm. The two scales reveal a tightly linked system whereby the microbial ecology controls mineral weathering, while the mineralogy and mineral chemistry control microbial colonization.

In this aquifer, carbonate chemistry is influenced primarily at the macroscale. With few native microorganisms observed on carbonate surfaces. In the upgradient oxidizing zone aerobic hydrocarbon oxidation produces excess carbon dioxide, accelerating the dissolution of calcite and dolomite, but with little weathering of silicates. Under the anoxic, leading edge, of the oil pool calcite (but not siderite) precipitates on uncolonized surfaces, while under the trailing edge of the oil, iron reduction dominates over methanogenesis and here siderite precipitates in addition to calcite. As molecular oxygen begins to diffuse into the aquifer, aerobes again dominate and residual hydrocarbons and ferrous iron are oxidized, resulting in macroscale carbonate mineral dissolution and iron precipitation.

Feldspars, in contrast, are weathered exclusively near attached microorganisms, and only at the leading edge of the anoxic sub-oil pool zone. Here native organisms preferentially colonize only those feldspars that contain trace phosphorus as apatite inclusions, apparently as a consequence to the P-limiting environment. These feldspars are rapidly weathered, while nearby feldspars without trace P are uncolonized and unweathered. The weathering of feldspars results in the release of dissolved silica which increases to near-equilibrium with amorphous silica. Comparison of the distribution of dissolved silica between 1990 and 1998 shows that the area of most intense feldspar weathering has moved downgradient, parallel with the area of most intense iron reduction.

We hypothesize that the weathering of the P-rich feldspar releases the limiting phosphate, offering the colonizing population a competitive advantage over planktonic organisms or organisms that occupy other mineral surfaces. This suggests that minerals, and the nutrient content of minerals can influence microbial processes, microbial colonization, and contaminant degradation efficiency, while the microbial ecology directly influences the mineral weathering rate and sequence.

## INTRODUCTION

At the Bemidji site, native microorganisms rapidly consume dissolved components of the petroleum, but with little addition of biomass. While there is abundant carbon substrate, and sufficient abundance of electron acceptor in the saturated zone under the oil, there is scant

available phosphorus or nitrogen, and the microbial community appears to be nutrient limited. In this same region, where iron reduction and methanogenesis are the dominant microbial processes, silicates rapidly weather, while carbonates precipitate, apparently in response microbial perturbation of specific mineral-water equilibria.

The role of microorganisms in feldspar weathering, however, is not well established or documented. Mounting evidence suggests that bacteria attached to feldspar surfaces can greatly accelerate the rate of feldspar dissolution (Barker, Welch, and others, 1998; Bennett and Hiebert, 1992; Bennett, Hiebert, and Choi, 1996; Ullman, Kirchman, and others, 1996), but two important questions remain - why, and how. Here we report the results of geochemical analysis of ground waters and field microcosm experiments that help constrain the question of how, and suggests a hypothesis for why; the native microorganisms in the Bemidji aquifer may destroy feldspars to gain access to trace or limiting nutrients.

## Site Background

The aquifer at the Bemidji site was contaminated by crude petroleum in 1979 when a high pressure pipeline ruptured, contaminating ~0.65 hectares of the surface, with both surface and subsurface accumulations of petroleum. The oil spilled at Bemidji is a light aliphatic crude (Eganhouse, Baedecker, and others, 1993), and dissolved aromatic hydrocarbons are present in the anoxic ground water under the oil, and are being rapidly degraded. Hydrocarbons in this zone are being biodegraded primarily by iron (III) reduction (Baedecker, Cozzarelli, and others, 1993; Lovley and Lonergan, 1990) and by secondary methanogenesis.

The contaminated aquifer consists of ~20 m of moderately calcareous, silty sand deposited as glacial morainal and outwash material overlying clayey till of unknown thickness, with thin discontinuous lacustrine silt layers interbedded with sand near the water table (Bennett, Siegel, and others, 1993). The native aquifer material is composed of ~ 57% quartz, 29% feldspars, 4-6% carbonates 2% hornblende, <1% clays, and < 0.2 % organic carbon. Degradation of the contaminating petroleum has produced a plume of inert and reactive organic and inorganic solutes, including a variety of organic acids (Baedecker, Cozzarelli, and others, 1993; Cozzarelli, Baedecker, and others, 1994; Cozzarelli, Eganhouse, and Baedecker, 1990), and etching of native quartz and feldspar grains has been

documented (Bennett and Casey, 1994; Bennett and Siegel, 1987).

## METHODS

For this study we used parallel field and laboratory methods to examine the role of mineralogy in microbial ecology. Complete sampling of ground waters at the Bemidji site wells were completed in September 1990 and July 1998, with additional selected wells sampled annually. Water was collected from up to 90, 5 cm OD PVC wells with stainless screens positioned to intersect the water table (1.5 meter screen length), and at specified intervals below the water table (0.15 meter length screens). Samples were collected using down-hole submersible pumps after evacuation of approximately 3 well volumes (see Bennett and others, 1993). During the 1990 sampling dissolved oxygen, pH, temperature, and specific conductance were measured at the surface using a flow cell. For the 1998 sampling, these constituents were measured *in situ* using down-hole data probes (Hydrolab Data Sonde), with readings recorded before and after sample collection. Analysis of very low dissolved oxygen (<20 ppb) was done at the surface using colorimetric techniques (Chemetrics) with a portable "Spec-20" spectrophotometer. Dissolved ferrous and ferrous+ferric iron were also determined immediately in the field using the bipyridine colorimetric method, and rechecked in the laboratory using a Perkin-Elmer Lambda 6 double-beam spectrophotometer. Alkalinity was determined on a 0.2 um filtered unpreserved sample by endpoint seeking titration with calibrated 0.1 N HCl.

Dissolved metals and silicon were determined by ICP on an acid-preserved sample filtered to 0.1 um, while ammonia was determined by single column ion chromatography (detection limit 10 ppb). Dissolved anions (F, Cl, NO<sub>2</sub>, NO<sub>3</sub>, SO<sub>4</sub>) were determined from a filtered unpreserved sample by single-column ion chromatography (Detection limit 20-50 ppb). Reactive orthophosphate was determined in the laboratory by standard colorimetric methods on a filtered sample preserved with HgCl<sub>2</sub>, with selected samples analyzed for total P by ICP-MS.

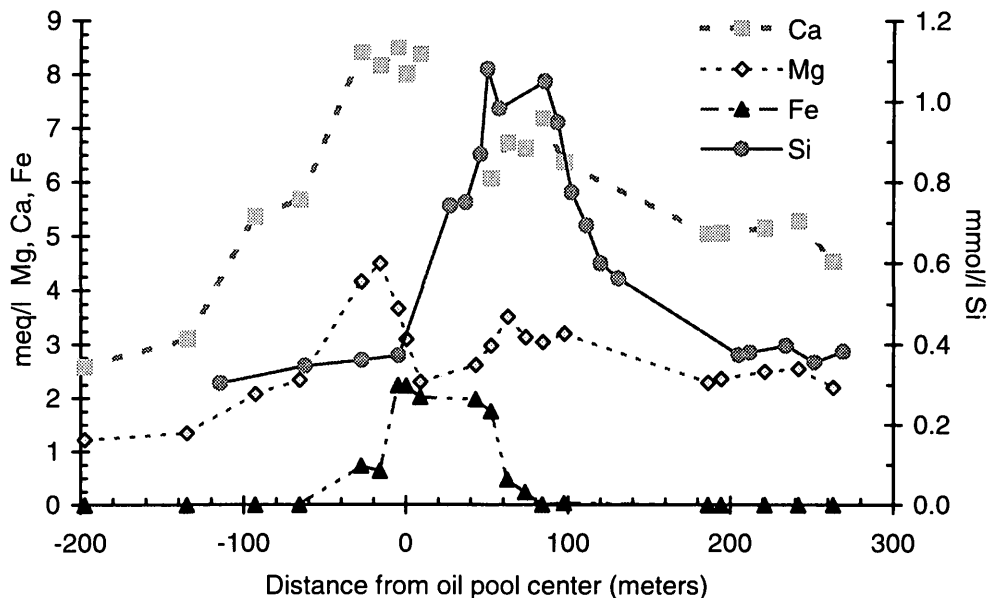


**Figure 1:** Solute concentrations along the primary transect. Ground water flow is from negative to positive distance.

Inorganic carbon was by measured using a Dohrman DC180 carbon analyzer.

Field microcosms of selected mineral chips were placed in different areas of a microbiologically active petroleum-contaminated aquifer for periods up to 12 months (Bennett, Hiebert, and Choi, 1996; Hiebert and Bennett, 1993; Rogers, Bennett, and Choi, 1998). In the aquifer the mineral chips were exposed to the native microbial population, and after recovery the pattern of colonization and the extent of reaction of the surface was characterized using SEM and related techniques (Rogers and others, this volume). At the time of microcosm placement and recovery, the ground water chemistry and microbiology were characterized and compared to over 15 years of record established for this site (Bennett, Siegel, and others, 1993).

Using the same mineral specimens, we also examined some of the fundamental controls on feldspar dissolution kinetics within the context of a limited experimental question - how can a microorganism accelerate the dissolution rate of a feldspar orders of magnitude over the rate of an uncolonized surface? Specimens of Bancroft albite and a South Dakota microcline were ground

to a uniform size fraction, cleaned, and dissolved in an all-Teflon mixed flow reactor system (Bennett, Hiebert, and Choi, 1996; Choi, 1997; Choi and Bennett, 1995). Dissolution rate was examined as a function of pH, ionic strength, and the concentration of 3 target organic ligands: citrate, dihydroxy benzoate, and tropolone. The effect of these variables was monitored by measuring the change in absolute dissolution rate and *apparent* activation energy (the observed relationship between dissolution rate and temperature not corrected for the enthalpy of proton adsorption, (Casey and Sposito, 1992).

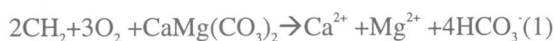
## FIELD OBSERVATIONS AND EXPERIMENTAL FINDINGS

### Macroscale Calcite Diagenesis

Upgradient of the oil pool oxidation of vadose-zone petroleum proceeds by aerobic beta-oxidation and oxygenlytic cleavage of simple aromatic compounds depleting the reservoir of dissolved oxygen. This produces substantial acidity from carbon dioxide as well as minor and transient quantities of simple and complex organic acids, resulting in a downward trend in pH along the flow path. The acid production is buffered by carbonate dissolution, resulting in an

increase in the concentration of dissolved Ca, Mg, and HCO<sub>3</sub> along the flow path, but little increase in dissolved silica or iron (Figure 1).

Examination of mineral surfaces reacted in this region shows evidence of a macroscale perturbation in mineral water equilibria, and both calcite and dolomite show evidence of aggressive chemical weathering, with distinct etch pits and solution channels (Figure 3). Microorganisms were rarely found on the carbonate mineral surfaces, and the weathering appears to be a macroscale effect: microbial production of acidity from hydrocarbons dissolves calcite, but the microorganism itself is distant from the region of weathering:



where CH<sub>2</sub> represents an average mid-chain alkyl carbon (C<sup>II</sup>) and dolomite as the reacting carbonate. We found no evidence of significant feldspar weathering in the aerobic oxidation region, either from changes in the geochemistry, or from direct examination of mineral surfaces.

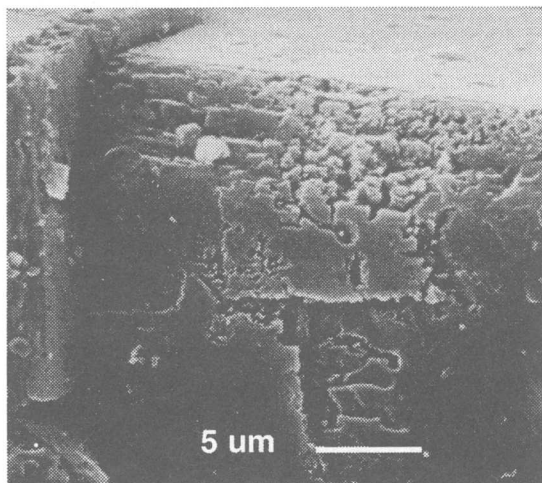


**Figure 2.** SEM micrograph of dolomite reacted in the oxic region of the aquifer for 1 year. Extensive etching without attached organisms is found on all surfaces.

In the anoxic region beneath the oil pool calcite had sparse dissolution pitting, but only at the microscale associated with microbial colonization. In this region, calcite were typically covered with a variety of precipitation features (Figure 4). Spikes appear to nucleate along cleavage, forming regular rows and rhombic

outlines, eventually filling to form rhombic “mesas”. The measured geochemical trends in this region support precipitation, probably driven by iron reduction:

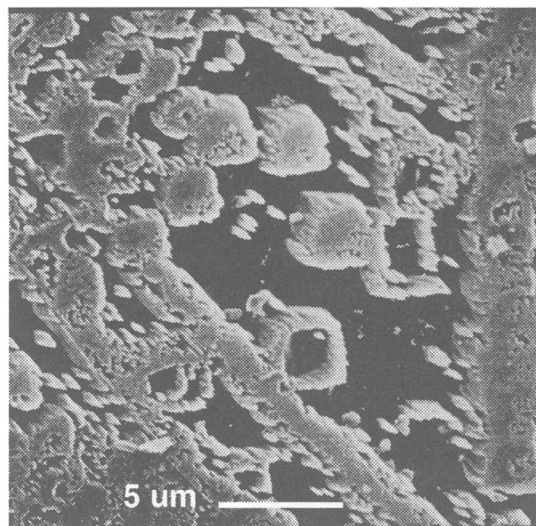


**Figure 3.** SEM micrograph of calcite reacted in the anoxic region of the aquifer for 1 year. Extensive precipitation without attached organisms is found on all surfaces.

Sequential leaching experiments suggests that the precipitated mineral in the upgradient anoxic region is pure calcium carbonate, with only trace magnesium, strontium, and iron (Hiebert, 1994). In the upgradient portion of the anoxic zone, where methanogenesis may dominate over iron reduction in some regions, in situ experiments show that siderite is uncolonized, and generally dissolving, not precipitating. Further downgradient, however, where iron reduction dominates over methanogenesis, siderite may also precipitate in addition to calcite.

### Microscale Silicate Weathering

In the most organic-rich area of this aquifer, the ground water is extremely reducing, and dissolved ferrous iron increases along the principle flow path, while pH decreases from ~7.8 to ~6.5 (Figure 1). Dissolved silica increases



from 0.3 mmole l<sup>-1</sup> to > 1 mmole l<sup>-1</sup> associated with the greatly accelerated dissolution of quartz and feldspars (Bennett and Casey, 1994; Bennett and Siegel, 1987).

In 1990, the highest silica concentration was found under the center of the floating oil pool, where the greatest iron reduction activity was found (Figure 2). In 1998, the original contaminated area is increasingly dominated by methanogenesis as the available iron is consumed, and the greatest iron reduction activity was found down gradient toward the trailing edge of the oil pool. Concurrent with the downgradient shift in iron reduction activity is documented a shift in the highest silica concentration, which in 1998 exceeded 1.3 mmole l<sup>-1</sup> and was also found downgradient of the trailing edge of the oil. From the geochemical data it appears that the feldspar weathering follows the iron reducing bacteria.

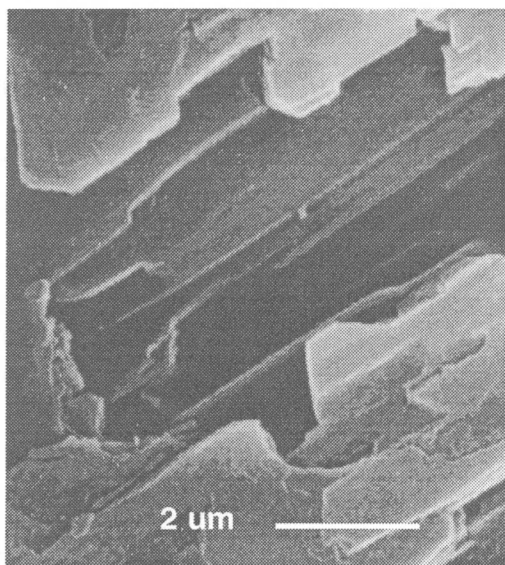


**Figure 4.** SEM micrograph of a single etch pit on South Dakota Microcline reacted in the anoxic region of the aquifer for 1 year, and then cleaned by brief ultrasonification. The pit is probably the result of the dissolution of an apatite inclusion..

The field microcosms experiments suggest that mineral weathering is primarily associated with surface colonizing bacteria, and that there is significant variability in colonization pattern and density (See Rogers and others, this volume), and density and depth of etch-pits, on different silicates. Significant colonization of feldspars is

only observed in the very anaerobic zone, and those feldspars that are colonized all show evidence of rapid and extensive dissolution. Other feldspars in the same location, however, are uncolonized and unweathered. The apparent rate of dissolution of the colonized surfaces, based on etch pit depth is *at least* a factor of 100 greater than the uncolonized surfaces (Bennett, Hiebert, and Choi, 1996).

We found that the feldspars that are colonized in this system all contain minor phosphorus, while virtually identical feldspars without phosphorus are uncolonized and unweathered (Rogers, Bennett, and Choi, 1998; Rogers, Bennett, and Ullman, 1998). The P is present as apatite inclusions, and based on simple leaching experiments appears to be in a form available to the microorganisms. Some etch features on the microcline surface appear to be the remnant of an apatite blade (Figure 5).

### Feldspar Dissolution Kinetics

The weathering pattern on the colonized feldspars suggest that the microorganisms are dissolving the feldspar matrix in addition to the exposed apatite inclusion. This is reasonable considering the exposed surface area of silicate vs. the surface area of exposed apatite inclusion. Assuming the organism is colonizing these surfaces to gain access to limiting P (and no other systematic difference has been identified to date) feldspar matrix must eventually be removed to expose new P. There are, however, a limited number of mechanisms available to accelerate silicate dissolution. Principally this can be accomplished by perturbing temperature, pH or ionic strength, or by the production of metal chelating ligands (Brady and Walther, 1989; Welch and Ullman, 1993; Welch and Vandevivere, 1995).

In the laboratory experiments, we examined the dissolution dynamics of one feldspar that consistently is colonized and weathered (microcline) and one feldspar that consistently is uncolonized and unweathered (albite). The results of our experiments were then compared to other published results using similar material to try and identify possible mechanisms for the microbial acceleration of weathering. We found

that the dissolution rate of both feldspars is nearly independent of proton activity between pH 6.5 (the ground water pH) and pH 4.5, while the rate of dissolution only increases by a factor of ~3.3 between pH 4.5 and 3.0 for the microcline. Dissolution rate *decreases* with increasing ionic strength (using LiCl as an ionic strength buffer) by 50-75% up to I = 0.05 molar, with a larger effect found at lower temperature. These results suggest that ionic strength is not a factor, and the pH around the attached microorganism would have to be substantially less than 3.0 to achieve the observed field rate of microcline dissolution, an unreasonable expectation (Barker, Welch, and others, 1998).

The dissolution rate of both the albite and microcline, however, increased by a factor of 10-50 with even low (0.1-1.0 mM) concentrations of the iron-chelating ligands, while the apparent activation energy is substantially lower (decreasing from 50 kJ/mol to 32 kJ/mol for microcline). The increase in rate, and decrease in the apparent activation energy suggests that these organic ligands can substantially increase feldspar weathering rate, particularly at low temperature or under a biofilm layer where ligand concentration could be quite high.

## IMPLICATIONS

We propose that microorganisms attached to feldspars in this environment are producing reactive ligands, potentially as a mechanism to scavenge scarce ferric iron for metabolic processes. While the concentration of these ligands in the aquifer is only 0.1-1.0  $\mu\text{M}$ , the concentration would be much higher near the attached organism. The result of this ligand excretion therefore is the accelerated weathering of the feldspar, and in some cases, the release of a limiting nutrient. The presence of a limiting nutrient will act as a positive feedback for further metabolism, and possibly, additional colonization. The end result of this interaction is the selective weathering of only those feldspars that provide a nutritive advantage to the microorganism, while almost identical feldspars without nutritive benefit will be left untouched, and presumably preserved in the rock record.

These results represent a unique observation of the interaction of microorganisms with minerals *in situ* and the influence of microbial metabolism on mineral weathering and secondary mineral precipitation. Destruction of silicate minerals to access limiting inorganic nutrients appears to be a fundamental aspect of subsurface microbial ecology, and of the natural attenuation of oil by native microorganisms. This also has implications for our conceptual understanding of mineral diagenesis and the time-sequence of mineral weathering. A basic tenet of sediment diagenesis is the "Goldich Weathering Sequence" (Goldich, 1938), which states that the most unstable silicate mineral will weather (dissolve) first, with more resistant silicates taking progressively longer to dissolve. The ideal weathering sequence for the minerals examined in this study (from most to least rapidly weathered) *should* be: Olivine > Plagioclase > Albite > Anorthoclase > Microcline > Quartz, But the weathering sequence observed here is almost opposite, with olivine stable with respect to quartz and microcline. The evidence from this study suggests that in *some* environments the indigenous microorganisms may significantly alter weathering patterns as they aggressively scavenge limiting nutrients.

If microorganisms are colonizing and destroying specific feldspars in order to release limiting nutrients, then feldspar weathering is not simply a random event controlled by simple abiotic kinetic rate laws and mechanisms. In this microbial weathering scenario, colonized feldspars containing trace nutrients of value may weather very quickly and early, leaving only a clay residuum and those feldspars without nutritive value.

## REFERENCES

- Baedecker, M.J., Cozzarelli, I.M., Siegel, D.I., Bennett, P.C., and Eganhouse, R.P., 1993, Crude oil in a shallow sand and gravel aquifer-III. Biochemical reactions and mass balance modeling in anoxic groundwater: Applied Geochemistry, v. 8, p. 569-586.
- Barker, W.W., Welch, S.A., Chu, S., and Banfield, J.F., 1998, Experimental observations of the effects of bacteria on

- aluminosilicate weathering: *American Mineralogist*, v. 83, p. 1551-1563.
- Bennett, P.C., and Casey, W.H., 1994, Organic acids and the dissolution of silicates, *in* Pittman, E.D., and Lewan, M., eds., *The role of organic acids in geological processes*, Springer-Verlag, p. 162-201.
- Bennett, P.C., and Hiebert, F.K., 1992, Microbial mediation of silicate diagenesis in organic-rich natural waters: *Proceedings International Symposium on Water Rock Interaction*, p. 7; Pages 267-270.
- Bennett, P.C., Hiebert, F.K., and Choi, W.J., 1996, Rates of Microbial Weathering of Silicates in Ground Water: *Chemical Geology*, v. 132, p. 45-53.
- Bennett, P.C., and Siegel, D.I., 1987, Increased solubility of quartz in water due to complexation by dissolved organic compounds: *Nature*, v. 326, p. 684-687.
- Bennett, P.C., Siegel, D.I., Baedeker, M.J., Cozzarelli, I., and Hult, M., 1993, The fate of crude oil in a sand and gravel aquifer I. *Inorganic geochemistry: Applied Geochemistry*, v. 8, p. 529-549.
- Brady, P.V., and Walther, J.V., 1989, Controls on silicate dissolution rates in neutral and basic pH solutions at 25 C.: *Geochimica et Cosmochimica Acta*, v. 53, p. 2823-2830.
- Casey, W.H., and Sposito, G., 1992, On the temperature dependence of mineral dissolution rates: *Geochim. Cosmochim. Acta*, v. 56, p. 3825-3830.
- Choi, W.J., 1997, Silicate dissolution kinetics in organic electrolyte solutions: Austin, Texas, The University of Texas at Austin, Ph.D. Dissertation.
- Choi, W.J., and Bennett, P.C., 1995, Dynamics of silicate dissolution in organic and inorganic electrolyte solutions: *GSA Abstracts with Programs*, v. 27, p. A-44.
- Cozzarelli, I.M., Baedeker, M.J., Eganhouse, R.P., and Goerlitz, D.F., 1994, Geochemical evolution of low-molecular-weight organic acids derived from the degradation of petroleum contaminants in ground water: *Geochimica et Cosmochimica Acta*, v. 58, no. 2, p. 863-877.
- Cozzarelli, I.M., Eganhouse, R.P., and Baedeker, M.J., 1990, Transformation of monoaromatic hydrocarbons to organic acids in anoxic groundwater environment: *Environmental Geology and Water Science*, v. 16, p. 135-41.
- Eganhouse, R.P., Baedeker, M.J., Cozzarelli, I.M., Aiken, G.R., Thorn, K.A., and Dorsey, T.F., 1993, Crude oil in a shallow sand and gravel aquifer-II. *Organic geochemistry: Applied Geochemistry*, v. 8, p. 551-567.
- Goldich, S.S., 1938, A study in rock weathering: *Journal of Geology*, v. 46, p. 17-58.
- Hiebert, F.K., 1994, *Microbial Diagenesis in Terrestrial Aquifer Conditions: Laboratory and Field Studies.*: Austin, TX, University of Texas, Dissertation, 198 p.
- Hiebert, F.K., and Bennett, P.C., 1993, Microbial diagenesis of silicates and calcite in an organic-rich aquifer: *Abstracts with Programs Geological Society of America*, v. 25, no. 6, p. 202.
- Lovley, D.R., and Lonergan, D.J., 1990, Anaerobic oxidation of toluene, phenol, and *p*-cresol by the dissimilatory iron reducing organism GS-15: *Applied Environmental Microbiology*, v. 56, no. 1858-1864.
- Rogers, J.R., Bennett, P.C., and Choi, W.J., 1998, Feldspars as a source of nutrients for microorganisms: *American Mineralogist*, v. 83, p. 1532-1540.
- Rogers, J.R., Bennett, P.C., and Ullman, W.J., 1998, Biochemical release of a limiting nutrient from feldspars, *in* Goldschmidt Conference, Toulouse, France.
- Ullman, W.J., Kirchman, D.L., Welch, S.A., and Vandevivere, P., 1996, Laboratory evidence for microbially mediated silicate mineral dissolution in nature: *Chemical Geology*, v. 132, no. 1-4, p. 11-17.
- Welch, S.A., and Ullman, W.J., 1993, The effect of soluble organic acids on feldspar dissolution rates and stoichiometry: *Geochimica et Cosmochimica Acta*, v. 57, p. 2725-2736.
- Welch, S.A., and Vandevivere, P., 1995, Effect of microbial and other naturally occurring polymers on mineral dissolution: *Geomicrobiology Journal*, v. 12, p. 227-238.

## **AUTHOR INFORMATION**

Philip C. Bennett, Jennifer Roberts Rogers, and  
Wan Joo Choi, Dept. of Geological Sciences,  
University of Texas, Austin, TX 78712  
pbennett@mail.utexas.edu

Franz K. Hiebert, RMT Inc. 912 Captial of Texas  
Hwy, Suite 300, Austin, TX 78746-5210

# Aromatic and Polyaromatic Hydrocarbon Degradation under Fe(III)-Reducing Conditions

Robert T. Anderson, Juliette N. Rooney-Varga, Catherine V. Gaw, Derek R. Lovley  
University of Massachusetts, Amherst, MA 01003

## ABSTRACT

Investigations of the Bemidji aquifer have demonstrated that important ground water contaminants such as benzene and naphthalene can be degraded under Fe(III)-reducing conditions found in situ. Mineralization of both compounds occurred without a lag period suggesting that Fe(III)-reducers found in the sediment were oxidizing these contaminants in situ. The area of greatest mineralization activity was confined to a narrow region at the downgradient edge of the Fe(III)-reducing zone. Microbial community analysis using 16S rRNA-based techniques indicated that members of the *Geobacter* family were enriched in sediments collected from this active zone. Furthermore, phylogenetic analyses of DNA sequences recovered from benzene-degrading sediments and enrichment cultures clustered with *Geobacteraceae* known to degrade aromatic compounds while sequences from uncontaminated, background sediments did not. These results could lead to the development of a rapid assay for assessing anaerobic benzene degradation potential at petroleum-contaminated sites.

## INTRODUCTION

Petroleum hydrocarbon contamination of aquifers presents a serious threat to ground water resources. While most hydrocarbon compounds are known to be degraded under aerobic conditions many petroleum-contaminated aquifers contain large areas where anaerobic processes are dominant (Anderson and Lovley, 1997; Lovley, 1997b). Specifically, microbial Fe(III) reduction is predicted to be a dominant anaerobic process because Fe(III) is generally the most abundant potential electron acceptor found in aquifer sediments (Lovley, 1997a; Lovley, 1997b). Large decreases in ground water contaminant concentrations are observed in many aquifers where large areas of Fe(III) reduction are observed (Borden and others, 1995; Cozzarelli and others, 1990).

Benzene, a known carcinogen, is relatively mobile in ground water and is often observed to persist in anaerobic environments (Barbaro and others, 1992; Flyvbjerg and others, 1993). Laboratory incubations of sediment have indicated a potential for anaerobic benzene

degradation under a variety of anaerobic conditions but the onset of degradation activity is often preceded by long lag periods suggesting that benzene degradation was not occurring in situ (Edwards and Grbic-Galic, 1992; Kazumi and others, 1997; Lovley and others, 1996). Evidence of in situ benzene degradation has been demonstrated in contaminated harbor sediments under sulfate reducing conditions (Coates and others, 1996) and recently in contaminated aquifer sediments under Fe(III)-reducing conditions (Anderson and others, 1998).

Polyaromatic hydrocarbons (PAHs) are also potential ground water contaminants found in petroleum contaminated environments. Many PAHs are known to be carcinogenic and when present in aquifers tend to be associated with the sediment. However some PAHs such as naphthalene do migrate with the ground water and can pose a threat to downgradient water resources (Goerlitz and others, 1985). Most low molecular weight PAH compounds are known to be degraded under aerobic conditions and until recently PAHs were generally thought to persist under anaerobic conditions (Cerniglia, 1992).

Anaerobic PAH degradation has been observed under a variety of electron-accepting conditions. Naphthalene degradation has been observed in laboratory sediment incubations where nitrate was supplied as the electron acceptor (Langenhoff and others, 1996; Thierry and others, 1996) and in contaminated harbor sediments under sulfate reducing conditions (Coates and others, 1996). While naphthalene degradation has also been observed in enrichment cultures established from aquifer sediment under sulfate reducing conditions (Bedessem and others, 1997) and in sulfate reducing ground water downgradient from a leaking underground storage tank (Thierrin and others, 1993), PAH degradation has not been previously observed under Fe(III)-reducing conditions.

This paper describes the results of a study to further examine anaerobic aromatic and polyaromatic degradation within petroleum-contaminated aquifers. The results demonstrate that benzene and naphthalene can be degraded under Fe(III)-reducing conditions found in some but not all petroleum-contaminated aquifers. When this activity is found it may be largely

restricted to narrow regions of the aquifer at the downgradient edge of the Fe(III) reduction zone. Furthermore, the detection of specific Fe(III)-reducing microorganisms could lead to the development of a rapid assay to assess benzene degradation potential in petroleum-contaminated aquifers.

## MATERIALS AND METHODS

### Sediment Collection and TEAP Determination

Sediment samples were collected from a variety of petroleum-contaminated aquifers and evaluated for the potential to anaerobically degrade aromatic and polyaromatic compounds as previously described (Anderson and Lovley, 1999; Anderson and others, 1998; Murphy and Herkelrath, 1996). All sediment samples were collected using either a truck mounted drill rig or hand augers. Sediments collected at the Bemidji aquifer in 1997 are from sites shown in Figure 1.

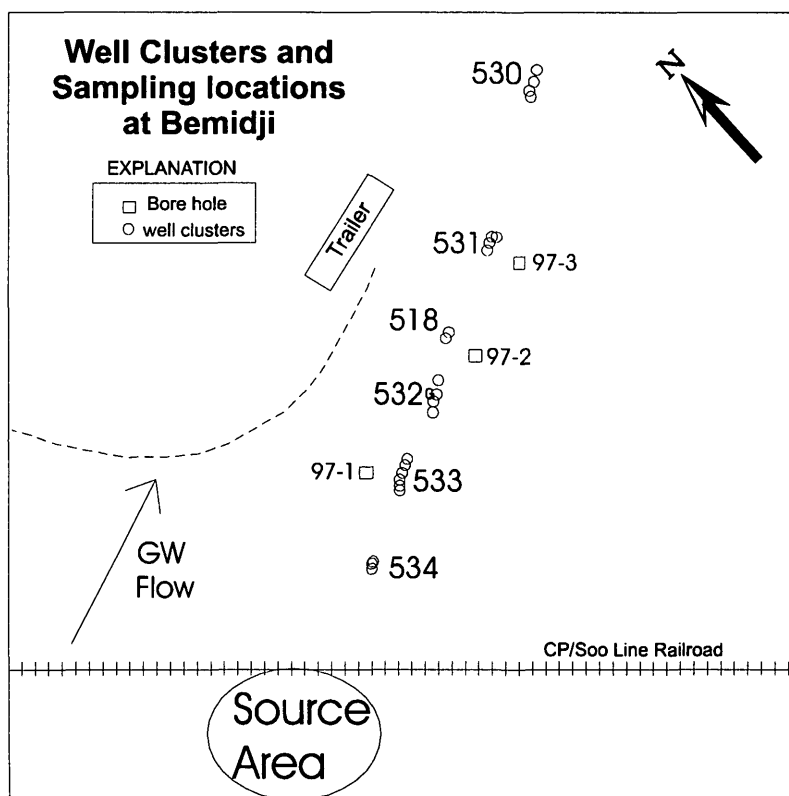


**Figure 1.** Well clusters and sediment sampling locations at the Bemidji site (adapted from Anderson and others, 1998).

The dominant terminal electron accepting process (TEAP) in collected sediments was assessed using [2-<sup>14</sup>C]acetate as previously described (Anderson and others, 1998). Fe(III)-reducing conditions are confirmed as the dominant anaerobic process in sampled sediments if the following criteria are met: 1) ground water is depleted of nitrate, 2) Fe(II) is present in the sediments, 3) mineralization of [2-<sup>14</sup>C]acetate is not inhibited by molybdate, 4) no <sup>14</sup>CH<sub>4</sub> production observed when sediments are incubated with [2-<sup>14</sup>C]acetate. The Fe(II) content of the sediments was evaluated using a 0.5N HCl extraction followed by measurement with ferrozine.

### Ground Water Analysis

Ground water samples for anion analysis were collected in 40 mL vials or 58 mL serum bottles, chilled on ice and sent via overnight carrier to the laboratory. Once in the laboratory, the samples were immediately analyzed for nitrate and sulfate by ion chromatography (Dionex, DX-100, Sunnyvale, CA). Ground water samples for benzene analysis were placed into no-headspace 40 mL vials and preserved with HCl prior to overnight shipment to the laboratory. Benzene samples were analyzed by gas chromatography (HP6890, Wilmington, DE) coupled with a purge and trap autosampler (OI-Analytical, DPM-16, College Station, TX) according to a modification of EPA method 8015/8020.

### Mineralization of Radiolabeled Substrates

The potential for benzene, toluene, naphthalene and phenanthrene degradation in sediments was assessed using [<sup>14</sup>C]-labeled substrates as previously described (Anderson and Lovley, 1999; Anderson and others, 1998). Sediments (30g) were dispensed into triplicate sets of serum bottles inside an N<sub>2</sub>-filled glove bag and stoppered with thick butyl rubber stoppers. Anaerobic stock solutions of [<sup>14</sup>C]-labeled benzene and toluene were prepared using an adaptation of the manufacturer's recommended

method of transfer and were added to provide 1 μCi of labeled substrate to each sediment bottle.

Radiolabeled naphthalene and phenanthrene, supplied in methanol stocks, were first applied to sediment pellets prepared from the tested sediments and the methanol allowed to evaporate (Anderson and Lovley, 1999). The sediment pellets were then added to serum bottles while under a stream of anaerobic N<sub>2</sub>. The bottles were vigorously shaken to break up and disperse the pellets inside the bottles.

Headspace samples (1ml) of bottles containing radiolabeled substrates were removed over time and analyzed for <sup>14</sup>CO<sub>2</sub> and <sup>14</sup>CH<sub>4</sub> using gas chromatography and gas proportional counting detection. Total mineralization percentages were calculated based on the partitioning of H<sup>14</sup>CO<sub>2</sub> between bottle headspaces and the sediment.

### Analysis of Microbial Populations in the Sediment

Analyses of the microbial subsurface community was performed using 16S rRNA-based techniques as previously described (Anderson and others, 1998; Rooney-Varga and others, 1999). Since cultivation-based community analyses can selectively bias the results, a more direct approach was applied at the Bemidji site. DNA was extracted directly from sediments and analyzed using both DGGE and MPN-PCR. Briefly, DNA was extracted from triplicate sediment samples using a freeze-thaw method of cell disruption followed by phenol-chloroform extraction or with the FastDNA soil extraction kit (Bio 101, Vista, CA). For bacterial community analyses, portions of the 16S rDNA sequences were amplified using the PCR and primers 338F-GC and 907R. For analysis of the *Geobacteraceae* community within sediments, 16S rDNA sequences were amplified using primers 338F-GC and Geo825R. The resulting PCR products were subsequently separated on a denaturing gradient electrophoresis gel and resolved with ethidium bromide/transillumination. Excised bands were later sequenced for identification. For MPN-PCR analyses, the extracted DNA was first serially

diluted 10-fold into sterile Milli-Q water and portions of each dilutions were used as template in the PCR. In these analyses, *Geobacteraceae* sequences were amplified using primers 8F and Geo825R. Resulting PCR products were analyzed by gel electrophoresis in agarose (1%) containing ethidium bromide and visualized by transillumination.

## RESULTS AND DISCUSSION

### Anaerobic Aromatic and Polyaromatic Degradation

Of several sites investigated (Anderson and others, 1998), Bemidji aquifer sediments were the

only samples collected that demonstrated a potential for benzene degradation under Fe(III)-reducing conditions. While all sediments from all sites demonstrated a potential for toluene degradation only sediments from a narrow region at the downgradient edge of the Fe(III) reduction zone (site 97-3) at Bemidji readily mineralized [<sup>14</sup>C]benzene to <sup>14</sup>CO<sub>2</sub> (Figure 2). No lag period was observed prior to the onset of mineralization suggesting that the organisms within the sediment were preadapted for benzene oxidation and therefore must be oxidizing benzene in situ. No benzene mineralization was observed in uncontaminated, background sediments from Bemidji implying that the observed benzene degradation is associated with petroleum contamination.

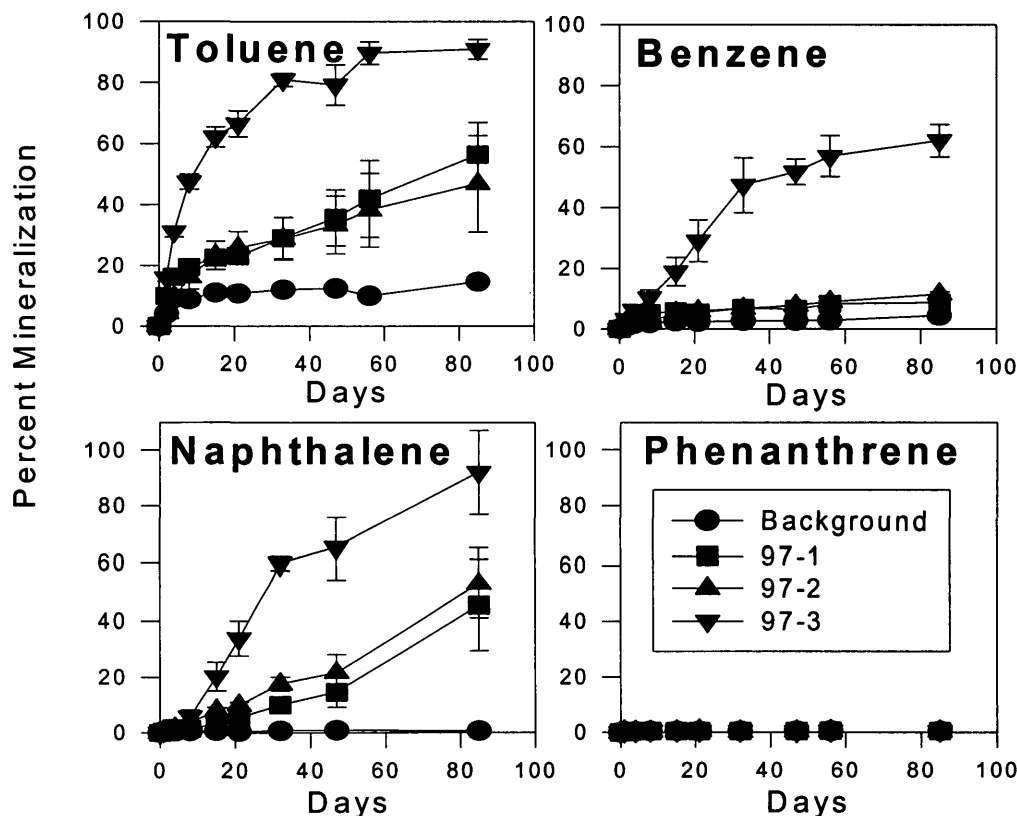


**Figure 2.** Mineralization [<sup>14</sup>C] toluene, benzene, naphthalene and phenanthrene in sediments collected from the Bemidji aquifer (adapted from Anderson and Lovley, 1999; Anderson and others, 1998). Results are averages of triplicate analyses.



Bemidji sediments not only rapidly mineralized benzene under Fe(III)-reducing conditions but also readily mineralized [ $^{14}\text{C}$ ]naphthalene to  $^{14}\text{CO}_2$ . Again, the onset of mineralization was immediate with no lag period suggesting that organisms present within the subsurface were preadapted for naphthalene degradation and were likely mineralizing this compound *in situ*. No naphthalene degradation was observed in uncontaminated sediments again indicating that this activity is associated with petroleum contamination. In addition, no mineralization of [ $^{14}\text{C}$ ]phenanthrene was observed in any Bemidji sediments under Fe(III)-reducing conditions demonstrating that oxygen contamination could not account for the observed benzene or naphthalene degradation in contaminated sediments. Phenanthrene is readily oxidized under aerobic conditions but its anaerobic degradation potential may be hindered due to solubility limitations.

These results are the first documented evidence of the potential for *in situ* oxidation of benzene and naphthalene under Fe(III)-reducing conditions found in petroleum-contaminated aquifers. The greatest rates of toluene, benzene

and naphthalene degradation were restricted to a narrow region at the downgradient edge of the Fe(III) reduction zone. These observations indicate that the downgradient edge of Fe(III) reduction zone at Bemidji is an area of intense microbial activity. Detection of similar zones in other petroleum-contaminated aquifers could lead to better understanding of the contribution of anaerobic process to the natural attenuation of ground water contaminants.

### Association of *Geobacteraceae* with Anaerobic Benzene Degradation

Investigation of the microbial communities within the Bemidji aquifer focused on organisms involved in the degradation of benzene under Fe(III)-reducing conditions because benzene is frequently the contaminant of greatest concern when present in ground water. DGGE analysis of Bemidji sediments using *Bacteria* primers indicated that relatively few species dominated at each site, particularly the background site (Figure 3).

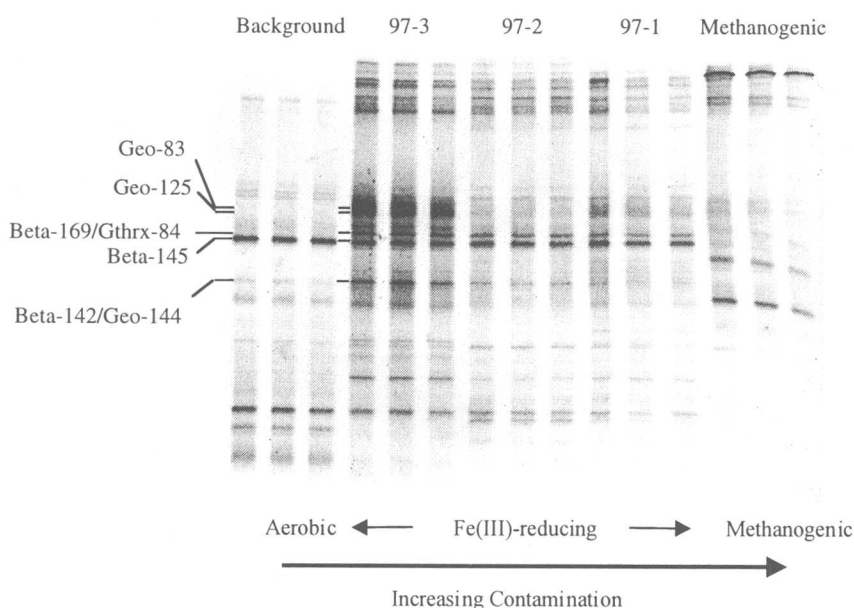


**Figure 3.** DGGE analysis of DNA extracted from triplicate samples of Bemidji sediment and amplified using *Bacteria* specific primers (adapted from Rooney-Varga and others, 1999). Methanogenic sediments were collected near well cluster 534.

Differences in community composition between background sediments and contaminated sediments were clearly evident as well as differences among the different TEAP zones. More bands were recovered from sediments within contaminated portions of the aquifer than in uncontaminated portions suggesting that the presence of crude oil in the subsurface stimulated the growth of microorganisms that were not previously dominant in the sediments

Previous cultivation-based results suggested that *Geobacteraceae* were enriched in benzene-degrading sediments collected at site 97-3 (Anderson and others, 1998). While the DGGE results using primers specific for *Bacteria* indicated no dramatic differences among the three Fe(III)-reducing sites investigated, a few bands of much higher intensity corresponding to *Geobacteraceae* (Geo-83, Geo-125) were found in sediments from site 97-3 (Figure 3) suggesting that these organisms were selectively enriched in 97-3 sediments. Members of the *Geobacteraceae* are strict Fe(III)-reducers many of which are known to completely oxidize aromatic compounds. Bands corresponding to *Geothrix* species (Gthrx-84) were found among all Fe(III)-

reducing sites while a sequence from the  $\beta$ -proteobacteria (Beta-145) was found in both the background and all Fe(III)-reducing sites. These organisms are not known to oxidize aromatic compounds.

MPN-PCR analysis of DNA extracted from sediments provides an unbiased analysis of the numerical abundance of microbial species relative to cultivation-based techniques. When Fe(III)-reducing sediments collected from the Bemidji aquifer were analyzed by MPN-PCR, *Geobacteraceae* were found to be enriched in sediments known to degrade benzene (Figure 4). *Geobacteraceae* sequences enumerated in benzene-degrading sediments from site 97-3 were more than four orders of magnitude greater than background sediments and more than three orders of magnitude greater than other Fe(III)-reducing sediments that did not degrade benzene (97-1, 97-2). Site 97-3 is located near wells where the concentration of benzene in the ground water sharply decreases with downgradient distance (Figure 5). These results suggest that elevated numbers *Geobacteraceae* detected in benzene-degrading sediment play an important role in removing benzene from the ground water.

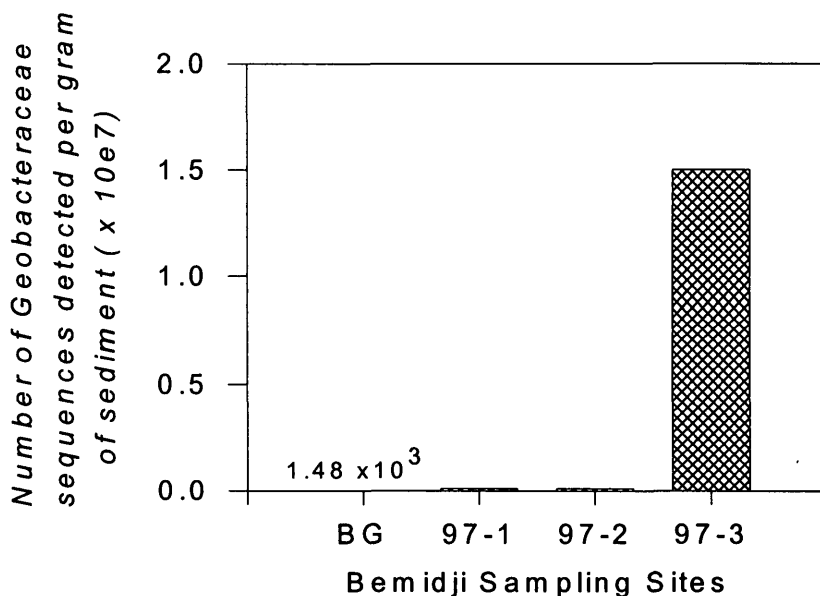


**Figure 4.** Enumeration of *Geobacteraceae* by MPN-PCR in sediments collected from the Bemidji aquifer (adapted from Anderson and others, 1998). BG is the background site.

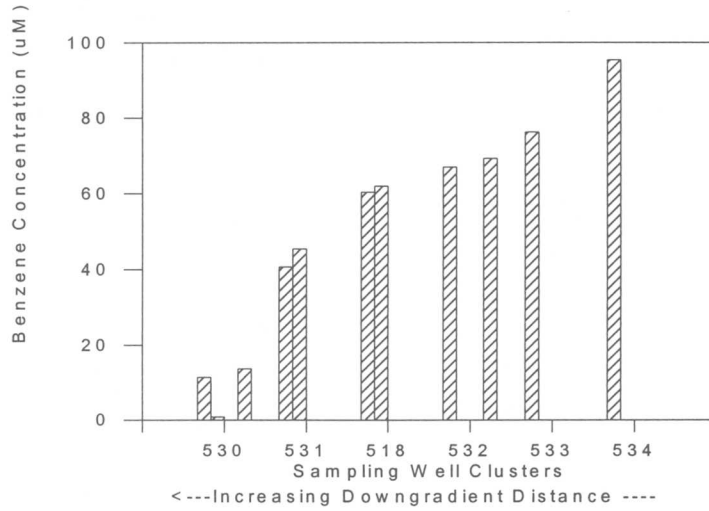


**Figure 5.** Ground water benzene concentrations in wells at increasing distances downgradient from the source area. Results are averages of triplicate analyses. Sediments sampling site 97-3 is near well cluster 531.

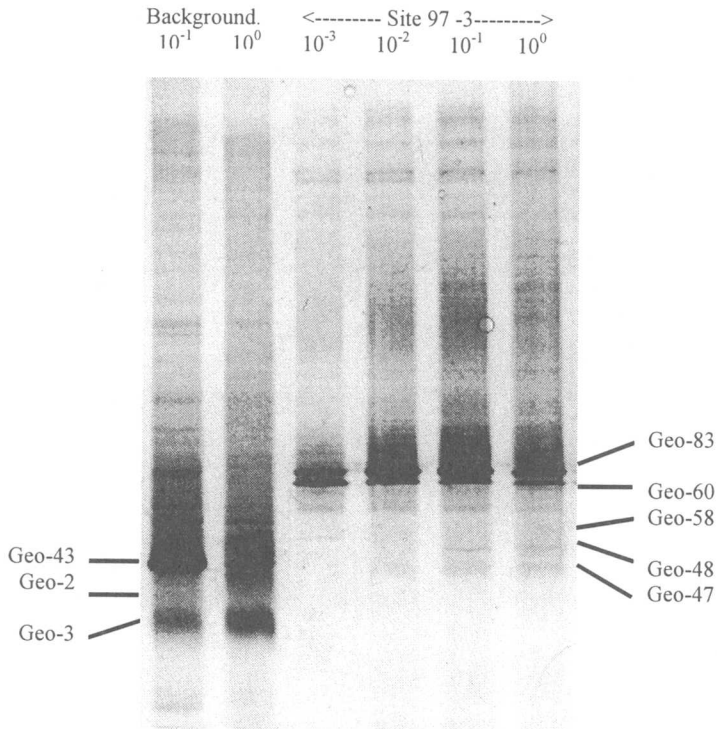


**Figure 6.** Comparison of *Geobacteraceae* detected in benzene-degrading sediment from site 97-3 and an uncontaminated background sediment (adapted from Rooney-Varga and others, 1999).

More intensive DGGE analysis contrasted the differences between *Geobacteraceae* recovered from site 97-3 and the background sites (Figure 6). Bands from benzene-degrading sediment were clearly different than those from background sediments with no shared bands between the two sites suggesting that different populations of *Geobacteraceae* were found in each sediment. When sequences recovered from both sites were analyzed to infer phylogenetic relationships, two distinct clusters of organisms were observed which correlated with the location of sediment samples. Sequences from the benzene-degrading site (97-3) clustered among

*Geobacteraceae* known to degrade aromatic compounds while sequences from the background site did not. Furthermore, DNA extracted from a benzene-degrading enrichment culture established from benzene-degrading sediment collected at Bemidji also contained a sequence (Benz-76, Figure 7) that clustered among the *Geobacteraceae*. These results suggest that a rapid assay could be developed to detect *Geobacteraceae* in contaminated sediments in order to assess the potential for anaerobic benzene degradation in contaminated aquifers.

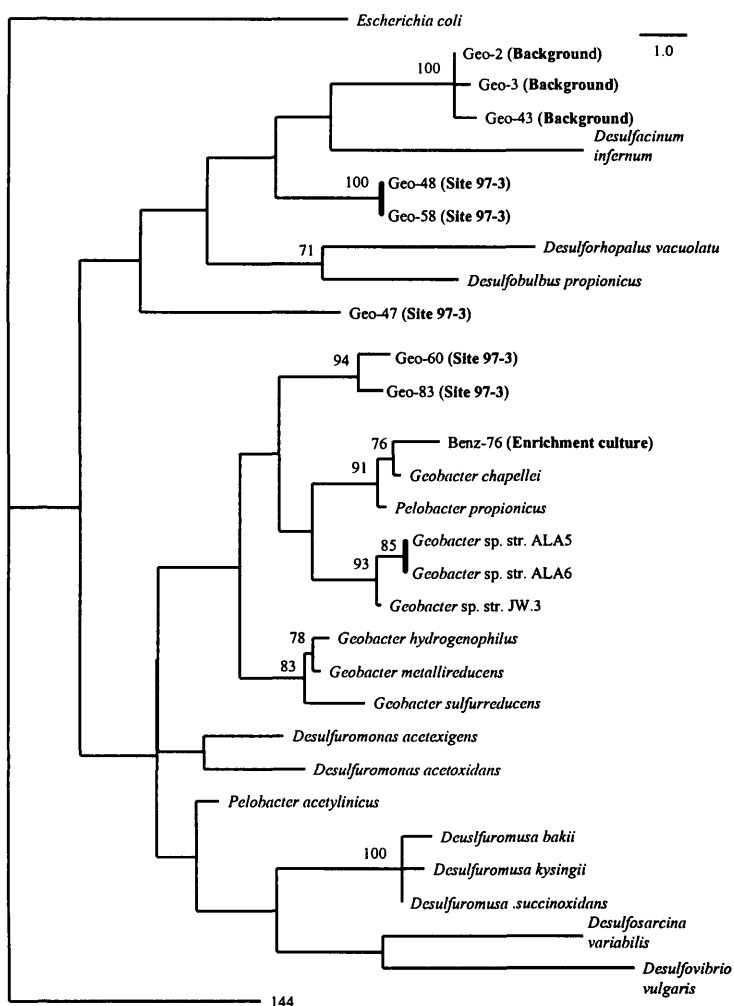


**Figure 7.** Phylogenetic relationship of sequences detected in benzene-degrading sediment from site 97-3, from an background site and a benzene-degrading enrichment culture developed from benzene degrading sediment collected at the Bemidji site (adapted from Rooney-Varga and others, 1999).

## REFERENCES

- Anderson, R.T. and Lovley, D.R. 1997. "Ecology and biogeochemistry of in situ groundwater bioremediation." In: (J. G. Jones, ed.) *Advances in Microbial Ecology*, vol. 15, pp. 289-350, Plenum Press, New York.
- Anderson, R.T. and Lovley, D.R. 1999. "Naphthalene and benzene degradation under Fe(III)-reducing conditions in petroleum-contaminated aquifers." *Bioremediation Journal*, (in press).
- Anderson, R.T., Rooney-Varga, J.N., Gaw, C.V., Lovley, D.R., 1998. "Anaerobic benzene oxidation in the Fe(III) reduction zone of petroleum-contaminated aquifers." *Environmental Science and Technology*, 32(9):1222-1229.
- Barbaro, J.R., Barker, J.F., Lemon, L.A., Mayfield, C.I., 1992. "Biotransformation of BTEX under anaerobic, denitrifying conditions: field and laboratory observations." *Journal of Contaminant Hydrology*, 11:245-272.
- Bedessem, M.E., Swoboda-Colberg, N.G., Colberg, P.J.S., 1997. "Naphthalene mineralization coupled to sulfate reduction in aquifer-derived enrichments." *FEMS Microbiology Letters*, 152:213-218.
- Borden, R.C., Gomez, C.A., Becker, M.T., 1995. "Geochemical indicators of intrinsic bioremediation." *Ground Water*, 33:180-189.
- Cerniglia, C., E. 1992., "Biodegradation of polycyclic aromatic hydrocarbons." *Biodegradation*, 3:351-368.
- Coates, J.D., Anderson, R.T., Lovley, D.R., 1996. "Oxidation of polycyclic aromatic hydrocarbons under sulfate-reducing conditions." *Applied and Environmental Microbiology*, 62(3):1099-1101.
- Cozzarelli, I.M., Eganhouse, R.P, Baedecker, M.J., 1990. "Transformation of monoaromatic hydrocarbons to organic acids in anoxic groundwater environment." *Environmental Geology and Water Science*, 16(2):135-141.
- Edwards, E.A. and Grbic-Galic, D., 1992. "Complete mineralization of benzene by aquifer microorganisms under strictly anaerobic conditions." *Applied and Environmental Microbiology*, 58:2663-2666.
- Flyvbjerg, J., Arvin, E., Jensen, B.K., Olsen, S.K., 1993. "Microbial degradation of phenols and aromatic hydrocarbons in creosote-contaminated groundwater under nitrate-reducing conditions." *Journal of Contaminant Hydrology*, 12:133-150.
- Goerlitz, D.F., Trouman, D.W., Godsy, E.M., Franks, B.J. 1985. "Migration of wood-preserving chemicals in contaminated groundwater in a sand aquifer at Pensacola, Florida." *Environmental and Science Technology*, 19:955-961.
- Kazumi, J., Caldwell, M.E., Suflita, J.M., Lovley, D.R., Young, L.Y., 1997. "Anaerobic degradation of benzene in diverse anoxic environments." *Environmental Science and Technology*, 31:813-818.
- Langenhoff, A.A.M., Zehnder, A.J.B., Schraa, G., 1996. "Behavior of toluene, benzene and naphthalene under anaerobic conditions in sediment columns." *Biodegradation*, 7:267-274.
- Lovley, D.R. 1997a. "Microbial Fe(III) reduction in subsurface environments." *FEMS Microbiology Reviews*, 20:305-313.
- Lovley, D.R. 1997b. "Potential for anaerobic bioremediation of BTEX in petroleum-contaminated aquifers." *Journal of Industrial Microbiology*, 18:75-81.
- Lovley, D.R., Woodward, J.C., Chapelle, F.H., 1996. "Rapid anaerobic benzene oxidation with a variety of chelated Fe(III) forms." *Applied and Environmental Microbiology*, 62:288-291.
- Murphy, F. and Herkelrath, W.N. 1996. "A sample-freezing drive shoe for a wire line piston core sampler." *Ground Water Monitoring and Remediation*, 16(3):86-90.
- Rooney-Varga, J., Anderson, R.T., Fraga, J. L., Ringelberg, D., Lovley, D.R., 1999. "Microbial communities associated with anaerobic benzene degradation in a petroleum-contaminated aquifer." *Applied and Environmental Microbiology*, (submitted).

- Thierrin, J., Davis, G.B., Barber, C., Patterson, B.M., Pribac, F., Power, T.R., Lambert, M., 1993. "Natural degradation rates of BTEX compounds and naphthalene in a sulphate reducing groundwater environment." *Hydrological Sciences*, 38:309-322.
- Thierry, P.-A.B., Hohener, P., Haner, A., Zeyer, J., 1996. "Degradation of weathered diesel fuel by microorganisms from a contaminated aquifer in aerobic and anaerobic microcosms." *Environmental Toxicology and Chemistry*, 15(3):299-307.

# Electrical Geophysics at the Bemidji Research Site

By Robert J. Bisdorf

## ABSTRACT

Self-potential (SP), induced polarization (IP), and direct-current (DC) resistivity electrical geophysical methods were used to study the effect of crude oil on the resistivity of a sand and gravel aquifer near Bemidji, Minnesota. The SP measurements do not show any trends that correspond with the oil spill. The IP data show resistivities consistent with the DC measurements, but only a slight polarization effect. Direct-current resistivity measurements made into maps and cross sections, detect lower resistivities associated with the oil spill, especially in areas where the oil soaked into the sand and gravel. The observed resistivity measurements show a larger resistivity decrease than can be explained by laboratory measurements made on selected samples of the sand and oil.

## INTRODUCTION

In 1979 a crude oil pipeline burst spilling about 1,700,000 L of oil onto the glacial outwash aquifer about 16 km northwest of Bemidji, Minnesota. Initial cleanup efforts recovered about 1,300,000 L of crude oil leaving about 400,000 L in the aquifer. Figure 1 shows the general location of the research site, the spray zone, the oil drainage area, and the excavated area. The broken pipeline sprayed crude oil to the northwest. This oil drained from the topographic high through the drainage area to the south oil pool. The excavated area is the area around the pipeline excavated for repair of the pipe as well as for oil recovery.

The glacial outwash sand and gravel is about 8m thick and is underlain by other stratified glacial deposits. A uniform glacial till underlies the stratified glacial deposits at a depth of about 25 meters (Smith and Hult, 1993). In 1998 the U.S. Geological Survey made surface electrical geophysical measurements at this site to determine the effect of crude oil on the electrical properties of the sand and gravel aquifer. Self-potential (SP), induced polarization (IP), and Direct-current (DC) resistivity electrical geophysical methods were used. The site is generally clear of cultural features except for many metallic well casings, the crude oil

pipelines, a buried telephone line, and buried power cables.

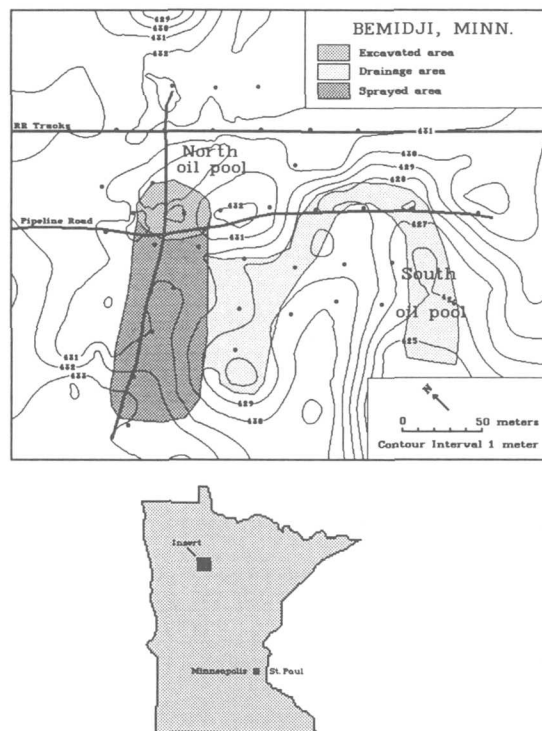


**Figure 1.** Location of research site near Bemidji, Minnesota (modified from Smith and Hult, 1993) including the location of the north and south oil pools, the excavated area, the spray zone, and the oil drainage area.

## INDUCED POLARIZATION

Induced polarization (IP) is a technique that measures the delay in the response of earth materials to an electrical signal. The delay is caused by the build up of charge on metal in an electrolyte or due to membrane effects in clays (Sumner, 1976). The IP response is frequency dependent and measurements made using multiple frequencies are called complex resistivity (CR) or spectral IP (SIP). The frequency domain measurements made for this survey express the IP effect as phase in milliradians. Because the IP response is also dependent on the resistivity/conductivity of the rock, conductivity measurements are also made. Measurements were made at multiple frequencies, but results will only be presented for the lowest frequency (0.125 Hz). The IP measurements were made to detect variations in the clay content of the aquifer, and possible reactions of the crude oil with the clays. Because of its greater signal generation, measurements were made to an "n" of 10, using the pole-dipole array instead of the more conventional dipole-dipole array. The "infinite" current electrode was placed about 245 meters away from the close current electrode. Data were inverted using a computer program licensed from the University of British Columbia-Geophysical Inversion Facility under a consortium research project "Joint/cooperative inversion of geophysical and geological data". The program is based on the work of Oldenburg and Li (1994).

## SP MEASUREMENTS

The SP method measures natural potential fields in the earth caused by electrokinetic coupling, thermoelectric coupling, and electrochemical reactions (Corwin, 1990). Man made sources of potential from electric power lines and associated equipment are the main source of noise for this method. About 180 total-field SP measurements were made in two sets of

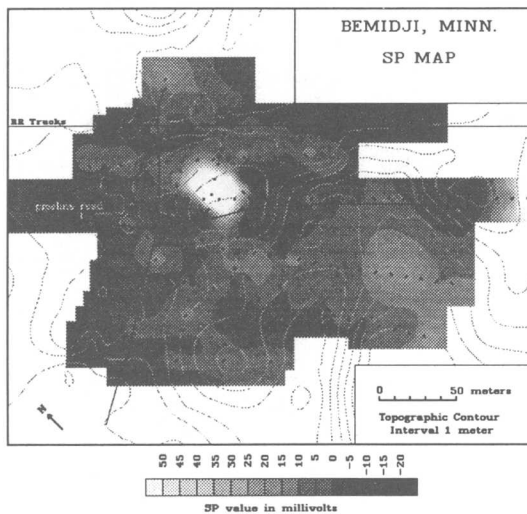


**Figure 2.** Map of SP values. Black dots indicate measurement locations. Gray scale represents measured voltage in millivolts.

semi-orthogonal lines each with its own zero reference electrode. The 2 data sets were consistent enough to combine into one map. Figure 2 shows a map of the combined data sets. The small black dots represent the measurement locations. Contours of elevation and road locations are overlain for reference. The main feature of the map is a small area of very high (190 mv) SP that occurs just north of the pipeline road. This anomaly is close to the pipeline break and the subsurface oil pool, but I think that the anomaly is generated by electric power lines that were installed to power the automated data loggers. In general the SP trends/anomalies shown on the map can not be correlated with the pooled oil, the oil spray zone, the areas of oil flow, or topography.

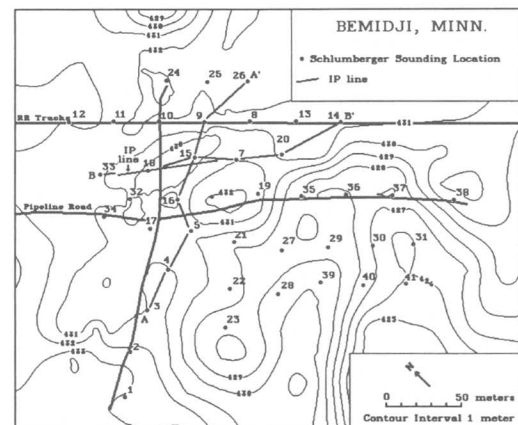


**Figure 3.** Map showing the location of the Schlumberger soundings, the IP line, and cross sections A-A' and B-B'.



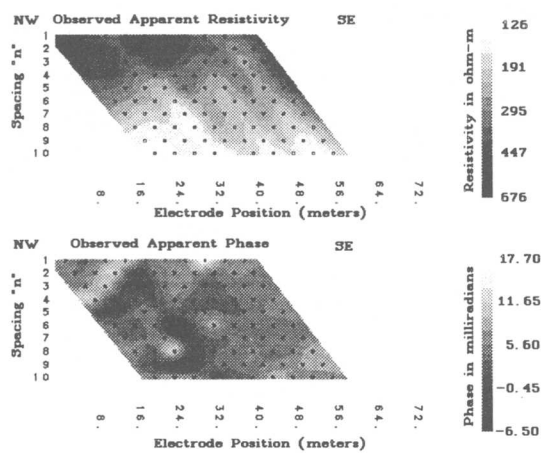


**Figure 4.** Pseudo sections of apparent IP resistivity and phase.

Figure 3 is a location map that shows the location of the IP cross section, and the DC resistivity sounding locations. Contours of elevation, and road locations are displayed for reference. Figure 4 shows pseudo sections of the IP resistivity and phase measurements. The apparent resistivities are high (greater than 700 ohm-m) at the surface and decrease with depth. In addition, the apparent resistivities get lower to the southeast toward the north oil pool. The apparent phase pseudo section shows a phase increase in the area of "n" of 8 to 10 and at an electrode position of 40 to 46 meters. Small phase anomalies are present in the near surface.

Figure 5 shows the IP resistivity and phase models. The resistivity model shows a high resistivity (greater than 700 ohm-m) layer over a zone of dome shaped lower resistivity (less than 100 ohm-m). The phase model shows a low phase layer (less than 5 milliradians) over a dome shaped zone of slightly higher phase (greater than 5 milliradians). To the southeast of electrode position 58 exists a higher phase (7 to 16 milliradians) anomaly that is near the main portion of the north oil pool. This may be caused by the oil pool, but, unfortunately, the anomaly is on the edge of the data set and may not be directly related to the data, but only to initial model parameters and boundary values.

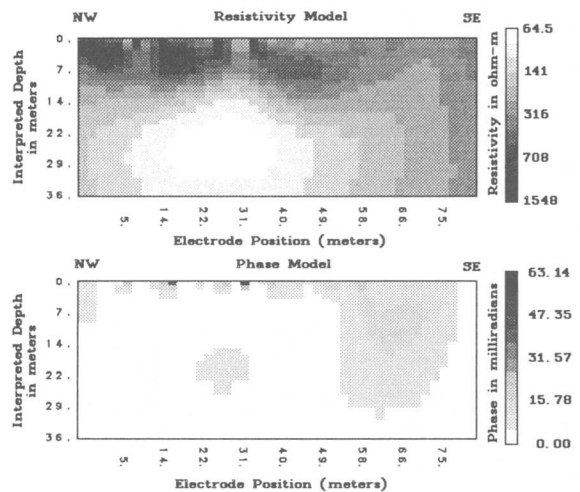


**Figure 5.** Cross sections of interpreted IP resistivity and phase.

## DC RESISTIVITY SOUNDINGS

DC resistivity sounding is a geophysical technique that uses variations in the electrical resistivity of earth materials to help detect buried geologic structures. Resistivity (the inverse of conductivity) is a fundamental rock property that varies due to rock type, clay content, porosity and the quantity and quality of the pore water. Resistivity is normally expressed in ohm-m. Generally speaking, higher clay content and/or poorer quality (more dissolved solids) ground water lowers the rock resistivity.

For this survey the Schlumberger array (Zohdy and others, 1974) was used to vertically explore the subsurface. The name Schlumberger derives from Conrad Schlumberger, an early proponent of the array geometry. Schlumberger soundings are processed by computer modeling of the sounding data as a series of horizontal layers (Zohdy, 1989 and Zohdy and Bisdorf, 1989). More detailed explanations of the processing and automatic interpretation procedure can be found in Bisdorf (1985) and Zohdy and others (1993). A series of individual soundings can be combined to generate either a geoelectrical cross section or a map view of interpreted resistivity. Cross sections, which can be thought of as vertical slices through the ground similar to a road cut, show lateral as well as vertical variations of resistivity. Maps of interpreted resistivity show areal distributions at a particular depth or

elevation and can be thought of as horizontal slices through the earth.

The resistivity of selected samples of sand and crude oil from the site was measured in the laboratory. Table 1 summarizes the results. The resistivity of the crude oil is as expected, very high, but the fact that the resistivity of the wet sand/oil mix was not much different than that of water saturated sand came as a surprise. In fact the resistivity of the oil/water-saturated sand was lower than that of the water-saturated sand. These measurements need to be repeated to verify this result, but as it stands it appears that the oil somehow increases conduction, possibly by forcing the water into more coherent paths. These data indicate that the oil floating on the water table should not be detectable as a resistivity anomaly since the resistivity contrast is small (376/320). Of course mixing oil, sand and water in the lab may not accurately reflect conditions in situ.

**Table 1.** Measured resistivity of selected samples.

sample description	resistivity (ohm-m)
6/17/98 crude oil	13 meg
moist uncontaminated sand 6/17/98	820
sand saturated with distilled water	376
wet sand saturated with crude oil	320
dry oil contaminated sand	20 meg

Figure 3 shows the Schlumberger sounding locations. The locations of 2 interpreted resistivity cross sections are indicated by the heavy lines labeled A-A' and B-B'. Sounding expansion was limited to a maximum of about 600 meters between the current electrodes (300 meters AB/2). In general, neither the well casings nor the pipeline influenced the Schlumberger sounding measurements. Surface areas of dry, oil coated sand caused some contact resistance problems that were solved by adding water to the electrode holes and stirring to lower the contact

resistance.

## CROSS SECTIONS OF INTERPRETED RESISTIVITY

Resistivity cross sections are generated from individual sounding interpretations. Each sounding interpretation is sampled in a manner to approximate a continuous vertical distribution of resistivity with depth (Bisdorf, 1982). These vertical distributions are then horizontally interpolated to create a grid. Shades of gray are assigned based on the interpolated resistivity values and the desired contour levels. Triangles on the upper surface of the cross section designate the sounding locations. Topographic information, input as sounding elevations, is represented by connecting the surface location of the soundings by straight lines.

Figure 6 shows the geoelectrical cross section labeled A-A' in Figure 3. This cross section extends across the northern oil pool from southwest to northeast. High resistivities (greater than 700 ohm-m) dominate the upper 10 to 12 meters of this cross section except under soundings 15 and 16 where resistivities are moderate (300 to 700 ohm-m). These high resistivity sediments are similar in resistivity to the moist uncontaminated sand in Table 1. The moderate resistivities are in the area of the oil pool. Sounding 15 is the area where the early oil recovery was done and sounding 16 is close to where the pipeline broke. These moderate resistivities could be due to the oil-recovery/pipeline-repair activities or to some effect of the oil on the sand that would reduce the resistivity of the material. The water table in the area is between 423 and 424 meters in elevation (Smith and Hult, 1993). Under soundings 15 and 16 low resistivity material becomes shallower, with the 150 ohm-m contour rising almost 10 meters. This low resistivity material could be the underlying till, but wells 606 and 607, shown on the cross section, encountered the till between the elevations of 405 and 410 meters. Since this shallowing of the deeper low resistivity zone is in the area of the oil plume, it is possible that it is due, in some unknown fashion, to the effect of the oil.

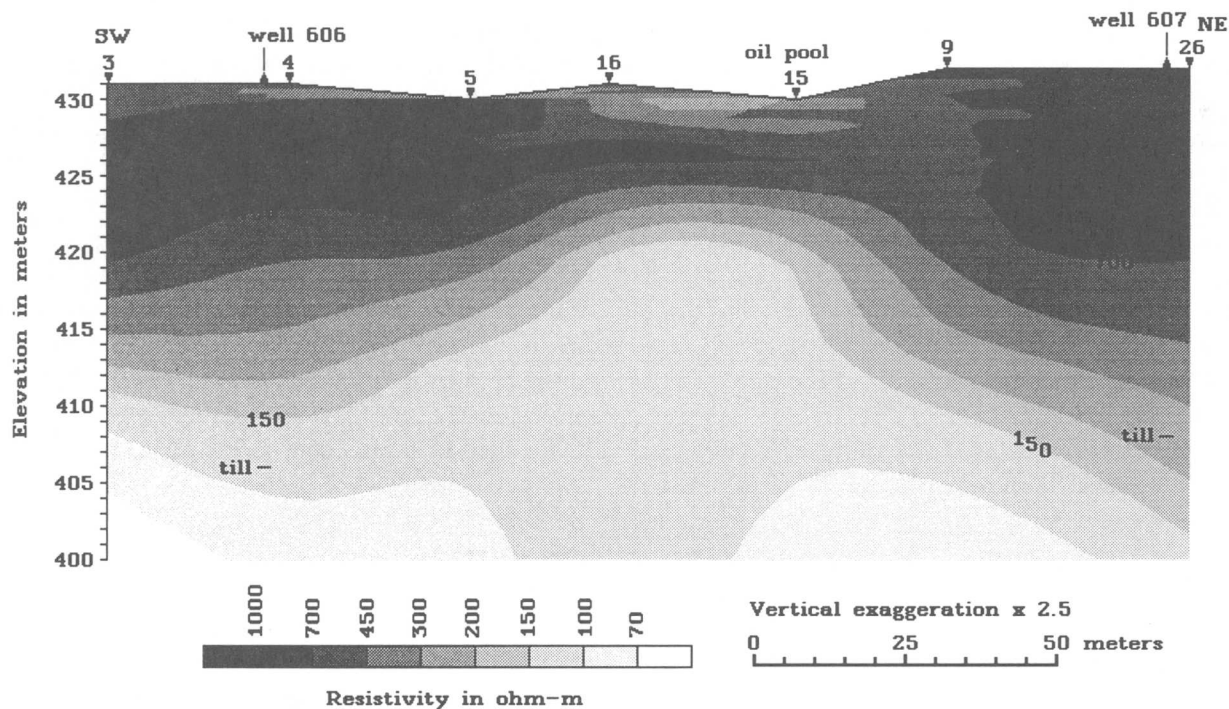


**Figure 6.** Cross section of interpreted resistivity designated A-A' on figure 3. The gray scale represents interpreted resistivity values in ohm-m. The surface location of the soundings are indicated by the triangles.

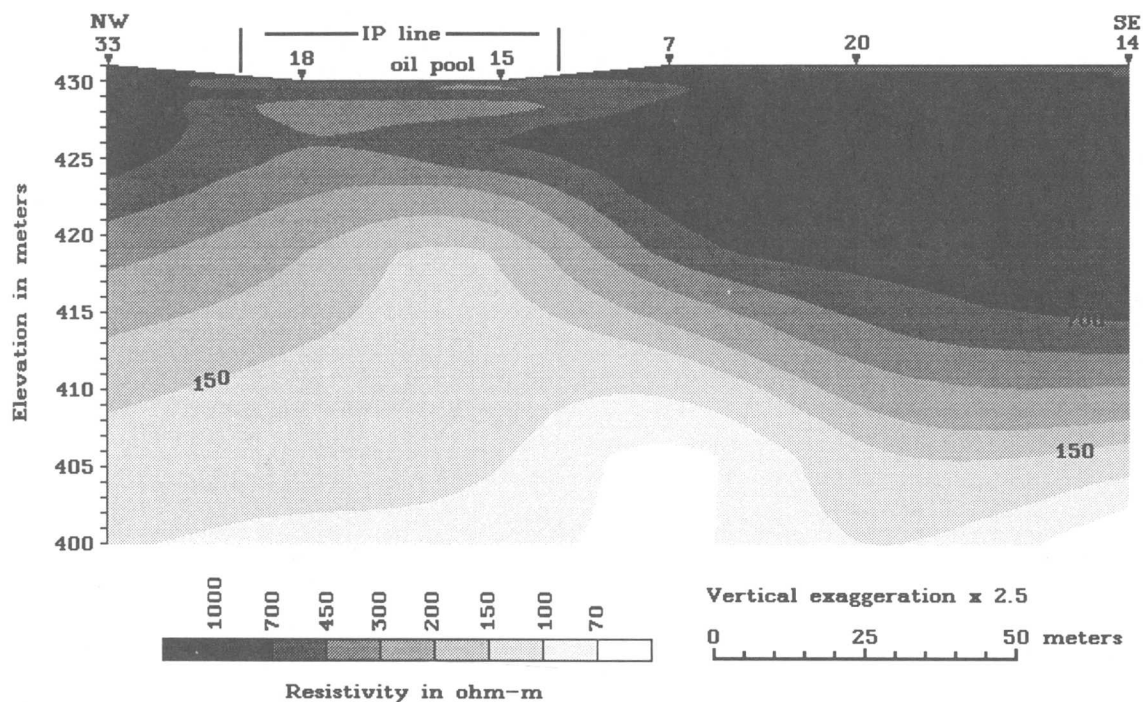


**Figure 7.** Cross section of interpreted resistivity designated B-B' on figure 3. The gray scale represents interpreted resistivity values in ohm-m. The surface location of the soundings are indicated by the triangles.

Figure 7 shows the geoelectrical cross section labeled B-B' in Figure 3. This cross section extends across the northern oil pool from northwest to southeast. High resistivities of greater than 700 ohm-m dominate the upper 10 to 12 meters of the cross section except under soundings 18, 15, and 7 where resistivities are moderate (300 to 700 ohm-m). This is the area where oil pooled and much of the early oil recovery was done. As in cross section A-A', the 150 ohm-m contour rises to about 10 meters under sounding 15.

It is interesting to note that the water table is not delineated on the eastern portions of these cross sections. High resistivity continues to an elevation of as low as 415 meters. This may be due to coarser sand and gravel being more predominate to the east and south of the plume area effectively masking the effect of the water table. The modeled IP data shown in figure 5 corresponds well with the applicable portion of cross section B-B'. High resistivities to the northwest moderating onto the oil pool area. At depth, low resistivities become more shallow just southeast of sounding 18.

## RESISTIVITY MAPS AT SELECTED ELEVATIONS

Maps of interpreted resistivity at a particular elevation are generated by sampling the sounding interpretations at depths determined by the difference between the surface elevation at that sounding and the desired elevation. The resultant sampled interpreted resistivities and the corresponding location values are gridded using a minimum-curvature algorithm (Webring, 1981). To prevent possible interpolated resistivities of less than zero, the logarithm of the resistivities is used for gridding. Shades of gray are assigned based on the grid value and the desired logarithmically spaced contour levels. Since these maps are raster (pixel) based, a bicubic interpolation program is used to increase the size of the resultant image. An interpolating program is used to resample the grid, as opposed to simply gridding the data at the desired final interval, because the minimum-curvature algorithm

generates undesirable results if the data are over sampled. The Kolor-map and section program (Zohdy, 1993) uses similar procedures and provides a discussion of the nuances of resistivity map generation.

Figure 8 shows a map of interpreted resistivity made at an elevation of 424 meters. This elevation is just at or above the water table. High resistivities are associated with topographic highs and low resistivities are associated with topographic lows. The area of the north oil pool is designated by "A" in the figure. Letter "B" is associated with moderate to low resistivities in the area where the oil drained after the pipeline break and the southern oil pool. Again, moderate and low resistivities are associated with the presence of a very high resistivity crude oil.

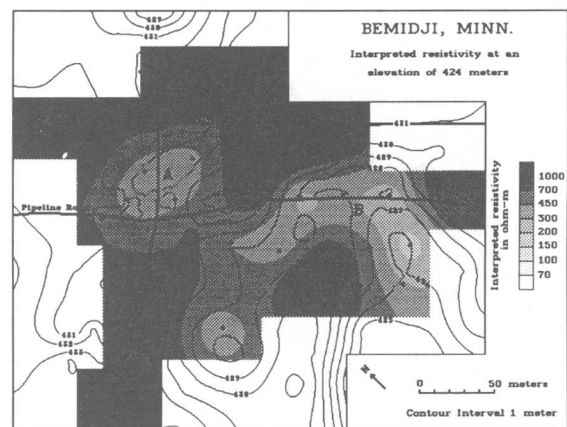


**Figure 8.** Map of interpreted resistivity at an elevation of 424 meters. The gray scale represents interpreted resistivity in ohm-m. The sounding locations are indicated by the black dots.

## SUMMARY

SP data did not show anomalies that correlated with pooled oil, or areas of oil contamination. IP measurements showed an area of low resistivity at depth in the area of the northern oil pool. A small phase anomaly is also associated with this oil pool, although the anomaly is not very large. Additional frequencies need to be modeled to confirm the phase information. DC resistivity sounding data showed a lower resistivity anomaly in areas were

the crude oil had soaked into the sand and in the known pool areas. This is surprising because lab measurements made on selected sand, oil, and sand-oil mixture indicated only a small resistivity contrast. Some mechanism lowering resistivities is in place at the site that is not reflected in my sand samples. It is possible that by products of bacterial activity are lowering the in situ resistivities, or possibly that some fraction of the oil has gone into solution and is lowering the resistivity.

## REFERENCES

- Bisdorf, R.J., 1982, Schlumberger sounding investigations in the Date Creek Basin, Arizona: U.S. Geological Survey Open-File Report 82-953, 55 p.
- \_\_\_\_\_, 1985, Electrical techniques for engineering applications: Bulletin of the Association of Engineering Geologists, v. XXII, no. 4, p. 421-433.
- Corwin, R.F., 1990, The self-potential method for environmental and engineering applications in Ward, Stanley H., ed., Geotechnical and environmental geophysics, Vol. I, Review and tutorial: Investigations in Geophysics, 5, p. 127-145.
- Lucius, J. E., and Bisdorf, R. J., 1995, Results of geophysical investigations near the Norman, Oklahoma, municipal landfill, 1995: U.S. Geological Survey Open-File report 95-825, 125 p.
- Oldenburg, D.W., and Li, Yaoguo. 1994, Inversion of induced polarization data: Geophysics, v. 59, p 1327-1341.
- Smith, S.E., and Hult, M.F., 1993, Hydrogeologic data collected from a crude-oil spill site near Bemidji, Minnesota, 1983-91: U.S. Geological Survey Open-File Report 93-496, 158 p.
- Sumner, J.S., 1976, Principles of induced polarization for geophysical exploration: Elsevier Scientific Publishing Company, New York, NY, 277 p.
- Webring, Michael, 1981, MINC: A gridding program based on minimum curvature: U.S. Geological Survey Open-File Report 81-1224, 12 p.
- Zohdy, A.A.R., 1989, A new method for the automatic interpretation of Schlumberger and Wenner sounding curves: Geophysics, v. 54, p. 245-253.
- \_\_\_\_\_, 1993, Program Kolor-Map & Section, Amiga Version: U.S. Geological Survey Open-File Report 93-585, 113 p.
- Zohdy, A.A.R., and Bisdorf, R.J., 1989, Programs for the automatic processing and interpretation of Schlumberger sounding curves in QuickBASIC 4.0: U.S. Geological Survey Open-File Report 89- 137 A&B, 64 p., + disk.
- Zohdy, A.A.R., Eaton, G.P., and Maybey, D.R., 1974, Application of surface geophysics to ground-water investigations, Techniques of ground water investigations of the U.S. Geological Survey, Book 2, Chapter D1:U.S. Geological Survey, Denver, CO, 116 p.
- Zohdy, A.A.R., Bisdorf, R.J., and Martin, Peter, 1993, A study of sea-water intrusion using Schlumberger soundings near Oxnard, California: U.S. Geological Survey Open-File Report 93-524, 139 p.



# Impacts of Remediation at the Bemidji Oil-Spill Site

By William N. Herkelrath

## ABSTRACT

The U.S. Geological Survey has conducted a multidisciplinary investigation of the fate and transport of subsurface petroleum hydrocarbons at the site of crude-oil spill near Bemidji, Minnesota, since 1983. For 19 years, the Bemidji site provided a unique natural laboratory for scientists to study a subsurface oil spill that was virtually undisturbed. However, in order to ensure compliance with the law, Minnesota State authorities have recently mandated oil-recovery remediation of the site. The aim of the remediation is to remove the separate-phase oil that is presently located near the water table. In this paper, simple models were used to obtain first-order estimates of how much subsurface oil is now present at the Bemidji site, and how much oil is likely to be recovered during the remediation. These preliminary results indicate that about 241,000 liters of oil are now present, and about 41,000 liters (17% of the present oil volume) will be recovered during the remediation.

## INTRODUCTION

The U.S. Geological Survey, in cooperation with several academic institutions, has conducted a multidisciplinary investigation of the fate and transport of petroleum hydrocarbons within an aquifer at the site of a crude-oil spill near Bemidji, Minnesota, since 1983. A wide range of research has been conducted at the site. Much of the research focused on understanding processes that lead to the natural bioremediation of dissolved hydrocarbons. Work also was done on studying the complex, interrelated inorganic and organic geochemical reactions that occur within a contaminated aquifer. The factors that influence the oil-saturation distribution and the rate of dissolution of separate-phase oil within the aquifer and in the unsaturated zone also were investigated. In the process of the research, a large number of sediment cores were obtained and analyzed in order to create a large database of particle-size and porosity distributions that is useful in developing model representations of the heterogeneous aquifer.

In the past, remediation efforts at the site were limited to a cleanup that was carried out within one month of the pipeline break that caused the spill in August, 1979. Because the site is located in a remote area, there was little

demand for further remediation. For 19 years, the Bemidji site provided a unique natural laboratory for scientists to study a subsurface oil spill that was virtually undisturbed. However, in order to ensure compliance with state law, the Minnesota Pollution Control Agency has recently mandated further remediation. The aim of the remediation is to remove the separate-phase oil that is located near the water table at the Bemidji site. Installation of remediation equipment began in 1998, and it is anticipated that oil removal will begin in 1999.

Remediation activities will disrupt much of the ongoing research at the site. It is anticipated that large amounts of water will be pumped out of several wells, which will change the ground-water flow regime and alter the subsurface conditions that have resulted in natural biological degradation of the dissolved contaminants. However, the remediation of the Bemidji site provides an important opportunity to investigate the impact and efficacy of remediation at a well-characterized site. Although the Nation has made a large investment in research, development, and implementation of remediation techniques for petroleum spill sites, very few well-documented field-scale case studies have been published.

This paper reports preliminary quantitative estimates of the anticipated impacts of the proposed remediation on the amount and distribution of subsurface oil at the Bemidji oil-spill site.

### Subsurface Oil Prior to Remediation

The primary goal of the remediation will be the removal of some of the separate-phase oil. In order to estimate how much oil is likely to be removed, I first estimated the amount and distribution of oil present prior to remediation. Since 1989, sediment cores were periodically obtained within the two major subsurface oil pools (the “north” and “south” pools) at the Bemidji site. Using the methods described in Hess and others (1992) and Murphy and Herkelrath (1996), the cores were analyzed in order to measure the vertical distribution of oil, air, and water saturation within each core. Because the oil is less dense than water, the oil tends to “float” on the water table. Oil saturation rapidly decreases below the water table. Oil also was found in the unsaturated zone above the water table. Essaid and others (1993) and Dillard and others (1997) published detailed analyses of the oil saturation data.

In order to estimate the total amount of oil present in the north and south pools at the site, I first calculated  $L_o$ , the total volume of oil per unit cross-sectional area in each borehole.  $L_o$  has dimensions of length, and is equivalent to the length that the oil phase would occupy if the oil were present in a core liner without any sediment. I then interpolated between values of  $L_o$  measured at the boreholes in order to create a matrix of estimated values of  $L_o$  on a uniform grid. A contour map of the interpolated total volume of oil per unit cross section at the Bemidji north oil pool is shown in figure 1. A contour map of the  $L_o$  distribution at the south pool is shown in figure 2. By integrating over the interpolated matrices, I estimated that the total amount of oil present at the north and south pools is 147,000 and 94,000 liters, respectively.

A significant fraction of the oil at the north pool is located above the water table in the unsaturated zone. The water table at the north pool is about six meters below the surface. The

“unsaturated zone” oil is probably located beneath areas where the oil originally infiltrated into the soil, and represents a “residual” saturation of oil that is “trapped” or flows very slowly downward. This oil probably will not be mobilized in the proposed “pump and treat” remediation.

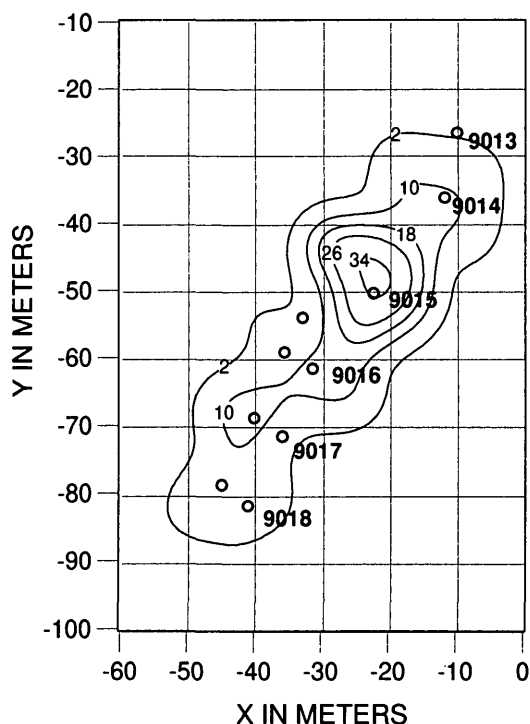


**Figure 1.** Contour map of the total volume of oil per unit cross section (in centimeters) at the Bemidji north oil pool. Circles indicate borehole locations. USGS well numbers are shown in bold print.

In order to estimate the total amount of oil that may be influenced by the north pool remediation, I assumed that oil that is more than one meter above the water table (or above an elevation of 424.5 meters above sea level) will not be influenced. The cutoff elevation was somewhat arbitrarily selected to roughly correspond to the top of the “capillary fringe,” a zone in which both the water and oil saturation rapidly declined above the water table. I calculated  $L_1$ , the total volume of oil per unit cross sectional area below 424.5 m in each borehole. A contour map of the interpolated distribution of  $L_1$ , which illustrates the areal distribution of oil at the water table at the north pool, is shown in figure 3. By integrating over the interpolated matrix, I



estimated that the total amount of oil near the water table at the north pool is 88,000 liters, and the total amount of oil in the unsaturated zone at the north pool is 59,000 liters.

At the Bemidji south oil pool, the water table is only 2 meters below the surface, and almost all of the oil is near the water table. I assume that all of the oil at the south pool will be influenced by remediation.

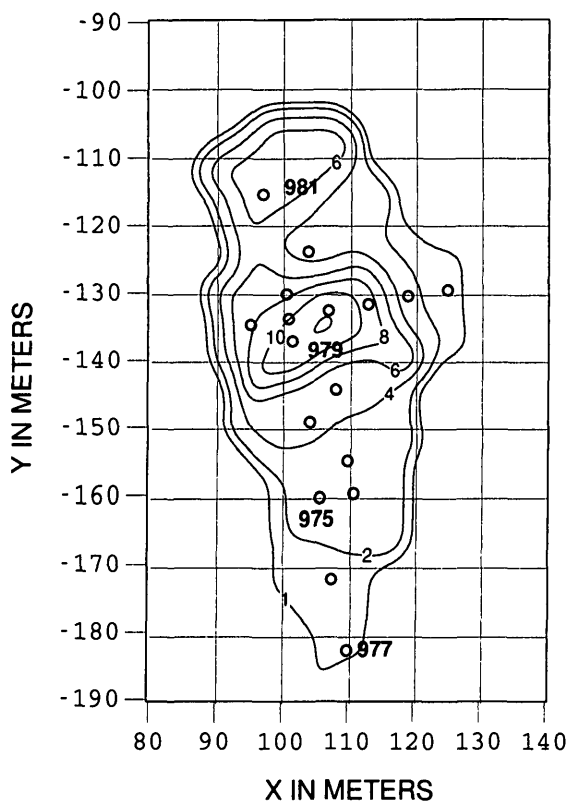


**Figure 2.** Contour map of the total volume of oil per unit cross section (in centimeters) at the Bemidji south oil pool. Circles indicate borehole locations. USGS well numbers are shown in bold print.

In a reconnaissance carried out in 1998, Lakehead Pipe Line Company discovered another, smaller subsurface oil pool (the “middle pool”), which is located between the north and south pool. The USGS has not cored the middle pool, and I cannot estimate the amount of oil present.

## The Remediation Plan

A plan for remediating the Bemidji site was developed by the Lakehead Pipe Line Company (1998). According to the plan, two oil-recovery wells (RW-1N and RW-2N) will be installed at the north oil pool (figure 3). Each of these wells will have a 254-mm diameter and a 3-m long screen that straddles the water table. The plan is to pump water from each well at a rate of 45 liters/minute for 5 years. The idea is to create a depression in the water table near the wells within which oil will tend to collect. It is expected that oil will slowly flow into the wells, where it will be skimmed off of the surface of the water and injected into a nearby oil pipeline. Water removed from the wells will be pumped into an infiltration gallery that is located upgradient.

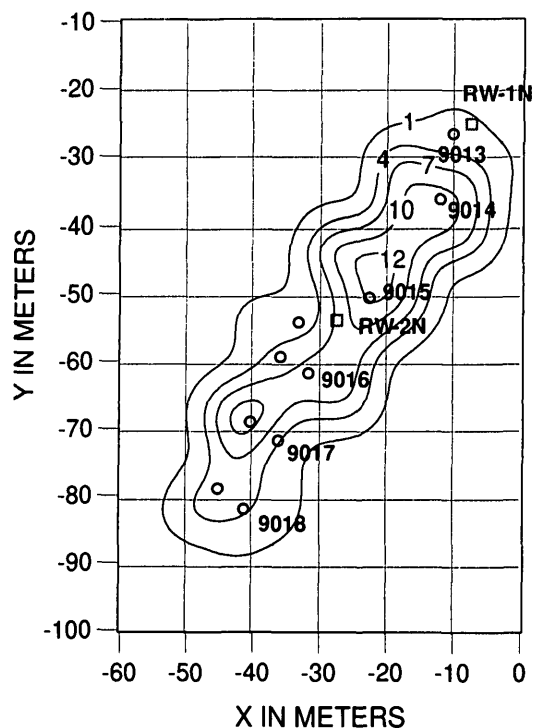


**Figure 3.** Contour map of the volume of oil per unit cross section (in centimeters) that is located less than one meter above the water table at the Bemidji north oil pool. Circles indicate borehole locations, and squares indicate oil-recovery well locations.

Two oil-recovery wells will also be placed at the middle pool. A total of about 70 liters of water per minute will be pumped from the middle pool area.

A drain tile that is approximately 30 meters long will be installed along the main axis of the south oil pool just below the water table. Water will be pumped from the drain tile at a rate of 80 liters/minute in order to create a linear depression in the water table. It is anticipated that oil will flow into the drain tile and be skimmed off of the surface of the water.

## Predicted Oil Recovery

In order to obtain a first-order estimate of the amount of oil that can be recovered by remediation, I adopted the concept of “residual oil saturation,” which is commonly used in petroleum engineering (Dullien, 1992). I assumed that wherever the oil saturation is initially above a “residual” value of  $S_{or}$ , oil would be removed until the oil saturation was reduced to  $S_{or}$ . Therefore, I assumed that the maximum oil saturation after remediation would be  $S_{or}$ . Wherever the initial oil saturation was below  $S_{or}$ , the oil was assumed to be immobile, and the oil saturation would not change during the remediation.

Residual oil saturation is difficult to estimate.  $S_{or}$  has been found to depend on many factors and to vary widely from site to site. For example, Abdul (1992) reported that  $S_{or}$  ranged from 0.08 to 0.32 (8 to 32% of the pore space) in small funnels of sand and can be higher in a heterogeneous field environment. At the Bemidji site, one indicator of  $S_{or}$  is the level of oil saturation found in the unsaturated zone beneath the location where oil infiltration occurred. After 19 years of drainage, the very oily sediments found in the unsaturated zone near the center of the north oil pool have drained to an oil saturation of 0.25 +/- 0.05. In order to cover the probable range indicated by this data, I calculated oil recovery assuming both  $S_{or} = 0.2$  and 0.3.

The “recoverable” oil volume,  $V_{rec}$ , that was found in each 75-mm-long core section was used to estimate total oil recovery.  $V_{rec}$  was calculated from

$$V_{rec} = V\phi(S_o - S_{or}) \quad (\text{for } S_o > S_{or}), \quad (1)$$

where

- $V$  is the volume of the core section,
- $\phi$  is the porosity of the core section, and

$S_o$  is the oil saturation in the core section.

$V_{rec}$  was assumed to be zero if  $S_o < S_{or}$ .

Individual  $V_{rec}$  values were summed in order to obtain an estimate of the recoverable oil volume per unit cross section,  $L_{rec}$ , at each borehole location. For  $S_{or} = 0.3$ , a contour map of interpolated  $L_{rec}$  values at the north pool is shown in figure 4. By integrating over the interpolated  $L_{rec}$  matrices, I estimate that 23,000 ( $S_{or} = 0.3$ ) to 37,000 ( $S_{or} = 0.2$ ) liters of oil can be recovered from the north oil pool. Similar calculations using the south pool data indicate that 6,000 to 16,000 liters of oil can be recovered there.

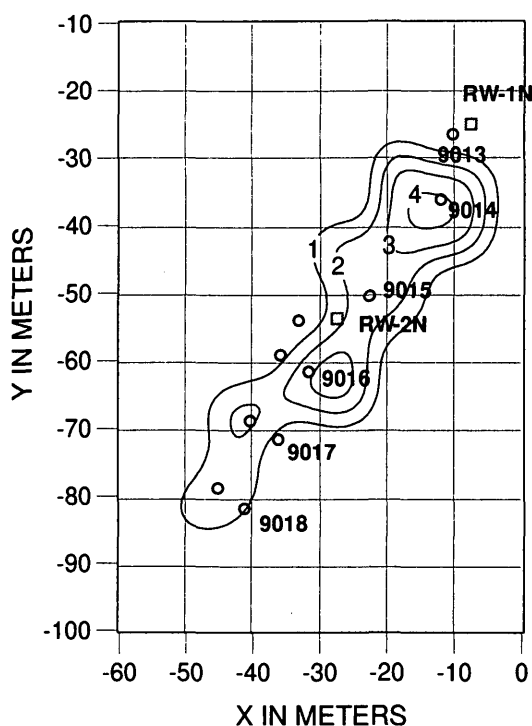


**Figure 4.** Contour map of the volume of oil per unit cross section (in centimeters) that is likely to be recovered by remediation at the Bemidji north oil pool. Circles indicate borehole locations, and squares indicate oil-recovery well locations.

## Subsurface Oil after the Remediation

These preliminary estimates indicate that after the oil-recovery remediation there will still be 110,000 to 124,000 liters of oil at the Bemidji north oil pool. I estimate that 16 to 25% of the

original oil in place will be removed during the north pool remediation. The oil that remains should be spread over roughly the same area outlined by contours in figure 1. At the south pool, I estimate that 7 to 17% of the oil will be removed, and there should still be 78,000 to 88,000 liters in place after the remediation.

## SUMMARY AND CONCLUSIONS

The State of Minnesota has mandated oil-recovery remediation of the Bemidji oil-spill site. The USGS has carried out research into the fate and transport of hydrocarbons in the subsurface at this site since 1983. The aim of the remediation, which is scheduled to begin in 1999, is to recover and remove separate-phase oil that is presently located near the water table. The remediation plan calls for pumping large amounts of water out of several recovery wells. Oil will be drawn into the wells, where it will be skimmed off of the water surface and injected into an oil pipeline. Because the natural ground-water flow regime will be greatly changed, most of the ongoing research at the site will be disrupted.

Using extensive data obtained from field cores, I estimated the amount of oil in place at the Bemidji site at present. By applying a simple model based on the concept of residual oil saturation, I obtained a first-order estimate of the amount of oil that can be recovered by the remediation. Oil volumes estimated in this analysis are summarized in table 1. The low oil recoveries predicted (16 to 25% at the north oil pool; 7 to 17% at the south oil pool) are in good agreement with other case studies (Abdul, 1992), and with the experience of the oil industry. These calculations reemphasize how difficult it is to remove separate-phase oil from sediments using pump-and-treat technology.

**Table 1.** Summary of Bemidji oil volume estimates. All volumes are in liters.

### North oil pool:

Total initial volume of oil in the unsaturated zone	59,000	Liters
Total initial volume of oil near the water table	88,000	liters
Total initial volume of oil at the north pool	147,000	liters
Assumed residual oil saturation	0.3	0.2
Estimated recoverable oil volume	23,000	37,000
Recoverable oil volume/initial oil volume	16%	25%

### South oil pool:

Total initial volume of oil at the south pool	94,000	liters
Assumed residual saturation	0.3	0.2
Estimated recoverable oil volume	6,000	16,000
Recoverable oil volume/initial oil volume	7%	17%

## REFERENCES

- Abdul, Abdul S., 1992, A new pumping strategy for petroleum product recovery from contaminated hydrogeologic systems: Laboratory and field evaluations: *Ground Water Monitoring Review*, v. 12, no. 1, p. 105-114.
- Dillard, L.A., Essaid, H.I., and Herkelrath, W.N., 1997, Multiphase flow modeling of a crude-oil spill site with a bimodal permeability distribution: *Water Resources Research*, v. 33, no. 7, p. 1617-1632.
- Dullien, F.A.L., 1992, *Porous media fluid transport and pore structure* (2<sup>nd</sup> ed.): San Diego, Academic Press, 574 p.
- Essaid, H.I., Herkelrath, W.N., and Hess, K.M., 1993, Simulation of fluid distributions observed at a crude oil spill site incorporating hysteresis, oil entrapment, and spatial variability of hydraulic properties: *Water*

Resources Research, v. 29, no. 6, p.  
1753-1770.

Hess, K.M., Herkelrath, W.N., and Essaid, H.I.,  
1992, Determination of subsurface fluid  
contents at a crude-oil spill site: Journal of  
Contaminant Hydrology, v. 10, p. 75-96.

Lakehead Pipe Line Company, 1998, Remedial  
investigation and corrective action design  
report, milepost 926.53, Pinewood,  
Minnesota, 30 p.

Murphy, Fred and Herkelrath, W.N., 1996, A  
sample-freezing drive shoe for a wire line  
piston core sampler: Ground Water  
Monitoring & Remediation, v. 16, no. 3, p.  
86-90.

## **AUTHOR INFORMATION**

William N. Herkelrath, U.S. Geological Survey,  
Menlo Park, California ([wnherkel@usgs.gov](mailto:wnherkel@usgs.gov))

# Ground Penetrating Radar Research at the Bemidji, Minnesota, Crude-Oil Spill Site

By Jeffrey E. Lucius

## ABSTRACT

At the Bemidji, Minnesota, crude-oil spill site, the USGS collected ground penetrating radar (GPR) data to determine the distribution of oil concentrated in two subsurface pools, which remained after cleanup efforts. Physical property information from analysis of mixtures of sand and crude oil assisted in the interpretation of the GPR data. Laboratory measurements show that the crude oil is still very electrically resistive (greater than  $10^6$  ohm-m). Mixing clean sand with crude oil does not significantly change the relative dielectric permittivity (RDP) or electrical conductivity of the mixture. Four GPR lines were selected, from the large number of radar lines collected at the spill site since 1984, as typical examples of 80 MHz and 300 MHz data collected over the oil pools. At the spill site, GPR is sensitive to changes in electrical conductivity and RDP related to variations in water content, due to grain size and porosity, rather than variations in the oil saturation distribution (fraction of pore space occupied by oil). The oil pools at the Bemidji site are not easily detected using GPR. Nonetheless, GPR can detect those geologic features, such as silt or gravel layers in sand, that may affect the transport and fate of petroleum in the subsurface.

## INTRODUCTION

In 1979 near Bemidji, Minnesota, one of three buried pipelines broke releasing approximately 1.7 million liters of crude oil contaminating the land surface and shallow subsurface (Hult, 1984; Delin and others, 1998). After cleanup efforts were completed, about one-quarter of the oil remained, mostly concentrated in two subsurface pools near the water table (fig. 1). Since 1979, the oil at the north pool has advanced about 80 m away from the pipelines down the hydrologic gradient (Dillard and others, 1997).

The site of the crude-oil spill is located approximately 16 km northwest of Bemidji. The site is located on a glacial outwash plain consisting of medium- to coarse-grained, calcareous, quartz-rich sand with silt and fine-grained sand lenses, dissected by gravel-filled channels, and underlain by glacial till at a depth of about 25 m (Hult, 1991). Local topographic depressions in the area may be caused by the melting of stagnant ice blocks during the retreat of the glacial ice front.

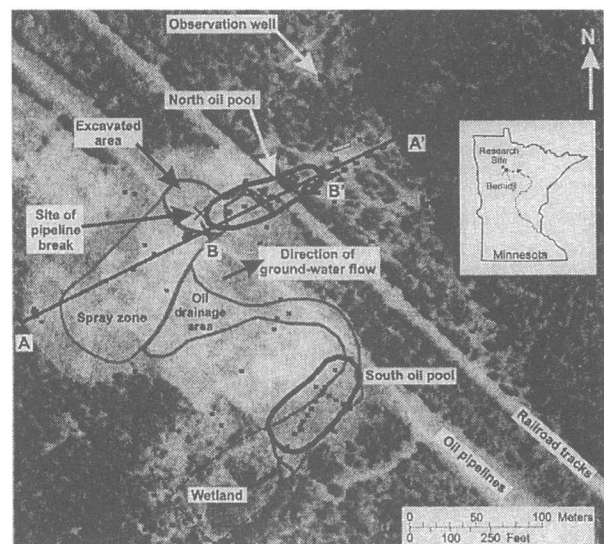


**Figure 1.** Aerial photograph from 1991 showing features of the Bemidji crude-oil spill research site (from Delin and others, 1998).

The overall objectives for U.S. Geological Survey (USGS) research at the site are to acquire a more complete understanding of the mobilization, transport, and fate of petroleum and petroleum derivatives in the shallow subsurface and to develop predictive models of contaminant behavior (Hult, 1984). Specific objectives for the use of geophysics are to (1) determine the distribution of hydrocarbons using GPR and other electrical methods, (2) characterize the vadose zone in terms of geometry, structure, and scale lengths, and (3) correlate GPR measurements with site hydrogeologic properties.

The USGS has collected ground penetrating radar (GPR) data and other geophysical information at the research site since 1984. This paper describes the use of GPR data and petrophysical information to map the subsurface distribution of oil. A brief overview of the GPR method and data imaging is presented and GPR data collected over the oil pools are displayed and discussed.

## **GPR METHOD OVERVIEW AND DATA DISPLAY**

The GPR data were collected with Subsurface Interface Radar (SIR) Systems 7 and 10 manufactured by Geophysical Survey Systems, Inc. (GSSI, North Salem, NH, USA). The radar systems operate by periodically transmitting radio-frequency electromagnetic (EM) pulses, or waves, into the earth. Under the right conditions, the radiated wave propagates through the near surface. When changes in electromagnetic properties are encountered, the wave partially reflects back toward the surface where it can be detected by the GPR system. Electromagnetic properties of the earth include dielectric permittivity ( $\epsilon$ ), electrical conductivity ( $\sigma$ ), and magnetic permeability. For a good overview of the GPR method, see Daniels (1989).

Changes in EM properties of the earth are controlled dominantly by water content, water quality, lithology, and porosity. Pore water is important because it is highly polarizable (a high value of  $\epsilon$ ) and holds free ions in solution. The propagation velocity of radar waves is controlled mostly by  $\epsilon$ , which is often presented as relative dielectric permittivity (RDP), the ratio of  $\epsilon$  to the

dielectric permittivity of free space. Intrinsic attenuation of radar waves is controlled mostly by the  $\sigma$  of the medium. Conductivity is always a GPR loss mechanism as EM field energy is converted to heat due to resistance to transport. Most common earth materials have very low magnetic permeability, but where iron, cobalt, or nickel are present, as for example in magnetite, the magnetic permeability can significantly affect the velocity and attenuation of GPR energy.

From the large collection of GPR data, four typical lines near the oil pools were selected. Locations of the radar lines discussed in this paper are shown in figure 2 along with selected USGS observation wells along the lines. The images displayed here are of GPR data that have been processed to remove system noise and to add a geometric correction factor. The radar images are approximate depth sections based on an average velocity for radar waves in material above the water table. The vertical scale is exaggerated by a factor of two or three to better show features in the records. There is also a time-dependent amplitude gain applied to the data to enhance signal strength from deeper features.

## **PHYSICAL PROPERTIES**

Several physical properties of various mixtures of distilled water with sand and oil from the Bemidji site were measured in the USGS Petrophysics Lab. Table 1 summarizes the laboratory measurements. The two oil samples were collected from wells in the north pool, Oil1 from well 301 in 1983 and Oil2 from well 412B in 1998. See Smith and Hult (1993) for locations of observation wells at this site. Sand1 is oily and dry sand collected in 1987 in the spray zone (fig. 1) near well 708. Also collected in 1987 is an oil-free sand and gravel mixture, Sand2, from well 701 at a depth of about 2.7 m. Sand3 is moist, fine-grained sand collected near the Benchmark (fig. 2) in 1998 at 0.3 m depth. The average in situ porosity of sand at the site is probably less than that measured in the lab for sample Sand3, and is likely to be around 40 percent, which agrees favorably to the value used in Dillard and others (1997). Distilled water did not mix readily with the contaminated sample, Sand1 from the

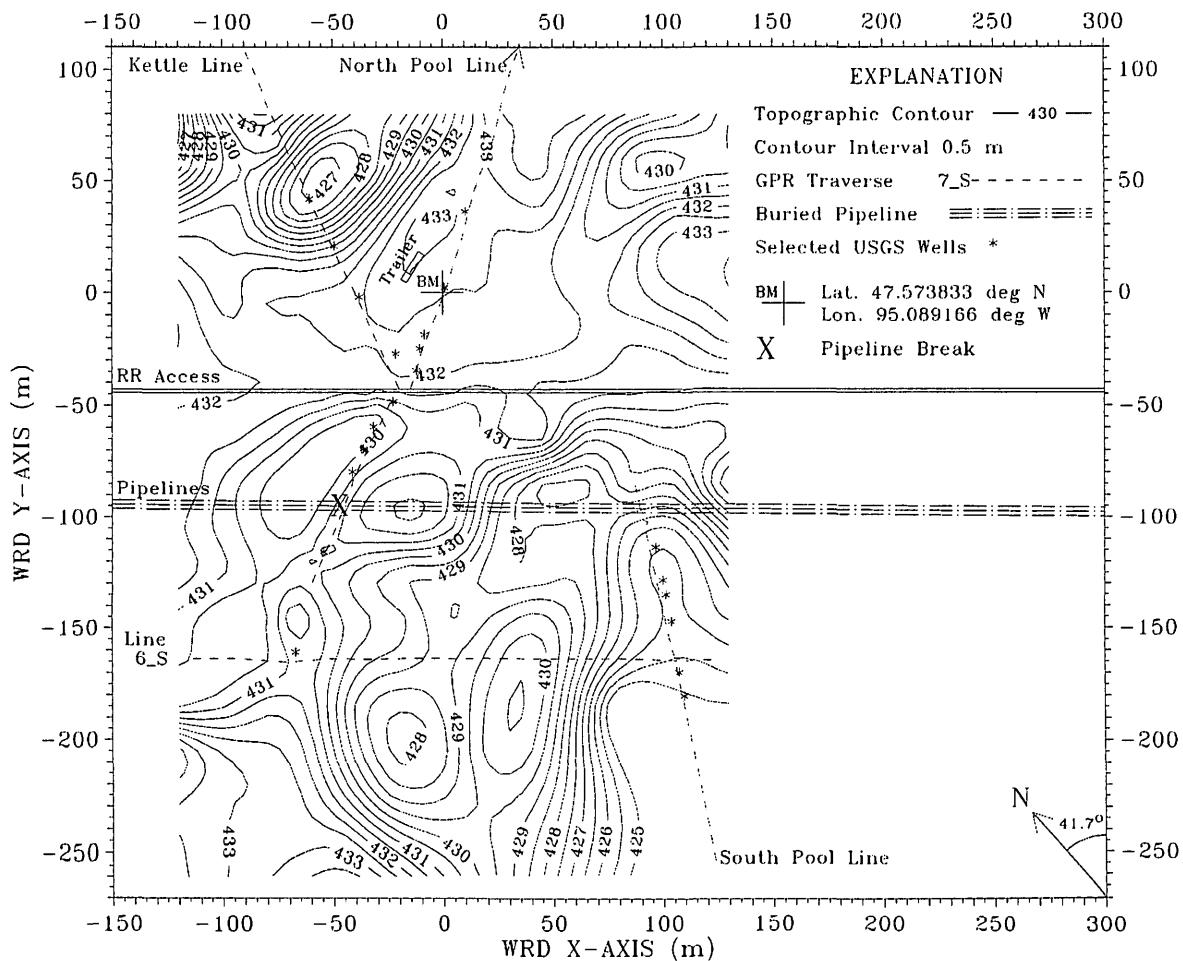


**Figure 2.** Topographic map of the Bemidji, Minnesota, crude-oil spill site showing selected GPR lines and observation wells.

spray zone, and required vigorous shaking and stirring.

The laboratory measurements show the oil is very resistive (very low electrical conductivity). Dry sand, whether contaminated or not, also has a low to very low conductivity. Sand saturated with water, or water and oil, has a low conductivity of less than 3.2 mS/m.

Bulk electrical conductivity at the site was measured using EM induction meters and dc resistivity soundings (Bisdorf, 1999). Both methods indicate the near surface has a conductivity of about 1 mS/m and the saturated zone conductivity is about 3 to 10 mS/m. These in situ values are similar to the laboratory values shown in table 1.

Dielectric permittivity can be approximated by a 3-phase mixing formula based on the 2-phase formulas of Sen and others (1981). Figure 3 shows calculated RDP for mixtures of sand, water, and air and for mixtures of sand, water,

and oil. Note the similarity of the curves. It is assumed that the materials do not electrochemically interact and that the RDP for water, quartz sand, crude oil, and air are, respectively, 80, 4.5, 2.3, and 1. Predicted values of RDP at various water saturation levels are listed for porosities of 30 and 40 percent. At 100 percent saturation, water fills all pore space. At saturation levels less than 100 percent, air or oil occupies some portion of the pore space.

As an example with conditions similar to that found at the Bemidji site, if quartz sand with a porosity of 40 percent is saturated with water, RDP of 25 is predicted. In that same sand, if a mixture of equal amounts of water and oil occupies pore space, an RDP is predicted to be 9.9. If air is substituted for oil, the predicted RDP only drops to 8.4. If porosity were only 30 percent in this same example, predicted RDP for 50/50 mixtures of water and oil and water and air in pore space would drop to 8.6 and 7.8 respectively.

**Table 1.** Summary of physical properties of various mixtures of distilled water with sand and oil from the Bemidji crude-oil spill site, determined in the USGS Petrophysics Lab. "Wet/oil" means the sample was saturated with distilled water, then gravity drained, then filled with oil. NA indicates data are not available or not applicable.

Sample Description	Conductivity (mS/m)	Resistivity (Ohm-m)	Wgt. % H <sub>2</sub> O	Wgt. % Oil	Porosity	Bulk Density (g/cc)
Oil1	6.6x10 <sup>-8</sup>	15x10 <sup>6</sup>	0.0	100.0	NA	NA
Oil2	7.6x10 <sup>-8</sup>	13x10 <sup>6</sup>	0.0	100.0	NA	0.906
Sand1 dry	5x10 <sup>-8</sup>	20x10 <sup>6</sup>	0.0	NA <sup>1</sup>	NA	1.52
Sand1 sat	2.04	489	14.8	NA <sup>1</sup>	>0.26 <sup>1</sup>	1.79
Sand2 dry	0.18	5444	0.0	0.0	NA	1.60
Sand3 dry	<10 <sup>-9</sup>	>10 <sup>9</sup>	0.0	0.0	0.44	1.61 <sup>2</sup>
Sand3 moist	0.12	820	5.37	0.0	0.44	1.70
Sand3 sat	2.66	376	21.5	0.0	0.44	2.05
Sand3 wet/oil	3.13	320	20.8	3.5	0.44	2.02

<sup>1</sup>Amount of adsorbed oil unknown

<sup>2</sup>Calculated

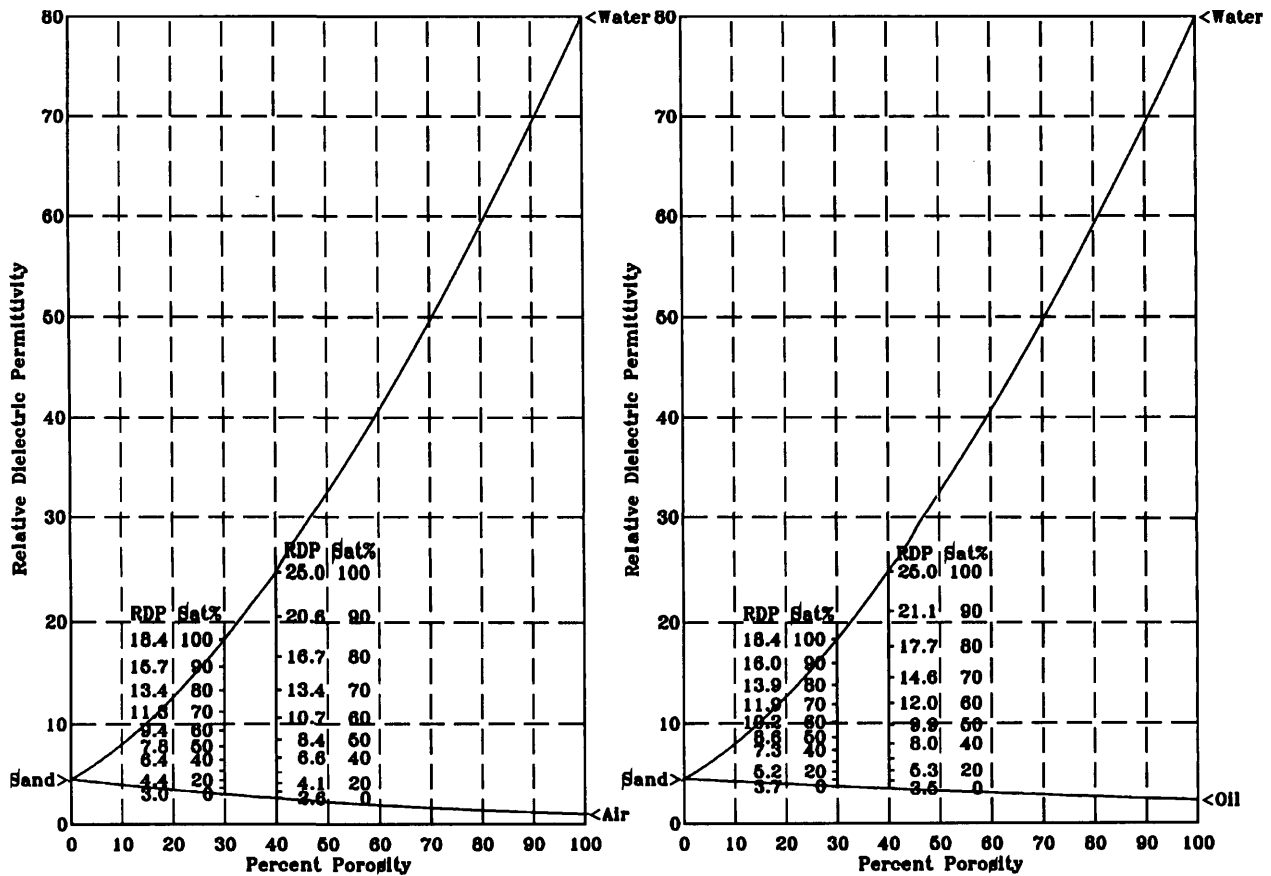


**Figure 3.** Calculated relative dielectric permittivity versus porosity are shown for sand-water-air mixtures and sand-water-oil mixtures



This example shows that variations in porosity and saturation levels can mask the effect of changes in oil saturation on the RDP of sand mixtures at the site.

## DATA INTERPRETATION

### Kettle Line

Figure 4 shows processed GPR data using 3 different antenna configurations collected along the Kettle Line in May 1987. The water table (WT) elevation, at 423 m, was established using

data from Smith and Hult (1993). The data collected with the 80 MHz dual antennas (fig. 4c) readily show the top of saturated zone (SZ) as the discontinuous series of sub-horizontal reflections, near the WT level, that cross reflections from stratigraphic sequences. The top of saturated zone, rather than the water table, can generate radar reflections because EM waves are sensitive to water content, not barometric pressure, within the earth. A radar reflection from the top of SZ is much less apparent in data collected with the 80 MHz single antenna (fig. 4b) and 300 MHz dual antennas (fig. 4a).

In the topographic depression near well 702A, all three data images show dipping

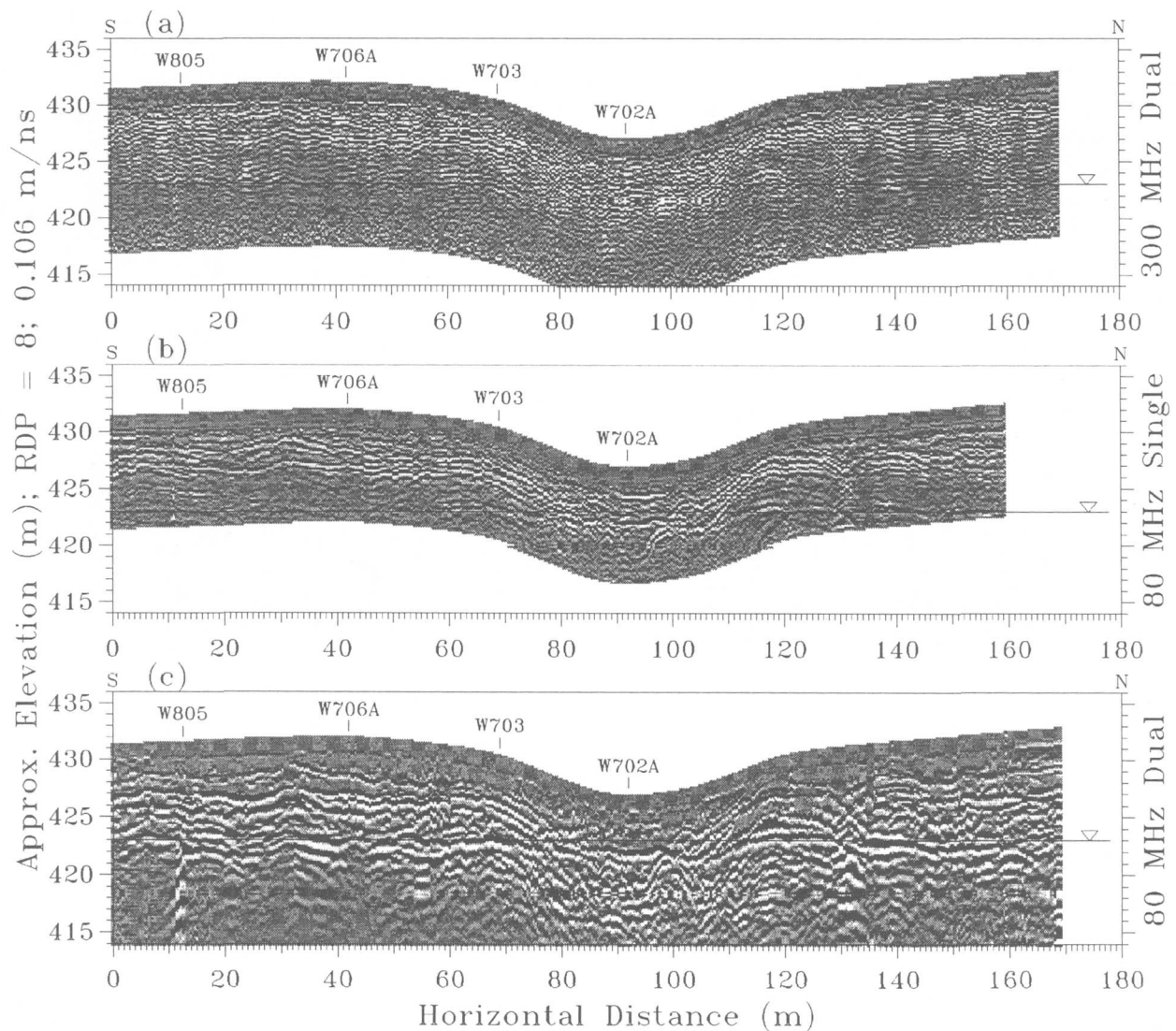


**Figure 4.** GPR data collected along the Kettle Line at the Bemidji, Minnesota, crude-oil spill site (see figs. 1 and 2 for location) using 3 different antenna configurations. Vertical exaggeration is 2. Selected USGS observation wells along the line are indicated for reference.

reflections indicating deposition, subsidence, and collapse related to the formation of a kettle. The oil pool extends a short distance beyond well 805 (from the left side of the figures) but does not reach well 706A (Smith and Hult, 1993). The location of the oil pool cannot be determined easily from data in figure 4.

In the unsaturated zone, GPR is mostly sensitive to changes in water content. When all water has been removed, most earth materials (including sand and clay) have a low relative dielectric permittivity of 7 or less (Telford and others, 1976; Keller, 1966). The RDP of oil is also within this range. Clay has a relatively high conductivity when wet, but lab and field measurements indicate that electrical conductivity is low for the materials at this site, and so clay content must be low. Water, however, has a RDP of about 80. Small changes in water content, not oil content, cause radar reflections above the water table.

### North Oil Pool Line

Data in figure 5 were collected above the long axis of the north pool (see location in figures 1 and 2) in June 1998 using 300 MHz dual

antennas. The horizontal scale shows distance from the pipelines. The gap between records is due to the railroad access. The water table, determined at the time of data collection, is shown as the sloping line at about 424-m elevation. Beneath the radar image is a cross section produced by Dillard and others (1997) that shows the oil saturation distribution (the fraction of pore space occupied by oil) determined from cores. The cross section is at the same horizontal and vertical scale as the radar image. For reference, selected well locations are shown in both the cross section and in the radar image.

The three pipelines are indicated in the radar image by the hyperbolic reflections near the origin. Curved reflections of this sort are generated because objects are detected both in front of and behind the antennas as they move across the earth. Other hyperbolic reflections present near the surface are due to wires associated with instruments at the site and are missing from data collected before 1991. The edges of the trench constructed in 1979 (fig. 1) to remove oil from the subsurface can be identified by the radar reflections sloping downward near wells 9017 and 9015.

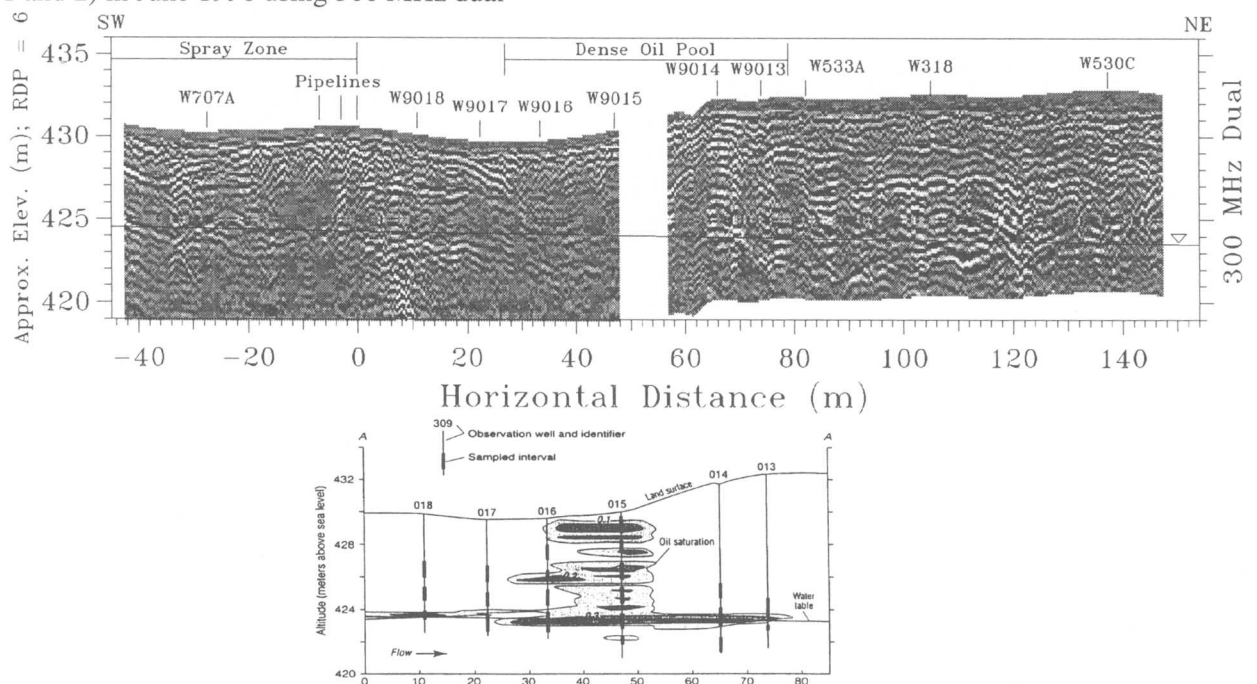


**Figure 5.** GPR data collected above the north oil pool at the Bemidji, Minnesota, crude-oil spill site (see figs. 1 and 2 for location). Vertical exaggeration is 3. Selected USGS observation wells along the line are indicated for reference. The cross section showing oil saturation distribution (from Dillard and others, 1997) is at the same scale as the radar image.

Using core samples, Dillard and others (1997) determined there are many fine-grained lenses in the unsaturated zone plus a distinct fine-grained layer at an elevation of about 423 m. The water table also occurs at about this elevation or slightly higher. Radar reflections from these two features cannot be distinguished in figure 5, and combine to produce a discontinuous reflection across the record. Correlation of oil saturation with grain size in Dillard and others (1997) suggests that the fine-grained lenses impede oil migration and trap the oil.

The cross section from Dillard and others (1997) in figure 5 shows that the densest part of

the oil pool is between wells 9017 and 9013. Oil can be found in a few wells beyond these limits. The radar reflections are not significantly different in this area as compared to others at about the same depth.

### SOUTH OIL POOL LINE AND LINE 6\_S

GPR data shown in Figure 6 were collected above the long axis of the south pool (see location in figs. 1 and 2). A single 80 MHz antenna was used in January 1985 and 300 MHz dual antennas were used in October 1996. The elevation of the

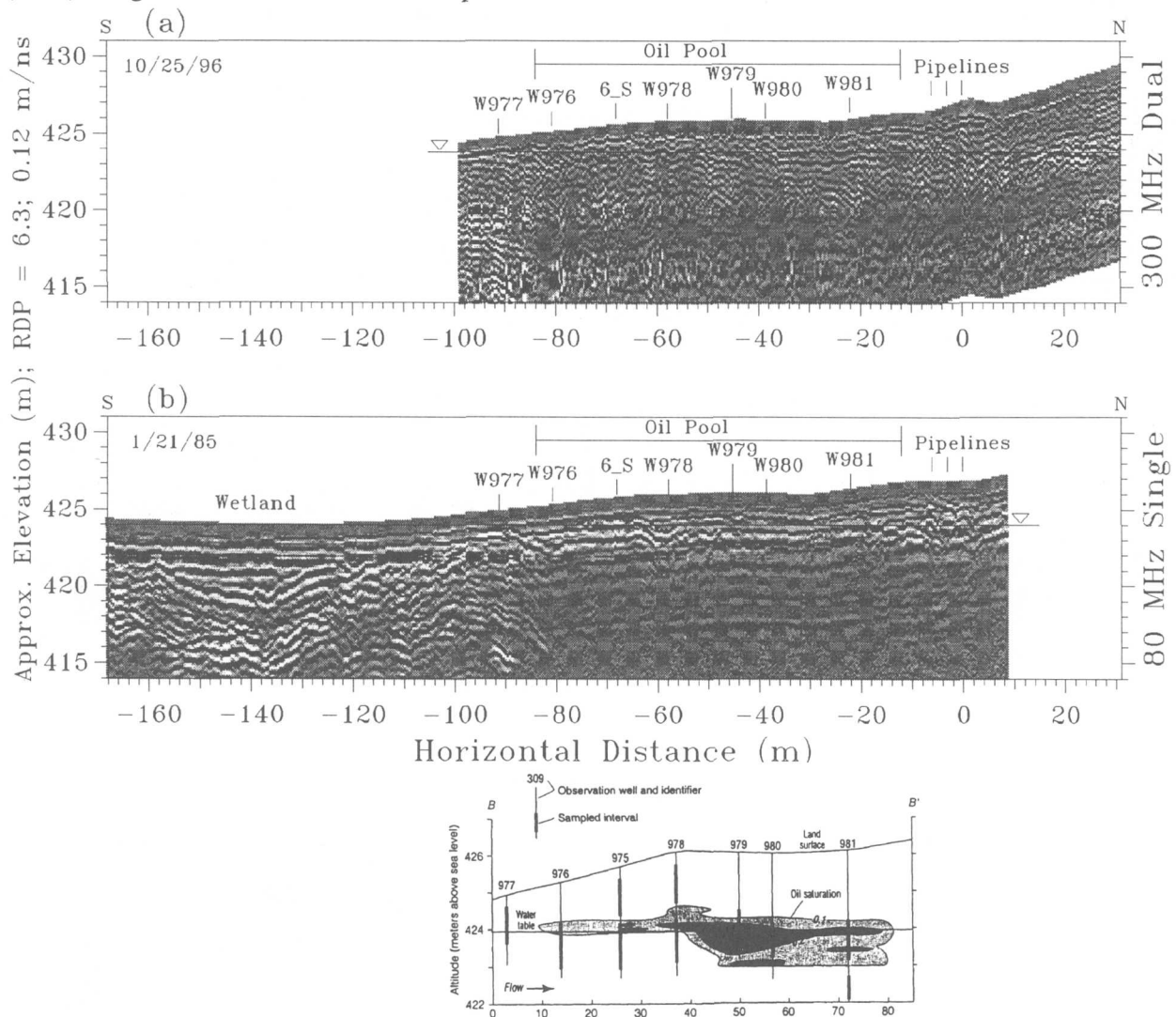


**Figure 6.** GPR data collected above the south oil pool at the Bemidji, Minnesota, crude-oil spill site (see figs. 1 and 2 for location) using two antenna configurations. Vertical exaggeration is 3. Selected USGS observation wells along the line and the location of Line 6\_S are indicated for reference. The cross section showing oil saturation distribution (from Dillard and others, 1997) is at the same horizontal scale as the radar images, but has a different vertical scale.

water table, determined from Smith and Hult (1993), is shown at approximately 424 m. The horizontal scale for the radar images shows distance from the pipelines. Locations of selected wells next to the line are noted for reference. The cross section showing oil distribution is from Dillard and others (1997) and is at the same horizontal scale, but different vertical scale, as the radar images above it.

Radar reflections from sedimentary structures associated with kettle formation are evident in both images in the topographic low to the left of well 976. GPR reflections from below the water table are muted (attenuated) to the right (north) of well 976 in the 80 MHz data (fig. 6b). Reflections are also muted in the 300 MHz data (fig. 6a), but at a depth of about 5m below the land surface. It is tempting to correlate the oil pool location with the muted reflections in the 80 MHz data. However, this is not the case. The cross section below figure 6b shows that the oil pool, at oil saturation levels greater than 10 percent, does extend south to about well 976 but does not extend north past the pipelines to

correlate with the attenuated reflections. The attenuation of radar reflections appears to be caused by differences in penetration depth related to changes in stratigraphy related to formation of the kettle.

Radar reflections away from kettle structures at the Bemidji site are often attenuated near the water table. This may be caused by the increase in electrical conductivity in the saturated zone and associated loss in radar signal strength. Figure 7 shows radar data along line 6\_S that crosses the south pool line at the location shown in figure 6. The water table elevation, determined from Smith and Hult (1993), is at approximately 424 m. The 80-MHz data sets, figures 6b and 7b, were collected on the same day and have the same amplitude gain function applied. The two 300-MHz data sets, figures 6a and 7a, were collected in different years with different antenna configurations. The muted reflections clearly are related to lithologic and conductivity changes within the saturated zone and to antenna configuration, not to the distribution of the crude oil.

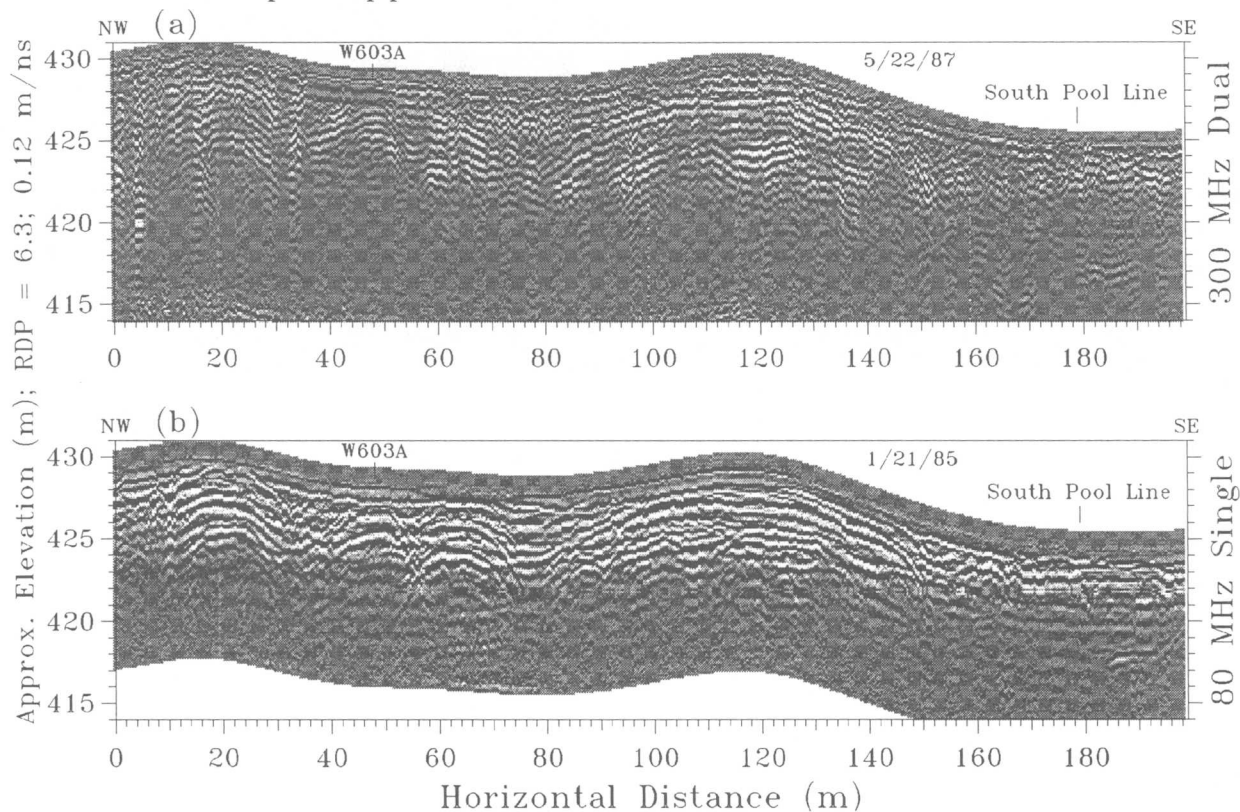


**Figure 7.** GPR data collected along Line 6\_S at the Bemidji, Minnesota, crude-oil spill site (see figs. 1 and 2 for location). Vertical exaggeration is 3. Selected USGS observation wells along the line and the location of the South Pool Line are indicated for reference. The water table is at an elevation of about 424 meters.

## CONCLUSIONS

Laboratory measurements of Bemidji crude oil indicate that the oil is still very resistive (greater than  $10^6$  ohm-m) even after 20 years of biodegradation, geochemical reactions, and dissolution. Mixing the crude oil with sand does not significantly affect the electrical conductivity or dielectric permittivity of the mixture, whether at the surface in the spray zone or at depth above the water table. This is illustrated by comparing GPR images with cross sections of oil saturation distribution.

Silt and gravel units within the sandier, glacial-outwash material can be imaged and mapped using GPR. Deposition, subsidence, and collapse features related to glacial kettle formation are identified in both 80 MHz and 300 MHz data. The top of the saturated zone can be detected and mapped easier with 80 MHz dual antennas than with other configurations. The GPR data do not show any reflections from the glacial till at about 25-m depth.

Because electromagnetic properties of oil and air are similar, small changes in water content, not oil content, cause radar reflections above the water table. GPR does not easily detect the oil pools at depth or the oil-contaminated sand near the surface. Nonetheless, GPR can detect those geologic features likely to impede oil migration or trap oil, for example, layers of silt or clay within the sand.

## REFERENCES

- Bisdorf, R.J., 1999, Electrical geophysics at the Bemidji research site, in Morganwelp, D.W., and Buxton, H.T., eds., U.S. Geological Survey Toxic Substances Hydrology Program -- Proceedings of the Technical Meeting, Charleston, SC, March 8-12, 1999 -- Volume 3 -- Subsurface Contamination from Point Sources: U.S. Geological Survey Water-Resources Investigations Report 99-4018C, this volume.
- Daniels, J.J., 1989, Fundamentals of ground penetrating radar, in Proceedings of the Symposium on the Application of Geophysics to Engineering and Environmental Problems (SAGEEP '89), March 13-16, 1989, Golden, CO, USA: The Society of Engineering and Mineral Exploration Geophysicists, p. 62-142.
- Delin, G.N., Essaid, H.I., Cozzarelli, I.M., Lahvis, M.H., and Bekins, B.A., 1998, Ground water contamination by crude oil near Bemidji, Minnesota: U.S. Geological Survey Fact Sheet 084-98, 4 p.
- Dillard, L.A., Essaid, H.I., and Herkelwrath, W.N., 1997, Multiphase flow modeling of a crude-oil spill site with a bimodal permeability distribution: *Water Resources Research*, v. 33, no. 7, p. 1617-1632.
- Hult, M.F., ed., 1984, Ground-water contamination by crude oil at the Bemidji, Minnesota, Research Site -- U. S. Geological Survey Toxic Waste -- Ground-Water Contamination Study: U.S. Geological Survey Water-Resources Investigations Report 84-4188, 107 p.
- Hult, M.F., 1991, Overview of research on contamination of the subsurface by crude oil at the Bemidji, Minnesota, Toxic Substances Research Site, in Mallard, G.E. and Aronson, D.A., eds., U.S. Geological Survey Toxic Substances Hydrology Program -- Proceedings of the technical meeting, Monterey, California, March 11-15, 1991: U.S. Geological Survey Water-Resources Investigations Report 91-4034, p. 611-613.
- Keller, G.V., 1966, Electrical properties of rocks and minerals, in Clark, S.P., ed., *Handbook of Physical Constants*: Geological Society of America Memoir 97, p. 553-577.
- Sen, P.N., Scala, C., and Cohen, M.H., 1981, A self-similar model for sedimentary rocks with application to the dielectric constant of fused glass beads: *Geophysics*, vol. 46, no. 5, p. 781-795.
- Smith, S.E., and Hult, M.F., 1993, Hydrogeologic data collected from a crude-oil spill site near Bemidji, Minnesota, 1983-91: U.S. Geological Survey Open-File Report 93-496, 158 p.
- Telford, W.M., Geldhart, L.P., Sheriff, R.E., and Keys, D.A., 1976, *Applied Geophysics*: New York, Cambridge University Press, p. 456.

## AUTHOR INFORMATION

Jeffrey E. Lucius, U.S. Geological Survey, Lakewood, Colorado, USA ([lucius@usgs.gov](mailto:lucius@usgs.gov))



# Investigating the Potential for Colloid- and Organic Matter-Facilitated Transport of Polycyclic Aromatic Hydrocarbons in Crude Oil-Contaminated Ground Water

By Joseph N. Ryan, George R. Aiken, Debera A. Backhus, Karen G. Villholth, and Christine M. Hawley

## ABSTRACT

The potential for colloid- and organic matter-facilitated transport of polycyclic aromatic hydrocarbons (PAHs) was investigated at a crude oil-contaminated field site near Bemidji, Minnesota. Field tests focused on sampling and characterization of the ground water colloids and assessment of the partitioning of PAHs to the colloids. The colloids were mostly iron-rich spheres of 100-300 nm diameter. Their concentration reached a maximum of about  $2 \times 10^{10}$  particles per liter (0.75 NTU) at a distance 50 m down-gradient from the oil spill and decreased with distance to a background concentration of about  $7 \times 10^8$  particles per liter at a distance of 140 m. During well purging, stable colloid concentrations decreased slightly with increasing pumping rate. Fluorescence quenching experiments revealed that partitioning of perylene to organic matter in the unaltered ground water was significant. Laboratory tests examined the effect of ferrous iron, present in high concentrations near the oil spill, on the partitioning of phenanthrene to aliphatic and aromatic carboxylic acids typical of crude oil degradation and hydrophobic acid fractions of natural organic matter. Ferrous iron increased the partitioning of phenanthrene to the organic acids by 11 to 250%, with the largest increase occurring for aromatic carboxylic acids. The data suggest that ferrous iron increased the partition coefficient by causing aggregation of the organic acids.

## INTRODUCTION

Colloids, both organic and inorganic, have been implicated in the transport of metals, radionuclides, and certain ionizable organic pesticides in laboratory and field tests (Jury and others, 1986; Buddemeier and Hunt, 1988; Amrhein and others, 1993; de Jonge and others, 1998). Laboratory tests also indicate that colloids facilitate the transport of hydrophobic organic compounds (Vinten and others, 1983; Magee and others, 1991; Dunnivant and others, 1992); however, colloid-facilitated transport of hydrophobic organic compounds has only infrequently been observed in the field (Villholth, in press). To assess the potential for colloid-facilitated transport of hydrophobic organic compounds in the field, we examined the association of colloids and polycyclic aromatic

hydrocarbons (PAHs) in a crude oil-contaminated ground water at Bemidji, Minnesota.

The Bemidji site was considered a good candidate for detecting colloid-facilitated transport of hydrophobic organic compounds. Phenanthrene and fluorene, two PAHs in the crude oil, were measured in the ground water down-gradient of the oil spill at concentrations 26% and 300% greater than concentration estimates based on equilibrium between the crude oil and the surrounding water (Aiken and others, 1991). The transport distances for phenanthrene and fluorene also exceed expectations based on two-phase transport estimates (Hawley, 1995). These observations suggest sorption of the PAHs to a third phase -- a mobile colloid phase.

We suspected that organic and inorganic colloids would be abundant near the oil spill. The dissolved organic matter concentration of the



ground water increased to 50 mg C L<sup>-1</sup> adjacent to the oil spill. Degradation of the oil produced an anoxic plume of ground water and high ferrous iron concentration. These conditions have been associated with colloid mobilization in iron oxide-coated sediments (Ryan and Gschwend, 1990; 1992).

Our investigation included both field and laboratory components. In the field, we tested the dependence of the stable colloid concentration on the pumping rate and characterized the colloids collected in the samples. Using the field samples, we measured the partitioning of perylene, a five-ring PAH, to the colloids at *in situ* concentrations. In the laboratory, we tested the effect of ferrous iron on the partitioning of phenanthrene, a three-ring PAH, to different types of organic matter ranging from high molecular weight aliphatic and aromatic carboxylic acids to isolated fractions of natural organic matter.

## MATERIALS AND METHODS

In this section, we describe the field site, the methods of sampling the ground water, the measurement of partition coefficients by fluorescence quenching, and the measurement of partition coefficients by solubility enhancement in the presence and absence of ferrous iron.

### Field Site

The field tests were conducted at the U.S. Geological Survey Toxic Substances Hydrology research site at Bemidji, Minnesota. In August 1979, a pipeline near Bemidji burst and sprayed light crude oil on the ground surface. After cleanup, an estimated 400,000 L of oil remained in the unsaturated zone of the soil perched in a lens on the water table (Hult, 1987). Since the spill, the oil body has migrated about 30 m down-gradient and oil dissolution and degradation products have traveled at least 200 m down-gradient (Hult, 1989).

The saturated sediment at the site is a calcareous silty sand deposited as glacial moraine and outwash. The sand and silt fraction is composed of quartz, feldspar, dolomite, calcite, hornblende, and ilmenite. The clay fraction (<1%) is composed of kaolinite, smectite, and chlorite

(Bennett and others, 1993). Ground water flow is advancing at a rate of about 0.08 m d<sup>-1</sup> (Baedecker and others, 1993).

The supply of oil degradation products to the ground water has created five distinct zones of ground water chemistry (Baedecker and others, 1993) (fig. 1). Near the oil body, dissolved oxygen decreases to zero from near saturation, dissolved organic matter increases to 50 mg C L<sup>-1</sup> from 2 mg C L<sup>-1</sup>, and ferrous iron increases to about 1 mM from micromolar levels.

### Ground Water Sampling

Ground water was sampled from five monitoring wells aligned with the axis of ground water flow past the oil body (fig. 1) in July 1995. These wells provided samples from the uncontaminated background zone, near the oil body, and down-gradient of the oil body. The sampling apparatus and procedures were designed to minimize suspension of colloids by pumping and preserve sample chemistry.

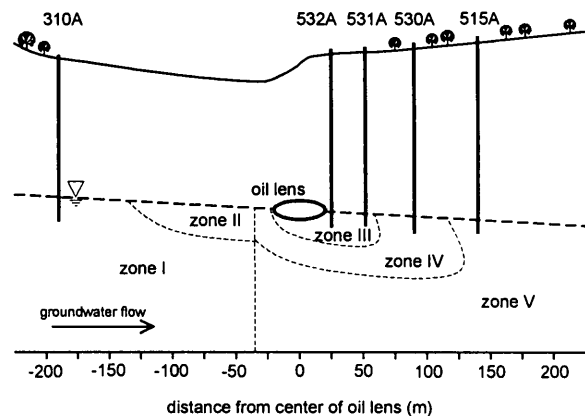


**Figure 1.** Locations of the monitoring wells sampled in this investigation shown with oil body and geochemical zones of contamination designated by Baedecker and others (1993). The ground water zones have the following characteristics: (I) native uncontaminated ground water, oxic; (II) high organic and inorganic carbon, sub-oxic; (III) high hydrocarbons, Mn<sup>2+</sup>, Fe<sup>2+</sup>, methane, anoxic; (IV) transition zone between III and V, sub-oxic; and (V) slightly elevated benzene, toluene, ethylbenzene, and xylenes, oxic. The water table depth ranges from 8 to 9 m for the wells shown.

Ground water was removed from the wells using a positive-displacement gear-driven pump



made of stainless steel and Teflon. The pumping zone was partially isolated by a packer inflated with argon above the pump. Aluminum and stainless steel tubing (pre-rinsed with acetone and deionized water) was used to connect the pump with the surface. A low flow rate (about  $0.1 \text{ L min}^{-1}$ ) was used to minimize suspension of colloids.

In one well (532A), ground water sampling was conducted at 4 different pumping rates (0.15, 0.35, 1.1, and  $1.8 \text{ L min}^{-1}$ ) on successive days to test the effect of pumping rate on colloid sampling. These pumping rates span the range commonly used in ground water sampling. After sampling at the highest pumping rate on the fourth day, the pumping rate was decreased to the medium and low rates to determine the effect on turbidity.

Flow from the pump tubing was directed to the bottom of an inverted, overflowing glass funnel for measurement of pH, specific conductance, and dissolved oxygen (colorimetric vacuum ampoules; Chemetrics, Inc.). Flow was also diverted to glass vials for frequent turbidity (Hach, model Ratio X/R) and total iron measurement (Hach, field titration) during well purging. Samples were collected when the field parameters stabilized. This purging of the wells required removal of 100 well volumes over 7 h. Ground water was collected in ground glass-stoppered bottles pre-filled with argon and contained in sealed plastic bags after allowing approximately one volume of overflow. The bottles were capped, covered with plastic caps, and stored on ice in coolers.

Colloids were sampled by collecting 20 to 60 mL of ground water in glass syringes and filtering through  $0.1 \mu\text{m}$  membranes. The membranes were rinsed with 10 mL of deionized water and stored in sealed petri dishes.

## Laboratory Analysis

### Ground Water Chemistry

Samples were analyzed for major cations and metals (Al, Ca, Fe, K, Mg, Mn, Na, and Si) in whole and  $0.1 \mu\text{m}$ -filtered samples by inductively coupled plasma-atomic emission spectrophotometry (ICP-AES). Sample handling

and filtering was conducted in an argon-filled glove box. Total and dissolved organic carbon concentrations were determined by ultrafiltration (500 molecular weight cutoff), high-temperature platinum catalyst combustion of the samples from which inorganic carbon and volatile organic carbon had been purged, and infrared detection of carbon dioxide.

### Colloid Characterization

The abundance of inorganic colloids on gold-coated filters was determined by scanning electron microscopy (SEM) at 20,000 times magnification and 30 kV accelerating voltage. From 40 to 100 randomly located fields were counted. Fields with colloids too numerous to count were excluded; these fields were photographed. Elemental composition of the colloids was estimated by energy-dispersive x-ray (EDX) analysis with count times of 60 s.

### Fluorescence Quenching

Fluorescence quenching (Backhus and Gschwend, 1990) was used to determine the partitioning of a probe PAH, perylene, to the organic colloids present in ground water samples examined under in situ conditions. Organic colloids were operationally defined as organic matter that did not pass through a 500 molecular weight ultrafiltration membrane.

### Solubility Enhancement

Solubility enhancement experiments (e.g., Chiou and others, 1986) were performed to determine the effect of ferrous iron on the partitioning of a PAH, phenanthrene, to various types of high molecular weight organic acids. The organic acids tested included the hydrophobic acid fractions of organic matter isolated by XAD-8 resin (Aiken and others, 1992) from the site ground water and the Suwannee River and high molecular weight aliphatic and aromatic carboxylic acids (table 1). The carboxylic acids (fig. 2) were chosen to represent typical oil degradation products found at the site (Eganhouse and others, 1993). The hydrophobic acid fractions were added at a concentration of  $50 \text{ mg L}^{-1}$ . The carboxylic acids were added at a concentration of

20 mg L<sup>-1</sup>, an order of magnitude below the critical micelle concentration of any of the carboxylic acids (Mukerjee and Mysels, 1971).

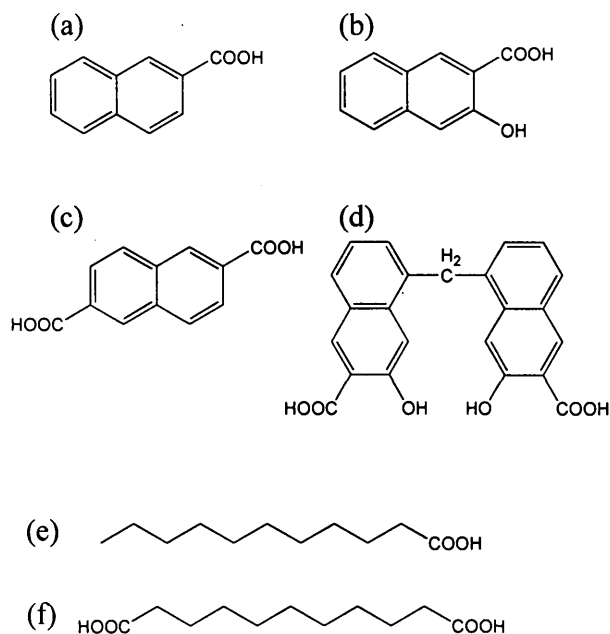


**Figure 2.** The aromatic and aliphatic carboxylic acids used in the solubility enhancement experiments: (a) 2-naphthoic acid, (b) 3-hydroxy-2-naphthoic acid, (c) 2,6-naphthdioic acid, (d) pamoic acid, (e) undecanoic acid, and (f) 1,11-undecanedioic acid.

Ferrous iron was added as Fe<sub>2</sub>SO<sub>4</sub>·4H<sub>2</sub>O at concentrations of 0.9 and 2.7 mM. The lower concentration is about 25% higher than the maximum total iron concentration measured in the contaminated Bemidji ground water. Potassium nitrate was added to control ionic strength at a concentration of 0.01 M, approximately the ionic strength of the contaminated Bemidji ground water. Phenanthrene was added in a radiolabeled form (phenanthrene-9-<sup>14</sup>C).

The phenanthrene was placed in glass centrifuge tubes with plastic caps and Teflon-lined septa. The organic acid/potassium nitrate solutions were sparged with argon to remove oxygen (<10 ppb) and added to the tubes. Sparged ferrous iron solution was spiked into the tubes and pH was adjusted to 6.5 with a sodium hydroxide solution. This pH was at least 1.5 pH units above the pK<sub>a</sub> values of the carboxylic acids. The headspace in the tubes was replaced

with argon and sealed for 14 d (an equilibration time chosen by kinetic tests) at room temperature (20±2°C). The vials were centrifuged (1750 g, 1 h) to force the excess phenanthrene to the argon-water interface. An aliquot of the aqueous solution was withdrawn by syringe for determination of phenanthrene concentration by liquid scintillation counting. All solution preparation was performed in an argon-filled glove box. Duplicate experiments were conducted for all data reported.

**Table 1.** Characteristics of the hydrophobic acid fractions (XAD-8) of the natural organic matter and the carboxylic acids used in the solubility enhancement experiments. The Number-averaged molecular weight (M<sub>n</sub>), aromaticity, carboxyl content, and oxygen/carbon (O/C) ratio are shown. Aromaticity and carboxyl content calculated for the carboxylic acids and measured by <sup>13</sup>C-nuclear magnetic resonance analysis for the hydrophobic acid fractions.

organic acid	M <sub>n</sub> (Da)	aromaticity (%)	carboxyl content (%)	O/C ratio
well 310A <sup>1</sup> (XAD-8)	536	18	15	0.66
well 532A <sup>2</sup> (XAD-8)	350	n.d.	n.d.	n.d.
well 530A <sup>3</sup> (XAD-8)	362	19	14	0.47
SR FA <sup>4</sup> (XAD-8)	826	25	21	0.71
2-naphthoic	160	91	9.1	0.24
2,6-naphthdioic	204	83	17	0.44
3-hydroxy-2-naphthoic	200	91	9.1	0.36
pamoic	388	91	9.1	0.35
undecanoic	186	0	9.1	0.24
1,11-undecanedioic	216	0	18	0.48

<sup>1</sup>Aiken and Thorn (unpublished data)

<sup>2</sup>Eganhouse and others (1993)

<sup>3</sup>Aiken (unpublished data)

<sup>4</sup>SR FA is Suwannee River fulvic acid (Aiken and Malcolm, 1987)

## RESULTS

### Pumping Rates during Sampling

Well 532A was purged at increasing pumping rates before sampling on four successive days. Turbidity and dissolved oxygen decreased

during purging, while pH and specific conductance were fairly constant (fig. 3).

The purging time required to reach a stable turbidity level decreased as the pumping rate increased (fig. 4). The stable turbidity values were highest at the lowest pumping rate. On the fourth day, when the pumping rate was decreased to medium and low rates after purging and sampling at  $1.8 \text{ L min}^{-1}$ , turbidity increased by 15 to 35% above the stable turbidity level. Only turbidity showed a significant variation as the pumping rate was increased.

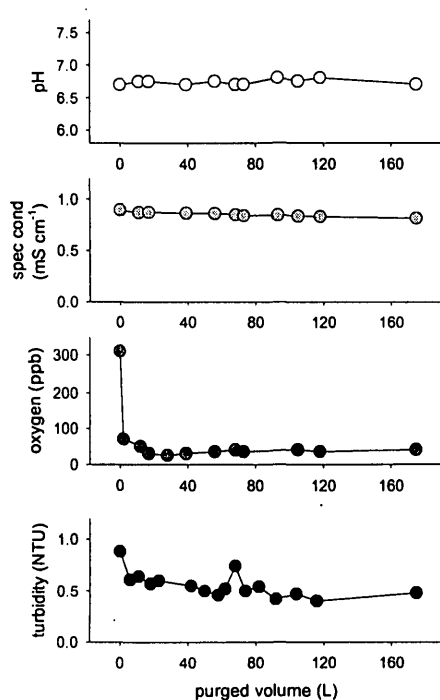


**Figure 3.** Changes in pH, specific conductance (spec cond), dissolved oxygen, and turbidity during the purging of well 532A at  $0.35 \text{ L min}^{-1}$ .

### Ground Water Chemistry

The ground water sampling conducted during this study echoed results obtained in previous studies (Baedecker and others, 1993; Eganhouse and others, 1993) as shown in fig. 5. Near the oil body, pH decreased slightly and specific conductance roughly doubled. Dissolved oxygen decreased from near saturation to undetectable levels ( $<0.1 \text{ mg L}^{-1}$ ). Dissolved iron increased from undetectable levels ( $<2 \mu\text{M}$ ) to

$0.72 \text{ mM}$ . Ground water from the background well (310A) was similar to ground water from the well most down-gradient (515A). Filtered ( $0.1 \mu\text{m}$ ) and unfiltered ground water samples displayed no significant difference in major cation and metal concentrations. Field measurements of total iron agreed well with laboratory measurements by ICP-AES. In contrast, the organic carbon concentration of material trapped on 500 molecular weight cutoff ultrafilters ranged from  $0.4$  to  $5.9 \text{ mg C L}^{-1}$  (table 2).

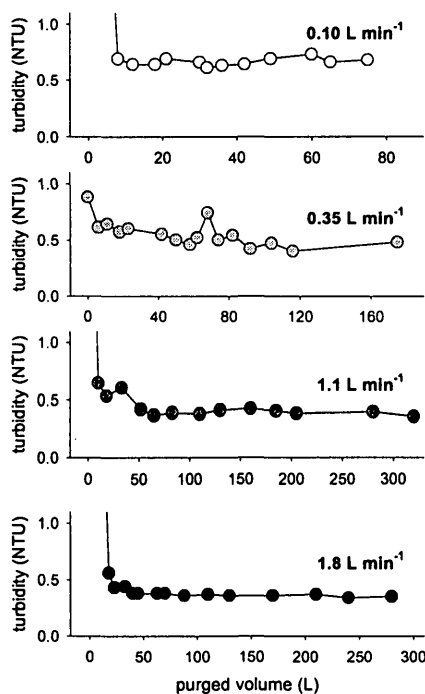


**Figure 4.** Changes in turbidity during purging of well 532A at four different pumping rates on four different days.

### Inorganic Colloids

Turbidity measurements ranged from near zero in the background and distant downgradient wells to  $0.75 \text{ NTU}$  in the wells near the oil body (fig. 5). Estimates of particle number concentrations revealed about 30 times higher colloid concentrations in ground water near the oil body. Assuming an inorganic colloid density range of  $2\text{-}4 \text{ g cm}^{-3}$ , colloid mass concentrations ranged from about  $1\text{-}2 \mu\text{g L}^{-1}$  in the background

ground water to about 20-40  $\mu\text{g L}^{-1}$  near the oil body. These mass concentrations are much less than the organic colloid concentration (table 2).

The inorganic colloids were roughly uniform in size (100-300 nm diameter) and shape (spherical) (fig. 6). Iron predominated the EDX scans of the colloids. Very few larger particles (approximately 1%) with elemental compositions similar to clay minerals (Al, Si, K) and organic matter (no elements above F) were also detected.

## Fluorescence Quenching

The fluorescence quenching experiments showed that perylene associates significantly with the organic colloids in the ground water down-gradient from the oil body (wells 531A, 530A, and 515A; table 2). No perylene binding was observed for the background ground water (well 310A). The extent of solubility enhancement decreased with distance down-gradient of the oil body. Some of this decrease may be attributed to the decrease in colloidal organic matter concentration with distance from the oil body; however, the organic matter partition coefficient ( $K_{om}$ ) also decreased slightly with distance from the oil body.

**Table 2.** Fluorescence quenching results for the partitioning of perylene to colloids in the Bemidji ground water. Solubility enhancement is the ratio of the apparent solubility to the predicted solubility.  $K_{om}$  is the organic matter-normalized partition coefficient.

well	distance from oil (m)	organic colloid (mg C L <sup>-1</sup> )	solubility enhancement	$K_{om}$ (mL g <sup>-1</sup> )
310A	-190	0.4	1.0	no quench
531A	25	5.9	2.2	$4.0 \times 10^5$
530A	50	3.3	1.5	$3.2 \times 10^5$
515A	140	2.2	1.3	$3.0 \times 10^5$

## Solubility Enhancement

The results of the solubility enhancement experiments are shown in table 3. The aliphatic carboxylic acids (undecanoic and 1,11-undecanedioic acids) and pamoic acid were most effective at binding phenanthrene, but ferrous iron did not significantly improve their ability to bind

phenanthrene. The hydrophobic acid fractions and the remaining aromatic carboxylic acids were roughly equal in their ability to bind phenanthrene. At a concentration of 0.9 mM, ferrous iron somewhat improved phenanthrene binding of the hydrophobic acid fractions of the natural organic matter (11 to 55% increase in  $K_{om}$ ). For the aromatic carboxylic acids (except pamoic acid), ferrous iron approximately doubled phenanthrene binding (205 to 250% increase in  $K_{om}$ ).

**Table 3.** Solubility enhancements and organic matter-water partition coefficients ( $K_{om}$ ) for phenanthrene with various organic acids in the absence and presence of ferrous iron at a concentration of 0.9 mM.

organic acid	relative solubility enhancement		$K_{om}$ (mL g <sup>-1</sup> )	
	without Fe <sup>2+</sup>	with Fe <sup>2+</sup>	without Fe <sup>2+</sup>	with Fe <sup>2+</sup>
blank <sup>1</sup>	1 (±0.008)	1.03 (±0.010)	--	$10^{3.16}$
well 310A (XAD-8)	1.36 (±0.015)	1.55 (±0.017)	$10^{3.85}$	$10^{4.05}$
well 532A (XAD-8)	1.51 (±0.022)	1.62 (±0.024)	$10^{4.01}$	$10^{4.10}$
SR FA <sup>2</sup> (XAD-8)	1.40 (±0.015)	1.45 (±0.020)	$10^{3.90}$	$10^{3.95}$
2-naphthoic	1.14 (±0.022)	1.35 (±0.028)	$10^{3.85}$	$10^{4.25}$
3-hydroxy-2-naphthoic	1.21 (±0.022)	1.44 (±0.017)	$10^{4.03}$	$10^{4.34}$
2,6-naphth-dioic	1.19 (±0.025)	1.45 (±0.010)	$10^{3.99}$	$10^{4.35}$
pamoic	1.40 (±0.008)	1.39 (±0.011)	$10^{4.30}$	$10^{4.30}$
undecanoic <sup>3</sup>	1.44 (±0.006)	1.34 (±0.015)	$10^{4.34}$	$10^{4.24}$
1,11-undecane-dioic	1.34 (±0.008)	1.41 (±0.010)	$10^{4.23}$	$10^{4.31}$

<sup>1</sup>The solubility enhancement caused by Fe<sup>2+</sup> alone was used to correct the organic acid solubility enhancements.

<sup>2</sup>SR FA is Suwannee River fulvic acid.

<sup>3</sup>black precipitate was observed.

For the undecanoic acid, repeated trials at a ferrous iron concentration of 0.9 mM produced a black precipitate after centrifugation. We suspect that the black precipitate reduced the solution concentration of phenanthrene, resulting in a solubility enhancement and  $K_{om}$  value lower than

expected in the presence of ferrous iron. At the higher ferrous iron concentration, 2.7 mM, black precipitates were produced in all of the solutions. The solubility enhancement caused by the higher ferrous iron concentration was  $1.03 \pm 0.010$ , the same value observed at the lower ferrous iron concentration.

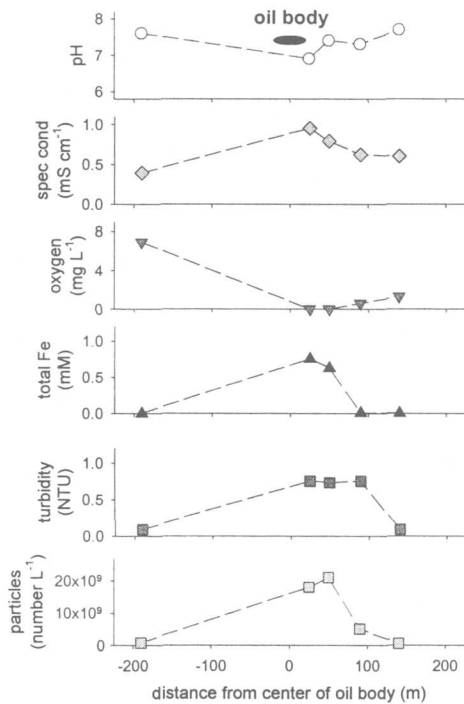


**Figure 5.** Variations in pH, specific conductance (spec cond), dissolved oxygen, turbidity, and particle number concentration as a function of distance from the oil body.

## DISCUSSION

### Pumping Rates during Sampling

Ground water sampling protocols have typically required the removal of three to five well volumes of ground water prior to sample collection. This purging of the well is meant to assure collection of ground water representative of the ground water in the formation, unaffected by the presence of the well. From this study and others (Puls and others, 1992; Backhus and others, 1993), it is clear that turbidity is still

decreasing at three to five well volumes, while parameters like pH and specific conductance have reached steady levels. At this site, as many as 100 well volumes were removed before reaching a stable turbidity level.

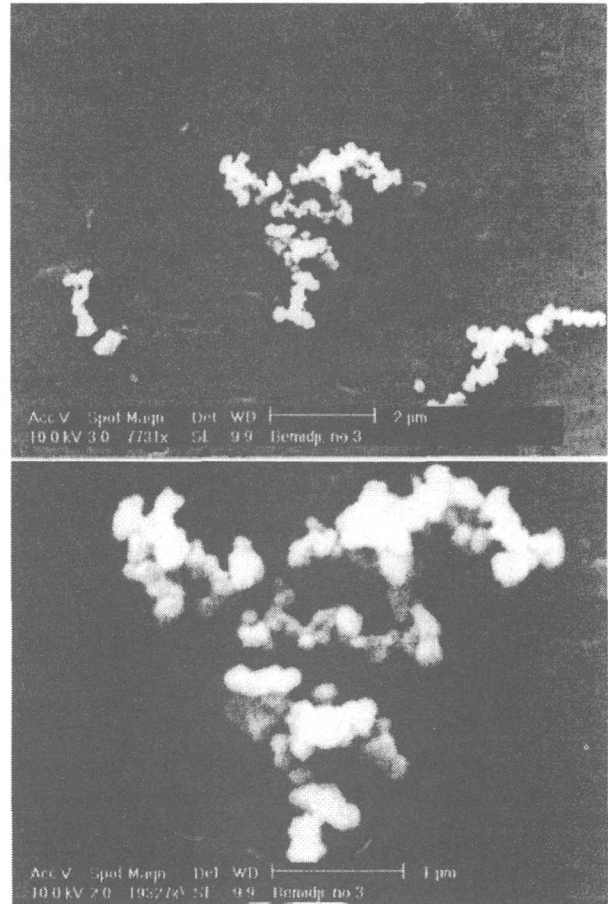


**Figure 6.** SEM images of colloids from well 532A (25 m down-gradient from oil body) trapped on 0.1 μm filters. Colloids are composed mostly of iron. Magnification of 7,700 times (top) and 19,000 times (bottom). Scale bars of 1 μm are shown.

Previous research on the effect of pumping rate on colloid concentrations concluded that higher pumping rates resulted in higher stable colloid concentrations (Puls and others, 1992; Backhus and others, 1993). Higher pumping rates produce greater shear on colloids attached to the framework grains. In this study, however, there was a slight decrease in the stable turbidity level as the pumping rate was increased. We suspect that the slight decrease may have resulted from depletion of the supply of colloids that could be mobilized by shear. Note that the stable turbidity level decreased with successive tests (from low to

high pumping). Inexplicably, decreases in the pumping rate after purging and sampling at a high rate also caused a decrease in the stable turbidity level. The higher stable turbidity level measured on the first day (at the lowest rate) may also be attributable to disturbance of colloids in the well. After the first day, the pump was left in the well. Puls and others (1992) observed the same effect in their studies and recommended that dedicated sampling equipment be used to more accurately sample colloids in ground water.

### **Colloid Mobilization and Transport**

Given the significant difference between the colloid concentrations of the background well (310A) and the wells near the oil body (532A, 531A) (fig. 5), we surmise that the change in ground water chemistry caused by the oil spill is responsible for the mobilization of colloids near the oil body. A coincidence of reducing conditions and high colloid concentrations was observed by Ryan and Gschwend (1990; 1992) in Atlantic Coastal Plain sediments below an organic matter-rich swamp. At Bemidji, the degradation of oil is responsible for the onset of reducing conditions (Cozzarelli and others, 1994).

For the Atlantic Coastal Plain sediments, Ryan and Gschwend (1990; 1992) hypothesized that the mobilization of colloids (mainly clay minerals) was caused by the reductive dissolution of ferric oxyhydroxide coatings binding clay colloids to the framework grains. At Bemidji, ferric oxyhydroxides were not listed as significant components of the sediments, but ilmenite ( $\text{FeTiO}_3$ ) is present in the heavy mineral fraction (Bennett and others, 1993). Ilmenite is also present in the Atlantic Coastal Plain sediments examined by Ryan and Gschwend (1992) and its weathering under oxidizing conditions released ferric iron that accumulated as oxyhydroxide coatings on grains. It is likely that the native Bemidji sediments are also coated by iron oxyhydroxides. The high concentrations of ferrous iron in the anoxic, organic carbon-rich ground water near the oil body also indicates that iron oxyhydroxide coatings must be present on the Bemidji sediments.

Despite the apparent similarity in colloid mobilization conditions, far fewer inorganic colloids were mobilized in the Bemidji ground

water than in the Atlantic Coastal Plain ground waters. At Bemidji, the colloids mobilized (up to an estimated  $30 \mu\text{g L}^{-1}$ ) are primarily small amorphous iron-rich spheres with a few clay colloids. In the Atlantic Coastal Plains sediments, the mobilized colloids (up to  $60 \text{mg L}^{-1}$ ) were mainly clay minerals with a few crystalline goethite particles. The difference in colloid concentrations may be attributed to the difference in the clay content of the sediments. The clay content of the Bemidji sediments is less than 1% and the Atlantic Coastal Plain sediments contain nearly 4% clay. In addition, the relatively high ionic strength of the Bemidji ground water (estimated at approximately 10 mM near the oil body) may prevent colloid mobilization. The ionic strengths of the Atlantic Coastal Plain ground waters were about one to two orders of magnitude lower than that of the contaminated Bemidji ground water.

The morphology of the iron-rich colloids suggests that they formed by relatively rapid oxidation of ferrous iron. While it may seem likely that these colloids formed after sampling, we believe that they are present in the ground water because we assiduously avoided exposure of the samples to the atmosphere. Colloid abundance on the filters correlated well with the turbidity of the samples and turbidity was measured in the field before any significant ferrous iron oxidation could occur at the pH of these samples (6.5 to 7.0). Samples returned to the laboratory and filtered in an argon-filled glove box contained the same colloids at similar concentrations. We surmise that these colloids were formed by ferrous iron oxidation brought on by the diffusion of trace levels of oxygen (<10 ppb) into the Zone III and IV ground water (fig. 1). The wells sampled were screened within one meter of the water table.

### **Perylene Binding in Bemidji Ground Water**

The fluorescence quenching experiments indicate that the oil degradation products present near the oil body enhance the apparent solubility of perylene. The natural organic matter in the background well (310A) is not present at sufficiently high concentration to enhance

perylene solubility. If the oil degradation products are mobile, they could facilitate the transport of perylene and other PAHs of similar hydrophobicity down-gradient. Given the low concentrations of inorganic colloids, it appears that the oil degradation products may be responsible for the observation of phenanthrene and fluorene concentrations above solubility at the site and the detection of these PAHs at distances down-gradient further than expected (Aiken and others, 1991).

The perylene  $K_{om}$  values measured by fluorescence quenching ( $10^{5.5}$  to  $10^{5.6}$  mL g<sup>-1</sup>) are slightly lower than the  $K_{om}$  value predicted using the  $K_{om}$ - $K_{ow}$  linear free energy relationship (LFER) developed by Karickhoff (1981) for PAH binding by soil organic matter. Using a  $K_{ow}$  value of  $10^{6.50}$  for perylene, this LFER predicts a  $K_{om}$  value of  $10^{5.85}$  mL g<sup>-1</sup>. This difference may reflect a difference in the aromaticity of the organic matter responsible for perylene binding. The oil degradation products are predominantly aliphatic (Eganhouse and others, 1993) and the soil organic matter used by Karickhoff (1981) is probably more aromatic. Chin and others (1997) showed that the  $K_{om}$  values of PAHs decrease with increasing aliphatic content of the organic matter.

### Phenanthrene Binding by Organic Matter

The organic matter partition coefficients for phenanthrene measured in the absence of ferrous iron compare favorably with  $K_{om}$  values estimated for aromatic hydrocarbons with  $K_{ow}$  values (Karickhoff, 1981). This LFER produces a  $K_{om}$  estimate of  $10^{3.90}$  mL g<sup>-1</sup> using a  $K_{ow}$  value of  $10^{4.57}$ . The  $K_{om}$  values for the hydrophobic acid fractions (well 310A, SR FA) were within 10% of this estimate; however, the hydrophobic acid fraction from ground water near the oil body (well 532A) was about 30% more effective at binding phenanthrene. Given the predominance of aliphatic oil degradation products in the well 532A ground water (Eganhouse and others, 1993), we expected a lower  $K_{om}$ , similar to the effect observed for perylene binding measured by fluorescence quenching.

The binding of hydrophobic organic compounds by organic matter generally increases with the molecular weight of the organic matter

(Chin and others, 1997). In contrast, we observed that the lower molecular weight carboxylic acids were at least as or more effective at binding perylene than the higher molecular weight hydrophobic acid fractions. On the basis of these differences, it appears that  $K_{om}$  increases with increasing aliphatic content and decreasing oxygen/carbon ratios. To enhance phenanthrene binding, the long hydrocarbon chains of the aliphatic carboxylic acids must provide more accessible hydrophobic surface area than the hydrophobic acid fractions.

### Effect of Ferrous Iron on Phenanthrene Binding

The presence of ferrous iron alone in solution very slightly enhanced the solubility of phenanthrene. While this solubility enhancement was subtracted from the solubility enhancements caused by the organic acids as a blank correction, some association between ferrous iron and PAHs is not unexpected. Metal ions can form charge transfer complexes with pi electrons in aromatic rings (e.g., the Ag<sup>+</sup>-naphthalene binding constant is log K = 0.49; Smith and Martell, 1989). To check this effect, a higher concentration of ferrous iron, 2.7 mM, was added to the aqueous solution and equilibrated with phenanthrene. The solubility enhancement, however, was not significantly different than that measured at 0.9 mM ferrous iron.

The presence of ferrous iron had no significant effect on the  $K_{om}$  values for the aliphatic carboxylic acids, although the black precipitate that appeared in the undecanoic acid solution may have artificially lowered the measured  $K_{om}$  value. Ferrous iron slightly increased the  $K_{om}$  values of the hydrophobic acid fractions and roughly doubled the  $K_{om}$  values of the aromatic carboxylic acids, with the exception of pamoic acid. We surmise that ferrous iron is promoting greater association of the organic acids with each other, resulting in an effective increase in the molecular weight of the organic acids. This increase in molecular weight would provide a more hydrophobic partitioning environment and higher  $K_{om}$  values.

Bivalent cations that do not bind strongly with carboxyl groups promote the aggregation of humic substances by charge suppression. Cations

that bind to carboxyl groups more strongly, like  $\text{Cu}^{2+}$ , are thought to form multiligand complexes that more effectively promote organic matter aggregation (Underdown and others, 1985). If ferrous iron behaved as  $\text{Cu}^{2+}$  did for fulvic acid, we would expect the solubility enhancement caused by ferrous iron for 3-hydroxy-2-naphthoic acid to be greater than that for 2-naphthoic acid because the 3-hydroxy-2-naphthoic acid can form a strong bidentate complex. Ferrous iron complexation constants are not available for these compounds, but we know that hydroxybenzoic acid ( $\log K = 10.13$ ) forms much stronger copper(II) complexes than benzoic acid ( $\log K = 1.76$ ) (Smith and Martell, 1989). Contrary to the strong multiligand aggregation hypothesis, the solubility enhancement for 2-naphthoic acid was slightly greater than that for the 3-hydroxy-2-naphthoic acid. It appears to be more likely that ferrous iron is increasing the solubility enhancement by allowing organic acid association through charge suppression.

## CONCLUSIONS

The geochemical changes caused by oil degradation have mobilized a small amount of iron-rich colloids in the Bemidji ground water. The organic colloids in the contaminated ground water are capable of enhancing the solubility of very hydrophobic PAHs. Potentially, this solubility enhancement may have contributed to the transport of such PAHs over distances greater than expected (Aiken and others, 1991). The presence of high ferrous iron concentrations in the contaminated Bemidji ground water may increase the ability of the the oil degradation products to enhance the solubility of PAHs.

## REFERENCES

Aiken, G.R., Capel, P.D., Furlong, E.T., Hult, M.F. and Thorn, K.A., 1991, Mechanisms controlling the transport of organic chemicals in subsurface environments, Mallard, G.E., and Aronson, D.A., eds., U.S. Geological Survey Toxic Substances Hydrology Program--Proceedings of the Technical Meeting, Monterey, California, March 11-15, 1991: U.S. Geological Survey Water-

- Resources Investigation Report 91-4034, p. 633-637.
- Aiken, G.R. and Malcolm, R.L., 1987, Molecular weight of aquatic fulvic acids by vapor pressure osmometry: *Geochimica Cosmochimica Acta*, v. 51, p. 2177-2184.
- Aiken, G.R., McKnight, D.M., Thorn, K.A., and Thurman, E.M., 1992, Isolation of hydrophilic organic acids from water using nonionic macroporous resins: *Organic Geochemistry*, v. 18, p. 567-573.
- Amrhein, C., Mosher, P.A. and Strong, J.E., 1993, Colloid-assisted transport of trace metals in roadside soils receiving deicing salts: *Soil Science Society of America Journal*, v. 57, p. 1212-1217.
- Backhus, D.A. and Gschwend, P.M., 1990, Fluorescent polycyclic aromatic hydrocarbons as probes of studying the impact of colloid on pollutant transport in groundwater: *Environmental Science & Technology*, v. 24, p. 1214-1223.
- Backhus, D.A., Ryan, J.N., Groher, D.M., MacFarlane, J.K. and Gschwend, P.M., 1993, Sampling colloids and colloid-associated contaminants in ground water: *Ground Water*, v. 31, p. 466-479.
- Baedecker, M.J., Cozzarelli, I.M., Eganhouse, R.P., Siegel, D.I. and Bennett, P.C., 1993, Crude oil in a shallow sand and gravel aquifer--III. Biogeochemical reactions and mass balance modeling in anoxic groundwater: *Applied Geochemistry*, v. 8, p. 569-586.
- Bennett, P.C., Siegel, D.I., Baedecker, M.J. and Hult, M.F., 1993, Crude oil in a shallow sand and gravel aquifer--I. Hydrogeology and inorganic geochemistry: *Applied Geochemistry*, v. 8, p. 529-549.
- Buddemeier, R.W. and Hunt, J.R., 1988, Transport of colloidal contaminants in groundwater: Radionuclide migration at the Nevada Test Site: *Applied Geochemistry*, v. 3, p. 535-548.
- Chin, Y.-P., Aiken, G.R. and Danielsen, K.M., 1997, Binding of pyrene to aquatic and commercial humic substances: The role of molecular weight and aromaticity: *Environmental Science & Technology*, v. 31, p. 1630-1635.



- Chiou, C.T., Malcolm, R.L., Brinton, T.I. and Kile, D.E., 1986, Water solubility enhancement of some organic pollutants and pesticides by dissolved humic and fulvic acids: *Environmental Science & Technology*, v. 20, p. 502-508.
- Cozzarelli, I.M., Baedecker, M.J., Eganhouse, R.P., and Goerlitz, D.F., 1994, Geochemical evolution of low-molecular weight organic acids derived from the degradation of petroleum contaminants in groundwater: *Geochimica Cosmochimica Acta*, v. 58, p. 863-877.
- De Jonge, H., Jacobsen, O.H., de Jonge, L.W. and Moldrup, P., 1998, Particle-facilitated transport of prochloraz in undisturbed sandy loam soil columns: *Soil Science Society of America Journal*, v. 27, p. 1495-1503.
- Dunnivant, F., Jardine, P.M., Taylor, D. and McCarthy, J.F., 1992, Cotransport of cadmium and hexachlorobiphenyl by dissolved organic matter through columns containing aquifer material: *Environmental Science & Technology*, v. 26, p. 360-368.
- Eganhouse, R.P., Baedecker, M.J., Cozzarelli, I.M., Aiken, G.R., Thorn, K.A. and Dorsey, T.F., 1993, Crude oil in a shallow sand and gravel aquifer--II. Organic geochemistry: *Applied Geochemistry*, v. 8, p. 551-567.
- Hawley, C. M., 1995, A field and laboratory study of the mechanisms of facilitated transport of hydrophobic organic contaminants: Boulder, Colorado, University of Colorado, Department of Civil, Environmental, and Architectural Engineering, unpublished M.S. thesis, 119 p.
- Hult, M. F., 1987, Movement and fate of crude oil contaminants in the subsurface environment at Bemidji, Minnesota, Franks, B. J., ed., U.S. Geological Survey. U.S. Geological Survey Program on Toxic Waste -- Ground-Water Contamination Proceedings of the Third Technical Meeting, Pensacola, Florida, March 23-27, 1987: U.S. Geological Survey Open-File Report 87-109, p. C3-C5.
- Hult, M. F., 1989, Mobilization, transport, and fate of hydrocarbons in the unsaturated zone, Mallard, G. E. and Ragone, S. E., eds., U.S. Geological Survey Toxic Substances Hydrology Program -- Proceedings of the Technical Meeting, Phoenix, Arizona, September 26-30, 1988: U.S. Geological Survey Water-Resources Investigation Report 88-4220, p. 53-53.
- Jury, W.A., Elabd, H. and Resteko, M., 1986, Field study of napromide movement through unsaturated soil: *Water Resources Research*, v. 22, p. 749-755.
- Karickhoff, S.W., 1981, Semi-empirical estimation of sorption of hydrophobic pollutants on natural sediments and soils: *Chemosphere*, v. 10, p. 833-846.
- Magee, B.R., Lion, L.W. and Lemley, A.T., 1991, Transport of dissolved organic macromolecules and their effect on the transport of phenanthrene in porous media: *Environmental Science & Technology*, v. 25, p. 323-331.
- Mukerjee, P. and Mysels, K. J., 1971, Critical micelle concentrations of aqueous surfactant systems: National Bureau of Standards Report NSRDS-NBS 36, 227 p.
- Puls, R.W., Clark, D.A., Bledsoe, B., Powell, R.M. and Paul, C.J., 1992, Metals in ground water: sampling artifacts and reproducibility: *Hazardous Waste and Hazardous Materials*, v. 9, p. 149-162.
- Ryan, J.N. and Gschwend, P.M., 1990, Colloid mobilization in two Atlantic Coastal Plain aquifers: Field studies: *Water Resources Research*, v. 26, p. 307-322.
- Ryan, J.N. and Gschwend, P.M., 1992, Effect of iron diagenesis on the transport of colloidal clay in an unconfined sand aquifer: *Geochimica Cosmochimica Acta*, v. 56, p. 1507-1521.
- Smith, R.M. and Martell, A.E., 1989, Critical Stability Constants: New York: Plenum Press.
- Underdown, A.W., Langford, C.H. and Gamble, D.S., 1985, Light scattering studies of the relationship between cation binding and aggregation of a fulvic acid: *Environmental Science & Technology*, v. 19, p. 132-136.
- Villholth, K.G., in press, Colloid characterization and colloidal phase partitioning of polycyclic aromatic hydrocarbons in two creosote-containing aquifers in Denmark: *Environmental Science & Technology*, to appear in February 1999.
- Vinten, A.J.A., Yaron, B. and Nye, P.H., 1983, Vertical transport of pesticides into soil when adsorbed on suspended particles: *Journal of*

Agriculture and Food Chemistry, v. 31,  
p. 662-664.

## **AUTHOR INFORMATION**

Joseph N. Ryan and Christine M. Hawley,  
Department of Civil, Environmental, and  
Architectural Engineering, University of  
Colorado, Campus Box 428, Boulder, Colorado  
80309 (joe.ryan@colorado.edu)

George R. Aiken, U.S. Geological Survey, 3215  
Marine Street, Boulder, Colorado 80303

Debera A. Backhus, School of Public and  
Environmental Affairs, Bloomington, Indiana  
47405

Karen G. Villholth, VKI, Agern Alle 11, DK-  
2970 Hoersholm, Denmark.

# Inhibition of Acetoclastic Methanogenesis by Crude Oil from Bemidji, Minnesota

By Ean Warren, Barbara A. Bekins, and E. Michael Godsy

## ABSTRACT

The shallow ground water at a site near Bemidji, Minnesota is contaminated with crude oil spilled from a broken pipeline in 1979. With a continued source of dissolved crude oil components, the geochemical conditions in the aquifer have evolved into aerobic, iron-reducing, and methanogenic redox zones. The methanogenic zone starts within the crude oil-contaminated region and extends more than 60 meters downgradient. The methanogenic numbers in the aquifer are low, but variable, depending on the subpopulation of methanogen. In areas close to the crude-oil source, hydrogen- and formate-utilizing methanogens are found in numbers more than one hundred times higher than acetate-utilizers. The acetate-utilizers are found only well below the non-aqueous phase oil and further downgradient. This pattern of methanogen distribution suggests that growth of acetate-utilizers is limited near the source. Laboratory results suggest that toxicity of the dissolved crude-oil is an explanation.

Serum bottle assays were conducted using crude oil in a mineral salts solution inoculated with an enriched methanogenic consortia from a creosote-contaminated site in Pensacola, Florida. Acetate, hydrogen, and formate were added and gas volume change was monitored. Hydrogen- and formate-utilization were unaffected by the crude oil whereas acetate utilization was significantly inhibited. The distribution of aquifer methanogens together with the toxicity assays form a consistent picture with the hypothesis that acetoclastic methanogenesis is inhibited in the vicinity of the oil at the Bemidji site. Because acetate degradation has been widely documented as the rate-limiting step in anaerobic waste treatment processes, it is likely that the inhibition of acetoclastic methanogenesis by the crude oil affects the overall methanogenic degradation rates of the petroleum hydrocarbon contaminants.

## INTRODUCTION

In August 1979, a crude oil pipeline near Bemidji, Minnesota (fig. 1) burst, spilling about 1,700,000 L (liters) of crude oil. Cleanup efforts removed all but an estimated 400,000 L of crude oil (Hult, 1984). The crude oil has moved through the unsaturated zone contaminating the sediments down to the water table. A plume of the water-soluble components (including benzene, toluene, ethylbenzene, xylenes, and polynuclear aromatic hydrocarbons) has formed under the crude oil. In the past 20 years, the plume has changed the geochemical conditions in the aquifer near the oil body from aerobic to iron-reducing and methanogenic (Baedecker and others, 1993; Bekins and others, 1999).

A model of the plume using a two-dimensional, multispecies reactive solute

transport model with sequential aerobic and anaerobic degradation processes was successful in predicting the evolution of geochemical conditions in the plume (Essaid and others, 1995). However, the use of Monod kinetics to model microbial growth in the aquifer resulted in simulated microbial numbers that far exceeded the observed aquifer microbial numbers. One process that would act to limit the net growth is inhibition of crude-oil biodegradation due to contaminant toxicity.

Specific methanogens may be inhibited by the increased contaminant concentration near the crude oil or even by the non-aqueous phase of the crude oil itself. Several authors have found that acetoclastic methanogens are inhibited by toxic compounds [Hickey and others, 1987 (chloroform, bromoethanesulfonic acid, trichloroacetic acid, and formaldehyde); Patel and

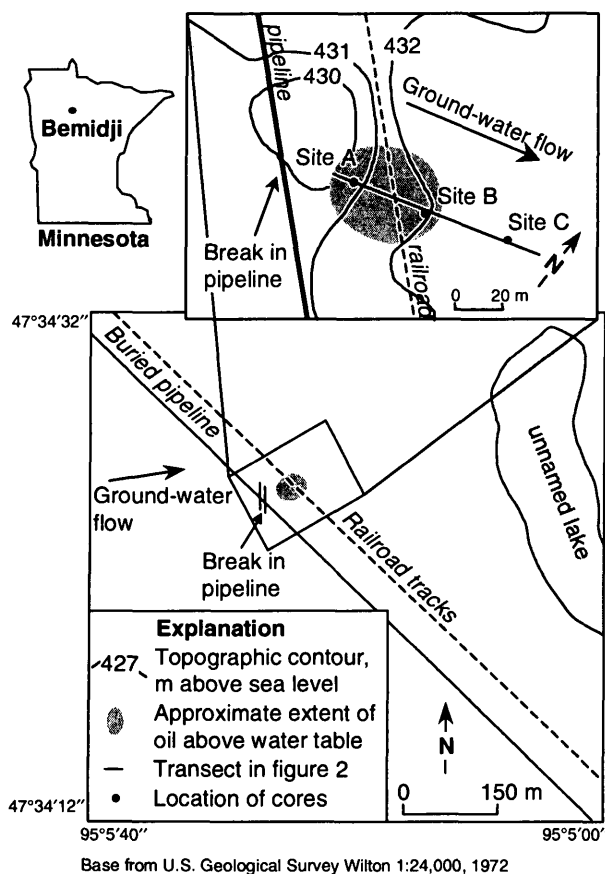


**Figure 1.** Site of 1979 crude oil spill near Bemidji, Minnesota, showing location of cores along a flow line.

others, 1991 (benzene ring compounds); Sierra-Alvarez and Lettinga, 1991 (monosubstituted benzenes, chlorobenzene, methoxybenzene, and benzaldehyde); Colleran and others, 1992 (chlorinated and fluorinated low molecular weight aliphatic and aromatic compounds); Davies-Venn and others, 1992 (chlorophenols and chloroanilines); van Beelen and Fleuren-Kemilä, 1993 (pentachlorophenol); and Donlon and others, 1995 (N-substituted aromatics)]. This is important because about 70 percent (%) of the methane produced comes from acetate fermentation by acetoclastic methanogens as opposed to carbon dioxide reduction by hydrogenophilic methanogens (Jeris and McCarty, 1965; Cappenberg, 1974; Cappenberg and Prins, 1974). Thus acetate fermentation is known to be the rate-limiting step in anaerobic wastewater-treatment processes. Parkin and Speece (1982) were able to model concentration-dependent inhibition of methanogenic

degradation of a variety of toxic compounds by modeling inhibition of the acetate utilization step.

Very little research has compared the inhibition of acetoclastic methanogens to other subpopulations. Colleran and others (1992) found acetoclastic species were significantly more inhibited by halogenated aliphatics than hydrogenophilic subpopulations. Bhattacharya and others (1995) found that whereas acetoclastic methanogens were inhibited by 4-nitrophenol, hydrogenophilic methanogens were not. Bekins and others (1997) found that acetoclastic methanogens were more susceptible to toxicity of water-soluble creosote compounds than were hydrogen- or formate-utilizing methanogens.

In this paper, we present evidence that inhibition can explain some aspects of methanogenic microbial numbers at the crude-oil spill site near Bemidji, Minnesota.

## METHODS

Most Probable Number (MPN) determinations were done on sediment from cores at three sites and compared with laboratory crude oil toxicity experiments. Inhibition of methanogens was measured by an anaerobic toxicity assay (Owen and others, 1979) in which the volume of gas produced in a methanogenic microcosm with crude oil was compared to that in a microcosm without crude oil.

### Most Probable Number Determination

Most Probable Number determinations were done on sediments from three sites located within the anoxic portion of the plume, labeled A, B, and C in figure 1. Cores containing aquifer sediments and the contaminated groundwater were collected with a 2.4 m (meter) freezing drive shoe (Murphy and Herkelrath, 1996). Data from sites A, B, and C were obtained from vertical profiles consisting of 3, 1, and 2 cores, respectively. The single core from site B was collected in 1996 while the five cores from sites A and C were collected in 1997. The method was the same for each core. The core was cut with a large tubing cutter exposing the aquifer material. Under a flow of oxygen-free nitrogen gas, the first few centimeters of the core material at the

cut were removed with a sterile spatula exposing an uncontaminated surface.

Approximately 10 g (grams) of sediment from the center of the core was added to a 25 x 142 mm (millimeter) anaerobic isolation roll streak tube (Bellco Glass Inc., Vineland, N.J. Note: Any use of trade, product, or firm names in this paper is for descriptive purposes only and does not imply endorsement by the U.S. Government.) filled with 20.0 mL (milliliter) of pre-reduced mineral salts solution. The mineral salts were prepared as follows (per liter): 0.75 g of  $\text{KH}_2\text{PO}_4$ ; 0.89 g of  $\text{K}_2\text{HPO}_4$ ; 0.36 g of  $\text{MgCl}_2 \cdot 6\text{H}_2\text{O}$ ; 0.9 g of  $\text{NH}_4\text{Cl}$ ; 9.0 mL of trace metal solution (Zeikus, 1977); 5.0 mL of vitamin solution (Wolin and others, 1963); and 10 mg (milligram) of Tween 80<sup>®</sup> [a nonionic surfactant added to remove microbes from the sediment (Yoon and Rosson, 1990)]. The pH was adjusted to 7.0 with phosphoric acid, and the solution was then boiled, cooled, and dispensed under a stream of oxygen-free nitrogen gas. The solution was sterilized at 121°C (degrees Celsius) [100 kPa (kilopascal)] for 15 minutes. All mineral salts solutions were amended with ferrous sulfide (FeS) as a reducing agent (Brock and O’Dea, 1977) to a final concentration of 1% by volume. Oxygen-free nitrogen gas was allowed to flow over the surface of the mineral salts solution as the sediment sample was added. The tube was then sealed, mixed well, and allowed to stand for 2 hours to allow penetration of Tween 80<sup>®</sup> into the sample. The tubes were then opened and sonicated [10 watts for 30 seconds] to dislodge the bacteria into the mineral salts using a Branson Sonifier<sup>®</sup>, Model 200, with the microtip attached (Branson Ultrasonics Corporation, Danbury, Conn.) with a flow of sterile oxygen-free nitrogen gas over the surface. The sediment samples in mineral salts were stored for not more than 4 hours at 20°C before inoculation of the growth media.

Microbial concentrations in sediment samples were determined using a five-tube MPN analysis. Samples were serially diluted by orders of magnitude into dilution mineral salts solutions that were pre-reduced and anaerobically sterilized as described by Holdeman and Moore (1972). Aliquots of the dilutions were inoculated into three different media, designed to promote growth

and the enumeration of acetate-, hydrogen-, and formate-utilizing methanogenic microorganisms. Acetoclastic and formate-utilizing organisms were enumerated with the addition to mineral salts of 2.5 g of sodium acetate·3H<sub>2</sub>O or 2.5 g sodium formate per liter, respectively. Hydrogen oxidizers were enumerated by aseptically pressurizing the serum bottles after inoculation with a 70:30 mix of H<sub>2</sub>:CO<sub>2</sub> to 140 kPa. The serum bottles were allowed to incubate for a minimum of six weeks at room temperature. The presence of the methanogen subpopulation was established by the detection of methane using a gas chromatograph with flame ionization detection (Godsy, 1980). Subsamples of sediments from site B (fig. 2) were taken for analysis of oil content using the method described by Hess and others (1992). Values for oil content at a site near site A were determined by Dillard and others (1997).

### Anaerobic Toxicity Assays

Anaerobic toxicity assays followed an adaptation of a protocol described by Owen and others (1979). Microcosms in 120 mL serum bottles were prepared to evaluate the toxicity of crude oil to formate-, hydrogen-, and acetate-utilizing methanogens. The serum bottles contained a total of 100 mL comprised of crude oil (10% by volume), mineral salts (70%), and an enriched methanogenic consortia suspended in

**Table 1.** Contents of serum bottles. Number indicates number of replicates. Check mark indicates either bottle was autoclaved or crude oil was present.

Bottle	Energy Source	Autoclaved	Crude Oil	No.
1	Acetate		√	2
2	Formate		√	2
3	Hydrogen		√	2
4	Acetate			1
5	Formate			1
6	Hydrogen			1
7	Acetate	√	√	1
8	Formate	√	√	1
9	Hydrogen	√	√	1
10	None		√	2
11	None	√		1

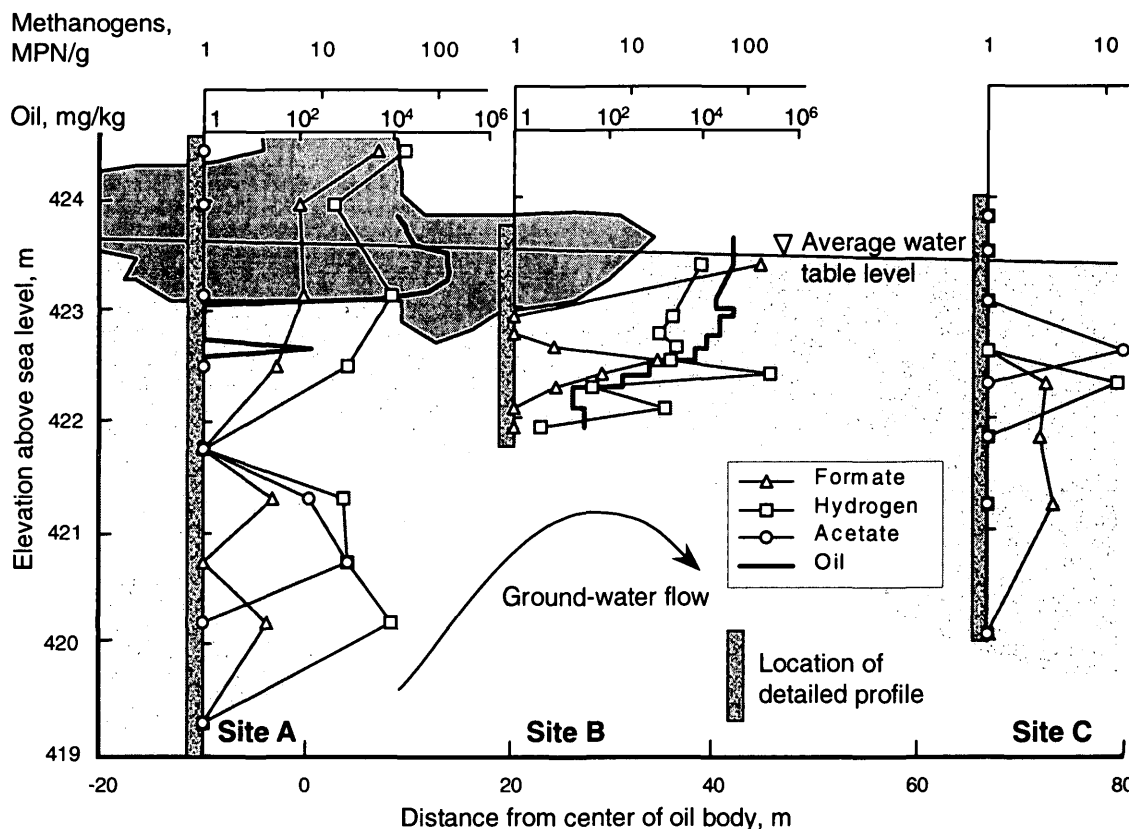


**Figure 2.** Formate-, hydrogen-, and acetate-utilizing microbial numbers [upper scale in graphs, shown in MPN/g (Most Probable Number per g)] from cores taken at sites A, B, and C, along with oil content [lower scale, shown in mg/kg (milligrams per kilogram of sediment)] at sites A and B. The dark gray area denotes greater than 10% oil saturation of pore space. Oil content for site A was determined by Dillard and others (1997). The light gray area corresponds to the anaerobic area of the plume (Bekins and others, 1999).

mineral salts (20%). The bottles were prepared in an anaerobic atmosphere and amended with ferrous sulfide (FeS) as a reducing agent (Brock and O'Dea, 1977) to a final concentration of 1% by volume. The bottles were sealed with solid butyl rubber stoppers and aluminum crimp seals. They were stored on their sides to reduce the possibility of gas leakage. Change of gas volume in the headspace was measured using a horizontal manometer.

Formate, hydrogen, or acetate were added to the bottles (table 1). The acetate and formate microcosms contained, respectively, 110 mg/L (milligrams per liter) acetate or 330 mg/L formate in mineral salts. The headspace of the formate and acetate microcosms were flushed with oxygen-free nitrogen and carbon dioxide at a 80:20 ratio by volume. The hydrogen microcosms were flushed with 80% hydrogen and 20% carbon

dioxide. At the start of the experiment, each microcosm was brought to equilibrium with atmospheric pressure using oxygen-free nitrogen.

Active microcosms were compared to controls to determine inhibition. Each active bottle containing crude oil was made in duplicate. Positive controls were made with acetate, hydrogen, and formate and no crude oil. Negative controls consisted of just the methanogenic consortium in mineral salts with the crude oil (in duplicate) as well as autoclaved bottles with acetate, hydrogen, and formate and the crude oil. The headspace was brought to atmospheric pressure with each measurement and any consumption of gas was replaced with nitrogen. All volume data were adjusted to standard temperature and pressure. Volumes from hydrogen microcosms were further normalized to

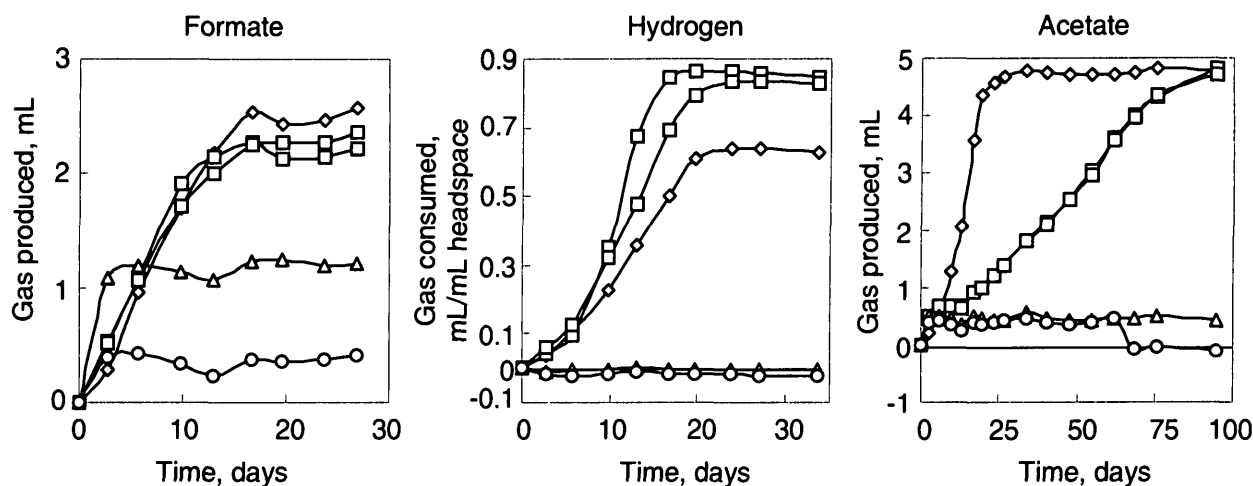


**Figure 3.** Gas production or consumption in microcosms fed with formate, hydrogen, or acetate. The legend is as follows: Active culture with crude oil (□), in duplicate; active culture without crude oil (◇); active culture with crude oil only (○); and average of two autoclaved cultures without crude oil (△).

the headspace volume to account for differing amounts of initial hydrogen mass.

## RESULTS

Most Probable Numbers from the site reveal that acetoclastic methanogens are not found near the oil body. In contrast, hydrogenophilic and formate-utilizers are found in similar numbers both within the oil body and outside it in the aqueous plume. The anaerobic toxicity assays show that the acetoclasts are inhibited significantly by the crude oil whereas the hydrogenophiles and formate-utilizers are not (figs. 2 and 3).

### Vertical Profiles of Methanogens

Vertical profiles of numbers of methanogens and oil concentrations through the plume of dissolved crude-oil compounds are shown in figure 2. The figure shows the microbial numbers of three subpopulations of methanogens at each location, along with oil content on sediments from sites A and B. Acetate-utilizing methanogens were found under the crude oil body at site A but only at a vertical distance of greater than 1 meter below the oil. At the center site, B, the anaerobic part of the plume is very narrow due to upwelling of oxygenated water below a low-permeability horizon. At this location there is

apparently no niche sufficiently distant from the oil for the acetate-utilizers to occupy. At the down-gradient site where there is no non-aqueous oil, acetate utilizers are again present. Hydrogen- and formate-utilizers are found both in the vicinity of the oil and also downgradient. All MPNs were below 100/g sediment. At site A, there were relatively high numbers of hydrogenophiles and formate-utilizers starting in the unsaturated zone in the oil. They remained high until about 1 meter below the oil where they dropped to less than 1/g. They were found again over the next 1.5 m, but hydrogenophiles were found in greater abundance in this interval than formate-utilizers. At site B, there was a peak of formate-utilizers in the oil and another at 422.5 m near the center of the aqueous plume. The hydrogenophiles were relatively high throughout the core. The hydrogen- and formate-utilizers do not seem to be affected by the oil. Site C contained all three subpopulations of methanogens, but at very low numbers (note the scale on the site C plot).

### Anaerobic Toxicity Assays

The results from the toxicity experiment are shown in figure 3. Formate-utilizing methanogens produced 2.5 mL of gas after 26 days. The microcosms with crude oil closely paralleled the active control indicating no detectable toxicity effect. After the first reading, gas in the killed

control increased. Since the microcosm remained inactive for the duration of the experiment, the likely source is due to an experimental error, possibly incomplete equilibrium with atmospheric pressure at the start of the experiment.

When hydrogen is utilized by methanogens, the net effect is a reduction of the gas volume in the headspace. The rates of hydrogen utilization in the microcosms with crude oil were similar to the active control indicating no discernable toxicity effect. Surprisingly, the hydrogen-utilizing methanogens used about 20% more gas in the presence of crude oil than in its absence. This indicates a slightly greater level of activity in the presence of the crude oil. The difference may be due to an initial excess of hydrogen in the headspace. Because hydrogen and carbon dioxide were added in stoichiometric amounts (table 2), if the hydrogen:carbon dioxide ratio in the headspace is too low, carbon dioxide-limiting conditions will occur when the as the hydrogen is exhausted. The microcosms with crude oil may have produced enough carbon dioxide from the degradation of organics to eliminate this limitation. Further studies including tighter controls of the headspace gas are planned to verify the possibility of carbon dioxide limitation.

The behavior of the acetate microcosms contrasts sharply with that of the hydrogen and formate microcosms. Production of methane and carbon dioxide in the acetate microcosms was

**Table 2.** Reactions and energy yields (kilojoules per mole) for acetate fermentation and carbon dioxide reduction using formate and hydrogen.

Acetate
$\text{CH}_3\text{COOH} \rightarrow \text{CH}_4 + \text{CO}_2$
-28.3 kJ/mol acetate
Hydrogen
$4\text{H}_2 + \text{CO}_2 \rightarrow \text{CH}_4 + 2\text{H}_2\text{O}$
-32.7 kJ/mol hydrogen
Formate
$4\text{HCOOH} \rightarrow \text{CH}_4 + 3\text{CO}_2 + 2\text{H}_2\text{O}$
-36.1 kJ/mol formate

affected significantly by the crude oil. All active microcosms produced 4.8 mL of gas. However, while the microcosm without crude oil took 30 days, the microcosms with crude oil took 100 days to reach completion.

## DISCUSSION AND CONCLUSIONS

Serum-bottle toxicity assays using crude oil and enriched methanogenic cultures with formate, hydrogen, and acetate showed that formate- and hydrogen-utilization were unaffected by the crude oil whereas acetate utilization was significantly inhibited. This result is consistent with observed numbers of methanogens found in the aquifer. Microbial numbers at the site indicate that formate- and hydrogen-utilizing methanogens are present near the non-aqueous oil whereas acetoclastic methanogens are found only at distances greater than 1 meter from the oil.

Anaerobic-toxicity experiments using water-soluble components from creosote also showed that acetoclastic methanogens were more susceptible to inhibition than the others were. This observed inhibition may be due to the lower energy yield (table 2) from the degradation of acetate. The energy gained from acetate fermentation may be inadequate to compensate for the toxicity near the oil. Methanogens from the two carbon dioxide reduction pathways may get just enough energy to overcome the toxic effects of the oil (Bekins and others, 1997).

Because the inhibition of acetoclastic methanogenesis by the crude oil would affect the overall methanogenic degradation rates of the petroleum hydrocarbon contaminants, it is important to identify sources and extent of inhibition.

## REFERENCES

- Baedecker, M.J., Cozzarelli, I.M., Eganhouse, R.P., Siegel, D.I., and Bennett, P.C., 1993, Crude oil in a shallow sand and gravel aquifer-III. Biogeochemical reactions and mass balance modeling in anoxic groundwater: *Applied Geochemistry*, v. 8, p. 569-586.



- Bekins, B.A., Cozzarelli, I.M., Godsy, E.M., Warren, Ean, Tuccillo, M.E., Essaid, H.I., and Paganelli, V.V., 1999, Chemical and physical controls on microbial populations in the Bemidji Toxics Site crude-oil plume, Morganwalp, D.W., and Buxton, H.T., eds., U.S. Geological Survey Toxic Substances Hydrology Program—Proceedings of the Technical Meeting, Charleston, South Carolina, March 8-12, 1999-- Volume 3 -- Subsurface Contamination from Point Sources: U.S. Geological Survey Water-Resources Investigations Report 99-4018C, this volume.
- Bekins, B.A., Godsy, E.M., and Warren, Ean, 1997, Inhibition of acetoclastic methanogenesis by complex mixtures of hydrocarbons: Eos, Transactions, American Geophysical Union, v. 78, no. 46, supplement, p. F289.
- Bhattacharya, S.K., Sluder, J.L., Jr., and Uberoi, V., 1995, Effects of 4-nitrophenol and H<sub>2</sub> and CO levels in anaerobic propionate systems: Water Research, v. 29, no. 5, p. 1249-1258.
- Brock, T.D. and O'Dea, K., 1977, Amorphous ferrous sulfide as a reducing agent for culture of anaerobes: Applied and Environmental Microbiology, v. 33, p. 254-256.
- Cappenberg, T.E., 1974, Interrelations between sulfate-reducing and methane-producing bacteria in bottom deposits of a fresh-water lake. II. Inhibition experiments: Antonie van Leeuwenhoek Journal of Microbiology and Serology, v. 40, no. 2, p. 297-306.
- Cappenberg, T.E. and Prins, R.A., 1974, Interrelations between sulfate-reducing and methane-producing bacteria in bottom deposits of a fresh-water lake. III. Experiments with <sup>14</sup>C-labeled substrates: Antonie van Leeuwenhoek Journal of Microbiology and Serology, v. 40, no. 3, p. 457-469.
- Colleran, Emer, Concannon, F., Golden, T., Geoghegan, F., Crumlish, B., Killilea, E., Henry, M., and Coates, J., 1992, Use of methanogenic activity tests to characterize anaerobic sludges, screen for anaerobic biodegradability and determine toxicity thresholds against individual anaerobic trophic groups and species: Water Science and Technology, v. 25, no. 7, p. 31-40.
- Davies-Venn, Christian, Young, J.C., and Tabak, H.H., 1992, Impact of chlorophenols and chloroanilines on the kinetics of acetoclastic methanogenesis: Environmental Science and Technology, v. 26, no. 8, p. 1627-1635.
- Dillard, L.A., Essaid, H.I., and Herkelrath, W.N., 1997, Multiphase flow modeling of a crude-oil spill site with a bimodal permeability distribution: Water Resources Research, v. 33, p. 1617-1632.
- Donlon, B.A., Razo-Flores, Elías, Field, J.A., and Lettinga, Gatze, 1995, Toxicity of N-substituted aromatics to acetoclastic methanogenic activity in granular sludge: Applied and Environmental Microbiology, v. 61, no. 11, p. 3889-3893.
- Essaid, H.I., Bekins, B.A., Godsy, E.M., Warren, Ean, Baedecker, M.J., and Cozzarelli, I.M., 1995, Simulation of aerobic and anaerobic biodegradation processes at a crude oil spill site: Water Resources Research, v. 31, no. 12, p. 3309-3327.
- Godsy, E.M., 1980, Isolation of *Methanobacterium bryantii* from a deep aquifer by using a novel broth-antibiotic disk method: Applied and Environmental Microbiology, v. 39, no. 5, p. 1074-1075.
- Hess, K.M., Herkelrath, W.N., and Essaid, H.I., 1992, Determination of subsurface fluid contents at a crude-oil spill site: Journal of Contaminant Hydrology, v. 10, p. 75-96.
- Hickey, R.F., Vanderwielen, J., and Switzenbuam, M.S., 1987, The effects of organic toxicants on methane production and hydrogen gas levels during the anaerobic digestion of waste activated sludge: Water Research, v. 21, no. 11, p. 1417-1427.
- Holdeman, L.V. and Moore, W.E.C., 1972, Anaerobe Laboratory Manual: Blacksburg, Virginia, Virginia Polytechnic Institute and State University, 156 p.
- Hult, M.F., 1984, Groundwater contamination by crude oil at the Bemidji, Minnesota, research site - An introduction, Hult, M.F. ed., Groundwater Contamination by Crude Oil at the Bemidji, Minnesota, Research Site: U.S. Geological Survey Water-Resources Investigations Report 84-4188, p. 1-15.

- Jeris, J.S. and McCarty, P.L., 1965, The Biochemistry of methane fermentation using C<sup>14</sup> tracers: *Journal of the Water Pollution Control Federation*, v. 37, no. 2, p. 178-192.
- Murphy, Fred and Herkelrath, W.N., 1996, A sample-freezing drive shoe for a wire line piston core sampler: *Ground Water Monitoring and Remediation*, v. 16, no. 3, p. 86-90.
- Owen, W.F., Stuckey, D.C., Healy, J.B., Jr., Young, L.Y., and McCarty, P.L., 1979, Bioassay for monitoring biochemical methane potential and anaerobic toxicity: *Water Research*, v. 13, p. 485-492.
- Parkin, G.F. and Speece, R.E., 1982, Modeling toxicity in methane fermentation systems: *Journal of Environmental Engineering*, v. 108, no. EE3, p. 515-531.
- Patel, G.B., Agnew, B.J., and Dicaire, C.J., 1991, Inhibition of pure cultures of methanogens by benzene ring compounds: *Applied and Environmental Microbiology*, v. 57, no. 10, p. 2969-2974.
- Sierra-Alvarez, Reyes and Lettinga, Gatzke, 1991, The effect of aromatic structure on the inhibition of acetoclastic methanogenesis in granular sludge: *Applied Microbiology and Biotechnology*, v. 34, no. 4, p. 544-550.
- van Beelen, P. and Fleuren-Kemilä, A.K., 1993, Toxic effects of pentachlorophenol and other pollutants on the mineralization of acetate in several soils: *Ecotoxicology and Environmental Safety*, v. 26, no. 1, p. 10-17.
- Wolin, E.A., Wolin, M.J., and Wolfe, R.S., 1963, Formation of methane by bacterial extracts: *Journal of Biological Chemistry*, v. 238, p. 2882-2886.
- Yoon, W.B. and Rosson, R.A., 1990, Improved Method of enumeration of attached bacteria for study of fluctuation in the abundance of attached and free-living bacteria in response to diel variation in seawater turbidity: *Applied and Environmental Microbiology*, v. 56, no. 3, p. 595-600.
- Zeikus, J.G., 1977, The biology of methanogenic bacteria: *Bacteriological Reviews*, v. 41, no. 2, p. 514-541.

## AUTHOR INFORMATION

Ean Warren, Barbara A. Bekins, and E. Michael Godsy, U.S. Geological Survey, Menlo Park, California (ewarren@usgs.gov)

# Polar Metabolites of Crude Oil

By Kevin A. Thorn and George R. Aiken

## ABSTRACT

Polar metabolites of crude oil in the form of nonvolatile organic acids were isolated from wells downgradient from the North oil pool and from the spray zone at the Bemidji site. The nonvolatile organic acids were subjected to spectroscopic and other characterization methods. The nonvolatile organic acids were distinguishable from naturally occurring ground-water humic substances in the aquifer, and appear to represent the partial oxidation products of the C<sub>18</sub> or greater alkylaromatic, naphthenoaromatic, and sulfur-containing constituents of the crude oil.

## INTRODUCTION

At the study site near Bemidji, Minnesota, biodegradation has resulted in a plume of dissolved organic carbon (DOC) that extends into zones III, IV, and V downgradient from the North oil pool (fig. 1). Ground-water in the spray zone (zone II) has also been contaminated from vertical infiltration of DOC resulting from biodegradation of crude oil in the overlying unsaturated zone, or from vertical infiltration of crude oil constituents followed by degradation in the saturated zone. The majority of DOC in zones II, III, IV, and V is comprised of nonvolatile organic acids (NVOA's) in the approximate molecular weight range from 360 to 410 daltons that represent the partial oxidation products (i.e. polar metabolites) of crude oil constituents. A study was undertaken to determine to what degree of resolution these NVOA's could be differentiated from the naturally occurring ground-water DOC in the aquifer, and to determine from which constituents in the crude oil the NVOA's are derived, using spectroscopic and other characterization techniques. The results from this study (Thorn and Aiken, 1998) are summarized here.

Hydrophilic acids, hydrophobic acids, and the hydrophobic neutral fraction of organic acids were isolated on XAD resins in samples from well 530 in zone IV (transition zone, DOC=21 mg C/L), well 603 in zone II (spray zone; DOC=15 mg C/L), and well 310 in zone I (background well; DOC= 2.9 mg C/L) that were collected during the 1986-1989 field seasons. These were characterized using liquid phase <sup>1</sup>H and <sup>13</sup>C NMR spectroscopy, elemental analyses, molecular weight determinations, δ <sup>13</sup>C's, and <sup>14</sup>C ages. The characterization data are presented in table 1. The naturally occurring ground-water

humic substances isolated from well 310 were distinguishable from the NVOA's isolated from contaminated water in wells 530 and 603. Based upon molecular weights, sulfur contents, carbon aromaticities, and the presence of methyl groups bonded to aromatic rings, the characterization data suggest that the NVOA's in wells 530 and 603 originate from the C<sub>18</sub> or greater alkylaromatic, naphthenoaromatic, and sulfur-containing constituents of the crude oil, including possibly the resins and asphaltenes. A scheme for the origin of the NVOA's in well 530 is shown in figure 2.

The generation and fate of the partial oxidation products of crude oil constituents is one of the least understood processes in the biodegradation of petroleum in ground-water. Some fundamental questions need to be addressed in future research. The hydrophobic neutrals are the least polar (i.e. least oxidized) fraction of dissolved organic acids isolated from the ground-water. The possibility that metabolites of petroleum constituents less polar than the hydrophobic neutrals are sorbed to the sediment grains within the vicinity of the oil body needs to be investigated. The concentration of total dissolved organic carbon (TDOC) downgradient from the North oil pool has remained relatively stable suggesting that degradation of the plume has reached equilibrium (Delin and others, 1998). This suggests three possible fates for the NVOA's: further degradation into lower molecular weight organic acids with subsequent microbial re-assimilation; mineralization to CO<sub>2</sub>; sorption onto aquifer sediments, possibly via ligand exchange complexation reactions.

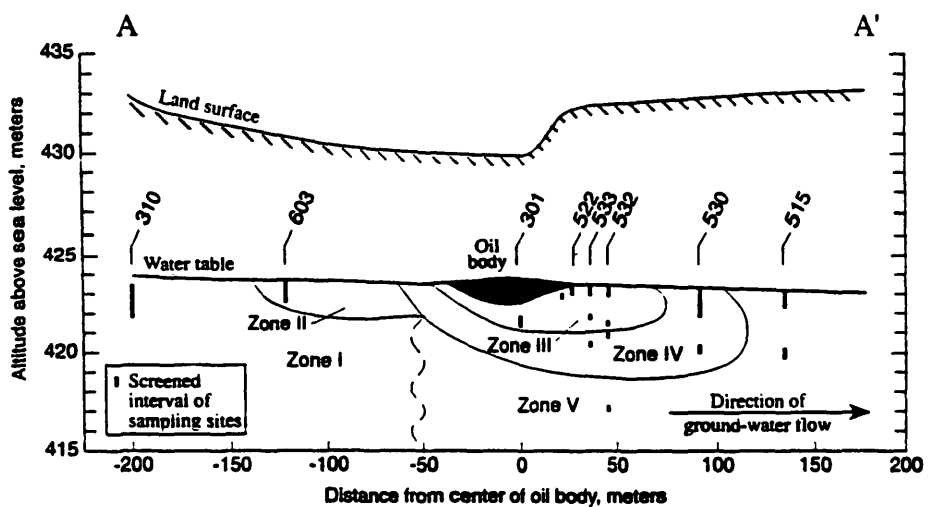
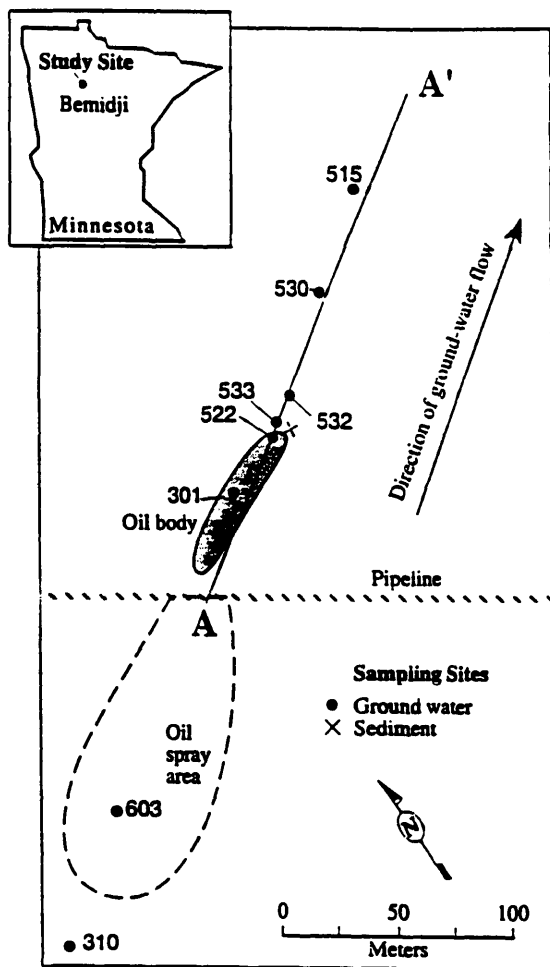


**Figure 1.** Bemidji study site showing locations of water table wells, North oil pool, and geochemical zones. Modified from Baedecker and others, 1993.

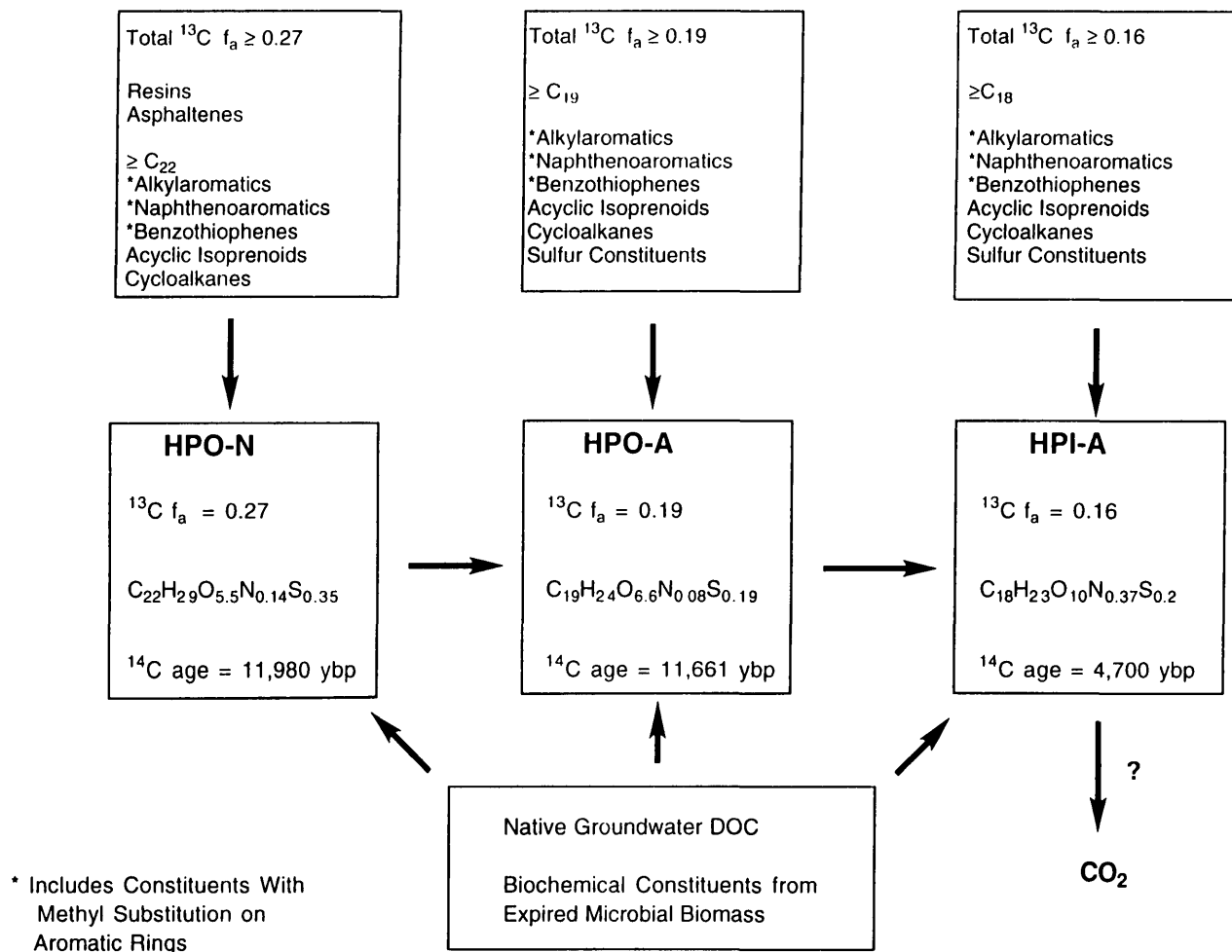


**Figure 2.** Scheme for the formation of NVOA's in well 530, using characterization data for the 530 NVOA's.  $f_a$  = carbon aromaticity determined from C-13 NMR, ybp = years before the present.

**Table 1.** Elemental Analyses, Molecular Weights,  $\delta^{13}\text{C}$  values, and  $^{14}\text{C}$  Ages for Crude Oil, Crude Oil Fractions, and Nonvolatile Organic Acids. HPI-A = hydrophilic acids; HPO-A = hydrophobic acids; HPO-N = hydrophobic neutral fraction of acids. Elemental C, H, O, N, and S contents reported on moisture free and ash free basis.  $M_n$  = number average molecular weight; C/M = number of carbons per average molecule; nd = not determined.

<u>SAMPLE</u>	<u>C</u>	<u>H</u>	<u>O</u>	<u>N</u>	<u>S</u>	<u>ASH</u>	<u>O/C</u>	<u><math>M_n</math></u>	<u>C/M</u>	<u><math>\delta^{13}\text{C}</math></u> (‰)	<u><math>^{14}\text{C}</math> Age</u> (ybp)
Crude Oil	86.41	12.83	0.47	0.38	0.64	<0.01	0.01	nd	nd	-28.4	
Aromatic	86.45	9.42	1.20	0.36	2.54	1.27	0.01	nd	nd	nd	
Resin	80.02	9.59	5.12	1.37	2.86	0.28	0.06	586	39	nd	
Asph.	86.45	7.22	2.58	1.39	3.09	<0.1	0.03	3598	259	nd	
530 HPO-N	67.47	7.27	22.56	0.49	2.85	3.53	0.33	395	22	-27.0	11,980 $\pm$ 105
530 HPO-A	62.18	6.75	29.09	0.32	1.66	2.32	0.47	362	19	-27.7	11,661 $\pm$ 89
530 HPI-A	52.66	5.52	38.99	1.27	1.56	3.26	0.74	412	18	-25.9	4,700 $\pm$ 55
603 HPO-N	64.32	7.63	24.44	0.18	3.42	19.92	0.38	nd	nd	nd	nd
603 HPO-A	62.5	6.4	27.8	0.4	2.71	3.8	0.44	nd	nd	nd	nd
603 HPI-A	50.62	5.8	39.69	0.72	3.13	4.20	0.78	nd	nd	nd	nd
310 HPO-A	55.95	5.88	37.08	0.71	0.39	5.06	0.66	536	25	-27.0	post bomb
310 HPI-A	52.20	5.05	40.34	1.75	0.67	2.02	0.77	513	22	-26.4	post bomb

## REFERENCES

- Baedecker, M.J., Cozzarelli, I.M., Siegel, D.I., Bennett, P.C., and Eganhouse, R.P., 1993, Crude oil in a shallow sand and gravel aquifer. III. Biogeochemical reactions and mass balance modeling in anoxic groundwater: *Applied Geochemistry*, v. 8, p. 569-586.
- Delin, G.N., Essaid, H.I., Cozzarelli, I.M., Lahvis, M.H., and Bekins, B.A., 1998, Ground water contamination by crude oil near Bemidji, Minnesota: U.S. Geological Survey Fact Sheet 084-98.
- Thorn, K.A., and Aiken, G.R., 1998, Biodegradation of crude oil into nonvolatile organic acids in a contaminated aquifer near Bemidji, Minnesota: *Organic Geochemistry*, v. 29, no. 4, p. 909-931.

## AUTHOR INFORMATION

Kevin A. Thorn and George R. Aiken, U.S. Geological Survey, Denver, Colorado





# Patterns of Microbial Colonization on Silicates

By Jennifer Roberts Rogers, Philip C. Bennett, and Franz K. Hiebert

## ABSTRACT

Several factors influence the attachment of microorganisms to mineral surfaces, such as surface charge, solution and mineral composition, and the types of organisms present in the ground water. In dilute groundwater systems inorganic nutrients can represent limiting components for growth of subsurface microorganisms and in these systems mineral composition may be an important factor in microbial colonization. In this study we examined microbial colonization of silicate minerals *in situ* using field microcosms, as well as in controlled laboratory microcosms. We found that in the petroleum-contaminated aquifer near Bemidji, MN where P is scarce, feldspars that contain inclusions of P-minerals such as apatite are preferentially colonized over similar feldspars without P. A microcline from S. Dakota, for example, which contains 1220 ppm P, was heavily colonized and deeply weathered after one year, while a similar microcline without detectable P was barren of attached organisms and completely unweathered. Anorthoclase (1050 ppm P) was very heavily colonized and weathered, whereas plagioclase specimens (<50 ppm) were uncolonized and unweathered. However, compositional differences in a limiting nutrient may not be the only controlling factor. In a stressed environment such as the aquifer near Bemidji, toxic elements may also influence colonization. Using silicate glasses, one with 4500 ppm Al and the other with 450 ppm Al, we found that Al appeared to be a deterrent to surface colonization, nor was olivine, with ~3000 ppm Ni, colonized. Quartz however was sparsely colonized and is most likely the result of no positive or negative compositional effects. Quartz with an iron hydroxide coating was heavily colonized with microorganisms remaining even after the iron was utilized. We propose that colonization in this system is particularly sensitive to the availability of P, and the native subsurface microorganisms tend to colonize and weather silicates, which contain apatite. Colonization may also be increased when more than one scarce nutrient is present. The result of this interaction is that nutrient-bearing silicates will be colonized, and preferentially destroyed, as the subsurface microbial community scavenges a limiting nutrient, while colonization of non-nutrient bearing minerals are colonized based on surface charge and toxic elements effects.

## INTRODUCTION

The influence of microorganisms on mineral-water interactions can be viewed at several scales, from a macro-scale examination of groundwater chemistry, to a micro-scale examination of the microbe-mineral interface. At the micro-scale, organisms that attach to surfaces can create reactive microenvironments due to the production of mineral and organic acidity and organic ligands, resulting in a perturbation of the mineral-water equilibria that may not be accurately reflected in the groundwater chemistry. In this study we examine the attachment of subsurface microorganisms to mineral surfaces both *in situ* and in the laboratory, and the possible controls on which mineral is colonized, and

which is weathered, in the microbial microenvironment.

There are several potential controls on microbial attachment to a mineral surface, both positive and negative. A mineral's surface charge can influence initial reversible attachment due to simple coulombic attraction or repulsion (e.g. Marshall, 1980; Scholl and others, 1990). Feldspar and quartz surfaces, for example, are uniformly negatively charged at environmental pHs, as are bacteria (e.g. Stumm and Morgan, 1996; Madigan and others, 1997), so attachment to that surface must overcome some degree of coulombic repulsion. Coulombic attraction or repulsion, however, is not an absolute control; bacteria can and will overcome an apparent

repulsion and attach to a negatively charged surface if that surface offers a competitive advantage.

The importance of other factors, such as surface roughness, and surface composition on initial colonization or subsequent growth is not well known. Potential influences might be the presence of adsorbed organic carbon, limiting nutrients, adsorbed iron or manganese oxides that alter surface charge, or toxic metals. The result however is a difference in colonization between two mineral surfaces that might otherwise be considered geologically similar, such as two different K-feldspars.

We are investigating specifically the presence of trace phosphorus in feldspars as a positive control on colonization. Most organisms require phosphorus as an essential macronutrient, and P is needed for the synthesis of nucleic acids, nucleotides, phosphoproteins and phospholipids (e.g., Ehrlich, 1996; Madigan and others, 1996). In many subsurface aqueous environments P is scarce, and tightly cycled within the community, limiting the size and growth of indigenous microbial populations (Ghiorse and Wilson, 1988).

Some microorganisms can extract phosphorus from insoluble mineral sources such as apatite, variscite, strengite and vivianite, by using organic acidity or chelators (e.g. Duff and others, 1963; Halder and Chaktabartty 1993; Goldstein, 1986). Many microorganisms, particularly those associated with soil rhizospheres are capable of solubilizing mineral phosphates. The mechanism of solubilization is typically by the formation of organic acids, such as gluconic and ketogluconic acid, and the resultant decrease in pH near the organism (e.g. Kim and others, 1997; Goldstein, 1986). Subba Rao (1982a, 1982b) found that bacteria isolated from the soil zone had the ability to solubilize mineral phosphates, and the expression of the mineral phosphate solubilizing (MPS) gene is suppressed with increasing concentration of dissolved orthophosphate (Goldstein, 1986). Solubilization of mineral phosphates by microorganisms has been primarily documented in soil zones where phosphates are applied as fertilizer however, these detrital phosphates are rarely abundant in the subsurface.

While phosphate minerals may not be widely distributed, phosphorus is a trace or minor constituent in many rocks. Pegmatitic feldspars can contain up to 2000 ppm phosphorus in the crystal matrix, while many igneous rocks including feldspars contain apatite as minor or trace inclusions. While the feldspar-bound P has not previously been considered a viable source of phosphorus, in very nutrient-limited environments silicate-bound nutrients may be an attractive source to colonizing microorganisms.

We propose that microorganisms extract phosphorus from apatite inclusions in feldspars, scavenging the nutrient while destroying the silicate matrix. We have observed this in carbon-rich, but phosphorus-poor, anaerobic groundwater.

## METHODS

We used both *in situ* and laboratory microcosms to examine the relationship between the P-content of feldspars and the microbial colonization of the mineral surface. We also examined the effects this interaction had on microbial biomass, substrate degradation, and mineral weathering.

### *In situ* Microcosms

Using *in situ* field microcosms (e.g. Hiebert and Bennett, 1992) we characterized the microbial colonization and weathering of a variety of feldspars, silicate glasses, quartz and iron-coated quartz (e.g. Grantham and Dove, 1996). An *in situ* microcosm consists of clean sterile mineral chips in a flow-through container that is suspended in a well for periods of months to years. For this study the microcosms were left in both aerobic and anaerobic zones in the petroleum-contaminated aquifer near Bemidji, Minnesota for periods up to one year. The anaerobic water has a pH of ~6.8, with very high DOC, ferrous iron and silica, while the aerobic region pH ranges from 6.2 to 7.0, and is dominated by the products of carbonate dissolution, with less DOC, little silica and no ferrous iron. The native microbial population in the anaerobic ground water consists of iron reducers, fermenters and methanogens, while the

aerobic groundwater is host to a variety of aerobes. Approximately 95% of the microorganisms are sessile, but the planktonic distribution is a good representation of the sessile population (Bekins, personal communication).

After microcosm removal, the biological tissue was fixed using a field critical point drying method (Nation, 1983; Vandevivere and Bevaye, 1993). Scanning electron microscopy was then used to characterize the types of microorganisms present, colonization patterns and weathering on the feldspar surfaces.

## Laboratory Microcosms

Laboratory microcosms were constructed from sterile glass bottles containing sterile mineral chips and native sediment and formation water. Sediments were collected using a freezing shoe core barrel (Murphy and Herkelrath, 1996), and the sealed core liner was moved immediately into a nitrogen-purged glove bag where the microcosms were constructed. To maintain anaerobic conditions the microcosms were also stored in an anaerobic chamber during the course of the experiment. The microcosms were amended with toluene at the start of the experiment, and reaction progress was characterized by chemical analysis of the microcosm water and vapor head-space. Production of methane and loss of toluene was determined by gas-solid gas chromatography (GC). Silicate dissolution was characterized by analysis of dissolved silica by ICP-OES and the reduced molybdate colorimetric method (Greenberg and others, 1992). Dissolved iron and orthophosphate were also measured colorimetrically as well as by ICP-OES. Minerals from sacrificed microcosms were fixed (as described above) then imaged using scanning electron microscopy (also described above) to observe differential colonization, extent of weathering and secondary phase generation.

Total viable microbial biomass and community structure were determined by PLFA analysis (Microbial Insights, Inc.) on samples of native anaerobic groundwater, sediment core from beneath the oil pool and anorthoclase chips left in situ in the anaerobic groundwater for 3 months.

## SILICATE CHEMISTRY

In this study five different feldspars as well as quartz, iron-coated quartz, olivine and two silicate glasses were exposed to the microbially active groundwater environment. It is assumed that the feldspars and quartz, as well as the two glasses, had similar starting surface charge and surface character, but with differing compositions. Whole rock, trace element, microprobe and light microscope analysis of all feldspars were used to determine compositional and mineralogical variations. The plagioclase (~Ab<sub>60</sub>) is a mixture of plagioclase, albite, and muscovite, with no detectable phosphorus, while oligoclase (~Ab<sub>75</sub>) had trace phosphorus, (<50ppm P) and iron of unknown redox state. The Ontario microcline was homogeneous with no detectable phosphorus, but trace iron.

The South Dakota microcline is more heterogeneous, with less iron than the Ontario microcline, but with 1220 ppm P, occurring as small apatite inclusions, intergrown with albite. The anorthoclase is also very heterogeneous, with 1050 ppm P occurring as mixed phosphate mineral inclusions. Inclusions are typically pure apatite, but some yttrium and barium were also detected. The anorthoclase also contained plagioclase and biotite, with iron/titanium oxides intergrown with apatite crystals. The apatite in both the South Dakota microcline and the anorthoclase was extractable with a weak acid solution and should be available to microorganisms. The aquifer sediment had 90 to 220 ppm total phosphorus of which only 0.9 to 3.6 ppm was available. Quartz had no impurities, while olivine contained ~3000 ppm Ni. Iron coatings on quartz were pure ferric hydroxide. The silicate glasses were obtained from NIST (standard 1830 and 1831) and had similar compositions with small differences in Al and K. The 1830 glass contained 450 ppm Al and 86 ppm K, while the 1831 glass contained 4500 ppm Al and 700 ppm K.

## SURFACE COLONIZATION

We found that microorganisms colonized some silicate surfaces to a greater degree than others, with weathering correlating directly with

the extent of colonization. Only those feldspars, which contain phosphorus were colonized, only colonized feldspars were weathered, and this only occurred in the anaerobic groundwater (e.g. Rogers and others, 1998).

SEM examination of mineral surfaces after reaction in the aquifer showed that quartz had colonization by a variety of microorganisms (based on morphological differences) and was lightly etched near attached organisms. The two glasses showed different colonization density, with biomass inversely correlated to the aluminum content of the glass. Olivine had little or no colonization, and this may be due to its high Ni content. The albite (Figure 1) and the Ontario

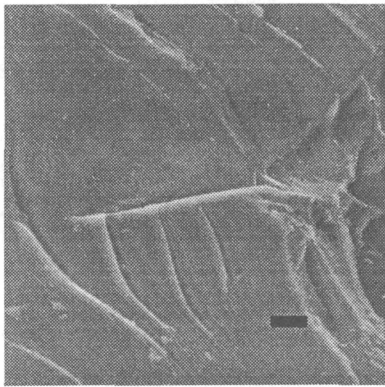


**Figure 1.** Photomicrograph of an albite surface after 1 year in the anaerobic groundwater at Bemidji. Scale bar is 5  $\mu\text{m}$ .

microcline had little or no colonization by microorganisms and no etching. The oligoclase had minor etching and a few microorganisms were detected. In contrast the South Dakota microcline and the anorthoclase (Figure 2) were

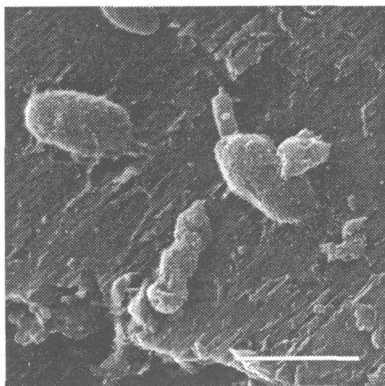


**Figure 2.** Photomicrograph of anorthoclase after 3 month in the aquifer. Attached organisms and etching are visible. Scale bar is 2  $\mu\text{m}$ .

both heavily colonized and etched.

Anorthoclase was the most heavily colonized and weathered possibly due to the presence of both P as apatite and Fe as iron oxides. The anaerobic groundwater is dominated by iron reducers and as Fe(III) is depleted iron may become limiting as a nutrient/TEA. Colonization of anorthoclase may be advantageous to this population by providing two necessary nutrients in one place.

While the colonization and weathering of the feldspars appears to be driven by P, colonization of quartz is anomalous to the theory that silicate colonization is nutrient controlled. Quartz may be a neutral surface on which microorganisms can attach although nutrients are not available. Conversely, surfaces such as olivine may contain a toxic factor, such as Ni, which interferes with microbial viability and may be particularly acute in stressed environments such as the anaerobic groundwater at Bemidji. The lack of colonization on the silicate glass, which contains Al, also suggests that even Al can have a negative effect on microorganisms. While Al is obviously present in the colonized feldspars, it may be tolerated by the attached organism if P is present as well. However, when P is not present the Al may be a deterrent to colonization, perhaps by chelating with ligands produced by the microorganism for sequestering essential metals such as iron.

Alteration of the quartz surface by precipitation of thin layer of amorphous iron sesquioxide, enhanced the colonization on that surface substantially, with thick colonization by organisms after only a few months. Here, unlike most surfaces examined to date, distinct colonies and biofilms are apparent. The change in colonization behavior with surface character is partly related to surface charge. Initial reversible attachment to the iron-coated quartz is enhanced by coulombic attraction between the positively charged iron sesquioxide surface and the negatively charged bacterial cell wall (Marshall, 1980). On the iron-coated surfaces the surface-attached organisms also form substantial colonies with evidence of attachment and glycocalyx development (Figure 3). This finding is in conflict with one prevalent hypothesis that iron reducing

organisms directly reduce the iron solid phase via membrane-bound iron reductase, and so must continuously move to fresh iron surfaces (Grantham and Dove, 1996). We observe the colony morphology even where no detectable iron coating remains.

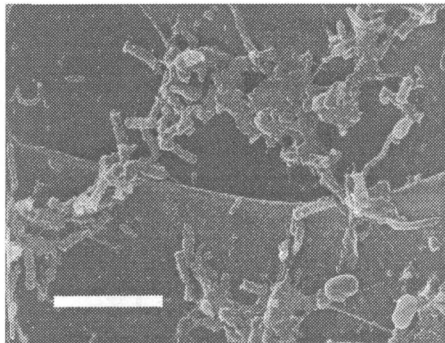


**Figure 3.** Photomicrograph of iron-coated quartz surface after 3 months in the aquifer. Several types of microorganisms and glycocalyx are visible. Scale bar is 6  $\mu\text{m}$ .

## SUBSTRATE UTILIZATION

Preliminary results from laboratory microcosm experiments suggest that P is released to the water when P-bearing feldspars are present. Further, microcosms containing anorthoclase as the sole source of P degraded toluene 90% faster than microcosms containing other feldspars or quartz, with no P. This suggests that not only is P released from the feldspars, but it is also available to the microorganisms, and the addition of P increases the rate of toluene degradation. It is not clear if an increase in the metabolism of the population or an increase in the size of the microbial population is responsible for the observed loss of toluene.

## MICROBIAL BIOMASS

Biomass determinations support the laboratory microcosm results. Anorthoclase chips colonized in the Bemidji aquifer for 3 months had approximately 15 times more biomass as aquifer sediment from the same interval. This suggests that biomass is actually increased by the presence of P as apatite in the mineral. The larger amount

of biomass may be due to an increase in the population size as a result of the addition of a limiting nutrient or may be a result of chemotaxis, where more organisms are attracted as the apatite is dissolved.

## IMPLICATIONS

We hypothesize that phosphorus in feldspars is released secondary to microbial production of ligands, which interact with the silicate matrix, dissolve it and expose the apatite inclusions in it. The release of phosphorus secondary to the silicate weathering provides a limiting nutrient to colonizing microorganisms, which promotes growth and in turn increases mineral weathering. However, nutrient limitation is not the sole factor in determining microbial colonization on mineral surfaces, though one of the more compelling ones. Colonization also depends on the composition of the mineral surface, and this may be more important in stressed or nutrient-limited environments.

## REFERENCES

- Duff, R.B., Webley, D.M., and Scott, R.O., 1963, Solubilization of minerals and related material by 2-ketogluconic acid producing bacteria: *Soil Science*, v. 95, p. 105-114.
- Ehrlich, H.L., 1996, *Geomicrobiology*: New York, Marcel Dekker, 719 p.
- Ghirorse, W.C. and Wilson, J.L., 1988, *Microbial ecology of the terrestrial subsurface*: *Advances in Applied Microbiology*, v. 33, p. 107-172.
- Grantham, M.C., and Dove, P.M., 1996, Investigation of bacterial-mineral interactions using Fluid Tapping Mode Atomic Force Microscopy: *Geochimica Cosmochimica Acta*, v.60, p. 2473-2480.
- Greenberg, A.E., Clesceri, L.S., and Eaton, A.D., 1992, *Standard Methods for Examination of Water and Wastewater*: Washington, D.C., APHA, 809 p.
- Halder, A.K., and Chakrabarty, P.K., 1993, Solubilization of inorganic phosphate by *Rhizobium*: *Folia Microbiologica*, v. 38, p. 325-330.

- Goldstein, A.H., 1986, Bacterial solubilization of mineral phosphates: *American Journal of Alternative Agriculture*, v. 1, p. 51-57.
- Hiebert, F.K. and Bennett, P.C., 1992, Microbial control of silicate weathering in an organic-rich ground water: *Science*, v. 258, p. 278-281.
- Kim, K.Y., Jordan, D., and Krishnan, H.B., 1997, *Rahnella aquatilis*, a bacterium isolated from soybean rhizosphere, can solubilize hydroxyapatite: *FEMS Microbiology Letters*, v. 153, p. 273-277.
- Madigan, M.T., Marinko, J.M., and Parker, J., 1997, *Brock Biology of Microorganisms*: Englewood Cliffs, Prentice Hall, 986 p.
- Marshall, K.C., 1980, Adsorption of Microorganisms to Surfaces: New York, John Wiley and Sons, p. 317-330.
- Murphy, F., and Herkelrath, W.N., 1996, A sample-freezing drive shoe for a wire-line piston core sampler: *Ground Water Monitoring and Remediation*, v. 16, p. 86-90.
- Nation, J.L., 1983, A new method for using hexamethyldisilazane for preparation of insect soft tissues for scanning electron microscopy: *Stain Technology*, v.58, p. 347-351.
- Rogers, J.R., Bennett, P.C., and Choi, W.J., 1998, *American Mineralogist*: v. 83, p. 1532-1540.
- Scholl, M.A., Mills, A.L., Herman, J.S., and Hornberger, G.M., 1990, *Journal of Contaminant Hydrology*, v.6, p. 321-330.
- Stumm, W., and Morgan, J.J., 1996, *Aquatic Chemistry*: New York, John Wiley and Sons, Inc., 780 p.
- Subba Rao, N.S., 1982a, *Biofertilizers: Interdisciplinary Science Reviews*, v. 7, p. 220-229.
- 1982b, Phosphate solubilization by soil microorganisms, in Subba Rao, N.S. ed., *Agricultural Microbiology*: Boston, MA, Butterworth, p. 295-305.
- Vandivivere, P. and Bavaye, P., 1993, Improved preservation of bacterial exopolymers for scanning electron microscopy: *Journal of Microscopy*, v. 167, p. 323-330.

## AUTHOR INFORMATION

Jennifer Roberts Rogers and Philip C. Bennett, Department of Geological Sciences, The University of Texas at Austin, Austin, Texas, 78712, ([jaroberts@mail.utexas.edu](mailto:jaroberts@mail.utexas.edu) and [pbennett@mail.utexas.edu](mailto:pbennett@mail.utexas.edu))

Franz K. Hiebert, RMT, Jones and Neuse, Inc., Austin, Texas.

# CONTENTS OF VOLUME 1 - CONTAMINATION FROM HARD-ROCK MINING

## KEYNOTE PAPER

Synthesis of watershed characterization for making remediation decisions by B.A. Kimball, K.E. Bencala, and J.M. Besser.

## SECTION A—A Watershed Approach to Contamination from Abandoned Mine Lands: The USGS Abandoned Mine Lands Initiative

Characterization of metals in water and bed sediment in two watersheds affected by historical mining in Montana and Colorado by D.A. Nimick, S.E. Church, T.E. Cleasby, D.L. Fey, B.A. Kimball, K.J. Leib, M.A. Mast, and W.G. Wright.

Determination of pre-mining geochemical conditions and paleoecology in the Animas River watershed, Colorado by S.E. Church, D.L. Fey, E.M. Brouwers, C.W. Holmes, and Robert Blair.

Use of tracer-injection and synoptic-sampling studies to quantify effects of metal loading from mine drainage by B.A. Kimball, R.L. Runkel, K.E. Bencala, and Katherine Walton-Day.

Application of the solute-transport models OTIS and OTEQ and implications for remediation in a watershed affected by acid mine drainage, Cement Creek, Animas River Basin, Colorado by Katherine Walton-Day, R.L. Runkel, B.A. Kimball, and K.E. Bencala.

Aquatic physical habitat and hydrology in abandoned mined land studies by R.T. Milhous.

Characterizing the aquatic health in the Boulder River watershed, Montana by A.M. Farag, D.F. Woodward, Don Skaar, and W.G. Brumbaugh.

Colloid formation and the transport of aluminum and iron in the Animas River near Silverton, Colorado by L.E. Schemel, B.A. Kimball, and K.E. Bencala.

Partitioning of zinc between dissolved and colloidal phases in the Animas River near Silverton, Colorado by L.E. Schemel, M.H. Cox, B.A. Kimball, and K.E. Bencala.

Oxygen isotopes of dissolved sulfate as a tool to distinguish natural and mining-related dissolved constituents by W.G. Wright and D.K. Nordstrom.

Modeling frequency of occurrence of toxic concentrations of zinc and copper in the Upper Animas River by J.M. Besser and K.J. Leib.

Overview of rare earth element investigations in acid waters of U. S. Geological Survey abandoned mine lands watersheds by P.L. Verplanck, D.K. Nordstrom, and H.E. Taylor.

Development of a passive integrative sampler for labile metals in water by W.G. Brumbaugh, J.D. Petty, J.N. Huckins, and S.E. Manahan.

Geomorphological context of metal-laden sediments the Animas River floodplain, Colorado by K.R. Vincent, S.E. Church, and D.L. Fey.

## SECTION B—Research on Hard-Rock Mining in Mountainous Terrains

Modeling solute transport and geochemistry in streams and rivers using OTIS and OTEQ by R.L. Runkel, K.E. Bencala, and B.A. Kimball.

Theory and(or) reality: Analysis of sulfate mass-balance at Summitville, Colorado, poses process questions about the estimation of metal loadings by K.E. Bencala and R.F. Ortiz .

Experimental diversion of acid mine drainage and the effects on a headwater stream by D.K. Niyogi, D.M. McKnight, W.M. Lewis, Jr., and B.A. Kimball.

Considerations of observational scale when evaluating the effect of, and remediation strategies for, a fluvial tailings deposit in the Upper Arkansas River Basin, Colorado by K.S. Smith, Katherine Walton-Day, and J.F. Ranville.

## SECTION C—Research on Hard-Rock Mining in Arid Southwest Alluvial Basins

- Geochemistry and reactive transport of metal contaminants in ground water, Pinal Creek Basin, Arizona by J.G. Brown, P.D. Glynn, and R.L. Bassett.
- Use of chlorofluorocarbons, dissolved gases, and water isotopes to characterize ground-water recharge in an aquifer contaminated by acidic, metal-laden wastewater by P.D. Glynn, Eurybiades Busenberg, and J.G. Brown.
- The effect of trace-metal reactive uptake in the hyporheic zone on reach-scale metal transport in Pinal Creek, Arizona by C.C. Fuller and J.W. Harvey.
- Environmental factors affecting oxidation of manganese in Pinal Creek, Arizona by J.C. Marble, T.L. Corley, M.H. Conklin and C.C. Fuller.
- Use of multi-parameter sensitivity analysis to determine relative importance of factors influencing natural attenuation of mining contaminants by J.Y. Choi, J.W. Harvey, and M.H. Conklin.
- Enhanced removal of dissolved manganese in hyporheic zones: centimeter-scale causes and kilometer-scale consequences by J.W. Harvey, C.C. Fuller, and M.H. Conklin.
- Evaluating the ability of tracer tests to quantify reactive solute transport in stream-aquifer systems by B.J. Wagner and J.W. Harvey.
- Preliminary model development of the ground- and surface-water system in Pinal Creek Basin, Arizona by C.E. Angerth, S.A. Leake, and B.J. Wagner.
- A flow-through cell for *in-situ*, real time X-ray absorption spectroscopy studies of geochemical reactions by J.E. Villinski, P.A. O'Day, T.L. Corley, and M.H. Conklin.
- Partitioning of trace metals between contaminated stream waters and manganese oxide minerals, Pinal Creek, Arizona by J.E. Best, K.E. Geiger, and P.A. O'Day.
- Representative plant and algal uptake of metals near Globe, Arizona by J.C. Marble, T.L. Corley, and M.H. Conklin.
- Manganese removal by the epilithic microbial consortium at Pinal Creek near Globe, Arizona by E.I. Robbins, T.L. Corley, and M.H. Conklin.

## SECTION D—Additional Research on Contamination from Mining-Related Activities

- Evaluation of the recovery of fish and invertebrate communities following reclamation of a watershed impacted by an abandoned coal surface mine by J.F. Fairchild, B.C. Poulton, T.W. May, and S.F. Miller.
- Factors explaining the distribution and site densities of the Neosho Madtom (*Noturus placidus*) in the Spring River, Missouri by M.L. Wildhaber, C.J. Schmitt, and A.L. Allert.
- Field demonstration of permeable reactive barriers to control radionuclide and trace-element contamination in ground water from abandoned mine lands by D.L. Naftz, J.A. Davis, C.C. Fuller, S.J. Morrison, G.W. Freethy, E.M. Feltcorn, R.G. Wilhelm, M.J. Piana, J. Joye, and R.C. Rowland.
- Geochemistry, toxicity, and sorption properties of contaminated sediments and pore waters from two reservoirs receiving acid mine drainage by D.K. Nordstrom, C.N. Alpers, J.A. Coston, H.E. Taylor, R.B. McCleskey, J.W. Ball, Scott Ogle, J.S. Cotsifas, and J.A. Davis.
- A new method for the direct determination of dissolved Fe(III) concentration in acid mine waters by J.W. Ball, D.K. Nordstrom, R.B. McCleskey, and T.B. To.
- Transport modeling of reactive and non-reactive constituents from Summitville, Colorado: Preliminary results from the application of the OTIS/OTEQ model to the Wightman Fork/Alamosa River System by J.W. Ball, R.L. Runkel, and D.K. Nordstrom.
- Frequency distribution of the pH of coal-mine drainage in Pennsylvania by C.A. Cravotta III, K.B.C. Brady, A.W. Rose, and J.B. Douds.



## CONTENTS OF VOLUME 2 - CONTAMINATION OF HYDROLOGIC SYSTEMS AND RELATED ECOSYSTEMS

### KEYNOTE PAPER

Emerging contaminant issues from an ecological perspective by S.N. Luoma.

### SECTION A—The San Francisco Bay-Estuary Toxics Study: Sustained Progress in a Unique Estuarine Laboratory

Studies relating pesticide concentrations to potential effects on aquatic organisms in the San Francisco Bay-Estuary, California by K.M. Kuivila.

Metal trends and effects in *Potamocorbula amurensis* in North San Francisco Bay by C.L. Brown and S.N. Luoma

Pesticides associated with suspended sediments in the San Francisco Bay during the first flush, December 1995 by B.A. Bergamaschi, K.M. Kuivila, and M.S. Fram.

Evaluation of polychlorinated biphenyl contamination in the Saginaw River using sediments, caged fish, and SPMDs by K.R. Echols, R.W. Gale, T.R. Schwartz, J.N. Huckins, L.L. Williams, J.C. Meadows, C.E. Orazio, J.D. Petty, and D.E. Tillitt.

Butyltin contamination in sediments and lipid tissues of the Asian clam, *Potamocorbula amurensis*, near Mare Island Naval Shipyard, San Francisco Bay by W.E. Pereira, F.D. Hostettler, and T.L. Wade.

Forecasting spring discharge in the west: A step towards forecasting stream chemistry by D.H. Peterson, R.E. Smith, Michael Dettinger, D.R. Cayan, S.W. Hager, and L.E. Schemel.

Reduced phosphate loading to South San Francisco Bay, California: Detection of effects in the water column by L.E. Schemel, S.W. Hager, and D.H. Peterson.

A Marine Nowcast System for San Francisco Bay, California by C.A. English, J.W. Gartner, R.E. Smith, and R.T. Cheng.

Herbicide concentrations in the Sacramento-San Joaquin Delta, California by K.M. Kuivila, H.D. Barnett, and J.L. Edmunds.

Do herbicides impair phytoplankton primary production in the Sacramento-San Joaquin River Delta? by J.L. Edmunds, K.M. Kuivila, B.E. Cole, and J.E. Cloern.

Degradation rates of six pesticides in water from the Sacramento River, California by Keith Starner, K.M. Kuivila, Bryan Jennings, and G.E. Moon.

The carbon isotopic composition of trihalomethanes formed from chemically distinct dissolved organic carbon isolates from the Sacramento-San Joaquin River Delta, California, USA by B.A. Bergamaschi, M.S. Fram, Roger Fujii, G.R. Aiken, Carol Kendall, and S.R. Silva.

Understanding the human influence on the San Francisco Bay-Delta Estuary Ecosystem - The Toxic Substances Hydrology Program and USGS Place-based Studies Program provide complementary approaches and results by J.S. Kuwabara, F.H. Nichols, K.M. Kuivila, and J.S. DiLeo.

Processes affecting the benthic flux of trace metals into the water column of San Francisco Bay by J.S. Kuwabara, B.R. Topping, K.H. Coale, and W.M. Berelson.

Redox gradients in the vicinity of the Santa Barbara Basin: Application of techniques developed within the San Francisco Bay Toxics Study by J.S. Kuwabara, Alexander van Geen, D.C. McCorkle, J.M. Bernhard, Yan Zheng, and B.R. Topping.

Flow-injection-ICP-MS method applied to benthic flux studies of San Francisco Bay by B.R. Topping and J.S. Kuwabara.

Aspects of the Exxon Valdez oil spill--A forensic study and a toxics controversy by F.D. Hostettler, K.A. Kvenvolden, R.J. Rosenbauer, and J.W. Short.

## SECTION B—Mercury Contamination of Aquatic Ecosystems

- A national pilot study of mercury contamination of aquatic ecosystems along multiple gradients by D.P. Krabbenhoft, J.G. Wiener, W.G. Brumbaugh, M.L. Olson, J.F. DeWild, and T.J. Sabin.
- Methylmercury in aquatic food webs: Consequences and management challenges by J.G. Wiener and D.P. Krabbenhoft.
- Mercury contamination: A nationwide threat to our aquatic resources, and a proposed research agenda for the USGS by D.P. Krabbenhoft, and J.G. Wiener.
- Mercury contamination from hydraulic placer-gold mining in the Dutch Flat mining district, California by M.P. Hunerlach, J.J. Rytuba, and C.N. Alpers.
- Techniques for the collection and species-specific analysis of low levels of mercury in water, sediment, and biota by M.L. Olson and J.F. DeWild.

## SECTION C—Occurrence, Distribution, and Fate of Agricultural Chemicals in the Mississippi River Basin

- Nitrogen flux and sources in the Mississippi River Basin by D.A. Goolsby, W.A. Battaglin, B.T. Aulenbach, and R.P. Hooper.
- Occurrence of sulfonylurea, sulfonamide, imidazolinone, and other herbicides in midwestern rivers, reservoirs, and ground water, 1998 by W.A. Battaglin, E.T. Furlong, M.R. Burkhardt, and C.J. Peter.
- Occurrence of cotton herbicides and insecticides in Playa Lakes of the High Plains of West Texas by E.M. Thurman, K.C. Bastian, and Tony Mollhagen.
- Trends in annual herbicide loads from the Mississippi River Basin to the Gulf of Mexico by G.M. Clark and D.A. Goolsby.
- Finding minimal herbicide concentrations in ground water? Try looking for the degradates by D.W. Kolpin, E.M. Thurman, and S.M. Linhart.
- Pesticides in the atmosphere of the Mississippi River Valley, Part I-Rain by M.S. Majewski, W.T. Foreman, and D.A. Goolsby.
- Pesticides in the atmosphere of the Mississippi River Valley, Part II-Air by W.T. Foreman, M.S. Majewski, D.A. Goolsby, F.W. Wiebe, and R.H. Coupe.
- Routine determination of sulfonylurea, imidazolinone, and sulfonamide herbicides at nanogram-per-liter concentrations by solid-phase extraction and liquid chromatography/mass spectrometry by E.T. Furlong, M.R. Burkhardt, P.M. Gates, S.L. Werner, and W.A. Battaglin.
- Herbicides and herbicide degradates in shallow ground water and the Cedar River near a municipal well field, Cedar Rapids, Iowa by R.A. Boyd.
- Occurrence of pesticides in rain and air in urban and agricultural areas of Mississippi, April-September 1995 by R.H. Coupe, M.A. Manning, W.T. Foreman, D.A. Goolsby, and M.S. Majewski.
- Changes in herbicide concentrations in midwestern streams in relation to changes in use, 1989-98 by E.A. Scribner, W.A. Battaglin, D.A. Goolsby, and E.M. Thurman.
- An ecological risk assessment of the potential for herbicide impacts on primary productivity of the Lower Missouri River by J.F. Fairchild, L.C. Sappington, and D.S. Ruessler.
- Atmospheric deposition of nitrogen in the Mississippi River Basin by G.B. Lawrence, D.A. Goolsby, and W.A. Battaglin.
- Isotopic tracing of nitrogen sources and cycling in the Mississippi River Basin by Carol Kendall, W.A. Battaglin, Gilbert Cabana, C.C. Chang, S.R. Silva, S.D. Porter, D.A. Goolsby, D.H. Campbell, R.P. Hooper, and C.J. Schmitt.
- Determination of chloroacetanilide herbicide metabolites in water using high-performance liquid chromatography-diode array detection and high-performance liquid chromatography/mass spectrometry by K.A. Hostetler and E.M. Thurman.

Analysis of selected herbicide metabolites in surface and ground water of the United States by E.A. Scribner, E.M. Thurman, and L.R. Zimmerman.

Detection of persistent organic pollutants in the Mississippi Delta using semipermeable membrane devices by L.R. Zimmerman, E.M. Thurman, and K.C. Bastian.

#### SECTION D—Additional Research on the Effects of Contamination on Hydrologic Systems and Related Ecosystems

Ratios of metolachlor to its metabolites in ground water, tile-drain discharge, and surface water in selected areas of New York State by P.J. Phillips, D.A. Eckhardt, E.M. Thurman, and S.A. Terracciano.

Herbicides and their metabolites in Cayuga Lake and its tributaries, New York by D.A.V. Eckhardt, W.M. Kappel, W.F. Coon, and P.J. Phillips.

Methyl tert-butyl ether (MTBE) in lakes in Byram Township, Sussex County, New Jersey, 1998 and vulnerability of ground water in lakeside communities by O.S. Zapecza and A.L. Baehr.

Halogenated organic compounds in endocrine-disrupted male carp from Las Vegas Wash and Lake Mead, Nevada by T.J. Leiker, H.E. Bevans and S.L. Goodbred.

How DOC composition may explain the poor correlation between specific trihalomethane formation potential and specific UV absorbance by M.S. Fram, Roger Fujii, J.L. Weishaar, B.A. Bergamaschi, and G.R. Aiken.

Wastewater analysis by gas chromatography/mass spectrometry by G.K. Brown, S.D. Zaugg, and L.B. Barber.

Biomonitoring of environmental status and trends (BEST) program: Contaminants and related effects in fish from the Mississippi, Columbia, and Rio Grande Basins by C.J. Schmitt, T.M. Bartish, V.S. Blazer, T.S. Gross, D.E. Tillitt, W.L. Bryant, and L.R. DeWeese.

A model fish system to test chemical effects on sexual differentiation and development by D.M. Papoulias, D.B. Noltie, and D.E. Tillitt.

The potential for contaminated ground water to adversely affect chinook salmon under exposure conditions simulating the Hanford Reach of the Columbia River, Washington, USA by D.F. Woodward, A.M. Farag, A.J. DeLonay, Laverne Cleveland, W.G. Brumbaugh, and E.E. Little.

A radioimmunoassay method to screen for antibiotics in liquid waste at confined livestock operations, with confirmation by liquid chromatography/mass spectrometry by M.T. Meyer, J.E. Bumgarner, E.M. Thurman, K.A. Hostetler, and J.V. Daughtridge.

Trends in sediment quality in response to urbanization by P.C. Van Metre, and Edward Callender.

Estimating the environmental behavior of inorganic and organometal contaminants: Solubilities, bioaccumulation, and acute aquatic toxicities by J.P. Hickey.

## CONTENTS OF VOLUME 3 - SUBSURFACE CONTAMINATION FROM POINT SOURCES

### KEYNOTE PAPERS

Scale considerations of chlorinated solvent source zones and contaminant fluxes: Insights from detailed field studies by B.L. Parker and J.A. Cherry

Selecting remediation goals by assessing the natural attenuation capacity of ground-water systems by F.H. Chapelle and P.M. Bradle

Sampling throughout the hydrologic cycle to characterize sources of volatile organic compounds in ground water by A.L. Baehr, L.J. Kauffman, E.G. Charles, R.J. Baker, P.E. Stackelberg, M.A. Ayers, and O.S. Zapecza

Capabilities and challenges of natural attenuation in the subsurface: Lessons from the U.S. Geological Survey Toxics and Substances Hydrology Program by B.A. Bekins, A.L. Baehr, I.M. Cozzarelli, H.I. Essaid, S.K. Haack, R.W. Harvey, A.M. Shapiro, J.A. Smith, and R.L. Smith

### SECTION A—Processes that Control the Natural Attenuation of Hydrocarbons and Fuel Oxygenates at Gasoline Release Sites

Fate of MTBE relative to benzene in a gasoline-contaminated aquifer (1993-98) by J.E. Landmeyer, P.M. Bradley, and F.H. Chapelle

Mass transport of methyl tert-butyl ether (MTBE) across the water table and significance for natural-attenuation remediation at a gasoline spill site in Beaufort, South Carolina by M.A. Lahvis, R.J. Baker, and A.L. Baehr

Aerobic mineralization of MTBE and *t*-butanol by stream-bed-sediment microorganisms by P.M. Bradley, J.E. Landmeyer, and F.H. Chapelle

Effects of environmental conditions on MTBE degradation in model column aquifers by C.D. Church, P.G. Tratnyek, J.F. Pankow, J.E. Landmeyer, A.L. Baehr, M.A. Thomas, and Mario Schirmer

Equilibrium vapor method to determine the concentration of inorganic carbon and other compounds in water samples by R.J. Baker, A.L. Baehr, and M.A. Lahvis

Transport of methyl tert-butyl ether (MTBE) and hydrocarbons to ground water from gasoline spills in the unsaturated zone by M.A. Lahvis and A.L. Baehr

### SECTION B—Ground Water Contamination by Crude Oil

Long-term geochemical evolution of a crude-oil plume at Bemidji, Minnesota by I.M. Cozzarelli, M.J. Baedecker, R.P. Eganhouse, M.E. Tuccillo, B.A. Bekins, G.R. Aiken, and J.B. Jaeschke

Chemical and physical controls on microbial populations in the Bemidji Toxics Site crude-oil plume by B.A. Bekins, I.M. Cozzarelli, E.M. Godsy, Ean Warren, M.E. Tuccillo, H.I. Essaid, and V.V. Paganelli

Long-term monitoring of unsaturated-zone properties to estimate recharge at the Bemidji crude-oil spill site by G.N. Delin and W.N. Herkelrath

Coupled biogeochemical modeling of ground-water contamination at the Bemidji, Minnesota, crude oil spill site by G.P. Curtis, I.M. Cozzarelli, M.J. Baedecker, and B.A. Bekins

Determining BTEX biodegradation rates using in-situ microcosms at the Bemidji site, Minnesota: Trials and tribulations by E.M. Godsy, Ean Warren, I.M. Cozzarelli, B.A. Bekins, and R.P. Eganhouse

Mineralogy and mineral weathering: Fundamental components of subsurface microbial ecology by P.C. Bennett, J.R. Rogers, F.K. Hiebert, and W.J. Choi

Aromatic and polyaromatic hydrocarbon degradation under Fe(III)-reducing conditions by R.T. Anderson, J.N. Rooney-Varga, C.V. Gaw, and D.R. Lovley

Electrical geophysics at the Bemidji Research Site by R.J. Bisdorf

- Impacts of remediation at the Bemidji oil-spill site by W.N. Herkelrath
- Ground penetrating radar research at the Bemidji, Minnesota, crude-oil spill site by J.E. Lucius
- Investigating the potential for colloid- and organic matter-facilitated transport of polycyclic aromatic hydrocarbons in crude oil-contaminated ground water by J.N. Ryan, G.R. Aiken, D.A. Backhus, K.G. Villholth, and C.M. Hawley
- Inhibition of acetoclastic methanogenesis by crude oil from Bemidji, Minnesota by Ean Warren, B.A. Bekins, and E.M. Godsy
- Polar metabolites of crude oil by K.A. Thorn and G.R. Aiken
- Patterns of microbial colonization on silicates by J.R. Rogers, P.C. Bennett, and F.K. Hiebert

## SECTION C—The Fate of Complex Contaminant Mixtures from Treated Wastewater Discharges

- Natural restoration of a sewage plume in a sand and gravel aquifer, Cape Cod, Massachusetts by D.R. LeBlanc, K.M. Hess, D.B. Kent, R.L. Smith, L.B. Barber, K.G. Stollenwerk, and K.W. Campo
- Evolution of a ground-water sewage plume after removal of the 60-year-long source, Cape Cod, Massachusetts: Changes in the distribution of dissolved oxygen, boron, and organic carbon by L.B. Barber and S.H. Keefe
- Evolution of a ground-water sewage plume after removal of a 60-year-long source, Cape Cod, Massachusetts: Fate of volatile organic compounds by K.W. Campo and K.M. Hess
- Evolution of a ground-water sewage plume after removal of the 60-year-long source, Cape Cod, Massachusetts: Inorganic nitrogen species by R.L. Smith, B.A. Rea Kumler, T.R. Peacock, and D.N. Miller
- Evolution of a ground-water sewage plume after removal of the 60-year-long source, Cape Cod, Massachusetts: pH and the fate of phosphate and metals by D.B. Kent and Valerie Maeder
- Phosphorus transport in sewage-contaminated ground water, Massachusetts Military Reservation, Cape Cod, Massachusetts by D.A. Walter, D.R. LeBlanc, K.G. Stollenwerk, and K.W. Campo
- In situ assessment of the transport and microbial consumption of oxygen in ground water, Cape Cod, Massachusetts by R.L. Smith, J.K. Böhlke, K.M. Revesz, Tadashi Yoshinari, P.B. Hatzinger, C.T. Penarrieta, and D.A. Repert
- Stable isotope composition of dissolved O<sub>2</sub> undergoing respiration in a ground-water contamination gradient by Kinga Révész, J.K. Böhlke, R.L. Smith, and Tadashi Yoshinari
- Nitrification in a shallow, nitrogen-contaminated aquifer, Cape Cod, Massachusetts by D.N. Miller, R.L. Smith, and J.K. Böhlke
- Recharge conditions and flow velocities of contaminated and uncontaminated ground waters at Cape Cod, Massachusetts: Evaluation of  $\delta^2\text{H}$ ,  $\delta^{18}\text{O}$ , and dissolved gases by J.K. Böhlke, R.L. Smith, T.B. Coplen, Eurybiades Busenberg, and D.R. LeBlanc
- Determination of temporal and spatial variability of hydraulic gradients in an unconfined aquifer using three-point triangulation, Cape Cod, Massachusetts by T.D. McCobb, D.R. LeBlanc, and K.M. Hess
- Modeling the influence of adsorption on the fate and transport of metals in shallow ground water: Zinc contamination in the sewage plume on Cape Cod, Massachusetts by D.B. Kent, R.H. Abrams, J.A. Davis, and J.A. Coston
- Modeling the evolution and natural remediation of a ground-water sewage plume by K.G. Stollenwerk and D.L. Parkhurst
- Multispecies reactive tracer test in an aquifer with spatially variable chemical conditions: An overview by J.A. Davis, D.B. Kent, J.A. Coston, K.M. Hess, and J.L. Joye
- Multispecies reactive transport in an aquifer with spatially variable chemical conditions: Dispersion of bromide and nickel tracers by K.M. Hess, J.A. Davis, J.A. Coston, and D.B. Kent

- Effect of growth conditions upon the subsurface transport behavior of a ground water protist by R.W. Harvey, N.A. Mayberry, N.E. Kinner, and D.W. Metge
- Mobilization and transport of natural and synthetic colloids and a virus in an iron oxide-coated, sewage-contaminated aquifer by J.N. Ryan, Menachem Elimelech, R.A. Ard, and R.D. Magelky
- Dual radioisotope labeling to monitor virus transport and identifying factors affecting viral inactivation in contaminated aquifer sediments from Cape Cod, Massachusetts by D.W. Metge, Theresa Navigato, J.E. Larson, J.N. Ryan, and R.W. Harvey
- Installation of deep reactive walls at MMR using a granular iron-guar slurry by D.W. Hubble and R.W. Gillham
- Monitoring a permeable reactive iron wall installation in unconsolidated sediments by using a cross-hole radar method by J.W. Lane, Jr., P.K. Joesten, and J.G. Savoie
- Robowell: A reliable and accurate automated data-collection process applied to reactive-wall monitoring at the Massachusetts Military Reservation, Cape Cod, Massachusetts by G.E. Granato and K.P. Smith

#### SECTION D—Factors and Processes that Affect Waste Disposal and Subsurface Transport of Contaminants in Arid Environments

- Overview of research on water, gas, and radionuclide transport at the Amargosa Desert Research Site, Nevada by B.J. Andraski and D.A. Stonestrom
- Isotopic composition of water in a deep unsaturated zone beside a radioactive-waste disposal area near Beatty, Nevada by D.A. Stonestrom, D.E. Prudic, and R.G. Striegl
- Tritium and  $^{14}\text{C}$  concentrations in unsaturated-zone gases at test hole UZB-2, Amargosa Desert Research Site, 1994-98 by D.E. Prudic, R.G. Striegl, R.W. Healy, R.L. Michel, and Herbert Haas
- Tritium in water vapor in the shallow unsaturated zone at the Amargosa Desert Research site by R.W. Healy, R.G. Striegl, R.L. Michel, D.E. Prudic, and B.J. Andraski
- Soil respiration at the Amargosa Desert Research site by A.C. Riggs, R.G. Striegl, and F.B. Maestas

#### SECTION E—Geochemical and Microbiological Processes in Ground Water and Surface Water Affected by Municipal Landfill Leachate

- Ground-water and surface-water hydrology of the Norman Landfill Research Site by Scott Christenson, M.A. Scholl, J.L. Schlottmann, and C.J. Becker
- Identifying ground-water and evaporated surface-water interactions near a landfill using Deuterium,  $^{18}\text{O}$ xygen, and Chloride, Norman, Oklahoma by J.L. Schlottmann, M.A. Scholl, and I.M. Cozzarelli
- Biogeochemical processes in a contaminant plume downgradient from a landfill, Norman, Oklahoma by I.M. Cozzarelli, J.M. Sufliata, G.A. Ulrich, S.H. Harris, M.A. Scholl, J.L. Schlottman, and J.B. Jaeschke
- Evidence for natural attenuation of volatile organic compounds in the leachate plume of a municipal landfill near Norman, Oklahoma by R.P. Eganhouse, L.L. Matthews, I.M. Cozzarelli, and M.A. Scholl
- Dominant terminal electron accepting processes occurring at a landfill leachate-impacted site as indicated by field and laboratory measures by S.H. Harris, G.A. Ulrich, and J.M. Sufliata
- Heterogeneous organic matter in a landfill aquifer material and its impact on contaminant sorption by H.K. Karapanagioti and D.A. Sabatini
- Aquifer heterogeneity at the Norman, Oklahoma, landfill and its effect on observations of biodegradation processes by M.A. Scholl, I.M. Cozzarelli, S.C. Christenson, G.N. Breit, and J.L. Schlottmann
- Hydraulic conductivity reductions resulting from clay dispersion within alluvial sediments impacted by sodium-rich water by L.J. King, H.W. Olsen, and G.N. Breit
- Mapping the Norman, Oklahoma, landfill contaminant plume using electrical geophysics by R.J. Bisdorf and J.E. Lucius

Shallow-depth seismic refraction studies near the Norman, Oklahoma Landfill by M.H. Powers and W.B. Hasbrouck

## SECTION F—Processes that Control the Natural Attenuation of Chlorinated Solvents

Using molecular approaches to describe microbial populations at contaminated sites by S.K. Haack and L.A. Reynolds

Methane as a product of chloroethene biodegradation under methanogenic conditions by P.M. Bradley and F.H. Chapelle

Chlorinated ethenes from ground water in tree trunks by D.A. Vroblesky, C.T. Nietch, and J.T. Morris

Relative importance of natural attenuation processes in a trichloroethene plume and comparison to pump-and-treat remediation at Picatinny Arsenal, New Jersey by T.E. Imbrigiotta and T.A. Ehlke

Unsaturated-zone air flow at Picatinny Arsenal, New Jersey: Implications for natural remediation of the trichloroethylene-contaminated aquifer by J.A. Smith, Whitney Katchmark, Jee-Won Choi, and F.D. Tillman, Jr.

Evaluation of RNA hybridization to assess bacterial population dynamics at natural attenuation sites by L.A. Reynolds and S.K. Haack

Temporal variations in biogeochemical processes that influence ground-water redox zonation by J.T. McGuire, E.W. Smith, D.T. Long, D.W. Hyndman, S.K. Haack, J.J. Kolak, M.J. Klug, M.A. Velbel, and L.J. Forney

Natural attenuation of chlorinated volatile organic compounds in a freshwater tidal wetland, Aberdeen Proving Ground, Maryland by M.M. Lorah and L.D. Olsen

## SECTION G—Research in Characterizing Fractured Rock Aquifers

Integrating multidisciplinary investigations in the characterization of fractured rock by A.M. Shapiro, P.A. Hsieh, and F.P. Haeni

Exchangeable ions, fracture volume, and specific surface area in fractured crystalline rocks by W.W. Wood, T.F. Kraemer, and Allen Shapiro

Geostatistical simulation of high-transmissivity zones at the Mirror Lake Site in New Hampshire: Conditioning to hydraulic information by F.D. Day-Lewis, P.A. Hsieh, A.M. Shapiro, and S.M. Gorelick

Microbial processes and down-hole mesocosms in two anaerobic fractured-rock aquifers by D.A. Vroblesky, P.M. Bradley, J.W. Lane, Jr., and J.F. Robertson

Bedrock geologic framework of the Mirror Lake research site, New Hampshire by W.C. Burton, T.R. Armstrong, and G.J. Walsh

Integrating surface and borehole geophysics--Examples based on electromagnetic sounding by F.L. Paillet and J.W. Lane, Jr.

Geophysical reconnaissance in bedrock boreholes--Finding and characterizing the hydraulically active fractures by F.L. Paillet

Relation between seismic velocity and hydraulic conductivity at the USGS Fractured Rock Research Site by K.J. Ellefsen, P.A. Hsieh, and A.M. Shapiro

Borehole radar tomography using saline tracer injections to image fluid flow in fractured rock by J.W. Lane, Jr., D.L. Wright, and F.P. Haeni

Integration of surface geophysical methods for fracture detection in bedrock at Mirror Lake, New Hampshire by C.J. Powers, Kamini Singha, and F.P. Haeni

Characterizing fractures in a bedrock outcrop using ground-penetrating radar at Mirror Lake, Grafton County, New Hampshire by M.L. Buursink and J.W. Lane, Jr.

Computer simulation of fluid flow in fractured rocks at the Mirror Lake FSE well field by P.A. Hsieh, A.M. Shapiro, and C.R. Tiedeman

Analysis of an open-hole aquifer test in fractured crystalline rock by C.R. Tiedeman and P.A. Hsieh

Effects of lithology and fracture characteristics on hydraulic properties in crystalline rock: Mirror Lake research site, Grafton County, New Hampshire by C.D. Johnson

Characterizing recharge to wells in carbonate aquifers using environmental and artificially recharged tracers by E.A. Greene

CFC's in the unsaturated zone and in shallow ground water at Mirror Lake, New Hampshire by D.J. Goode, Eurybiades Busenberg, L.N. Plummer, A.M. Shapiro, and D.A. Vroblesky

Modifications to the solute-transport model MOC3D for simple reactions, double porosity, and age, with application at Mirror Lake, New Hampshire, and other sites by D.J. Goode

Simulation of mass transport using the FracTran98 Module of FracSys2000 by D.M. Diodato

Borehole packers for *in situ* geophysical and microbial investigations in fractured rock by A.M. Shapiro, J.W. Lane, Jr., and J.R. Olimpio





Printed on recycled paper